Molecular and Functional Characterisation of the Chemopreventative Effects of Dietary Polyphenols in Intestinal Cancer

Thesis submitted for the award of Ph.D.

By

Stephanie May

Cardiff School of Biosciences

The European Cancer Stem Cell Research Institute

Cardiff University

2013 - 2017

Declarations

DECLARATION

This work has not been submitted in substance for any other degree or award at this or any other university or place of learning, nor is being submitted concurrently in candidature for any degree or other award.

Signed ..... (Candidate) Date 24/05/2017

STATEMENT 1

This thesis is being submitted in partial fulfillment of the requirements for the degree of Ph.D.

Signed ..... (Candidate) Date 24/05/2017

STATEMENT 2

This thesis is the result of my own independent work/investigation, except where otherwise stated, and the thesis has not been edited by a third party beyond what is permitted by Cardiff University's Policy on the Use of Third Party Editors by Research Degree Students. Other sources are acknowledged by explicit references. The views expressed are my own.

Signed ..... (Candidate) Date 24/05/2017

STATEMENT 3

I hereby give consent for my thesis, if accepted, to be available online in the University's Open Access repository and for inter-library loan, and for the title and summary to be made available to outside organisations.

Signed ..... (Candidate) Date 24/05/2017

STATEMENT 4: PREVIOUSLY APPROVED BAR ON ACCESS

I hereby give consent for my thesis, if accepted, to be available online in the University's Open Access repository and for inter-library loans **after expiry of a bar on access previously approved by the Academic Standards & Quality Committee.**

Signed ..... (Candidate) Date 24/05/2017

Acknowledgements

After five months of extensive writing, today is the day: writing this note of thanks is the finishing touch on my thesis. My Ph.D. has been a period of intense learning for me not only on a scientific level but also on a personal level. I would like to reflect on the people who have supported and helped me throughout this time.

First and foremost, I would like to thank my supervisors. I would like to thank Prof Alan Clarke, whom sadly passed away before the completion of my Ph.D. I would like to thank him for his scientific knowledge and guidance despite his aura of logical distortion, and for providing me with this opportunity to pursue such an interesting and exciting project. Secondly, I would like to thank Dr Lee Parry for his constant support, enthusiasm, coffee (and beer). Without his influence, I would not have had such an insightful and enjoyable start to my scientific career. And thirdly, huge thanks go to Prof Ros John for her unprecedented support during such a difficult time and whom without, this thesis would not have been finished. I would also like to thank Tenovus Cancer Care, in particular the Jane Hodge foundation for kindly funding my studentship. Thanks are also due to the BACR and Cardiff University Michael Banfill Scholarship and William Morgan Thomas funds for supporting my attendance at conferences and ECSCRI for support with binding this thesis.

Much of the research presented in this thesis would not have been possible without the technical assistance and guidance from a number of individuals. Huge thanks go to Derek Scarborough and his team for the copious amount of tissue processing and sectioning. Credit is due to Matt Zverev and Elaine Taylor for genotyping and ear clipping of animals. I am particularly indebted to Elaine for her endless support and assistance with animal procedures, dissections and IHC. I must also thank everyone in ECSCRI, in particular the ARC group, old and present, for their friendship and guidance over the past 4 years, you have all been a pleasure to work with. In particular, I would like to thank Dr Maddy Young for her time teaching me techniques and willingly taking on the arduous task of reading my work. I'd also like to thank Dr Karen Reed for her advice, support and scientific discussion and for her enjoyable company at several conferences. Last but not least, I would like to thank Dr Valerie Méniel for always lending a helping hand and advice and for being an ear to listen to when I've felt the pressure of Ph.D. life. This leads me in nicely to thank all my amazing friends, especially Elaine and Lili Ordonez for your continued friendship, nights out and holidays. You have both brought so much happiness and joy to my life.

On a more personal note, I owe my biggest thanks to my parents and grandparents, to whom this thesis is dedicated. I am indebted to you for your unconditional love and support, financially, personally and emotionally. Words cannot express how grateful I am for your selfless support throughout my school and higher education, and for your continual encouragement to fulfil my academic goals. Thank you for always being a phone call away and a smiley face to brighten my day.

"Being a Ph.D. student is like becoming all of the Seven Dwarves. In the beginning you're Dopey and Bashful. In the middle you are usually sick (Sneezy), tired (Sleepy), and irritable (Grumpy). But in the end, they call you Doc, and then you're Happy". Ronald T. Azuma

Contents

List of Figures

List of Tables

Abbreviations and Definitions

Symbols

°C= Degrees Celsius

βNF = β-napthoflavone

Δ = Delta

µg = Micrograms

µl = Microlitre

µm = Micrometre

µM = Micromolar

fl/fl = Homozygously floxed allele

fl/+ = Heterozygously floxed allele

+/+ = Wildtype allele

A

AC = Anthocyanin

ACF = Aberrant Crypt Foci

Ah = Aryl hydrocarbon

AICR = American Institute for Cancer Research

AML = Acute myelocitic leukemia

AOM = Azoxymethane

APC = Adenomatous Polyposis Coli

Ascl2 = Achaete Scute like 2

AXIN2 = Axis Inhibitor Protein 2

B

BCSC = Breast cancer stem cell

BE = Barrett's esophagus

Bmi1 = Polycomb ring finger oncogene

BMP = Bone Morphogenic Protein

bp = Base Pair

BRB = Black Raspberry

BrdU = 5'-bromo-2-deoxyuridine

BSA = Bovine Serum Albumin

C

CBC cells = Crypt Base Columnar cells

CC3 = Cleaved-caspase 3

cDNA = Complementary DNA

CD133 = Prominin1

CMS = Consensus molecular subtypes

Cox-2 = Cyclooxygenase 2

CRC = Colorectal Cancer

Cre = Cre recombinase

$CreER^{T2}$ = Cre recombinase-Estrogen receptor fusion transgene

CSC = Cancer Stem Cell

CSL = CBF1/RBP-Jκ/Suppressor of Hairless/LAG-1. A transcription factor important within the Notch signalling pathway

CT = Cycle threshold

CYP1A1 = Cytochrome P4501A1

D

DAB= Diaminobenzidine

DCAMKL-1 = Doublecortin and calcium/ calmodulin-dependent protein Kinase-Like-1

DCC = Deleted in colorectal cancer

DEPC= Diethylpyrocarbonate

dH_2O = Distilled H_2O

ddH_2O = Double Distilled H_2O

Dhh = Desert Hedgehog

DIG = Digoxigenin

Dkk1 = Dickkopf1, a Wnt inhibitor

Dll1 = Delta-Like Ligand 1, a notch ligand

Dll4 = Delta-Like Ligand 4, a notch ligand

DMEM/F12 = Dulbecco's Modified Eagle Medium, nutrient mixture F12

DNA = Deoxyribonucleic Acid

DNase = Deoxyribonuclease

DNMT = DNA Methyltransferase

dNTP = Deoxynucleotide triphosphate

DSH = Dishevelled

DSS = Dextran Sodium Sulphate

DTT = Dithiothreitol

E

EAC = Esophageal adenocarcinoma

EDTA = Ethylenediaminetetraacetic acid

EGCG = Epigallocatechin gallate

EGF = Epidermal Growth Factor

EGFR = Epidermal Growth Factor Receptor

EGTA = Ethyleneglycoltetraacetic acid

ENU = Ethylnitrosurea

EphB = Ephrin receptor B

EpCAM = Epithelial Cell Adhesion Molecule

ER = Estrogen Receptor

EtOH = Ethanol

F

FACs = Fluorescence Activated Cell Sorting

FAP = Familial Adenamatous Polyposis

FOXL1 = Forkhead Box L1

Fw = Fresh weight

Fzd = Frizzled

G

g = Gram

GEMM = Genetically Engineered Mouse Model

gDNA = Genomic Deoxyribonucleic Acid

GFP = Green Fluorescent Protein

GSK-3 = Glycogen Synthase Kinase-3

H

H&E = Haematoxylin and Eosin

HBSS = Hanks Balanced Salt Solution

Hes1 = Hairy and enhancer of split-1

HFD = High-fat diet

HopX = Homeodomain-only protein X

hr = Hour

HRP = Horse Radish Peroxidase

I

IC_{50} = The concentration of AC required to reduce organoid viability by half

IEN = Intraepithelial neoplasia

IHC = Immunohistochemistry

Ihh = Indian Hedgehog

IP = Intraperitoneal

ISC = Intestinal Stem Cell

K

kg = Kilogram

KRAS = Kirsten Rat Sarcoma viral oncogene homolog

L

L = Litre

lb = Pound (weight)

LDL = Low Density Lipoprotein

LEF = Lymphoid Enhancer-Binding Factor 1

LOH = Loss of heterozygosity

LoxP = Locus of crossover of Bacteriophage P1

Lgr5 = Leucine-rich repeat containing G protein coupled receptor 5

LPS = Lipopolysaccharide

LRC = Label Retaining Cells

Lrig1 = Leucine-Rich Repeats and Immunoglobulin-Like Domains

LRP = Low density lipoprotein receptor related protein complex

M

mCRC = Metastatic colorectal cancer

mg = Milligram

Min = Multiple Intestinal Neoplasia

mins = Minutes

ml = Millilitre

mM = Millimolar

mRNA = Messenger Ribonucleic Acid

MSI = Microsatellite instability

Msi1 = Musashi RNA-Binding Protein

mTERT = Mouse telomerase reverse transcriptase

Muc2 = Mucin 2

N

n = Number

NGS = Normal Goat Serum

NICD = Notch Intracellular Domain

NMBA = N-nitrosomethylbenzylamine

NOD/SCID = Non-obese diabetic/severe combined immune deficiency

NRS = Normal Rabbit Serum

O

Olfm4 = Olfactomedin 4

O/N = Overnight

P

PBS = Phosphate Buffered Saline

PBS/T = Phosphate Buffered Saline with 0.1% Tween

PCR = Polymerase Chain Reaction

PI = Post induction

PKA = Protein Kinase A

PLL = Poly-L-Lysine coated slides

PUFAs = Polyunsaturated fatty acids

Q

qRT-PCR = Quantitative Reverse Transcription Polymerase Chain Reaction

R

RFP = Red Fluorescent Protein

RNA = Ribonucleic Acid

RNase = Ribonuclease

Rnf43 = Ring Finger Protein 43

ROCK = Rho-associated protein kinase

ROS = Reactive oxygen species

rpm = Revolutions per minute

R-Smad = Receptor regulated Smad

Rspo1 = R-spondin 1

RT = Room Temperature

S

SCC = Squamous Cell Carcinoma

SDS = Sodium Dodecyl Sulphate

secs = Seconds

SEM = Standard error of mean

Sfrp = Secreted frizzled related protein

Shh = Sonic Hedgehog

SMADs = Intracellular proteins important within BMP signalling

T

TA = Transit amplifying

TACE = Tumour Necrosis Factor-α-Converting Enzyme

TBE = Tris borate EDTA

Taq = DNA polymerase derived from *Thermus aquaticus*

TBS/T = Tris Buffered Saline with 0.1% Tween

TCF = T cell-specific transcription factor

TGF-α = Transforming Growth Factor-α

TGF-β = Transforming Growth Factor-β

Tnfrsf19 = Tumour Necrosis Factor Receptor Superfamily Member 19

U

UC = Ulcerative Colitis

UV = Ultra Violet

V

VEGF = Vascular Endothelial Growth Factor

VEGFR = Vascular Endothelial Growth Factor Receptor

VillinCreER^{T2} = Villin Cre recombinase Estrogen Receptor Transgene

W

W = Watts

WCRF = World Cancer Research Fund

Wnt = Wingless

WT = Wild Type

w/v = Weight per volume

w/w = Weight per weight

Z

Znrf3 = Zinc and Ring Finger 3

123

+4 = Crypt cell located 4 cells from the top of the Paneth cells

2D = Two dimensional

3D = Three dimensional

5-FU = 5'-fluorouracil

Abstract

It is estimated that over half of colorectal cancer (CRC) cases in the UK are preventable through lifestyle changes. Perhaps unsurprisingly, bowel cancer is strongly linked to dietary choices. Diets that are high in fat and low in fibre are associated with increased risk of cancer while diets rich in fruit, vegetables and fibre have a reduced risk. Several studies have investigated the effect of certain dietary components in CRC initiation and development. Previous work, in humans and animals, has demonstrated that the polyphenols found in black raspberries (BRBs) have chemopreventative and therapeutic effects. However, the exact mechanism for these effects remain unknown. As CRC can originate from an intestinal stem cell (ISC) it is possible that the chemopreventative role is due to the impact BRBs have on the normal and/or malignant ISCs. This thesis aimed to investigate the chemopreventative effect of BRBS on normal intestinal tissue and on the initial and later stages of intestinal tumourigenesis, in the context of ISC dynamics and activated Wnt signalling. This was achieved using a Cre-loxP based approach to conditionally delete *Apc* (the negative regulator of the Wnt signalling pathway) within different compartments of the adult murine intestinal epithelium and also utilised the 3D intestinal organoid system.

Exposure to a BRB enriched diet is reported here to be well tolerated in mice and have no major detrimental effects on normal intestinal homeostasis and health. Feeding of BRB diet 2 weeks prior to *Apc* gene ablation is shown to partially attenuate the 'crypt-progenitor' phenotype typical of acute *Apc* loss. In this context of activated Wnt signalling, BRBs altered ISC dynamics *in vivo* and reduced the self-renewal capacity of *Apc* deficient cells *ex vivo*. Additionally, long-term feeding of BRB diet was shown to significantly improve survival of mice which developed macroscopic stem-cell derived Wnt-driven adenomas.

Together, these data are the first evidence that BRBs play a role in CRC chemoprevention by protectively regulating the ISC compartment. These findings further support the use of BRB intervention in cancer prevention in the context of Wnt-driven tumourigenesis.

1 General Introduction

1.1 Cancer

In 2014 the number of deaths from cancer in the UK was 163,444, accounting for about 29% of deaths. There are approximately 350,000 new cancer cases in the UK each year, and 14.1 million worldwide (Ferlay *et al.* 2015). Of the new cancer cases each year in the UK, lung, breast, bowel and prostate cancers represent over half (Parkin *et al.* 2011). With the ever-increasing ageing population it is anticipated that the number of cases will continue to rise. The risk of developing cancer depends on several factors including inherited and acquired genetic mutations. Furthermore, a number of environmental factors are known to contribute to the increased risk of cancer, which includes smoking, exposure to sunlight, obesity, high alcohol consumption, lack of exercise and poor diet (Whiteman and Wilson 2016).

1.1.1 Preventable cancers

Within the UK around 4 in 10 cancer cases a year (42%) are linked to lifestyle factors. The largest single cause of cancer is smoking, which is estimated to cause 19% of cancers, predominately in the lung. Thus, the most effective way to lower cancer risk is to eliminate tobacco use. Dietary factors also play a significant role in the aetiology of many cancers (around 9% of cancers in the UK), particularly bowel cancer. High fat/low fibre diets and diets high in red and processed meat are associated with increased risk whereas high fruit, vegetable and fibre intake decreases the risk of this disease (WCRF/AICR 2011). Risk factors closely linked to dietary factors are being overweight or obese and limited physical activity, which are estimated to contribute to 5% and 1% of cancer cases respectively. Cancers highly related to these lifestyle factors include aero-digestive and colorectal cancers (CRC). Table 1.1 highlights the main lifestyle factors attributable to CRC in the UK (WCRF/AICR 2011).

While several studies report the link between diet and cancer risk, the precise mechanisms are not well understood. For example, high fibre diets have been shown to be protective in CRC (Chan and Giovannucci 2010). This may be due to the role of fibre in diluting carcinogens found in the faecal content, reducing transit time through the colon or through the production of short chain fatty acids (the preferred respiratory fuel of colonocytes) from anaerobic bacterial fermentation which has been found to induce cell death (Chan and Giovannucci 2010). One area of intense research centres on the protective role of bioactive phytochemicals, in particular polyphenols, in CRC (discussed further in 1.12). Understanding the chemopreventative mechanisms underpinning dietary compounds requires both large-scale epidemiological studies and studies using animal models.

Colorectal Cancer Lifestyle Risk Factors in UK	
Red and processed meat consumption	21%
Overweight and obesity	13%
Inadequate fibre consumption	12%
Alcohol	12%
Smoking	8%
Physical inactivity	3%
Ionising radiation	2%

Table 1.1 Estimated percentage of CRC cases caused by identifiable and/or potentially preventable factors based on WCRF/AICR Report 2011

1.2 Colorectal cancer

CRC accounts for approximately 12% of all new cancer cases in the UK with around 41,000 people being diagnosed every year. CRC remains the second most common cause of death by cancer in the UK, even though it can be curable if diagnosed early (Cancer Research UK 2014). Over the last 40 years we have seen a reduction in mortality rates and the number of people surviving CRC has more than doubled. Therapeutic research into this disease has led to the development of several novel and effective drug strategies. However, the five-year survival rate remains at 57% for adults (Cancer Research UK 2014). The high incidence of CRC can be attributed to the high rate of cell division required for intestinal homeostasis, which can result in oncogenic DNA mutations (Barker 2014). CRC can also develop through the interplay of epigenetic and environmental factors such as diet, microbiome, stress and smoking which can further increase mutation rates (Paul *et al.* 2015). Over half of CRCs in the UK might have been prevented through lifestyle changes and this alone highlights the importance of chemoprevention. Chemoprevention refers to the use of synthetic, biological or natural compounds to reverse, suppress or delay processes at either the initiation or progression stages of carcinogenesis (Sporn 1976; Steward and Brown 2013) discussed further in section 1.12.

1.3 Anatomy and function of the murine intestine

CRC is thought to be one of the most common cancers in humans, in part due to the unique exposures of the intestines during the process of digestion and the rapid cell proliferation that takes place to renew lost or damaged cells (Barker 2014). The intestine forms part of the digestive system responsible for the breakdown and absorption of nutrients and water from ingested food (Williams *et al.* 1989). The intestine is consequently exposed to potentially carcinogenic substances and pathogens which can cause mutations in the cells that make up this structure (Barker 2014). The laboratory

mouse is widely used to study human genetics and model human cancers. Aside from the fact that mice are small, cheap and easy to use, they share extensive physiological, molecular and genetic similarities to humans, which makes them one of the best models to study human disease (Frese and Tuveson 2007). Structurally, the intestine is an open-ended tube that runs from the stomach to the anus, approximately 7.5 metres long in humans (Drake *et al.* 2005) and approxiamtely 49 cm in mice (Fox *et al.* 2006). This is divided into the small and large intestine.

The small intestine has three segments, the duodenum, the jejunum and the ileum. The luminal surface of the small intestine is covered in a single layer of polarised epithelial cells. The epithelial sheet is arranged into invaginations called the crypts of Lieberkühn (commonly known as crypts), which sit within the lamina propria (Williams *et al.* 1989). The lamina propria forms a supportive matrix of mesenchymal (stromal) fibroblasts around the crypts and extends into the villus. The villi are finger-like projections, which extend from the crypts that function to increase the surface area to enable maximal nutrient absorption. Encased within the lamina propria compartment of the small intestine is a blood supply, which carries absorbed nutrients, and lacteals, which transports lipids in the form of lipoproteins. The wall of the small intestine consists of a smooth muscle layer. This is responsible for the peristaltic action, which is essential for the movement of material through the intestine (Williams *et al.* 1989). The small intestine also contains nodules of lymphoid tissue called Peyer's patches, which are responsible for immune surveillance against pathogens that enter the body through ingestion (Williams *et al.* 1989). Figure 1.1 shows the small intestine structure.

The large intestine consists of the caecum, colon, rectum and anal canal. The large intestine is where the majority of the water is absorbed from ingested foodstuffs, and where faecal material is stored before egestion through the rectum and anal canal (Williams *et al.* 1989). Similar to the small intestine, the large intestine is composed of a single layer of columnar epithelium however, unlike the small intestine, the crypts are elongated without any villus projections and thus the epithelium is a flat surface (Williams *et al.* 1989) (Figure 1.1). The majority of the cells that make up the large intestine are the mucus secreting cells, whereas in comparison to the small intestine the most abundant cells are the absorptive cells (Barker *et al.* 2008).

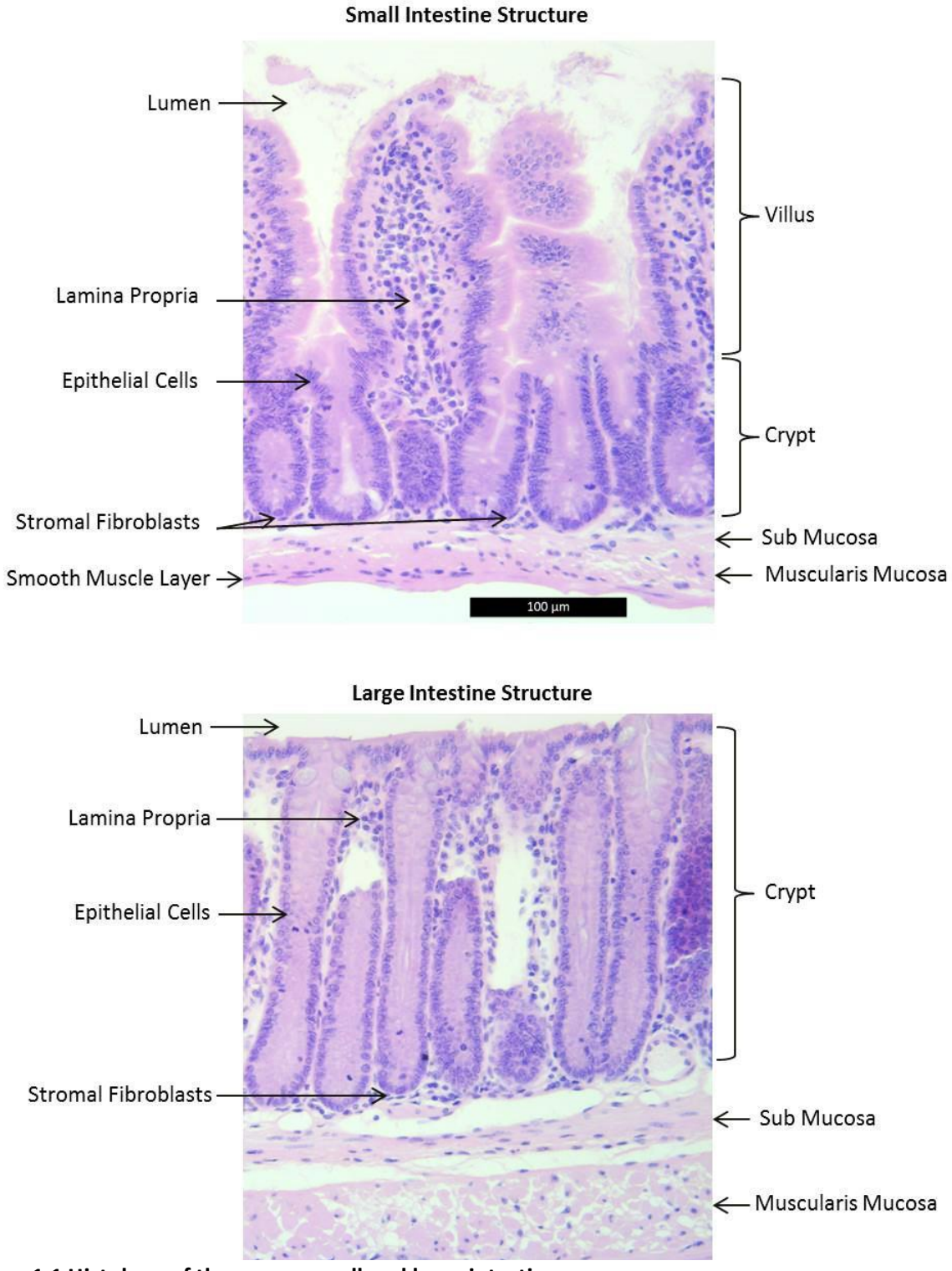

Figure 1.1 Histology of the mouse small and large intestine

The small intestine is comprised of finger-like projections called villi which face into the lumen and invaginations known as crypts. The epithelial layer is supported by stromal fibroblasts. Below the crypt is a smooth muscle layer. The large intestine is made up of a single epithelial layer in the form of crypts also supported by a smooth muscle layer. Scale bars represent 100 µm.

1.4 Small intestinal histology

The small intestinal epithelium is a highly regulated tissue, with six or more independent crypts feeding each villus (Barker *et al.* 2008). The epithelial layer is rapidly renewed every 5 - 6 days in humans and every 2 - 3 days in the mouse (Creamer 1967; Wright and Alison 1984), a process driven by the proliferative compartment within the crypts. This proliferation is pivotal for the generation and maintenance of the intestinal crypts. However, high cell turnover can contribute to cancer risk through *de novo* mutations during DNA replication (Tomasetti and Vogelstein 2015). The intestinal epithelium has a rapid turnover of cells which is maintained by the adult stem cell populations at the base of the crypt, which can produce any of the epithelial lineages in the intestine influenced by its microenvironment, or "niche" (Medema and Vermeulen 2011). The intestinal stem cells (ISCs) reside at the base of the crypt and give rise to their progeny, the transit amplifying (TA) cells (Figure 1.2). These cells divide 4 - 5 times as they migrate up towards the crypt-villus junction where they terminally differentiate. The intestine contains four main types of differentiated cells; the absorptive enterocytes and the secretory lineage of cells including goblet cells, enteroendocrine cells and Paneth cells (Barker *et al.* 2008). The differentiated cells with the exception of the Paneth cells, which reside at the bottom of the crypt, migrate up the villus where they are shed from the villus apex and are replaced by the constant renewal and migration of cells from the crypts (Marshman *et al.* 2002) (Figure 1.2).

1.4.1 Enterocytes

The enterocytes are the most abundant cell type found in the villi and are responsible for the absorption of nutrients from the intestinal lumen and secretion of hydrolytic enzymes which aid the breakdown of food. They are specialised, tightly packed cells that maintain cell polarity and also form an epithelial barrier against microbes (Barker 2014). These cells can be identified by their expression of the enzyme alkaline phosphatase.

1.4.2 Goblet Cells

The mucin secreting goblet cells lubricate and protect the intestinal epithelium from the aggressive environment and mechanical stress of food movement. Commonly found in higher number towards the distal end of the small intestine the goblet cells provide extra lubrication to aid the movement of compacting faecal matter towards the colon (Barker 2014). They are also involved in repairing damaged tissue by secreting trefoil proteins. In the normal intestine goblet cells are found throughout the villus, and most commonly at the crypt-villus junction. The goblet cells are easily identified by alcian blue staining which stains acidic mucins present in goblet cells.

1.4.3 Enteroendocrine Cells

Found throughout the crypt-villus axis are the enteroendocrine cells. These cells secrete hormones that facilitate the digestive functions of the intestine, including serotonine and secretin which act to facilitate gut movement and water homeostasis respectively (Schonhoff *et al.* 2004) These cells can be identified by their ability to reduce silver ions, forming black deposits when stained with grimelius silver.

1.4.4 Paneth Cells

It has long been thought that intestinal stem cells give rise to cells that terminally differentiate at the crypt-villus axis and either that migrate up the villus or in the instance of Paneth cells localise to the base of the crypt (Barker *et al.* 2008). It has recently been reported that Paneth cells arise directly from the quiescent intestinal cells as these cells are the precursors that are committed to differentiate into the secretory cell lineages (Buczacki *et al.* 2013). Paneth cells are long-lived secretory cells which constitute the ISC niche.

Cell positioning in the crypt-villus structure is also governed by a bidirectional gradient of Eph receptors and ephrin ligands, in particular EphB2, EphB3 and ephrin-B ligands. EphB2 is reported to be expressed throughout the proliferative region of the crypt, peaking at cell position 4 – 6 and decreases in concentration further up the crypt, mirroring Wnt gradients (discussed in section 1.6) (Batlle *et al.* 2002; Scoville *et al.* 2008). EphB3 is highly expressed in the stem cell compartment below position 4 and in Paneth cells, although it is often weakly expressed in some precursor cells. However, ephrin-B ligands are highly expressed in differentiated cells and decrease in expression towards to the crypt base but are completely absent within Paneth cells (Batlle *et al.* 2002; Scoville *et al.* 2008). These differential gradients of EphB-ephrin receptor expression cause cell compartmentalisation. Paneth cell positon is thus confined to the crypt base due to their high expression of EphB3 but not EphB2 or ephrin-B receptors (Batlle *et al.* 2002; Scoville *et al.* 2008).

Paneth cells are responsible for the protection and immunity within the crypt by secreting a range of anti-microbials such as cryptdins (Barker *et al.* 2008), enzymes including lysozyme and other factors including TGF-α and Wnt3a (Bevins and Salzman 2011). The ISC niche refers to the microenvironment in which the ISCs are located. The niche is comprised of epithelial and stromal cells as well as a range of ligands which interact with the ISCs to regulate cell fate see section 1.5.2.

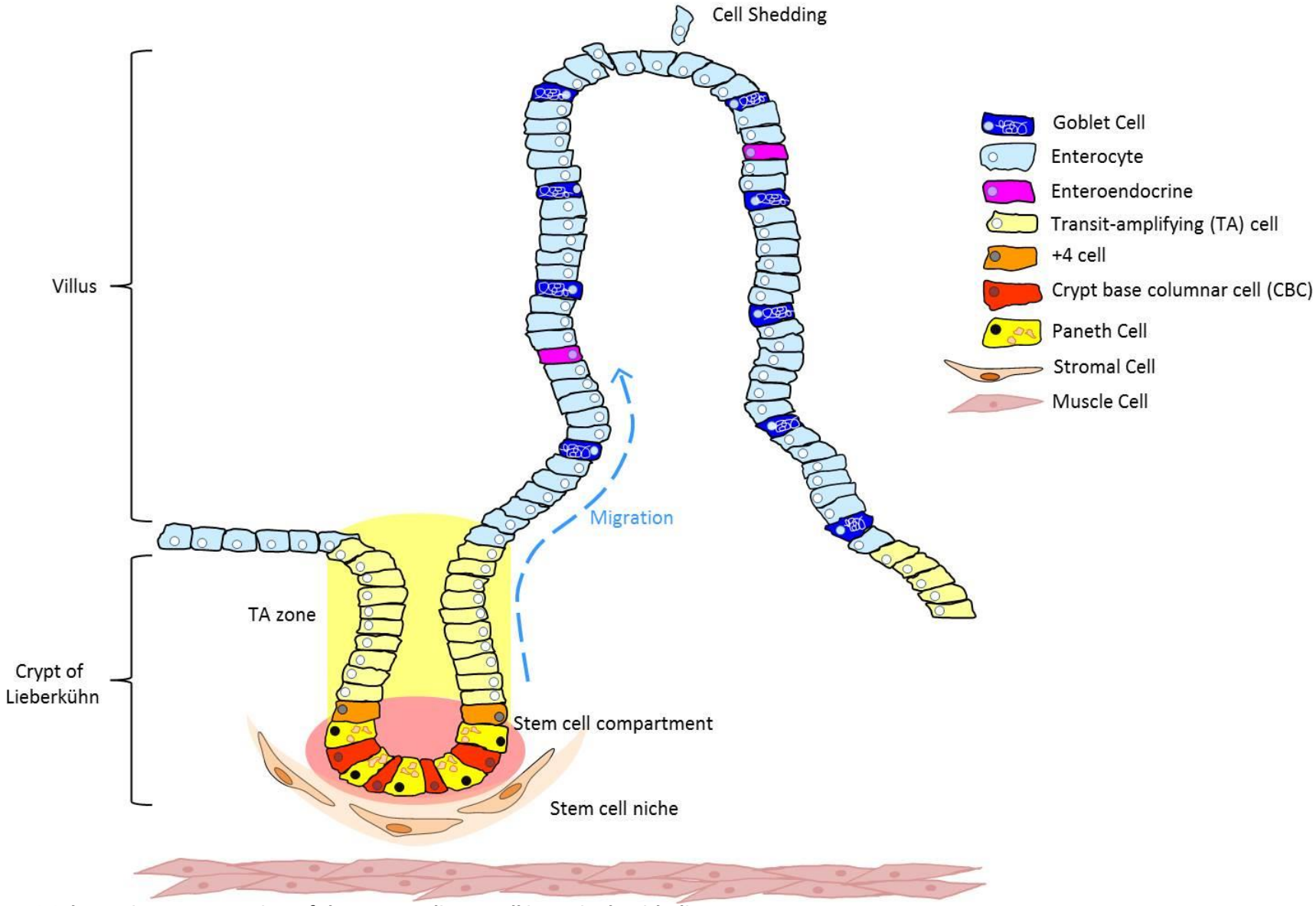

Figure 1.2 Schematic representation of the mammalian small intestinal epithelium

Crypt base columnar cells (CBCs, red) divide to produce progenitor transit amplifying (TA, pale yellow) cells. As TA cells migrate up through the crypt-villus axis they become more differentiated. Differentiated goblet (dark blue), enterocytes (light blue) and enteroendocrine (bright pink) cells reside in the villus. These cells continue to migrate along the villus where they are eventually shed into the intestinal lumen. Paneth cells (bright yellow) on the other hand migrate towards the base of the crypt where they support the stem cell niche, which contains stromal cells (pale orange). The intestinal epithelium is supported by a smooth muscle layer (pale pink) that facilitates the movement of food.

1.5 Intestinal Stem Cells

Stem cells are defined by two features; multipotency and self-renewal. Multipotency refers to the ability of undifferentiated stem cells to differentiate into all cell types within the tissue in which they reside (Barker *et al.* 2008). The dual ability of ISCs to indefinitely self-renew whilst simultaneously generating functioning epithelium makes them potential targets for regenerative medicine. Furthermore, these properties make stem cells targets for therapeutic strategies against cancer as, in some instances, ISCs are thought to be the cell of origin of mutations that promote carcinogenesis. Under normal circumstances ISCs cycle slowly (quiescent) and they readily undergo apoptosis following genetic insult. However, mutations in ISCs are also passed to all their daughter cells (Potten *et al.* 1978; Orford and Scadden 2008).

Previous studies have suggested that the ISC compartment is comprised of two distinct ISC populations. Cheng and Leblond identified the crypt base columnar cells (CBC), which are interspersed between the Paneth cells and are thought to be responsible for intestinal homeostasis (Cheng and Leblond 1974). This paper also reported that CBC cells have the ability to self-renew and are multipotent, thus supporting their role as stem cells. The CBC cells form part of the "stem cell zone" model for the intestine. This model proposes that the CBC stem cells exist within a stem-cell permissive environment or niche (see section 1.5.2), and the stem cell progeny leave this environment to differentiate into the intestinal cell lineages maintaining intestinal homeostasis (Bjerknes and Cheng 1999). However, the CBC cells were found to be rapidly cycling which is in contrast to the view that stem cells are slowly cycling (or quiescent) in order to preserve genome integrity.

The second proposed stem cell to exist alongside the CBCs is the +4 quiescent stem cells (Potten *et al.* 1974). These cells are resistant to damage but respond to an injury by becoming active after intestinal trauma to limit the accumulation of DNA damage in long-lived adult stem cells (Tian *et al.* 2011; Barker 2014). It has been proposed that these cells are a "reserve" stem cell potential population that are capable of replacing CBCs following injury (Montgomery *et al.* 2011). The quiescent cells in the +4 position within the crypt are thought to be a location of ISCs due to their DNA label retaining ability of thymidine labels when actively dividing over extended periods of time (Potten *et al.* 1974; Baker 2014).

The above evidence led to the hypothesis that there are two pools of ISCs that are active during homeostasis or during intestinal damage. The theory postulates that the cycling CBC cells are responsible for intestinal homeostasis, while a separate quiescent population, or population with 'reverse stem cell potential' only divide when injury occurs to the actively dividing stem cells. Three seminal papers have suggested that committed progenitor cells (both secretory and absorptive lineages) are extremely plastic and have the potential to revert to a stem cell state when subjected to

injury or stress (van Es *et al.* 2012; Buczacki *et al.* 2013; Tetteh *et al.* 2016a). These data argue against the traditional view of an adult-stem cell hierarchy in the intestinal crypt such that several committed progenitors have the potential to dedifferentiate into a stem cell-like cell when exposed to the ISC niche and stress

1.5.1 Identification of ISCs

There has been considerable controversy regarding the true stem cells of the mouse intestine (Barker *et al.* 2012). As a result there have been several suggested potential stem cell markers based on positional information of gene expression. However, positional information alone is inadequate evidence to define genes as markers of the ISC. Despite this, several gene markers have been proposed through genetic lineage tracing, xenograft transplantation (Barker and Clevers 2007) and *in situ* hybridisation (Gregorieff *et al.* 2005).

The generation of mouse models (see section 1.10) and the use of *in vivo* lineage tracing have identified *leucine-rich repeat containing G-protein coupled receptor 5* (*Lgr5*), a target gene of the Wnt (Wingless) signalling pathway (discussed in section 1.6.1), to be a marker of the rapidly dividing CBC cells (Barker *et al.* 2007). This led to the development of a genetically engineered mouse model (GEMM) which expressed GFP (green fluorescent protein) in the *Lgr5*$^{+}$ stem cells (Barker *et al.* 2007). This model was subsequently used to identify *Olfactomedin-4* (*Olfm4*), *Achaete Scute-Like 2* (*Ascl2*) and *Tumour necrosis factor receptor superfamily member 19* (*Tnfrsf19*) as markers of the CBC stem cell (van der Flier *et al.* 2009a; van der Flier *et al.* 2009b). The role of Ascl2 as a regulator of the CBC stem cells was confirmed when *in vivo* genetic ablation of *Ascl2* resulted in the rapid death of ISCs, and overexpression of the gene resulted in the expansion of the stem cell zone (van der Flier *et al.* 2009b). Other proposed CBC ISC markers include *Hairy and enhancer of split-1* (*Hes1*)*, Musashi homolog 1* (*Msi1*) (Kayahara *et al.* 2003), *Ring Finger Protein 43* (*Rnf43*) and *Zinc and Ring Finger 3* (*Znrf3*) (Koo *et al.* 2012).

Several markers of the +4 quiescent stem cell have been proposed, including Prominin1 (CD133), Homeodomain-only protein X (HopX), Mouse telomerase reverse transcriptase (mTERT), Leucine-rich repeats and immunoglobulin-like domains protein 1 (Lrig1) and Polycomb ring finger oncogene (Bmi1) (Sangiorgi and Capecchi 2008; Zhu et al. 2009; Montgomery et al. 2011; Takeda et al. 2011; Powell et al. 2012). The complexity in identifying markers that distinguish between distinct subsets of cells limits the use of some of these genes as true markers of the +4 stem cell (Barker et al. 2012; Beumer and Clevers 2016). In particular Bmi1 is commonly found throughout the proliferative zone of the crypt, including in the Lgr5^{+} CBC cells (Montgomery et al. 2011; Itzkovitz et al. 2012; Muñoz et al. 2012; Powell et al. 2012) and Bmi1^{+} cells have been reported to generate CBC cells during homeostasis (Tian et al. 2011; Li et al. 2014). It is evident that more research is required to define

markers associated with the +4 cells and to determine their homeostatic potential and relationship with CBCs. However, it can be concluded that stem cell markers appear as a gradient across CBCs and +4 cells, with only a few markers being uniquely expressed in CBCs (Muñoz et al. 2012). Figure 1.3 represents the commonly used markers of the ISC populations.

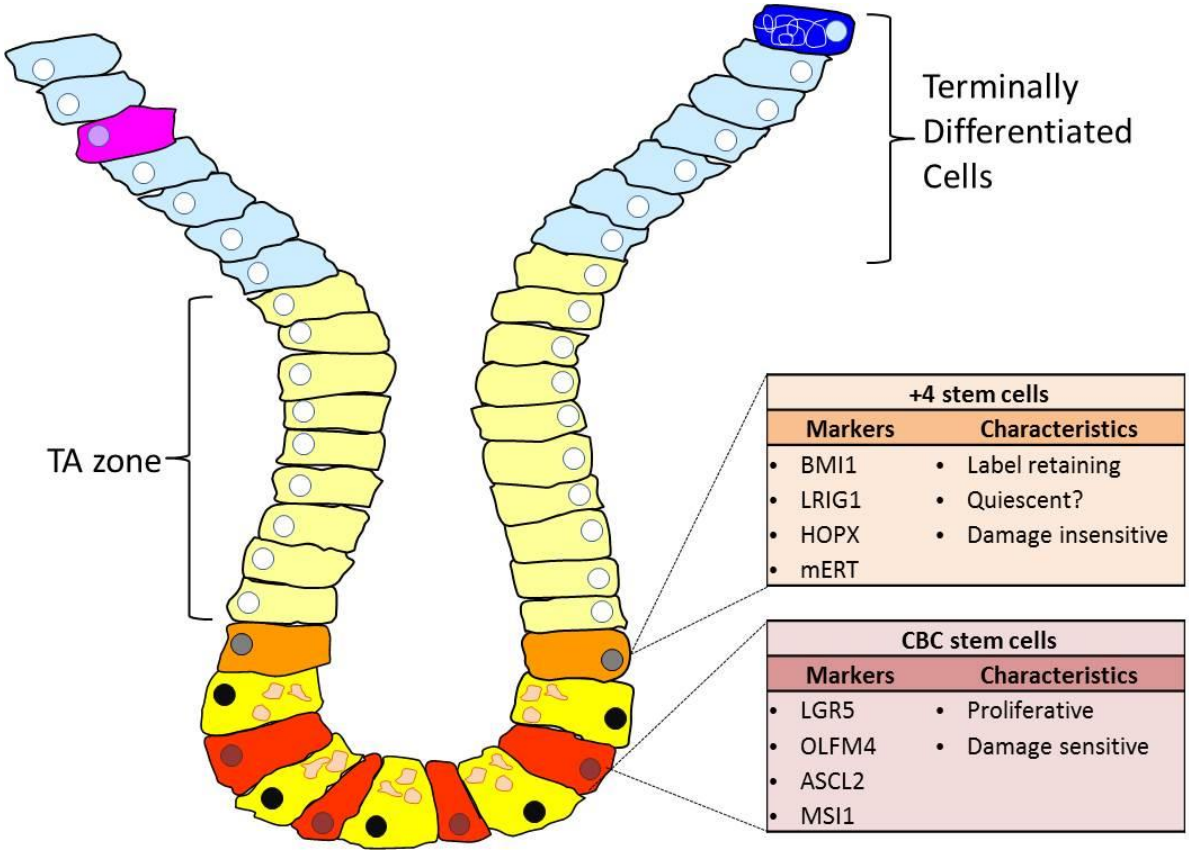

Figure 1.3 Location of putative intestinal stem cell markers

Proposed location and characteristics of ISC markers of the crypt base columnar cells (red) and +4 quiescent stem cell (orange).

1.5.2 Stem cell niche

The microenvironment that surrounds and nurtures ISCs is described as the stem cell niche. It is believed that the stem cell niche plays a role in maintaining a balance between stem cell quiescence and activity in order to establish homeostasis and safeguard against excessive stem cell expansion which could result in tumourigenesis. The intestinal niche is composed of the nearby proliferating and differentiating epithelial cells, surrounding mesenchymal cells such as blood vessels, intraepithelial lymphocytes, and fibroblasts and the extracellular matrix, which all provide stem cells with a range of signals. We have just started to understand the signals provided by the niche and how they help regulate self-renewal and differentiation of ISCs (Moore and Lemischka 2006; Umar 2010). It is apparent that a number of signalling pathways play important roles in the regulation of ISCs including Wnt, Notch, BMP and Hedgehog (discussed in section 1.6).

It has long been thought that Paneth cells are one of the main constituents of the ISC niche. This is because they express a range of ligands, in particular Wnt3, but also TGF-α and Dll4 (a Notch ligand) and antimicrobial factors (Ootani *et al.* 2009; Sato *et al.* 2009; Bevins and Salzman 2011; Sato *et al.* 2011b). The importance of Paneth cells to the stem cell niche is supported by a study which showed co-culturing of *Lgr5*$^{+}$ cells with Paneth cells increased the efficiency of ISCs to form intestinal organoids *ex vivo* (see section 1.10.3 on organoid culture) (Sato *et al.* 2011b). However, *in vivo* studies have shown that conditional Wnt3 deletion and Paneth cell ablation did not affect the maintenance of the ISC niche (Durand *et al.* 2012; Farin *et al.* 2012). These data propose that surrounding non-epithelial cells provide sources of Wnt ligands. Recent stuides have confirmed the role of non-epithelial cells in the maintenace of the ISC compartment. Kabiri *et al.* highlighted that organoids can form and expand in the absence of epithelial derived Wnts if supplemented with an intestinal myofibroblast-enriched stromal fraction that produces endogenous Wnt and R-spondin (Kabiri *et al.* 2014).

This highlights the importance of Wnt signalling in maintaining and regulating ISCs and their supporting niche.

1.5.3 Stem cell division

The DNA label retaining ability of stem cells led to the idea that stem cells divide asymmetrically to produce one ISC and one TA cell (Potten *et al.* 2002; Smith 2005) (Figure 1.4) This form of division is known as “invariant asymmetry”. However, asymmetric divisions do not support the phenomena that intestinal crypts appear to drive towards monoclonality (Loeffler *et al.* 1993). This means that over time an entire crypt will have descended from a single ISC. More recent studies reported that ISCs can divide symmetrically to produce either two TA cells or two ISCs (Figure 1.4).

These symmetric divisions occur in a stochastic manner, meaning that all ISCs have an equal chance of becoming the dominant clone within a crypt. This hypothesis is known as "neutral drift" and is supported by extensive evidence using mathematical modelling (Fletcher *et al.* 2012) and lineage tracing experiments (Lopez-Garcia *et al.* 2010; Snippert *et al.* 2010). ISCs possess both homeostatic and regenerative functions and so it could be argued that a combination of asymmetric and symmetric divisions may occur depending on the status and requirements of the intestinal epithelium.

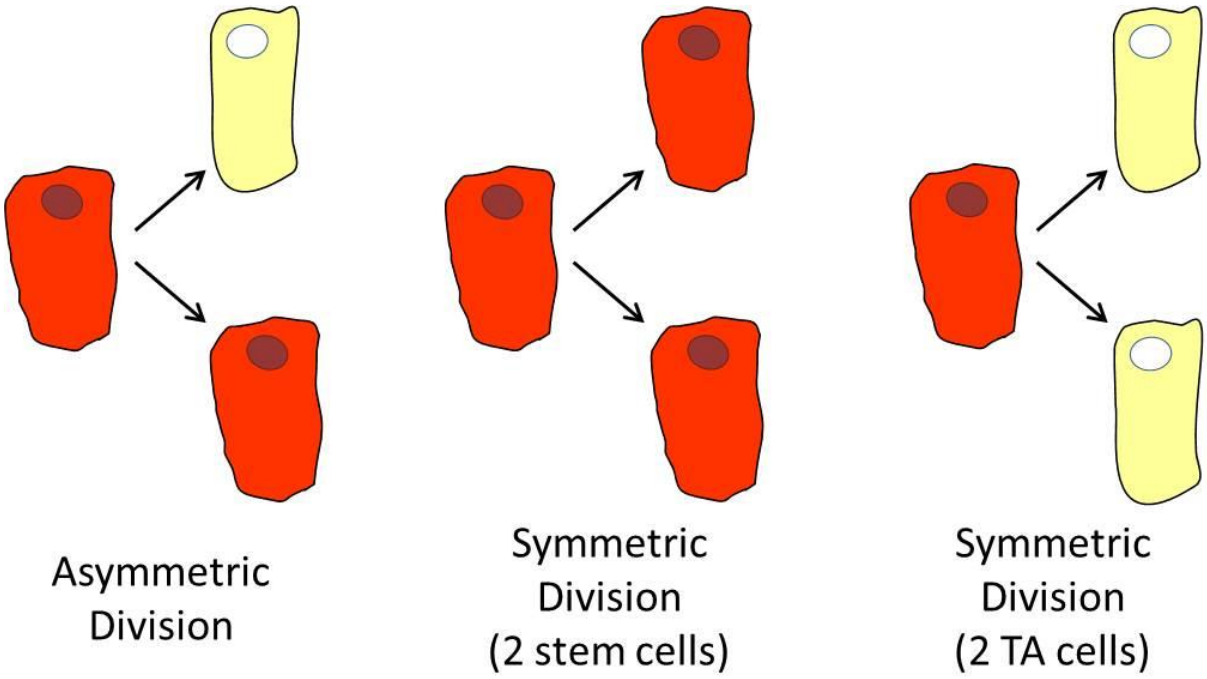

Figure 1.4 Diagrammatic representation of the potential outcomes of intestinal stem cell division

Stem cells = red; TA = transit amplifying cells, yellow.

1.6 Maintenance of intestinal homeostasis

Intestinal homeostasis is dependent on the fine balance of cell proliferation, apoptosis and migration. A slight change in favour of one of these cellular processes could result in a weakened intestinal structure and function. The function of the intestinal epithelium relies on the constant renewal of cells and thus demands a strict balance between proliferation and differentiation. The control of genes fundamental in these processes must be tightly regulated and this is achieved through a number of important signalling pathways. The most important pathways involved in intestinal homeostasis are Notch, TGF-β/BMP, Hedgehog and Wnt signalling. This thesis will focus on the Wnt

signalling pathway due to its roles in stem cell renewal but will very briefly describe the roles of the other signalling pathways.

1.6.1 Wnt Signalling Pathways

Wnt signalling is indispensable for embryonic development and tissue homeostasis. The Wnt pathways have been extensively studied and are known as the canonical Wnt/β-catenin pathway, the non-canonical planar cell polarity pathway and the non-canonical Wnt/calcium pathway. Planar polarity pathway is responsible for regulating cell shape through cytoskeletal changes (Zallen 2007) and the Wnt/calcium pathway controls calcium levels within cells (Kohn and Moon 2005). These two pathways are extremely important for planar cell polarity and extension movements during gastrulation or neuronal and epithelial cell migration, but they have distinctive roles compared to the canonical pathway. The canonical Wnt pathway is fundamental in development and maintenance of gut homeostasis through its regulation of several biological processes which include regulation of the stem cell pool, proliferation, differentiation and apoptosis. The canonical Wnt pathway is often implicated in many CRCs and other diseases due to its role in regulating ISC dynamics. For this reason this thesis will focus on the canonical Wnt pathway.

1.6.1.1 Canonical Wnt Signalling

The stem cell population and intestinal homeostasis is regulated by the canonical Wnt/β-catenin signalling pathway. This pathway also has important roles in embryonic development due to its role in establishing basic body pattern.

When the Wnt pathway is in its 'off state' (Figure 1.5), i.e. in the absence of a Wnt signal, dishevelled (DSH) is sequestered by the Frizzled (FZD) receptor. This allows the intracellular proteins which constitute the destruction complex, APC and AXIN, to be phosphorylated by glycogen synthase kinase-3β (GSK3). This enhances the ability of the destruction complex to bind and phosphorylate β-catenin. Phosphorylated β-catenin is targeted for degradation via the ubiquitin proteasome pathway (Logan and Nusse 2004), and thus cytoplasmic β-catenin levels are reduced.

The presence of a Wnt ligand binding to a Wnt receptor (FZD/low density lipoprotein (LDL) receptor-related protein (LRP) complex) induces an intracellular signalling pathway. DSH is released from FZD and binds to AXIN disrupting the destruction complex and inhibiting its ability to bind β-catenin. β-catenin is stabilised and accumulates in the cytoplasm. It can then translocate into the nucleus where it binds to the T-cell factor and lymphoid enhancer factor (TCF/LEF) which initiates the transcription of several downstream Wnt target genes (Behrens *et al.* 1996; Clevers and van de Wetering 1997) (Figure 1.5).

Activation of the Wnt signalling pathway drives proliferation and homeostasis in the intestine. The importance of Wnt signalling has been extensively studied and has shown that the normal intestinal structure is disturbed when Wnt signalling is lost. Dickkopf-1 (Dkk1) is a Wnt pathway antagonist, and its overexpression within the intestine resulted in the shortening of the intestinal crypts and villi, along with a lack of proliferation and secretory cells (Pinto *et al.* 2003; Kuhnert *et al.* 2004). Similarly, studies by Korinek *et al.* reported that the proliferative ISC compartment was lost *in vivo* following loss of *Tcf-4*, indicating that Wnt signalling is vital for the maintenance of the proliferative capacity of the ISCs (Korinek *et al.* 1998). Furthermore, constitutively active Wnt signalling through the homozygous deletion of *Apc* (the negative regulator of the Wnt pathway) resulted in a perturbed crypt-villus structure, known as the 'crypt progenitor phenotype'. This is characterised by an increase in proliferation, migration, mislocalisation of Paneth cells and a depletion of goblet, enterocyte and enteroendocrine cells (Sansom *et al.* 2004). It was later reported that although all cells of the intestinal epithelium were deficient for *Apc*, it is the crypt progenitor cells that are responsible for this phenotype as transformed villus cells were resistant to morphologically change and were unable to proliferate despite being Wnt-activated (Andreu *et al.* 2005).

It is clear that Wnt signalling is fundamental for homeostasis and regulation of the ISCs. Tight regulation of this pathway is governed by gradients of specific expression of Wnt pathway activators and repressors found throughout the epithelium and stromal cells. The highest levels of Wnt activity are found at the base of the crypts were the stem cells reside, diminishing closer to the differentiated cells (Gregorieff *et al.* 2005) (Figure 1.6).

1.6.2 Notch signalling

The Notch signalling pathway plays a role in intestinal homeostasis by regulating apoptosis, proliferation, determining cell fate and spatial patterning (Artavanis-Tsakonas *et al.* 1999). In more recent years Notch signalling has also been identified to play roles in controlling the differentiation of the intestinal epithelia cells.

Notch signalling is mediated by cell-to-cell signal transductions by direct contact between adjacent cells. Activation of the pathway depends on Notch ligand (Delta and/or Jagged) interaction with the Notch receptors on neighbouring cells. This interaction causes two proteolytic cleavage events. The extracellular domain of the Notch receptor is cleaved by tumour necrosis factor-α-converting enzyme (TACE). The second cleavage then occurs allowing the Notch intracellular domain (NCID) to translocate to the nucleus and activate transcription of several Notch target genes via binding to the CBF1/RBP-Jκ/Suppressor of Hairless/LAG-1 (CSL) transcription factor (Artavanis-Tsakonas *et al.* 1999) (Figure 1.5).

Notch is predominately active in the intestinal crypts were it is thought to keep progenitor cells in an undifferentiated state. It is proposed to do this via up-regulation of the transcription factor Hes1. Hes1 functions to repress the expression of *Math1* which is essential for the specification of the intestinal secretory progenitors (van Es *et al.* 2005). The importance of *Math1* expression to commit progenitor cells to the secretory lineage was shown through the use of mouse models. *Math1*$^{-/-}$ mice resulted in a lack of goblet, enteroendocrine and Paneth cells in the intestine (Yang *et al.* 2001; Van Es *et al.* 2010). In addition, immature progenitor cells have been shown to convert into terminally differentiated secretory cells upon Notch inhibition *in vivo* (Van Es *et al.* 2010; VanDussen and Samuelson 2010). The conversion of progenitor cells into differentiated secretory cells upon Notch inhibition in the intestine is further supported by studies by Pellegrinet *et al*. They showed that Delta-like1 (Dll1) and Delta-like4 (Dll4) (Notch ligands) loss *in vivo,* ablated the stem cell population suggesting that Notch signalling also plays a role in maintaining stemness (Pellegrinet *et al.* 2011).

Extensive *in vivo* murine studies have highlighted the fundamental role of Notch signalling in intestinal homeostasis and its importance of maintaining crypt progenitor status and stemness. Notch works in parallel with Wnt to prevent differentiation while Wnt regulates proliferation. Figure 1.6 highlights the interactions between the signalling pathways.

1.6.3 TGF-β/BMP signalling

The transforming growth factor beta (TGF-β)/bone morphogenetic protein (BMP) signalling pathway plays a fundamental role in embryonic development whereby it mainly regulates cell growth and proliferation. It also plays roles in differentiation, apoptosis and homeostasis. Pathway activation is dependent on ligand and type II receptor binding which allows dimerization with the type I receptor, consequently resulting in the phosphorylation of type I receptors cytoplasmic domain. The phosphorylated receptors can then recruit and phosphorylate Smad 2/3 proteins (TGF-β), or the Smad 1/5/8 proteins (BMP). Phosphorylated Smads are then known as receptor regulated Smads (R- Smad). The R- Smads are able to dissociate from the receptor and bind to Smad 4, forming a co-Smad, enabling it to enter the nucleus. Smad 4 is then able to activate transcription (Figure 1.5). The pathway is inactivated by the binding of inhibitory Smads (Smad 6 and 7) to Smad 4 instead of the R-Smad, preventing its translocation into the nucleus. The expression of TGF-β ligands are predominately at the tip of the villus notably in the lamina propria, but also in the muscularis. TGF-β/BMP signalling works in coordination with the rapid cell turnover of the intestine to prevent growth and proliferation (Barnard *et al.* 1989; Massagué *et al.* 2000). Members of this pathway are not usually found in the crypts of the small or large intestine. Noggin, an inhibitor of the BMP pathway, is found within the submucosal layer around the intestinal crypts (He *et al.* 2004).

1.6.4 Hedgehog Signalling

The Hedgehog signalling pathway is regulated by two membrane spanning proteins known as Patched and Smoothened. When the pathway is inactivated, i.e. no ligand present, Patched functions to supress the activation of Smoothened. This enables protein kinase A (PKA) to post-translationally modify the transcription factors Gli2/3. This preferentially targets Gli2 for degradation leaving a truncated Gli3 which can translocate to the nucleus and transcriptionally repress the Hedgehog target genes. In the presence of the Hedgehog ligands, Sonic Hedgehog (Shh), Indian Hedgehog (Ihh) or Desert Hedgehog (Dhh), the Patched receptor is unable to supress Smoothened. Activated Smoothened prevents the phosphorylation and subsequent degradation of Gli2. Active Gli2/3 is able to translocate to the nucleus and activate transcription of Hedgehog target genes (Madison *et al.* 2009) (Figure 1.5). Previous studies have shown that Hedgehog signalling is an upstream regulator of the canonical Wnt signalling pathway. The transcription factors *FoxL1* and *FoxF1* are Hedgehog target genes (Madison *et al.* 2009). It has been shown that deletion of *FoxL1* significantly down-regulates BMP ligands, consequently activating Wnt signalling (Kaestner *et al.* 1997). This was recently supported by two studies by Kosinski *et al.* and van Dop *et al.* They reported that loss of Ihh within the intestinal epithlieum caused a lack of normal crypt-villus architecture characterised by a marked increase in proliferation, expansion of the stem cell population, crypt fission, an increase in secretory cells but a lack of enterocyte differentiation and loss of the cellular components of the muscularis mucosa (Kosinski *et al.* 2010; van Dop *et al.* 2010). Mechanistic studies highlighted that this was due to the down-regualtion of BMPs simultaneously with up-regulation of Wnt signalling. Kosinski *et al.* also highlighted that Ihh signals to the stromal and smooth muscle fibroblasts in a paracrine manner (Kosinski *et al.* 2010). The findings from these studies implied that Hedgehog signalling is an inhibitor of the Wnt pathway by up-regulation of BMP signals, and its tight regulation is partially responsible for Wnt activation in normal gut homeostasis (Figure 1.6Figure 1.6 highlights these interactions).

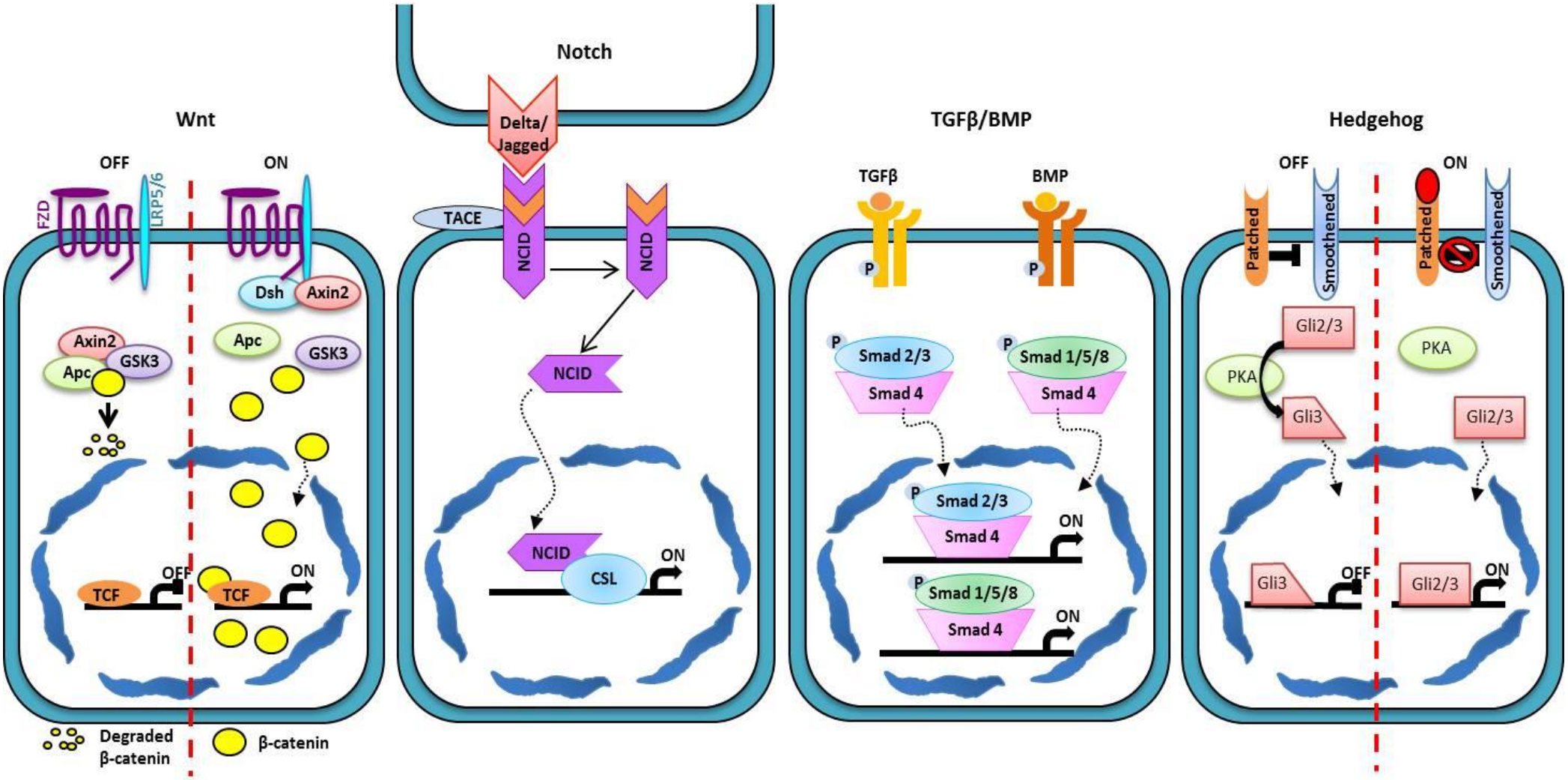

Figure 1.5 Schematic outline of four major signalling pathways involved in regulating intestinal homeostasis

The Wnt, Notch, TGFβ/BMP and Hedgehog signalling pathways are involved in controlling the transcription of genes that regulate and maintain normal homeostatic processes such as stem cell and progenitor cell fate, proliferation, apoptosis, differentiation and migration.

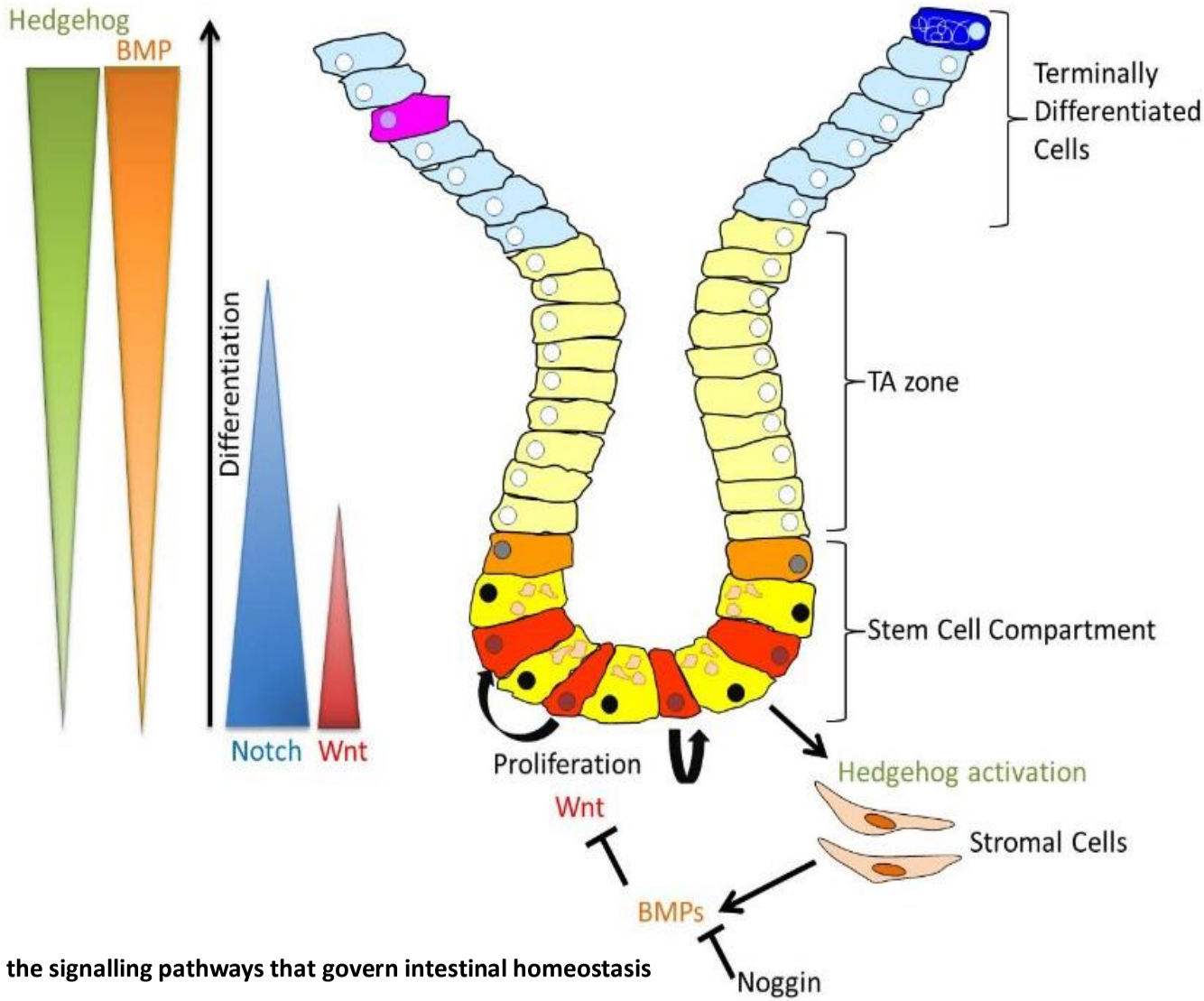

Figure 1.6 Interactions between the signalling pathways that govern intestinal homeostasis

The signalling pathways that regulate proliferation, cell death and differentiation are fundamental to intestinal homeostasis and must be tightly regulated. The canonical Wnt pathway drives proliferation of stem and progenitor cells to replace cells that are shed from the top of the villus. Wnt signalling is fundamental to maintain and stem and progenitor fate and thus, this pathways is tightly controlled by interactions with other signalling pathways. Epithelial cells in the stem cell compartment secrete Hedgehog ligands that activate Hedgehog signalling in neighbouring niche stromal cells. This up-regulates the production of BMP agonists, which inhibit Wnt signalling in adjacent epithelial cells. BMP signalling can be inhibited by the presence of the BMP antagonist, Noggin, in the submucosal layer around the crypts. In addition to Wnt signalling, Notch signalling maintains progenitor cells in an undifferentiated state within the crypt compartment. The highest levels of Wnt and Notch are found at the base of the crypt, decreasing along the crypt structure. Hedgehog and BMP signalling are lowest in the crypt but increase up the crypt in to the villus compartment.

1.7 Pathways implicated in CRC

Cancer arises when cells within a certain area of the body divide uncontrollably (Shen 2011). Intestinal homeostasis is governed by signalling pathways that regulate cell proliferation and stem cell dynamics (see section 1.6). The very same signalling pathways are thus, unsurprisingly, associated with CRC initiation and progression.

1.7.1 Molecular subtypes of CRC

1.7.1.1 Fearon and Vogelstein genetic model of progression

In 1990, it was proposed that sporadic CRC developed and progressed as a result of an accumulation of genetic mutations (Fearon and Vogelstein 1990). Through the use of genetic and histopathological data, Fearon and Vogelstein put forward a model of the genetic progression of CRC from normal intestinal epithelium, to dysplastic tissue, then adenoma through to metastatic carcinoma (Fearon and Vogelstein 1990). Using methods of measuring the frequency of gene mutations present at different stages of human CRC, it was proposed that the loss of function of *APC* in the intestine was sufficient to initiate the development of a benign adenoma. The accumulation of several other gene mutations including *KRAS* (*Kirsten rat sarcoma viral oncogene homologue*) activating mutations, loss of heterozygosity at the 5q and 18q locus and mutations in *Deleted in colorectal cancer* (*DCC*) and *p53* instigate disease progression and malignancy (Fearon and Vogelstein 1990) (Figure 1.7). It is important to note that although genetic alterations in these genes often presented in this order, progression to more advanced tumours is due to the gradual accumulation of mutations rather than following this specific sequence of events. However, initiation and progression of CRC is much more complex than this proposed model and as such, CRC can be classified into four consensus molecular subtypes (CMS), discussed below, in order to improve clinical stratification and aid therapeutic decisions and effective interventions.

1.7.1.2 Consensus molecular subtypes (CMS) of CRC

Through the use of large-scale data sharing and analytics, an international expert consortium have recently described four CMS subgroups of CRC characterised by different molecular and clinical features (Guinney *et al.* 2015). Although more research is required in order to confirm this classification system, these subgroups may prove useful in bettering clinical trial design and provide more effective therapeutics strategies dependent on tumour taxonomy.

CMS1 (MSI Immune, 14%): CRC classified in this group are characteristic of microsatellite instability (MSI) and hypermutations due to deregulated DNA mismatch repair due to hypermethyaltion and thus silencing of DNA mismatch repair gene promoters. In addition, these

tumours frequently presented with strong immune activation (Guinney *et al.* 2015; Müller *et al.* 2016). Patients with CMS1 CRC had poor survival outcomes following relapse (Guinney *et al.* 2015, Müller *et al.* 2016).

CMS2 (Canonical, 37%): Tumours from this subgroup predominately presented with epithelial differentiation signatures with marked activation of the WNT and MYC signalling pathways. Tumour suppressor genes were often lost in this subgroup while oncogenes had several more copy numbers (Guinney *et al.* 2015; Müller *et al.* 2016). However, patients with CMS2 tumours typically had the best survival outcomes after relapse (Guinney *et al*. 2015; Müller *et al.* 2016).

CMS3 (Metabolic, 13%): Akin to CMS2 tumours, CMS3 CRCs also have epithelial signatures but with enrichment of several metabolic pathways. These tumours frequently present with KRAS mutations (Guinney *et al.* 2015), which has previously been reported to maintain tumour cells by metabolic adaptations (Ying *et al.* 2012).

CMS4 (Mesenchymal, 23%): CRCs in this subgroup have enhanced TGF-β activation and increased expression of genes involved in epithelial–mesenchymal transition which ultimately results in stromal invasion and metastasis. In addition, these tumours often presented with increased angiogenesis, inflammation and matrix remodelling (Guinney *et al.* 2015; Müller *et al.* 2016). CMS4 patients had increased risk of metastasis, worse relapse-free survival and worse overall survival than patients with other subgroups (Guinney *et al.* 2015; Müller *et al.* 2016).

The remaining 13% represents a group of tumours with mixed features and thus could not be classified. This group is likely to represent a transition phenotype or intratumoral heterogeneity (Guinney *et al.* 2015)

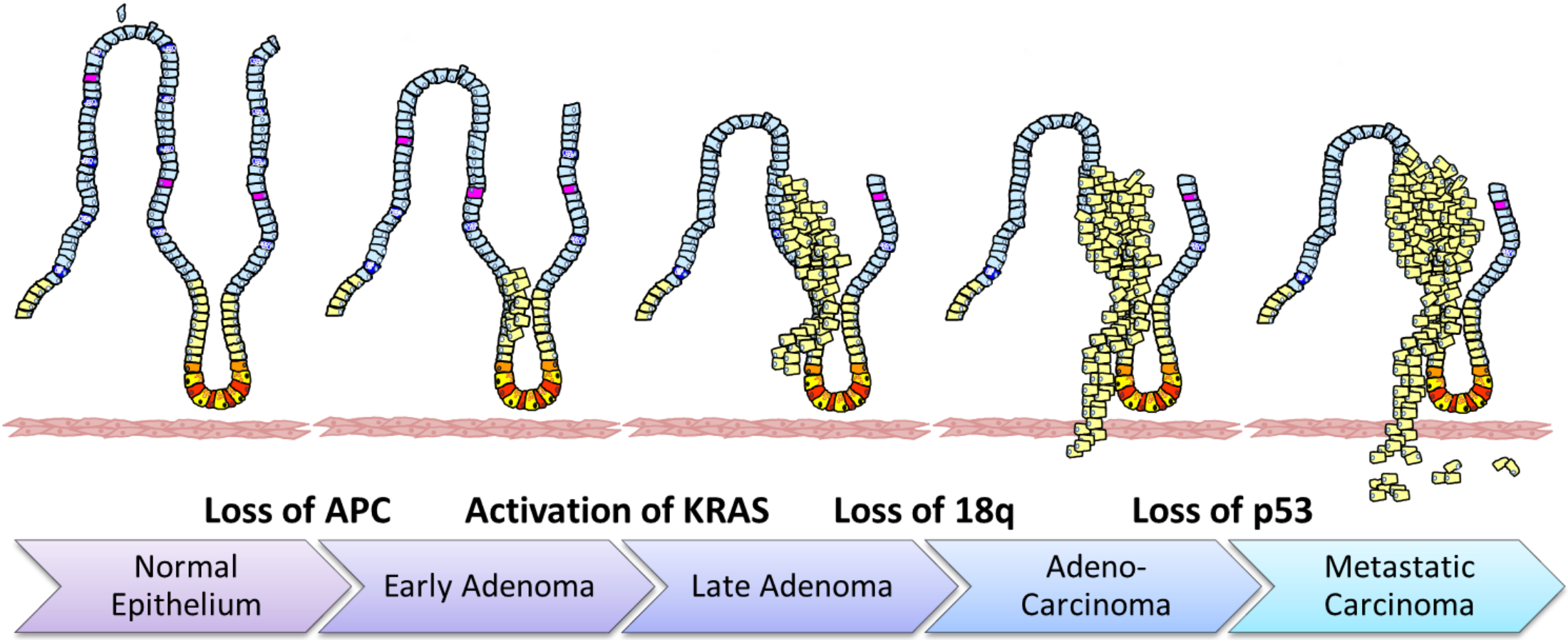

Figure 1.7 The Fearon-Vogelstein model of CRC initiation and progression

The schematic diagram represents the proposed stepwise progression to metastatic colorectal cancer from normal intestinal epithelium. Loss of APC is thought to be the initiating event in tumour formation. Subsequent activation of the KRAS oncogene and loss of the 18q chromosome results in the generation of advanced adenocarcinomas. Metastasis is driven by loss of the tumour suppressor p53.

1.7.2 Wnt and Cancer

As described in section 1.6.1.1 Apc is one of the negative regulators involved in the destruction of β-catenin in the Wnt signalling pathway. Inactivating mutations in *APC* are seen in more than 80% of CRC tumours and are thought to be the initiating event in this malignant disease (Powell *et al.* 1992; Leslie 2002). Loss of functional APC results in the accumulation of nuclear β-catenin and subsequently causes the constitutive transcription of several Wnt target genes involved in the initial and progressive stages of CRC (Komiya and Habas 2008). Exploiting therapeutics to target this pathway could aid in the prevention and treatment of CRC.

Other characterised mutations involved in the development of CRC include activating mutations of *β-catenin* (*Ctnnb1*) which are seen in less than 5% of CRCs. Activating mutations in the gene encoding β-catenin enables this protein to escape from proteasomeal degradation and thus causes constitutive activation of the signalling pathway (Morin *et al.* 1997). Axin (AXIN1) is a scaffold protein involved in stabilising the destruction complex which marks β-catenin for degradation. Mutations in *AXIN1* have been reported in CRC cell lines (Webster *et al.* 2000) which suggests that mutations in this component of the Wnt pathway are likely to augment Wnt signalling due to ineffective degradation of β-catenin. Wnt activation has also been reported through mutations in the transcription factor *TCF4* which has been found in microsatellite-unstable CRCs. Mutations in *TCF4* produce a truncated protein which is more transcriptionally active resulting in the up-regulation of genes involved in proliferation, migration and survival (Duval *et al.* 2000).

Therapeutically targeting the Wnt signalling pathway holds great promise for the treatment of CRC. Several studies are working on the development of novel Wnt inhibitors to target colorectal tumourigenesis and metastasis (Dihlmann and von Knebel Doeberitz 2005). It is important to fully eludicate the interactions involved between Wnt signalling in the normal intestinal epithlieum and CRC in order to develop effective and novel strategies. Therapeutics which target this signalling pathway have been effective, however drug specificity, toxicity and undesirable side effects still remain a problem. Again, this highlights the importance of investigation into chemopreventative therapeutics.

1.8 ISC as the cells of origin of CRC

It has been proposed that stem cells are the cells of origin of many cancers including ISCs. This concept in colorectal tumourigenesis evolved after a study in 2009 whereby *Apc* was deleted specifically in the long-lived ISC cells through the expression of a Cre recombinase driven by an Lgr5 promoter (see section 1.10.1.2). The study reported that these mice developed microadenomas in the intestine and within 3-5 weeks they had rapidly developed into adenomas. This is in contrast to mice

which were deficient of *Apc* in the progenitor and early differentiated cells of the intestine, as they rarely developed large adenomas even after 30 weeks (Barker *et al.* 2009). It is thought that ISCs are the cell or origin of CRC because when *Apc* is mutated in $Lgr5^{+}$ cells, which represent the ISCs, they repopulate the entire crypt and villus with *Apc* deficient cells and thus enable tumourigenesis. Whereas, due to the rapid turnover of the intestinal epithelium, when *Apc* is lost in the differentiated cells these are rapidly lost from the villus and unable to instigate tumourigenesis. This work highlights the importance of ISCs and cancer development; such that stem cells have the aptitude to indefinitely self-renew and potentially accumulate mutations (Barker 2014). Mutations which lead to an expansion of the ISC population mean there are large numbers of cells with the potential to initiate carcinogenesis. It is important to note that although ISCs have been described as the cell of origin of CRC, it has been shown that other epithelial cells have the potential to drive tumourigenesis but cancers derived from the ISC population are much more aggressive (Barker *et al.* 2009).

1.9 Cancer Stem Cells

As a result of the complexity and heterogeneity of tumours, the specific molecular mechanism of how tumours develop is still not clearly defined. The idea that cancer stem cells (CSCs) are the cells which propagate tumourigenesis have been of great interest over the years. The 'stochastic' theory for cancer growth argues cancer cells are not part of a hierarchical system and all cell types have an equal intrinsic potential to divide and contribute to malignancy, but the fate of the individual cells to tumour bulk cells or self-renewal is completely random (Figure 1.8). It was also thought that the phenotypical differences between tumours were due to the genomic instability of cells and influences from the microenvironment (Lobo *et al.* 2007).

Cells that are present within a tumour closely resemble the cells of the tissue in which they were derived. Furthermore, they have similar responses and interactions with the environment and molecular control mechanisms, suggesting that the tumour forming cells are organised into a hierarchy with differing cell potencies (Tan *et al.* 2006). This idea developed the cancer stem cell hypothesis (Figure 1.8), which proposes that only a sub-population of cancer cells have the ability to populate and maintain a tumour, as well as enabling metastasis. This hypothesis is supported with a substantial amount of evidence which have shown that blood cancers such as leukaemia (Lapidot *et al.* 1994) and a range of solid tumours, including breast (Al-Hajj *et al.* 2003), liver (Ma *et al.* 2007), colon (O'Brien *et al.* 2007) and brain (Singh *et al*. 2004), develop from a sub-population of cells when transplanted into an immune deficient mouse, therefore providing evidence against the 'stochastic' theory of cancer development. The clinical implications surrounding the cancer stem cell hypothesis could have profound effects in the battle to find a cure for cancer. Therapeutics targeting the CSC population are essential in the prevention and treatment of this malignant disease. However, it is

possible that by only killing the stem cells within the tumour, non-stem cell or quiescent stem cell populations could revert to stem-cell like cells and repopulate a tumour. Identification of novel and effective therapeutics against CSCs rely heavily on the ability to identify pools of tumour driving cells, highlighting the importance of identifying and confirming specific markers for CSCs in each type of cancer.

CD133 was the first surface marker identified for the ISCs in intestinal cancer. CD133 was enriched in the proliferative cells and these cells were found to have a high tumour-initiating ability when transplanted into non-obese diabetic/severe combined immune deficiency (NOD/SCID) mice when compared to $CD133^-$ cells (O'Brien *et al.* 2007). Similarly in human brain and liver tumours, only $CD133^+$ cells were capable of tumour initiation in NOD/SCID mice (Singh *et al.* 2004; Suetsugu *et al.* 2006). In addition to this, it was also found that a subpopulation of CRC cells that highly expressed epithelial cell adhesion molecule (EpCAM) and CD44 (a known breast CSC marker) were the only cells capable of engraftment in NOD/SCID mice forming lesions which were morphologically similar to the primary human tumour (Dalerba *et al.* 2007). This suggested that EpCAM and CD44 can act as CSC markers. Other intestinal CSC markers identified through similar techniques as CD133, CD44 and EpCAM include D166, CD29, CD24 and Lgr5 (Vermeulen *et al.* 2008).

Identification of these cell surface markers enabled Barker and colleagues, and Zhu and colleagues to provide strong evidence in favour of the ISC being the origin of CRC. As described in section 1.8 conditional activation of the Wnt pathway through deletion of *Apc* specifically within $Lgr5^+$ cells resulted in adenoma formation (Barker *et al.* 2009). Similarly, mice with Wnt activation through a β-catenin mutation resulted in gross alteration in the crypt-villus architecture and a marked expansion of $CD133^+$ cells at the base of the crypt (CD133 has been shown to co-express with Lgr5). Lineage tracing of $CD133^+$ cells revealed that daughter cells repopulated the entire intestinal epithelium with neoplastic tissue (Zhu *et al.* 2009). Furthermore, the use of a *R26R-Confetti Cre*reporter validated that $Lgr5^+$ CSCs were capable of promoting intestinal adenoma growth and generated the different cell types within adenomas (Schepers *et al.* 2012). Crossing of Lgr5 knock in mice with the *R26R-Confetti Cre* mouse resulted in single $Lgr5^+$ cells being randomly labelled with one of four floursecent reporters encoded by the *R26R-Confetti* allele (blue, red, yellow or green) and thus cells were analysed through lineage tracing techniques (Livet *et al.* 2007; Snippert *et al.* 2010). It has also been shown that $Lgr5^+$ adenoma cells were intermingled between Paneth cells suggesting that, like normal ISCs, CSCs may require an environmental niche (Schepers *et al.* 2012). However, $Lgr5^+$ sorted intestinal tumour cells have not yet been shown capable of engraftment in immune deficient mice suggesting that they lack self-renewal abilities despite being multipotent (Schepers *et al.* 2012).

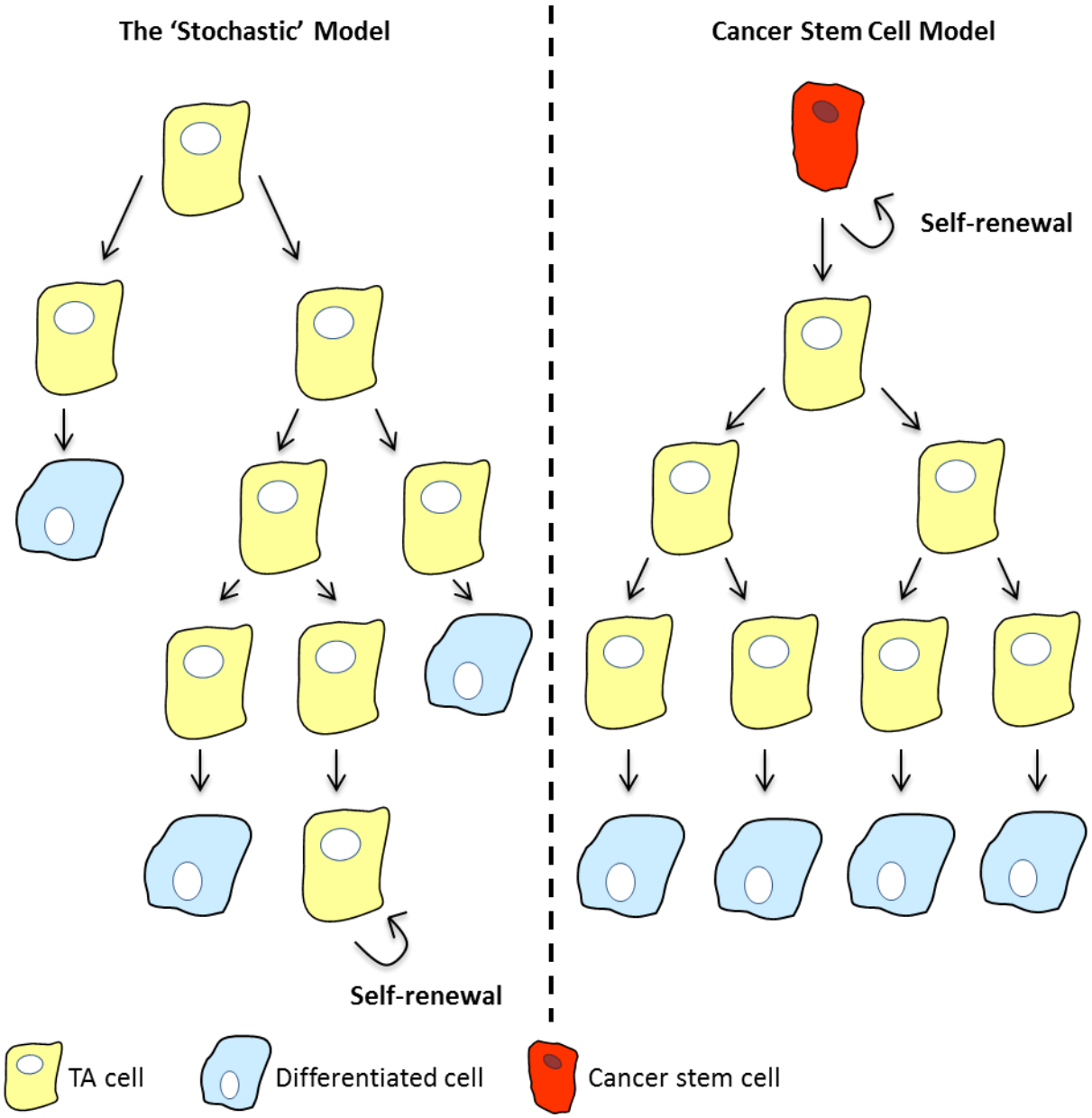

Figure 1.8 The origin of cancer theories

The stochastic model of cancer growth suggests that tumour development is a random process in which all cells have an equal potential to contribute to the growth. The cancer stem cell model proposes that tumour cells are organized into a hierarchy, and so only a sub-population of cells, termed the cancer stem cells (CSCs, red) can contribute to a tumours growth.

1.10 Modelling CRC

GEMMs are an extremely useful tool as they enable the long-term study of tumourigenesis and the earlier stages of carcinogenesis. Furthermore, they allow investigations into the role stem cells, diet and environmental factors play in tumourigenesis which is not always possible with other models such as human cancer cell lines.

Early studies of carcinogenesis relied upon the administration of chemicals that have mutagenic potential such as azoxymethane (AOM) and N-nitrosomethylbenzylamine (NMBA), which cause random mutations. Rodents injected with AOM commonly develop tumours which harbor mutations in the *β-catenin* gene (Johnson and Fleet 2013). One of the first mouse models which demonstrated intestinal tumourigenesis was the Apc^{Min} mouse. The phenotype of these mice was developed through the administration of ethylnitrosurea (ENU) and resulted in severe anemia and often death as a result of multiple intestinal neoplasms (Min). The formation of numerous polyps in the small and large intestine of these mice was found to be due to a germline heterozygous mutation in the tumour suppressor gene *Apc* (Moser *et al.* 1990; Moser *et al.* 1992). The Apc^{Min} mouse has been at the forefront of cancer research since 1990 as it provides a useful model for human Familial adenomatous polyposis (FAP) disease (Su et al. *1992;* Yamada and Mori 2007). However, it is limited in its ability to model other stages of carcinogenesis such as progression and metastasis. In addition to FAP, the majority of spontaneous CRCs carry deactivating mutations in *Apc.* This has led to the development of several genetically modified *Apc* mouse models to study CRC initiation and progression.

1.10.1 Spatio-temporal control of gene expression *in vivo* using Cre-loxP technology

In mice, homozygous *Apc* loss was found to be embryonic lethal (Fodde *et al.* 1994). Despite the potential of the Apc^{Min} mouse, studying early stages of intestinal tumourigenesis was rather limited. As one of the earliest stages of the disease requires inactivation of both alleles of *Apc*, a conditional model of *Apc* deletion was generated. This was achieved through the use of the Cre-loxP recombination system (Schwenk *et al*. 1995).

Conditional alleles rely on a combination of loxP sites flanking the region to be deleted and the expression of Cre recombinase under a tissue-specific or a temporal-specific promoter and/or an inducible promoter. This results in the precise and controlled excision of a gene region. To study CRC, models driving tissue specific transgenic expression of Cre recombinase were developed including *AhCre* (intestinal and other epithelial tissues), $VillinCreER^{T2}$ (intestinal specific) and $Lgr5CreER^{T2}$ (ISC specific) (El Marjou *et al.* 2004; Ireland *et al.* 2004; Barker *et al.* 2007) (Figure 1.9).

1.10.1.1 AhCre Transgene

AhCre was developed to study the conditional loss of function of genes targeted to the intestinal crypt (Ireland *et al.* 2004). This line was generated by cloning the cytochrome P4501A1 (CYP1A1) promoter upstream of Cre recombinase (Ireland *et al.* 2004). The CYP1A1 promoter is usually transcriptionally silent, but is up-regulated on exposure to lipophilic xenobiotics, such as β-napthoflavone (βNF), which bind to the aryl hydrocarbon (Ah) receptor (Ireland *et al.* 2004). The application of βNF activates the *CYP1A1* promoter initiating transcription of the *Cre recombinase.* Activated Cre recombinase protein drives recombination at loxP sites (Figure 1.9). The *Ah* promoter induces recombination selectively in the epithelia of the GI tract and near constitutive recombination in the small intestine, liver and other tissues. Background recombination is thought to be a result of leaky expression of *Cre* during development. Although induction results in recombination in the intestinal epithelium, morphological changes occur in the crypt, with small changes seen in the lower villus. However, changes in the villus are thought to be from migration of cells from the crypt (Ireland *et al.* 2004).

1.10.1.2 VillinCreER^{T2} and Lgr5CreER^{T2} Transgenes

In addition to the *AhCre* transgene the *Villin* and *Lgr5* promoters drive DNA recombination in the entire intestinal epithelia and ISC compartment respectively. These lines were generated by cloning the *Villin* and *Lgr5* promoters upstream of a *Cre recombinase ER^{T2}* insert (El Marjou *et al.* 2004; Barker *et al.* 2007). The *VillinCreER^{T2}* and *Lgr5CreER^{T2}* transgene encode a Cre recombinase estrogen-receptor (ER) linked protein which enables conditional tissue specific knock out of genes by freeing Cre recombinase upon administration of tamoxifen (Marsh *et al.* 2008) (Figure 1.9).

Deletion of the *Apc* gene through the use of *Lgr5CreER^{T2} Apc$^{fl/fl}$* mouse not only enables investigation into the interaction of ISCs and carcinogenesis but also allows lineage tracing events of individual cells by using a lacZ reporter gene or fluorescent reporters such red fluorescent protein (RFP).

The majority of GEMMs develop tumours in the small intestine however, most human CRCs are found in the colon. In humans, there are approximately 150 times as many colonic stem cell divisions than small ISC divisions. It is important to note that mice commonly develop more small intestinal tumours rather than tumours of the colon, this may be because the number of stem divisions is the opposite in mice (Tomasetti and Vogelstein 2015). This provides plausible reasoning for why we analyse the small intestine when investigating human CRCs in murine models. Clevers group have very recently developed an inducible mouse model (*Car1^{CreER}*) that specifically develops colon tumours and faithfully recapitulates human colon cancer in terms of latency, intestinal location, and molecular signature (Tetteh *et al.* 2016b). Carbonic anhydrase I (*Car1*) is a gene that is specifically expressed in

the colonic epiethelium and so Cre induction drives gene recombination specifically in the cecum and proximal colon (Tetteh *et al.* 2016b). This mouse model will be fundamental for cancer research in the future. It will enable the mechanism of tumour intiation from differentiated cells to be identifed and for investigations into novel therapeutic strategies for the treatment of proximal cancers. However, as *Apc* mutations alone rarely result in invasive adenomas, mouse models encompassing later mutations within the adenoma-carcinome sequence have been developed to produce more accurate models of human CRC (Jackstadt and Sansom 2016).

1.10.2 Compound mutant mouse models of CRC

In order to make *in vivo* models of CRC more patient-relevant, mouse models combining mutations in *Apc* with other gene mutations leads to the more advanced and invasive tumours. *KRAS* is typically mutated in approxiamtely 40% of human CRC following *APC* loss (Fearon and Vogelstein 1990). The combination of *APC* and *KRAS* mutations is thought to be the early event leading to CRC progression (Jackstadt and Sansom 2016). Mouse models that combine *Apc* mutation and abberant *Kras* expression had a high tumour burden and increased number of invasive tumour cells which is not seen with *Kras* muatations alone (Sansom *et al.* 2006). However, these mice need to be culled before tumours have the ability to metastasise due to tumor burden (Jackstadt and Sansom 2016), which impedes their use to reflect the human disease. Similarily, the combination of *Apc* mutations with loss of function of the TGF-β signalliing pathway (for example mutations in *SMAD4*) in compound mice, which commonly leads to CRC progression in humans, results in invasive but not metastatic adenocarcinomas (Munoz *et al.* 2006). Gain-of-function mutations in *TP53* are commonly founf in human CRCs. Compound mutant mice expressing mutant *Tp53* and *Apc* loss contain tumours with an invasive phenotype (Muller *et al.* 2009).

Recent advancements have enabled mouse models to model CRC metastasis through *in vivo* genome editing and organoid transplantation (Roper *et al.* 2017) (organoids are discussed in more detail in section 1.10.3).

1.10.2.1 In vivo genome editing and organoid transplantation

GEMMs have provided a basis in which to identify and funcitonally assess genes that are involved in homeostasis and cancer. Mouse models which develop tumours in the small intestine are limited due to high tumour burden and humans rarely develop small intestinal tumours. In addition these models are often expensive and time consuming (Roper *et al.* 2017). Colon specific Cres such as the *Car1* driven Cre (Tetteh *et al.* 2016b) are limited by the slow latency of tumour growth (Roper *et al.* 2017).

Recent work has developed a genome editing system that enables one or several genes involved in CRC initiation and progression to be mutated in wildtype mice. This system is known as the CRISPR-Cas9 nuclease genome editing system (Sánchez-Rivera and Jacks 2015). The bacterial CRISPR-Cas9 technology enables gene editing by acting on the normal response of an organism to respond to and eliminate invading genetic material (Jinek *et al.* 2012). Foreign DNA is incorporated into the CRISPR locus in the genome of bacteria where it is transcribed and processed to produce small RNAs. Small RNAs are then used to localise Cas9 endonucleases to the invading DNA sequence which subsequently results in the excision of foreign DNA (Jinek *et al.* 2012). This system has been adapted to target Cas9 proteins to remove whole or parts of genes involved in carcinogenesis (Sánchez-Rivera and Jacks 2015).

Of particular interest currently, is utilising this CRISPR-Cas9 system to induce gene editing in normal intestinal organoids to mimic the sequential loss and gain of functions of genes involved human CRC initiation and progression and then orthotopically transplant these organoids in to specific mouse tissue to visualise and assess metastasis (Roper *et al.* 2017). Recent work by Yilmaz's group and others have successfully utilised this system to model CRC and metastasis (de Sousa e Melo *et al.*2017; Roper *et al.* 2017). In particular, this system has been utilised to induce individual or combinational gene mutations in *Apc*, *Trp53*, *Kras* in mouse and human colon organoids which were capable of engraftment in the distal colon of wildtype and immunodeficient mice. Orthotopic transplantation of mutant *Apc*, *Kras* and *Trp53* organoids into these mice resulted in metastasis to the liver, which modelled advanced human CRCs which metastatic ability (Roper *et al.* 2017).

This *in situ* epithelial gene editing system and orthotopic transplantation provides several benefits over the standard GEMM of CRC we currently utilise. It enables tumours to develop in the relevant tissue and quickly and advanced tumours recapitulate the genetic complexity and pathological features of human CRC including metastasis, which is often hard to achieve in GEMMs (Roper *et al.* 2017).

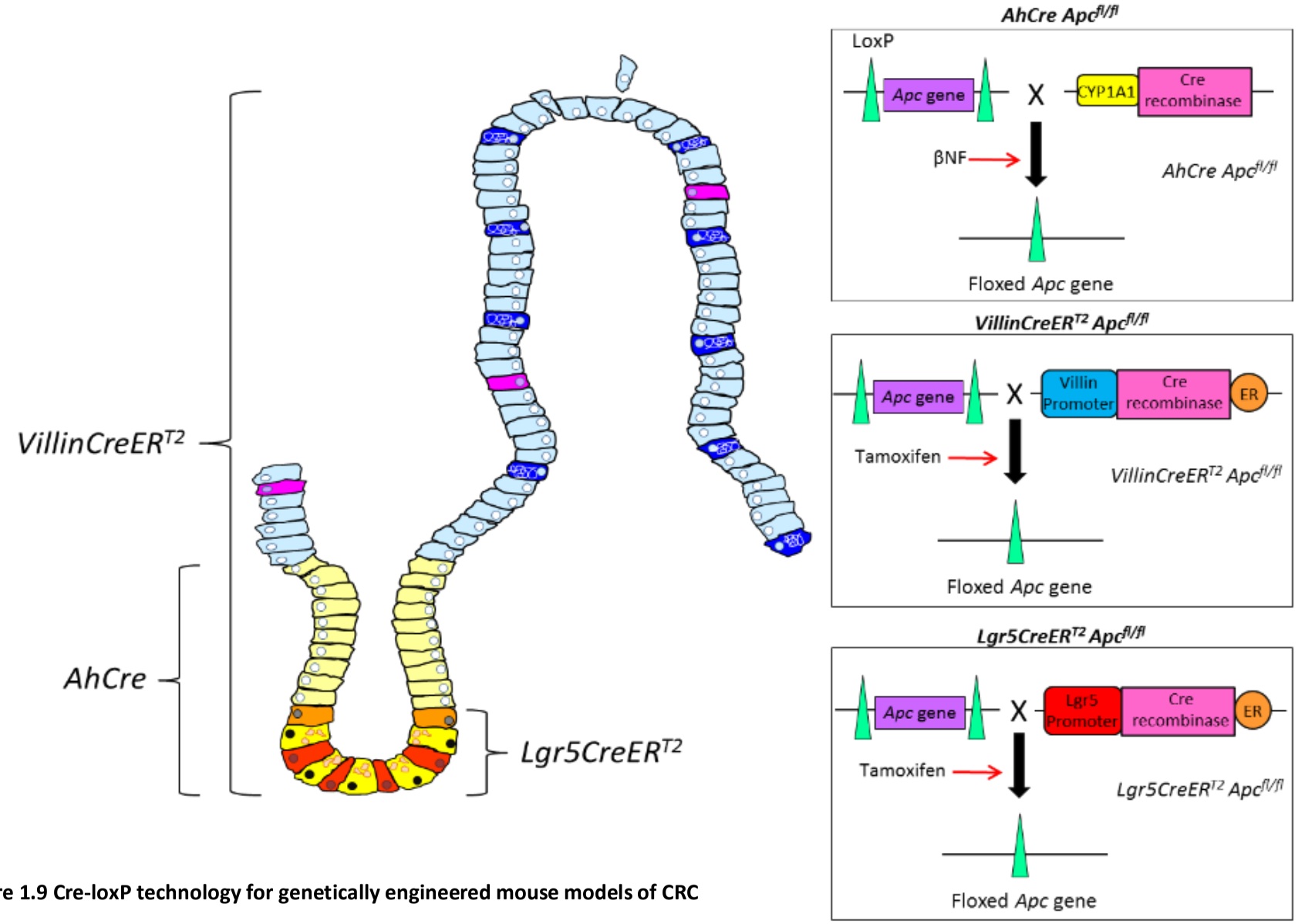

Figure 1.9 Cre-loxP technology for genetically engineered mouse models of CRC

Schematic representation of the inducible Cre recombinase utilised for *Apc* gene ablation. Administration of the relevant inducing agent, βNF or tamoxifen, to mice which have their *Apc* gene flanked by loxP sites (green) and a Cre recombinase under a specific tissue promoter, results in the activation of the Cre protein which subsequently recombines DNA between the two loxP sites, thus excising the *Apc* gene. The CYP1A1 promoter (*AhCre* mice) expresses Cre recombinase in the intestinal crypt epithelium excluding the Paneth cells. The Villin promoter drives Cre recombinase expression in the entire intestinal epithelium including thee Paneth cells. Lgr5 drives Cre recombinase in the intestinal stem cells. For further control of Cre activity a mutated estrogen receptor (ER) is combined to the Cre recombinase, the enzyme can only become free upon tamoxifen administration.

1.10.3 *Ex vivo* culture of ISCs

Over the years many culture systems have been established to look at intestinal crypt physiology and the self-renewal ability of the intestinal stem cells. These culture systems were among the first to report of clonogenic assays for epithelial cells from both murine and human normal intestinal and colonic epithelium. The main drawback of these culture techniques was their inability to sustain long-term culturing of cells (Perreault and Beaulieu 1996; Whitehead *et al.* 1999).

In 2009 Sato *et al.* described a method which enabled the long-term culture of mouse intestinal organoids from single crypts. The organoids form from expanding crypts which have undergone several crypt fission events giving rise to structures with villus-like epithelial regions (Figure 1.10A). In addition, Sato *et al.* were able to grow organoids from single $Lgr5^{+}$ cells, which were indistinguishable in morphology from those which formed from individual crypts (Sato *et al.* 2009). The organoids contained the main types of differentiated cells throughout the organoids structure and the Paneth cells were dispersed between the ISCs at the crypt base. They also report that only the Lgr5-GFP^{high} cells were capable of forming organoids, reinforcing *Lgr5* expression as a marker of the ISCs (Barker *et al.* 2007).

The establishment of this long-term culture system depended on growing organoids in the presence of the requirements of the intestinal epithelium *in vivo*. Firstly, organoids were grown in matrigel, which enables the cells to grow 3-dimensionally, but also prevents cell anoikis when outside of the normal tissue context due to the rich presence of laminin in the matrigel. Secondly, the addition of certain growth factors is fundamental to the growth of intestinal organoids. As Wnt signalling is fundamental for crypt proliferation, R-spondin 1 (Rspo1), a ligand for Lgr5, is required in the growth medium to activate Wnt signals within the crypts (Kim *et al.* 2005; Kim *et al*. 2008). In addition, BMP signalling is essential for cellular differentiation and has been shown to negatively regulate the number of ISCs. Suppression of this pathway is vital for increasing the self-renewal efficiency of ISCs to aid organoid growth (Haramis *et al.* 2004; He *et al.* 2004). This is achieved through the addition of Noggin, a BMP inhibitor in the culture medium. Epidermal growth factor (EGF) is also utilised in organoid crypt culture due to its involvement in cellular proliferation, differentiation and survival (Dignass and Sturm 2001).

When single cells are seeded in matrigel the "stem cell niche" is no longer present to support cell growth and survival, thus cells die immediately. To combat this, additional growth factors are added to the culture medium. The Notch signalling pathway is fundamental in regulating cell-cell communications (Li *et al.* 1998). In the absence of Paneth cells, activation of the Notch pathway in $Lgr5^{+}$ cells is not possible, for this reason Jagged, a notch ligand, is added. Rho-associated protein

kinases (ROCK) have been shown to be involved in detachment-induced cell death. To prevent anoikis of single ISCs a ROCK inhibitor, Y27632 is used (Watanabe *et al.* 2007; Sato *et al.* 2009).

The applications of this intestinal organoid system are extensive. It provides a solid platform in which to investigate basic stem cell biology but it also proves to be an extremely useful tool for clinical investigations including regenerative medicine, drug testing and disease modelling of epithelial derived diseases (Date and Sato 2015).

1.10.4 *Ex vivo* culture of *Apc* deficient cells

In addition to culturing ISCs and crypts from normal epithelium, this organoid culturing system enables the expansion of cells from both murine and human tumours. This has proven extremely beneficial in understanding tumour development, as organoids derived from adenomas recapitulate the events seen at all stages of adenoma progression. In addition, they are an exceptionally useful tool for use in drug screening assays as a way of stratifying medicines to an individual's needs.

It has previously been reported that cells of the small intestine with *Apc* loss are capable of forming organoids but are cyst-like in their structure (Jarde *et al.* 2013) (Figure 1.10B). Where normal organoids develop from an initial sphere their growth is characterised by budding of crypt-like structures and differentiated cell types. In contrast, cyst-like organoids maintain their spherical shape throughout growth and tend to lack differentiated cells. As a result of over activation of Wnt signalling either *in vitro* (Sato *et al.* 2011b; Onuma *et al.* 2013) or from the cells derived from adenomas (Sato *et al.* 2011a) cyst-like organoids are capable of growing in the absence of R-spondins. Germann *et al.* later reported that the organoids derived from cells deficient of *Apc* have a high organoid forming and self-renewal efficiency compared to cells with normally functioning *Apc* (Germann *et al.* 2014). These results confirm that the combination of an expansion in proliferative ISCs with hyperactive Wnt signalling is capable of initiating tumour formation. Thus, cyst-like organoids are a good model in which the earliest stages of *Apc* loss recapitulate *in vivo* tumourigenesis (Barker *et al.* 2009; Schepers *et al.* 2012).

Organoids derived from mouse and human tumours are providing a platform in which to understand cancer development, stratify individual treatments and better predict patients' response to therapies. However, organoid culture lacks essential components of *in vivo* models (microbiome, immune cells, vasculature etc) and so this reductionist approach can often impede analysis of tumour development with the native microenvironment (Hollins and Parry 2016) (discussed in more detail in sections 4.2.2 and 6.3).

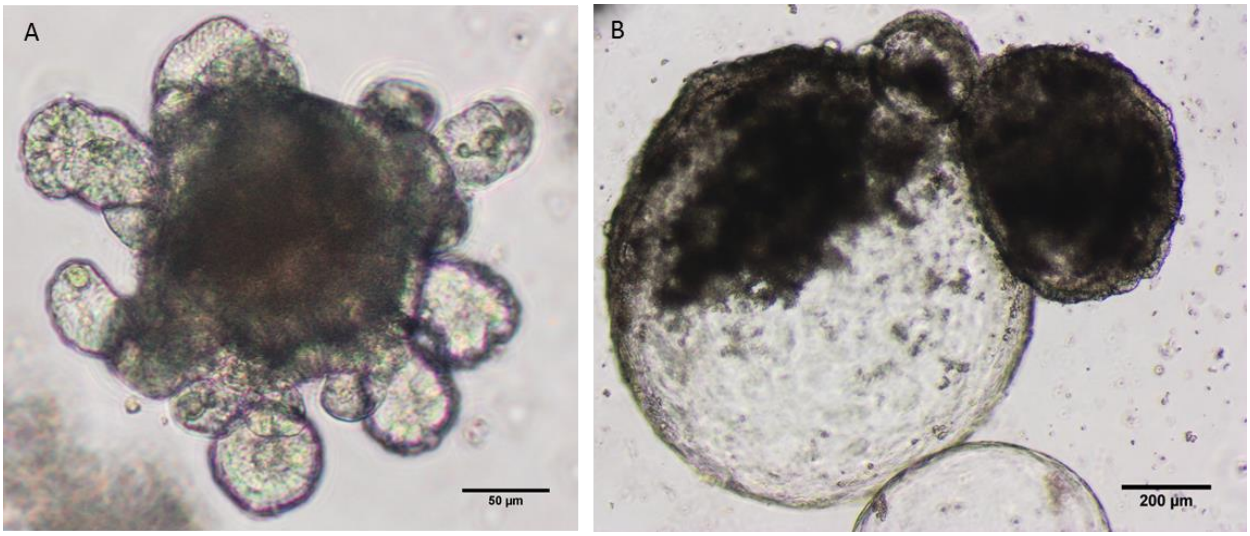

Figure 1.10 Organoids grown from wildtype and *Apc*$^{fl/fl}$ crypts

(A) Wildtype organoids have budding crypts projections. (B) *Apc* deficient organoids have a cyst-like morphology.

1.11 CRC Therapy

Current therapies for CRC depend largely on the tumours' stage of progression with surgery remaining the mainstay of treatment for CRC confined to the intestine (Bilchik *et al.* 2005). Conventional methods are often used to remove tumours and to prevent reoccurrence after surgery. In some instances patients may receive neo-adjuvant chemotherapy to reduce the tumour size before surgical removal (Bilchik *et al.* 2005). Although surgery can remove the majority of the tumour tissue, it cannot be guaranteed that all the cancer cells are removed. As a result of this chemotherapy is often used as an adjuvant treatment to eliminate remaining cancer cells and to prevent recurrence (Jessup *et al.* 2005). Chemotherapy is a standard of care in cancer treatment due to the observation that it often reduces tumour burden and improves survival outcomes. However, patients whom which chemotherapy has previously been successful frequently progress to a refractory state, this is commonly known as acquired or secondary resistance. The failure of many chemotherapeutic drugs can be attributed to this acquired resistance. It is known that intratumoural heterogeneity is responsible for acquired resistance (Vidal *et al.* 2014). The current cytotoxic chemotherapeutics target the rapidly dividing cells of the tumour bulk which accounts for about 99% of the tumour. But these therapies have very little effect against the CSCs which tend to cycle slower (Stoian *et al.* 2016). Evidence has shown that CSC populations develop resistance to conventional therapeutics and as a result, enables cancer recurrence and metastasis due to their ability to reform the tumour following treatment (Bu *et al.* 2014; Volk-Draper *et al.* 2014) (Figure 1.11). This has been shown *in vivo* and *in vitro* across a range of cancers including acute myelocitic leukemia (AML) (Gerber *et al.* 2012),

pancreatic cancer (Tajima *et al.* 2012*)* and gliobalstomas (Liu *et al.* 2006). Chemotherapeutic agents are often associated with many undesirable side effects such as hair loss, fatigue, mouth sores and heightened chance of infection. Accordingly, this has led research to aim at understanding CSCs response and sensitivity to drug treatments, emphasising the importance of understanding the molecular mechanisms in which drug therapies exert their anti-tumourigenic properties. It is clear that targeting CSCs specifically is required in the treatment of cancer however, this in itself also poses problems. Due to the similarities between ISCs and CSCs, novel therapies would need to distinguish between them in order to prevent any damage to the normal tissue which could be detrimental to life. In addition, as normal ISCs work in close association with its surrounding stem cell niche, it is likely that CSCs may also regulate and depend on its own microenvironment. If this is so, simply targeting the CSCs alone may not be an effective therapy, as the 'niche' may be able to aid the reversion of other cells to have stem-cell-like properties.

Targeted therapies, unlike the traditional cytotoxic chemotherapeutics which target any rapidly diving cell, interfere specifically with the proliferating process of cancer cells by inhibiting molecules vital for tumour development and survival. Due to having a better understanding of the molecular pathways involved in colorectal carcinogenesis, several targeted therapies have been established to exploit the pathways cancers use. Targeted therapies have advanced treatment of CRC (Johnston 2014), but they have only had a small impact on longer-term survival rates (Jonker *et al.* 2007). The median survival is around 2 years (Ohhara *et al.* 2016). Table 1.2 outlines some of the commonly utilised targeted therapies. Akin to conventional therapeutics, targeted therapies are also associated with complications and undesirable side effects. This emphasises the importance of cancer prevention and the development of alternative treatments. Several recent *in vitro* and *in vivo* studies have demonstrated the chemopreventative potential of naturally occurring dietary components which have a profound potential to target CSC self-renewal and vastly improve outcomes for patients (Huderson *et al.* 2013; Toden *et al.* 2016).

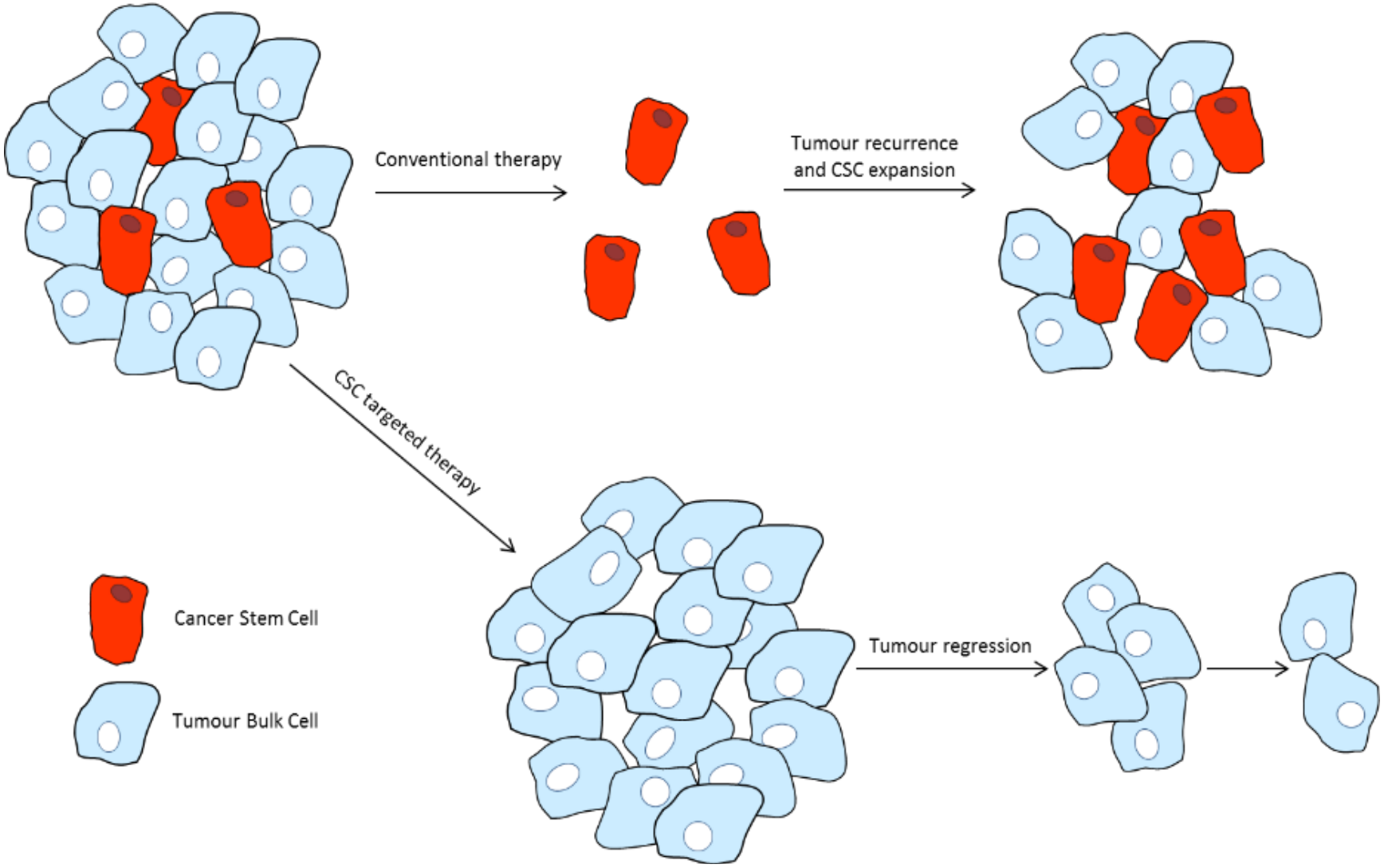

Figure 1.11 Cancer stem cell and chemotherapy

The CSC hypothesis proposes that tumour development is driven by a subpopulation of self-renewing cancer stem cells (red). Current conventional therapies target the rapidly dividing cells, reducing the tumour bulk (blue) thereby reducing tumour size. However, they have little effect on the CSCs. Remaining CSCs drives tumour formation and relapse. Therapies which specifically target the CSCs may enable tumour regression and prevent tumour metastasis, and so novel therapeutics which targets the CSC populations may have more beneficial effect clinically.

Targeted Therapy	Cancer Type	Mode of Action	Used in Combination?	Benefits	Side Effects	References
Bevacizumab	mCRC	Prevents interaction of VEGF-A with receptors on vascular cells. Thereby inhibiting the formation of a blood supply to tumours, that would otherwise aid tumour development and metastasis	Used in combination with chemotherapy	Improved survival of mCRC patients by around 5 months	Hypertension, proteinuria, wound-healing difficulties and gastrointestinal perforation	Hurwitz *et al.* 2004; Guan *et al.* 2011b; Samelis *et al.* 2011. Hagan *et al.* 2013; Hori *et al.* 2013.
Cetuximab and Panitumumab	mCRC	Binds to EGFR on the cell surface inhibiting cell proliferation and survival by blocking growth signals to cancer cells	Generally used as single agents in patients whose previous treatments with oxaliplatin, 5'-fluorouracil, leucovorin, and irinotecan chemotherapy have been unsuccessful; alternatively they can be given in combination with other chemotherapeutics	Increased progression-free survival and overall survival of mCRC patients with irinotecan-resistance. However, these drugs are only efficient in treating tumours wildtype for *Kras*	Skin toxicities on face, neck, scalp and trunk	Resnick *et al.* 2004; Jonker *et al.* 2007; Bokemeyer *et al.* 2009; Blanke 2009; Li and Perez-Soler 2009.

Table 1.2 Summary of commonly used targeted therapeutic drugs against metastatic colorectal cancer

mCRC = metastatic colorectal cancer; VEGF-A = vascular endothelial growth factor; EGFR = epidermal growth factor receptor; Kras = Kirsten rat sarcoma viral

1.12 Chemoprevention

The combination of an increasing ageing population and an increase in cancer incidence globally, together with the limitations of the therapeutic agents currently used in clinic, means there is an increasing demand for strategies for cancer prevention. An approach with great interest and potential is chemoprevention. Chemoprevention is defined as the "use of natural, synthetic or biological agents to reverse, suppress or prevent either the initial phases of carcinogenesis or the progression of premalignant cells to invasive disease" (Sporn 1976; Steward and Brown 2013).

One of the most studied drugs in CRC chemoprevention in humans is aspirin (Ulrich *et al.* 2006). Colon adenomas and invasive carcinomas often have increased levels of prostaglandins (Singh-Ranger 2016). Prostaglandins are fatty acids produced by cyclooxygenase (COX) enzymes during inflammation and thus, have a key role in cancer progression (Singh-Ranger 2016). Aspirin acts to inhibit COX activity and so aids in supressing the inflammatory process (Singh-Ranger 2016). As it often takes years for benign polyps to become cancerous, studies in to the use of aspirin as a long-term cancer preventative have been possible. A study by Rothwell *et al.* investigated the effect of aspirin (75 mg - 300 mg daily) on CRC incidence and mortality over 20 years during and after the start of five randomised clinical trial studies. Analysis of pooled individual patient data revealed that allocation to aspirin (75 mg a day, there was no added benefit of concentrations above this dose) for 5 or more years reduced the long-term incidence of CRC, reduced the risk of developing right-sided cancer by around 70% and reduced the risk of mortality due to CRC (Rothwell *et al.* 2010). It was shown that the largest benefit of long-term aspirin use was for prevention of proximal colon cancer where sigmoidoscopy and colonoscopy screening were usually not effective enough measures for prevention (Rothwell *et al.* 2010). It has been reported that high doses of aspirin ≥ 500 mg daily reduce long-term incidence of CRC (Rothwell *et al.* 2010) but higher doses are often associated with several adverse effects such as increased incidence of gastrointestinal bleeding (in a dose-dependent manner) and increased risk of hemorrhagic stroke, which could limit the chemopreventative potential for long-term aspirin administration (U.S. Preventive Services Task Force 2007), as the potential risks may outweigh the benefits. As a result it is thought that agents that are dietary derived may have the largest effects throughout the entire process of malignancy with fewer adverse effects (Steward and Brown 2013).

Previous studies have shown that a diet consisting of a high intake of red meat, saturated fats, refined carbohydrates (Willett *et al.* 1990) and alcohol (Giovannucci *et al.* 1995) correlate to significantly increased risk of CRC. However, a diet containing a high level of dietary fibre (Peters *et al.* 2003), folate (Sanjoaquin *et al.* 2005), fruit, vegetables (Millen *et al.* 2007), antioxidant vitamins and calcium (McCullough *et al.* 2003) appears to have a protective effect against the development of intestinal tumourigenesis.

Antioxidants are chemicals which scavenge and neutralise free radicals and reactive oxygen species (ROS) which are naturally produced chemicals in the body (Diplock *et al.* 1998). However, accumulation of these species can be detrimental. High concentrations of free radicals and ROS can cause DNA and protein damage which could potentiate the development of cancer from initiation to progression (Diplock *et al.* 1998). Endogenous antioxidants produced by the body remove free radicals and prevent cellular damage. However, the body heavily relies on the exogenous sources of antioxidants mainly from the diet (Valko *et al.* 2007). Polyphenols are commonly found in fruit and vegetables and are a major source of antioxidants in our diet. Several studies have characterised the anti-tumourigenic properties of dietary polyphenols *in vitro* and *in vivo* (discussed below), highlighting their potential use as chemopreventative agents

1.12.1 Dietary polyphenols

Over recent years several nutritional polyphenols have been investigated for their chemopreventative properties to alter cancer associated modifications. The most abundant antioxidants in our food are the polyphenols and several studies have shown them to be chemopreventative at the initiation and progression stages of carcinogenesis (Wang *et al.* 2013e). Based upon their chemical structure, nutritional polyphenols can be divided into several groups which include the flavonoids, phenolic acids, stilbenes and lignans (Bravo 1998; Manach *et al.* 2004). The flavonoids can be further divided into six subgroups, flavonols, flavones, isoflavones, flavanones, anthocyanidins and flavanols (catechins and proanthocyanidins). Although this thesis will briefly talk about some compounds in these subclasses it will mainly focus on the anthocyanidins.

With the increasing interest in dietary components there is growing evidence suggesting that plant-derived compounds have several protective biological roles including strong antioxidant, anti-inflammatory (Nijveldt *et al.* 2001), anti-carcinogenic (Middleton *et al.* 2000), anti-neurodegenerative (Soobrattee *et al.* 2006), anti-allergic, anti-thrombotic (Manach *et al.* 2004), and anti-viral (Lee *et al.* 2016) properties.

Epigallocatechin gallate (EGCG) is a catechin abundantly found in white and green tea, and has exceptional antioxidant activity that exceeds Vitamin C and E. Previous studies have shown that EGCG has chemopreventative properties through its ability to induce cell cycle arrest and apoptosis in several types of cancer cells, *in vitro* and *in vivo* (Ahmad *et al.* 2000). Specifically in a variety of colorectal cell lines, EGCG inhibited both EGFR (Shimizu *et al.* 2005) and vascular endothelial growth factor receptor (VEGFR) (Shimizu *et al.* 2010) which are utilised by cancer cells for tumour development, angiogenesis and metastasis, thereby exerting growth inhibitory effects on cancer cells. In addition, Adachi *et al.* found that EGCG specifically induced the internalisation of EGFR in colon cancer cells and thus elicited its chemopreventive effects by limiting activation of the EGF receptor

(Adachi *et al.* 2008). Thus, this inhibited downstream activation of pathways involved in cell proliferation and survival. It was recently shown that EGCG prevented colon cancer cell growth through inhibition of the Wnt/β-catenin signalling pathway. EGCG induced the phosphorylation of β-catenin targeting it for degradation but via a pathway independent of GSK3 mediated phosphorylation (Oh *et al.* 2014). However, the concentrations of EGCG used in these culture conditions were much higher than the physiological concentrations shown to be effective in animals (Moiseeva *et al.* 2007). These studies have shown promising results but haven't investigated the effect of EGCG on the CSCs. Recent studies have shown 5-FU resistant cell lines have an enhanced spheroid forming capacity suggestive of an increased CSC population. Exposure to EGCG limited the ability of 5-FU resistant cells to form spheroids and enhanced their sensitivity to 5-FU treatment. These results were also validated through *in vivo* experiments. The growth of spheroid derived CSCs which were xenografted into nude mice were significantly inhibited. These data indicated that EGCG induced sensitisation to 5-FU by specifically targeting the CSCs of CRC and suggested that EGCG could be used as an additional therapy with conventional chemotherapeutic agents (Toden *et al.* 2016).

Resveratrol, a natural phytoalexin found in a range of plants and grapes is classified as a stilbene. Studies have shown that resveratrol was capable of supressing growth of both Wnt-activated cells and Wnt-driven human CRC cell lines, revealing a novel therapeutic for Wnt-driven tumourigenesis *in vitro* (Hope *et al.* 2008; Chen *et al.* 2012). In addition to suppressing proliferation of the human CRC cell line, it has been reported that resveratrol can induce apoptosis. However, these effects were only visible at high concentrations. The preventive effects of resveratrol have also been investigated *in vivo* using a murine model of Apc^{Min}. Loss of *Apc* was induced using benzo(a)pyrene. The study reported that resveratrol induced apoptosis, arrested cell proliferation and growth of tumour cells and reduced tumour burden in Apc^{Min} mice (Huderson *et al.* 2013). Resveratrol has been evaluated as a dietary supplement in a CRC prevention trial. It was found that resveratrol reduced Wnt signalling, supporting the *in vitro* work presented by Chen and colleagues. It was also shown that *CD133* expression in the colonic epithelium was reduced following treatment with resveratrol, suggesting that it may target the CSCs. From this resveratrol is now under phase II clinical studies (Martinez *et al.* 2010). These data indicate that the anti-tumourigenic effects of some dietary compounds are via regulation of CSC populations.

1.12.1.1 Anthocyanins

The most abundant flavonoid found in fruit and vegetables are the anthocyanins. Anthocyanins are responsible for the variety of bright colours, most notably red, blue, purple and black, in leaves, stems, roots, flowers and fruits of plants (Wang and Stoner 2008). Anthocyanins are important in plants due to its ability to impart bright colours which helps in attracting animals for

pollination and seed dispersal. They also have defensive roles in plants helping to protect against extreme ultra violet (UV) exposure and providing antioxidant and antibacterial properties against viruses, bacteria, fungi and oxidative stress (Kong *et al.* 2003). In humans, anthocyanins have also been seen to be strong antioxidants and have anti-cancer and anti-inflammatory properties (Seeram 2008). In the USA it is estimated that the daily intake of anthocyanins is around 180 - 215 mg, approximately nine fold more than other dietary flavonoids which are consumed at about 23 mg/day (Wang and Stoner 2008). These natural anthocyanins are well represented in our diet as they occur in red, blue and purple fruits and vegetables such as carrots, onions and aubergines, and red wine but most abundantly in the berry fruits (Table 1.3) (Manach *et al.* 2004; Mazza 2007), having as high as 1480 mg of anthocyanin/ 100 g fresh weight berry (Wu *et al.* 2004). The concentration of anthocyanins in fruits is dependent on the cultiviator, growing conditions and season. Over 400 different anthocyanins have been identified but the 6 most common anthocyanidins (the sugar-free counterparts of anthocyanins) are pelargonidin, cyanidin, delphinidin, peonidin, petunidin, and malvidin, with cyanidin being the most abundant in nature. One berry known for its particularly high anthocyanin content is the black raspberry (BRB) (approximately 607 mg/ 100 g fresh weight) (Table 1.3). Studies have indicated that BRB anthocyanins have chemoprotective roles (Stoner *et al.* 2007; Kresty *et al.* 2016b) and thus may have a potential use as a chemopreventative strategy against CRC (discussed in more detail in section 1.12.2). The anthocyanins in BRBS have been identified as cyanidin-3-glucoside, cyanidin-3-sambubioside, cyanidin-3-xylosylrutinoside, cyanidin-3-rutinoside and pelargonidin-3-rutinoside (Tian *et al.* 2006).

Berry Type	Scientific Name	Anthocyanin Content (mg/100 g FW)	Reference
Black chokeberry	*Aronia melanocarpa*	307 ~ 1480	(Wu *et al.* 2004; Denev *et al.* 2012)
Elderberry	*Sambucus nigra*	332 ~ 1374	(Määttä-Riihinen *et al.* 2004; Wu *et al.* 2004)
Bilberry	*Vaccinium myrtillus*	300 ~ 808	(Prior *et al.* 1998; Määttä-Riihinen *et al.* 2004; Ogawa *et al.* 2008)
Black raspberry	*Rubus occidentalis*	145 ~ 607	(McGhie *et al.* 2002; Moyer *et al.* 2002)
Blueberry	*Vaccinium corymbosum*	63 ~ 430	(Prior *et al.* 1998; Moyer *et al.* 2002; Ogawa *et al.* 2008)
Cranberry	*Vaccinium macrocarpon*	20 ~ 360	(Prior *et al.* 1998; Moyer *et al.* 2002; Ogawa *et al.* 2008)
Evergreen blackberry	*Rubus laciniatus*	91 ~ 164	(Wada and Ou 2002; Siriwoharn *et al.* 2004; Ogawa *et al.* 2008)
Marionberry	*Rubus ursinus*	62 ~ 200	(Deighton *et al.* 2000 ; Wada and Ou 2002; Siriwoharn *et al.* 2004)
Red raspberry	*Rubus idaeus*	28 ~ 100	(McGhie *et al.* 2002; Moyer *et al.* 2002; Ogawa *et al.* 2008)
Strawberry	*Fragaria x ananassa*	13 ~ 55	(Cordenunsi *et al.* 2002; Ogawa *et al.* 2008)

Anthocyanin content (mg/ 100 g fresh weight (FW)) in selected berries.

Table 1.3 Approximate content of anthocyanin in different edible berry fruits

1.12.2 Black Raspberries

As already discussed, the most abundant flavonoid constituent in fruit and vegetables are the anthocyanins. Anthocyanins are polyphenols due to their phenolic structure which confers their antioxidant properties. Because of this anthocyanins have anti-mutagenic and anti-carcinogenic activities (Kong *et al.* 2003). Dietary anthocyanins are found in several fruits and BRBs are one of the richest dietary sources of anthocyanins (Tian *et al.* 2006).

Raspberries belong to the genus *Rubus* in the Rosaceae family. As they grow on woody stems known as canes they are often classified as caneberries. Raspberry fruits come in a range of colours including yellow, red, purple or black (Figure 1.12). Similarly to blackberries, raspberries are not considered true berries, but are in fact classified as aggregate fruits due to the clustering of several individual cells each with its' own seed (Johnson 2009). Black raspberries (*Rubus occidentalis*) are a minor but speciality fruit of eastern North America and share its name with its western North American relative *Rubus leucodermis*. The BRBs have been the most studied raspberry due to its extensive health benefits (Johnson 2009). BRBs have been shown to have chemopreventative properties in a range of human diseases including cancer. The chemopreventative properties of BRBs have been investigated *in vitro* and *in vivo* in both human and animal models (Kresty *et al.* 2016b) with the best documented studies being for oral, oesophageal and colon cancers (Zikri *et al.* 2009).

Figure 1.12 Picture of yellow, red, purple and black raspberries

1.12.2.1 Chemopreventive Studies of Black Raspberries

1.12.2.1.1 Chemopreventive Studies of Black Raspberries in Oral Cancer

In 2006, a study investigated the effects of freeze-dried BRB ethanol extracts at varying concentrations on cell lines derived from human oral squamous cell carcinoma (SCC) tumours *in vitro.* The results indicated that the extract had anti-proliferative effects on human oral SCC in a dose-dependent manner. The study also reported that BRBs were sufficient to induce apoptosis and terminal differentiation and supressed the translation of VEGF, thereby inhibiting angiogenesis which would aid tumour development (Rodrigo *et al.* 2006). These results highlighted the potential of BRBs as a chemopreventive therapy. In later years freeze-dried BRBs went into clinical studies. In patients with oral intraepithelial neoplasia (IEN), topical application of a 10% freeze-dried BRB gel was administered to the ventrolateral side of the tongue. The gel was applied here due to the high incidence of oral IEN and SCC found in that area. To ensure optimal delivery the gel was applied four times a day for 6 weeks, administering 0.5 g of BRB each application. Results showed that the lesional grade decreased in 41% of patients, 23% had an increase in lesional grade and 35% of participants remained at a stable state. The study also concluded that freeze-dried BRB gel is safe to use as none of the candidates developed BRB gel associated toxicities (Shumway *et al.* 2008).

The successes of this study lead to the development of a multi-centred placebo controlled trial, investigating the efficacy of the BRB gel over a 3 month period. The same dosing regime was utilised in patients with confirmed oral IEN. The study reported that patients treated with the BRB gel had a significant reduction in the size and grade of lesions compared to lesions which were treated with a placebo gel which continued to increase in size (Mallery *et al.* 2014). The chemopreventive properties of BRBs are supported by these data.

1.12.2.1.2 Chemopreventive Studies of Black Raspberries in Oesophageal Cancer

In 2001, *in vivo* studies using a rat model of NMBA-induced oesophageal tumourigenesis reported that feeding of 5 and 10% lyophilised BRBs for 2 weeks prior to induction with NMBA and then throughout a 30 week time period, significantly reduced tumour multiplicity by 39 and 49% respectively (Kresty *et al.* 2001). These results along with other preclinical animal studies (Kresty (Kresty *et al.* 2001; Stoner *et al.* 2006; Lechner *et al.* 2008; Zikri *et al.* 2009) led to the development of a phase I pilot study in patients with Barrett's esophagus (BE). BE is the known precursor lesion for oesophageal adenocarcinoma (EAC) and is becoming a much more common cancer with fairly poor survival rates. In order to determine the long-term tolerability of BRBs in oesophageal cancer, a 6 month pilot study was performed. Patients confirmed to have BE were administered lyophilised or freeze-dried BRB powder at 32 and 45 g once daily to women and men respectively. These weights

were determined based on preclinical studies which showed 5 and 10% BRBs were sufficient to inhibit tumourigenesis in rodents and approximately equated to 1.5 and 2 cups of whole fruit respectively (Kresty *et al.* 2001; Stoner *et al.* 2006; Lechner *et al.* 2008; Zikri *et al.* 2009). The BRBs were mixed with 6 ounces of water and taken every morning. Results showed that lyophilised BRBs were generally well tolerated with a few adverse effects including epigastric pain, diarrhoea and constipation (Kresty *et al.* 2016a).

In addition, the chemopreventive properties of BRBs in oesophageal cancer have been linked in part, to their effects on inflammation. Exposure to diets of 6.1% BRB or an anthocyanin-enriched fraction derived from BRBs, inhibited tumourigenesis in an NMBA-induced rat model of oesophageal cancer by inhibiting genes associated with inflammation such as *COX-2* (cyclooxygenase-2) an enzyme expressed during the inflammatory process (Peiffer *et al.* 2014). Furthermore, a diet containing 5% BRBs has recently been shown to inhibit NMBA-induced rat oesophageal tumourigenesis by inhibiting Wnt signalling via the reactivation of silenced Wnt pathway antagonists such as Sfrp4 (Secreted frizzled related protein 4) (Huang *et al.* 2016). These data highlight the potential of BRBs to prevent Wnt-driven tumourigenesis. Mutations in the Wnt signalling pathway are the most common drivers of colorectal cancer, and the chemopreventive potential of BRBs has been investigated in several models of CRC.

1.12.2.1.3 Chemopreventive Studies of Black Raspberries in Colorectal Cancer

In 2001 a study investigated the chemopreventive effects of lyophilised BRBs in a rat model of AOM-induced aberrant crypt foci (ACF) (Harris *et al.* 2001). ACF are early morphological changes that occur in rodents following exposure to a colon-specific carcinogen such as AOM (Suzuki *et al.* 2004). It is quite common in patients that develop sporadic or heredity forms of CRC to see similar lesions (Stevens *et al.* 2007), thus these rodent models recapitulate genetic, morphological and cellular changes that are present in human CRCs.

Following treatment with AOM, rats were fed 0, 2.5, 5 or 10% freeze-dried BRB diet for 9 and 33 weeks to analyse the number of ACF and tumours. ACF multiplicity decreased compared to the controls (0% BRB diet) following treatment with 2.5, 5 and 10% BRB diet by 36%, 24%, and 21% respectively. Similarly the total tumour multiplicity decreased 42%, 45%, and 71% respectively and also the adenocarcinoma multiplicity reduced in a likewise dose-dependent manner. These results are indicative that BRBs were sufficient in reducing tumourigenesis in an AOM-induced rodent model of colon carcinogenesis (Harris *et al.* 2001).

Previous studies by Wang *et al.* reported an association between BRB derived anthocyanins and decreased hypermethylation status seen in CRC. The data suggested that BRBs could play a role in modulating epigenetic events (Wang *et al.* 2013c). Epigenetics is defined as the study of heritable

changes in gene expression that do not involve changes to the DNA sequence; this commonly involves DNA methylation and modification to histones which has been reviewed in detail by Allis and Jenuwein (2016). Treatment with BRB-derived anthocyanins for three days at 0.5, 5, and 25 μg/ml suppressed DNA methyltransferase (DNMT) (an enzyme involved in methylating DNA) activity in three human CRC cell lines. Negative regulators of the Wnt signalling pathway (SFRP2/5 and WIF1) were reactivated presumably via demethylation of gene promoters. The group also found that anthocyanins induced apoptosis and caused cell cycle arrest in these CRC cell lines (Wang *et al.* 2013b).

In vivo studies have shown the chemopreventive effects of BRBs in rodent models of chemically induced CRC and oesophageal tumourigenesis (Harris *et al*. 2001; Kresty *et al.* 2001) however, they did not provide a mechanistic insight to how BRBs exert their preventative effects. In 2010, Bi and colleagues performed *in vivo* experiments in two murine models of human CRC to investigate whether BRBs would inhibit tumourigenesis and to determine a potential mechanism of action. The two mouse models used were *Apc*1638$^{+/-}$ which develop tumours as a result of only having one functional allele of *Apc* which leads to aberrant Wnt signalling (Fodde *et al.* 1994) and the *Muc2*$^{-/-}$ mouse which develop intestinal tumours in response to chronic inflammation (Velcich *et al.* 2002). A 12-week feeding of 10% freeze-dried BRBs in the diet significantly decreased tumour incidence and tumour multiplicity in *Apc*1638$^{+/-}$ mice by 45% and 60% respectively. Similarly in *Muc2*$^{-/-}$ mice, feeding of BRBs reduced tumour incidence and multiplicity by 50%. Levels of proliferation and differentiation were assessed and BRBs were found to inhibit proliferation in both animal models but had no effect on goblet cell differentiation. Mechanistic studies reported that BRBs elicited anti-tumour effects in *Apc*1638$^{+/-}$ mice through inhibiting Wnt/β-catenin signalling whereas in the *Muc2*$^{-/-}$ mouse BRBs down-regulated cytokines commonly associated with inflammation (Bi *et al.* 2010).

The hereditary disease FAP is characterised by an early onset of colonic polyposis and increased risk of developing CRC. A key phase Ib study was conducted to investigate whether BRBs were able to regress rectal polyps in FAP patients. Patients were divided into two groups. Group 1 received placebo powder slurry taken orally 3 times a day (60 g/day in total) and two BRB rectal suppositories at night (each containing 720 mg BRB powder), group 2 received a BRB powder slurry 3 times a day (60 g/day in total) plus two BRB rectal suppositories. Treatments were continued for 9 months. The study highlighted that BRB suppositories were sufficient to regress rectal polyps of FAP patients with no added benefit of oral BRB powder. Additionally, cellular proliferation and DNMT expression was decreased in adenomas from patients that responded to BRB treatment. These results suggested that BRBs may be a potential alternative treatment for FAP patients (Wang *et al.* 2014). These data are supported by another study that found oral administration of BRBs (60 g/day) for 4 weeks impacted epigenetic marks. Specifically, methylation of several genes involved in Wnt

signalling, proliferation, apoptosis and angiogenesis were reduced. This was associated with DNMT down-regulation (Wang *et al.* 2011) and further supported the protective effect of BRBs in a clinical setting.

Further evidence for the preventative roles of BRBs has been shown by Wang *et al.* who reported that a dextran sodium sulphate (DSS)-induced ulcerative colitis (UC) murine model fed a 5% BRB diet had reduced colonic ulceration, decreased activity of immune cells and promoter demethylation of tumour suppressor genes (Wang *et al.* 2013d). UC is characterised by chronic inflammation of the colon, which induces the release and accumulation of pro-inflammatory cytokines within the colon epithelium. This biological process is associated with an increase in DNMT activity and silencing of tumour suppressor genes and Wnt signalling antagonists alongside promoter methylation (Wang *et al.* 2013d), potentially leading to colorectal carcinogenesis. This data is supported by mouse models of UC which have the potential to progress to carcinogenesis (Wang *et al.* 2013c).

More recently the beneficial effects of BRBs have been attributed to metabolic changes in human CRC patients which may contribute towards an overall positive impact against CRC (Pan *et al.* 2015). In brief, urine and plasma samples were taken from CRC patients before and after BRB treatment. Patients consumed 60 g/day of BRB powder slurry for 1 - 9 weeks. Results indicated that metabolites associated with amino acid, energy, carbohydrate, lipid metabolism and xenobiotics were altered which could represent changes in the metabolic pathways utilised by tumours. The results varied between patients potentially as a result of different diets among patients, sample preparation and patient ethnicity. In addition, the level of apoptosis was increased after BRB treatment (Pan *et al.* 2015).

Current data suggests that BRBs could exert their effects at different stages of tumour development but the precise molecular mechanisms are unknown. Determining the molecular mechanism by which these dietary compounds employ their anti-tumourigenic properties, and how they modulate our epigenome will increase their relevance and efficacy as chemopreventative strategies. Previous studies have shown very promising results *in vitro* and *in vivo* in both animals and patients at different stages of colorectal tumourigenesis, however, they have not addressed a fundamental question, 'What effect do BRBs have on the intestinal stem cell and cancer stem cell populations in normal and malignant tissue?'

1.13 Aims and Objectives

There is strong supporting evidence indicating aberrant Wnt signalling is sufficient to initiate intestinal tumourigenesis. The link between intestinal carcinogenesis and the ISC population is very clear, as the ISCs have been identified as a "cell of origin" of CRC (Barker *et al.* 2008) and the early

stages of tumourigenesis are characterised by an expansion of the ISC compartment and a loss of differentiation following conditional homozygous loss of the *Apc* gene (Sansom *et al.* 2004). Diet plays a significant role in the aetiology of CRC, but there is a limited understanding of the chemopreventative mechanisms that underpin these associations. Previous research has indicated a protective role of the dietary polyphenols found in BRBs (Kresty *et al.* 2016b); however there is very little research on the effect of BRBs on a malignant ISC population.

Hypothesis: That BRB polyphenols will suppress Wnt-driven tumourigenesis through alteration of the Wnt signature modulating the intestinal stem cell compartment.

To begin to test this hypothesis, the action of dietary polyphenols on Wnt-driven tumourigenesis was examined *in vivo* and *ex vivo*, focusing on the ISC population at the initial stages of adenoma formation and on long-term intestinal tumourigenesis. Chapter 3 describes the application of dietary BRBs on normal intestinal homeostasis and in the short-term *Apc* floxed model using the *AhCre* $Apc^{fl/fl}$ and *VillinCreER*^{T2} $Apc^{fl/fl}$ mouse models. Chapter 4 describes the effect of BRB polyphenols in the intestinal crypt culture model, where individual *Apc* deficient cells form intestinal organoids *ex vivo* (Sato *et al.* 2009). Chapter 5 describes the effect of BRBs on long-term intestinal tumourigenesis using the *Lgr5CreER*^{T2} $Apc^{fl/fl}$ mouse model.

2 Materials and Methods

2.1 Experimental Animals

2.1.1 Animal Husbandry

2.1.1.1 Colony Maintenance

All animals were maintained on an outbred background and housed in a standard facility in accordance with institutional animal care guidelines and UK Home Office regulations. Animals were given access to RM3(E) Standard diet (Special Diets Service UK, expanded diet) and fresh water *ad libitum,* until the start of the experimental diets (discussed in 2.4).

2.1.1.2 Breeding

Mice of 6 weeks of age or older and of known genotype were bred in trios of one male and two females. At approximately 4 weeks of age, pups were weaned and housed according to sex. Ear biopsies were taken for identification and genotyping purposes (discussed in 2.3.2).

2.2 Genetic Mouse Models

The transgenic mouse models used within this project are outlined in Table 2.1. *AhCre*, *VillinCreER^{T2}* and *Lgr5CreER^{T2}* driven Cre recombinase transgenes were utilised to conditionally delete floxed *Apc* alleles in the crypt epithelium excluding Paneth cells, the entire intestinal epithelium and specifically in the ISCs, respectively. Expression of the Cre recombinase in the *AhCre* transgene was induced using beta-naphthoflavone (βNF). Expression of the Cre recombinase in the *VillinCreER^{T2}* and *Lgr5CreER^{T2}* transgenes were activated in the presence of tamoxifen.

Transgene	Transgene details
AhCre (Ireland *et al.* 2004)	Crypt epithelium (excluding Paneth cells), liver and skin cells
VillinCreER^{T2} (El Marjou *et al.* 2004)	Intestinal epithelial cells (including Paneth cells)
Lgr5CreER^{T2} (Barker *et al.* 2007)	Lgr5 positive intestinal stem cells
Apc$^{fl/fl}$ allele (Shibata *et al.* 1997)	Endogenous *Apc* allele bearing loxP sites flanking exon 14

Table 2.1 Outline of the transgenic mouse models utilised in this thesis

2.3 Experimental Procedures

All experiments involving animals were conducted according to the UK Home Office regulations under valid personal and project licenses and in accordance with the Animal [Scientific Procedures] Act 1986. Experimental procedures were carried out in designated procedure rooms.

2.3.1 Ear biopsy for identification and genotyping

To allow individual identification of animals', ear biopsies were taken using a 2mm ear punch (Harvard apparatus). DNA extracted from these biopsies was used for genotyping (see section 2.3.2).

2.3.2 Polymerase Chain Reaction (PCR) Genotyping

In order to genotype weaned mice, PCR was performed on genomic DNA (gDNA) extracted from ear biopsies. Genotyping was also performed at time of death to ensure each mouse was correctly assigned to the experimental cohorts. PCR was kindly performed by Matthew Zverev and Elaine Taylor.

2.3.2.1 DNA Extraction

Mouse ear biopsies were collected at weaning and temporarily stored at -20°C to prevent degradation. Each tissue sample was digested in 250 µl lysis buffer (VWR) containing 0.4 mg/ml proteinase K (Sigma), overnight (O/N) at 42°C with agitation. The protein was precipitated by the addition of 100 µl of protein precipitation solution (VWR). The solution was mixed by inversion and protein and insoluble debris was pelleted by centrifugation at 13000 rpm for 10 mins. The supernatant was added to a fresh eppendorf containing 250 µl of isopropanol (Thermo Fisher Scientific) to precipitate the DNA. The solution was mixed by inversion and centrifuged at 13000 rpm for 15 mins. The supernatant was discarded and the pellet was left to air dry for an hour before resuspending in 250 µl of Milli-Q water. For short-term storage gDNA was left at room temperature (RT) or stored at 4°C for longer-term storage.

2.3.2.2 PCR Protocol

PCR was carried out in 96 well semi skirted straight side pates (Alpha Labs). gDNA (3 µl) extracted from ear biopsies as described above, was added to each well. Then 47 µl of PCR mix (see Table 2.2) containing an appropriate DNA polymerase and buffer (Table 2.2) was added to each well. A control well was also made using the same PCR mix but with dH_20 instead of the DNA. The 96 well plates were then sealed with aluminium foil seals (Star Lab), and air bubbles were removed by tapping the plates on a hard surface. The reactions were run in a GS4 thermocycler (G storm). Reaction mixtures and cycling times for each PCR are outlined in Table 2.2. Primer sequences are shown in Table 2.3Table 2.3.

2.3.2.3 Visualisation of PCR Products

PCR products were visualised by gel electrophoresis using 2% agarose gels. The gels were made by dissolving agarose (Eurogentec) 2% [w/v] in 1X Tris Borate EDTA (TBE) buffer (National Diagnostic) and heated in a microwave until boiling. The solution was then cooled under a running tap

with agitation and 14 µl of Safe View fluorescent nucleic acid stain (NBS biological) was added per 400 ml. The gel solution was then poured into 2 clean moulds (Bio-Rad) and combs were added to create wells. Once set, the combs were carefully removed and the gels placed into an electrophoresis tank and covered with 1X TBE solution with Safe View (10 µl Safe View/100 ml 1X TBE). 5 µl of loading dye (50% Glycerol (Sigma), 50% dH_20, 0.1% bromophenol blue (Sigma)) was added to PCR product samples that utilised clear buffer and were gently mixed by pipetting. 20 µl of the PCR samples were added to individual wells of the agarose gel and run alongside a molecular weight marker. The gel was run at 120 V for approximately 30 mins or until the loading dye had run more than half way across the gel. The gel was then visualised for PCR products using a GelDoc UV Transilluminator (Bio-Rad) and images taken using the GelDoc software (Bio-Rad). PCR product sizes are outline in Table 2.3.

DNA extraction, PCR and visualisation of PCR products were repeated on all experimental mice following dissection to re-confirm the original PCR genotyping.

	AhCre	*VillinCreER* ^{T2}	*Lgr5CreER* ^{T2}	*Apc* -loxP
PCR mix				
DNA	3 µl	3 µl	3 µl	3 µl
Mili-Q water	31.7 µl	31.7 µl	31.7 µl	31.7 µl
Taq PCR buffer	10 µl	10 µl	10 µl	10 µl
Type of PCR buffer	Clear	Clear	Green	Green
5 mM $MgCl_2$	5 µl	5 µl	5 µl	5 µl
dNTPs	0.4 µl	0.4 µl	0.4 µl	0.4 µl
Primer 1 (100 mM)	0.1 µl	0.1 µl	0.1 µl	0.1 µl
Primer 2 (100 mM)	0.1 µl	0.1 µl	0.1 µl	0.1 µl
Taq DNA polymerase	0.2µl	0.2µl	0.2µl	0.2µl
Brand of Taq DNA polymer	GoTaq	GoTaq	Dream Taq	Dream Taq
PCR cycling conditions				
Initial denaturation	2.5 mins, 94°C	2.5 mins, 95°C	3 mins, 95°C	3 mins, 95°C
Cycle number	35	35	40	40
Step 1: denaturation	30 secs, 94°C	30 secs, 94°C	30 secs, 94°C	30 secs, 95°C
Step 2: annealing	1 min, 54°C	30 secs, 62°C	30 secs, 58°C	30 secs, 60°C
Step 3: extension	2 min, 72°C	1 min, 72°C	30 secs, 72°C	1 min, 72°C
Final extension	10 mins, 72°C	5 mins, 72°C	5 mins, 72°C	5 mins, 72°C
	Hold at 10°C	Hold at 10°C	Hold at 10°C	Hold at 10°C

Table 2.2 Genotyping PCR reaction conditions

Gene	Forward primer sequence (5'-3')	Reverse primer sequence (5'-3')	Product Size
AhCre	CCTGACTAGCATGGCGATAC	ATTGCCCCTGTTTCACTATC	1200 bp
VillinCreER^{T2}	CAAGCCTGGCTCGACGGCC	CGCGAACATCTTCAGGTTCT	220 bp
Lgr5CreER^{T2}	CTGCTCTCTGCTCCCAGTCT	Wildtype ATACCCCATCCCTTTTGAGC	WT = 298 bp, Mutant = 174 bp
		Mutant GAACTTCAGGGTCAGCTTGC	
Apc-loxP	GTTCTGTATCATGGAAAGATAGGTGGTC	CACTCAAAACGCTTTTGAGGGTTGATTC	WT = 266 bp, Targeted = 315 bp

Table 2.3 Outline of the primer sequences used for PCR and the product sizes

2.4 Experimental Cohorts

After the genotype of mice had been ascertained by PCR, mice of appropriate age were randomly placed into control and experimental cohorts. Where possible housing of single mice was avoided, in most cases animals were housed in cages with other mice. Mice were given fresh water and food *ad libitum* and were fed either the control or experimental diets discussed below, or in the absence of the control diet remained on the RM3(E) standard diet. After 2 weeks of feeding on their respective diets, Cre recombinase mediated recombination of the *Apc* allele was induced. Mice were monitored closely and short-term mice were sacrificed at days 4 and 5-post induction and long-term cohorts when they became symptomatic of an intestinal tumour phenotype (paling of feet/tail, piloerection, hunching of the body) or any other signs of loss of condition. Injections were performed using a 1 ml syringe (BD Plastipak) and 25 G needle (BD microlance).

2.4.1 Administration of Diet

2.4.1.1 Administration of 10% Black Raspberry Powder

Experimental *AhCre* mice were given access to 10% freeze-dried BRB powder supplemented in AIN76A powder *ad libitum* throughout the length of the experiment. Control mice were fed on the standard RM3(E) mouse diet. Mice were started on the BRB diet two weeks prior to induction. Administration of BRB powder was performed by Lucie Stocking and Kirsty Greenow.

2.4.1.2 Administration of AIN76A Diet

VillinCreER^{T2} and *Lgr5CreER^{T2}* mice in control cohorts were given access to the AIN76A purified rodent diet *ad libitum* throughout the length of the experiment. Control mice were started on the diet two weeks before induction. The diet was manufactured by Dyets Inc (diet formulation shown in Table 2.4).

2.4.1.3 Administration of 10% Black Raspberry Pellets

Experimental cohorts of *VillinCreER^{T2}* and *Lgr5CreER^{T2}* mice were given access to the modified AIN76A purified rodent diet with 10% w/w black raspberry powder *ad libitum* throughout the experiment (diet formulation shown in Table 2.5). Dyets Inc manufactured the diet. The black raspberry powder was purchased from Berrihealth, USA.

AIN76A Purified Rodent Diet DYET #100000	
Ingredient	**grams/kg**
Casein	200
Sucrose	500
Cornstarch	150
DL-Methionine	3
Cellulose	50
Corn Oil	50
Salt Mix #200000	35
Vitamin Mix # 300050	10
Choline Bitartrate	2
Journal of Nutrition v107, 1341(1977)	
Journal of Nutrition v110, 1726(1980)	

AIN76A Salt Mix DYET #200000	
Ingredient	**grams/kg**
Calcium Phosphate, dibasic	500
Sodium Chloride	74
Potassium Citrate.H2O	220
Potassium Sulfate	52
Magnesium Oxide	24
Manganous Carbonate	3.5
Ferric Citrate, U.S.P.	6
Zinc Carbonate	1.6
Cupric Carbonate	0.3
Potassium Iodate	0.01
Sodium Selenite	0.01
Chromium Potassium Sulfate.H2O	0.55
Sucrose	118.03
Journal of Nutrition v107, 1341(1977)	

AIN76A Vitamin Mixture DYET #300050	
Ingredient	**grams/kg**
Thiamin HCl	0.6
Riboflavin	0.6
Pyridoxine HCl	0.7
Niacin	3
Calcium Pantothenate	1.6
Folic Acid	0.2
Biotin	0.02
Vitamin B 12 (0.1%)	1
Vitamin A PalmitateU	0.8
Vitamin D3 (400,000 IU/g)	0.25
Vitamin E Acetate (500	10
Menadione Sodium	0.08
Sucrose, finely powdered	981.15
Journal of Nutrition 107, 1341(1977)	
Journal of Nutrition 110, 1726(1980)	

Table 2.4 Components of the purified rodent AIN76A control diet

Modified AIN76A Purified Rodent Diet with 10% w/w Black Raspberry Powder DYET #103649	
Ingredient	**grams/kg**
Casein	200
DL-Methionine	3
Sucrose	400
Cornstarch	150
Corn Oil	50
Cellulose	50
Mineral Mix #200000	35
Vitamin Mix # 300050	10
Choline Bitartrate	2
Black Raspberry Powder*	100
Journal of Nutrition v107, 1341(1977)	
Journal of Nutrition v110, 1726(1980)	
The Ohio State University, Bruce Casto, August 23, 2013	
*Black Raspberry Powder was supplied by Berrihealth, USA	

Table 2.5 Components of the modified AIN76A purified rodent diet with 10% w/w black raspberry powder

2.4.2 Induction of Cre-recombinase

2.4.2.1 Administration of beta-Napthoflavone

Cre recombinase from the *AhCre* transgene was induced by intraperitoneal injections (IP) of βNF (Sigma). Stocks of 10 mg/ml were produced by dissolving powdered βNF in corn oil (Sigma) by heating to 99°C in a water bath. When the βNF had completely dissolved, aliquots were frozen in small amber glass bottles at -20°C and defrosted when needed. Prior to induction, the βNF was defrosted and heated to 80°C in a water bath. Mice were administered with 3 x 80 mg/kg over 12 hrs by IP injection. Induction of *AhCre* recombinase was performed by Lucie Stocking and Kirsty Greenow.

2.4.2.2 Administration of tamoxifen

Induction of Cre recombinase activity in mice bearing the *VillinCreER^{T2}* and *Lgr5CreER^{T2}* transgenes was controlled by tamoxifen binding to a mutated ER^{T2} receptor fused to the Cre recombinase protein. Stocks of 10 mg/ml tamoxifen (Sigma) were produced by dissolving tamoxifen in corn oil in a water bath at 99°C. Samples were aliquoted and frozen at -20°C until required. Tamoxifen was defrosted by heating to 80°C in a water bath. *VillinCreER^{T2}* mice received 3 x 60 mg/kg tamoxifen over 12 hrs by IP injection. *Lgr5CreER^{T2}* mice were administered with 80 mg/kg tamoxifen via IP injection daily, for four consecutive days.

2.4.3 Labelling cells *in vivo* during S-phase by administration of 5-Bromo-2-deoxyuridine

To determine the rate of cell migration, animals were IP injected with 200 µl of 5-Bromo-2-deoxyuridine (BrdU, Thermo Fisher Scientific) either 2 or 24 hrs prior to sacrifice. BrdU, a thymidine analogue is bioavailable for 2 hrs and is incorporated in newly synthesised DNA strands during S-phase of the cell cycle.

2.5 Tissue Sample Preparation

In order to avoid degradation of RNA (Ribonucleic acid) and protein, all tissues were dissected immediately after animal sacrifice. Dissection and tissue harvesting of *AhCre* mice only was performed by Lucie Stocking and Kirsty Greenow.

2.5.1 Dissection of organs

Mice were culled by cervical dislocation. The abdomen was sprayed with 70% ethanol and the abdominal cavity was opened by cutting through the skin and smooth muscle wall. The intestines were dissected out first (see section 2.5.2). The heart, lungs, kidney, liver and spleen were dissected out and fixed as described in section 2.5.3. Part of the small and large intestines, kidney, liver and spleen were also frozen.

2.5.2 Dissection of Intestines

The stomach and intestines were carefully dissected out and the attached mesentery was removed. The stomach and caecum were removed and discarded. The small and large intestine were then flushed with water or 1X PBS (phosphate buffered saline; 1.44 g Sodium Phosphate Dibasic anhydride (Na_2HPO_4, Fluka), 8 g Sodium Chloride (NaCl, Sigma), 0.2 g Potassium Chloride (KCl, Fisher Scientific), 0.24 g Potassium Phosphate Monobasic (KH_2PO_4, Sigma), made up to 1 L in dH2O to pH 7.4) to remove the contents of the intestine and were then fixed as described in section 2.5.3. The small intestine was cut into several sections. The gut sections were either opened longitudinally and rolled into 'swiss roll-like' structures and secured with a needle or sectioned transversely. A section of small intestine was frozen (*AhCre* and *Lgr5CreER^{T2}*) or used for epithelial cell extraction using Weiser preparation (*VillinCreER^{T2}*) (described in 2.5.7). In addition, for some of the long-term cohorts, tumours were also dissected and frozen. The large intestine across all cohorts was also opened longitudinally and rolled into 'swiss roll-like' structures, and a small section was frozen for RNA extraction.

2.5.3 Formalin fixation of tissues

All tissues were fixed in ice cold 10% neutral buffered formalin (Sigma) for 24 hrs at 4°C. Samples were then stored in 70% ethanol (EtOH) in distilled H_2O (dH_2O) at 4°C until processing.

2.5.4 Processing of fixed tissue

After fixation, all tissues were placed in a cassette (Fisher) and processed using an automatic processor (Leica TP1050). The tissues were incubated in an increasing gradient of alcohols for dehydration (70% EtOH for 1 hr, 95% EtOH for 1 hr, 2 x 100% EtOH for 1 hr 30 mins and 100% EtOH for 2 hrs), then in xylene (2 x 2 hrs). The tissues were then placed in liquid paraffin for 1 hr and then twice more for 2 hrs. The samples were removed and embedded in paraffin wax by hand and allowed to harden.

2.5.5 Sectioning of fixed tissue

Tissues were then prepared for either H&E and cell type staining (described in sections 2.6.1, 2.6.2 and 2.6.3) or immunohistochemistry (IHC) (described in section 2.6.4). Paraffin embedded tissues were cut to 5 micron sections using a microtome (Leica RM2135) and placed on Poly-L-Lysine (PLL) coated slides and baked at 58°C for 24 hrs.

Paraffin embedding and sectioning was performed by Derek Scarborough.

2.5.6 Freezing tissue

Sections of the liver, kidney, spleen, small and large intestine were placed into individual lockable microtubes and placed on dry ice until frozen. The samples were then stored at -80°C until required. Where possible, intestinal tumour tissue and adjacent normal tissue from long-term cohorts was also frozen on dry ice.

2.5.7 Epithelial cell extraction using Weiser preparation

To avoid interference from stromal and smooth muscle compartments in subsequent RNA analysis, the intestinal epithelium was extracted from the small intestine of *VillinCreER*^{T2} cohorts. This was achieved by using a Weiser preparation. The second 10 cm of the small intestine closest to the pyloric junction was dissected out and flushed with ice cold 1X PBS (Gibco). The gut was then opened longitudinally and incubated in 15 ml of ice cold Wesier solution (recipe in Table 2.6) for 10 minutes with agitation. The supernatant was retained and kept on ice. The intestine was incubated in a further 15 ml of Wesier solution, this was repeated twice. The fractions were combined and centrifuged at 1500 rpm for 5 mins. The supernatant was discarded and the pellet was washed twice in 20 mls of ice cold 1X PBS. The pellet was then resuspended in 3 mls of PBS and aliquoted into three 1.5 ml eppendorfs, which were then centrifuged at 2000 rpm. The supernatant was discarded and the samples were stored at -80°C until required for RNA extraction (described in 2.9).

Weiser Solution for 1 Litre	
1M Na_2HPO_4 (Fluka)	5.56 ml
1M KH_2PO_4 (Sigma)	8 ml
5M NaCl (Sigma)	19.2 ml
1M KCl (Fisher Scientific)	1.5 ml
1M Na_3 Citrate (Fisher Scientific)	27 ml
Sucrose (Sigma)	15 g
D-sorbital (Sigma)	10 g
0.5M EGTA (Sigma)	8 ml
0.5M EDTA (Sigma)	12 ml
0.5mM DTT* (Sigma)	0.077 g

*DTT must be added fresh on the day of use

Table 2.6 Constituents of Weiser Solution for epithelial cell extraction

2.6 Histological Analysis

2.6.1 Preparation of sections for staining or IHC

Paraffin embedded tissue sections on PLL slides were dewaxed by placing in a bath of xylene for 2 x 5 min incubations to remove all the paraffin wax. The sections were then rehydrated through 2 min incubations down a decreasing gradient of EtOH baths; 2 x 100%, 1 x 95%, 1 x 70%). The slides were then placed in water in preparation for IHC staining.

2.6.2 Haematoxylin and Eosin (H&E) staining

Phenotypic analysis was possible by staining tissue sections with haematoxylin to stain the cell nuclei and eosin to mark the cytoplasm. Paraffin embedded tissue sections on PLL coated slides were dewaxed and rehydrated as previously described. The sections were then immersed in a bath of Mayer's Haemalum (R. A. Lamb) for 45 secs and then washed in running tap water for 5 mins. The sections were then counterstained in an aqueous solution of 1% Eosin (R. A. Lamb) for 5 mins before washing in running tap water to remove excess stain. The sections were then dehydrated, cleared and mounted as described in section 2.6.4.8.

2.6.3 Cell type specific stains

2.6.3.1 Alcian blue staining

Alcian blue stains the mucins present in the goblet cells. PLL sections were dewaxed and rehydrated as previously described, then immersed in a bath of alcian blue staining solutions (1% Alcian blue (Sigma), 3% Acetic acid (Fisher Scientific) in dH_2O at pH 2.5) for 5 mins then washed in

dH_2O for 5 mins. Slides were then counterstained in 0.1% nuclear fast red in 5% aluminium sulphate (Sigma) for 5 mins and washed in running tap water before dehydrating, clearing and mounting as described in section 2.6.4.8.

2.6.3.2 Grimelius silver staining

Grimelius silver staining was utilised to stain for argyrophilic granules in enteroendocrine cells. PLL tissue sections were dewaxed and dehydrated as previously described; all glassware was rinsed in ultrapure double distilled water (ddH_2O) (Sigma) to remove any reducing agents that were present. Solutions were freshly prepared following the recipe in Table 2.7. Slides were immersed in a preheated silver solution at 60°C for 3 hrs, then incubated in a reducing solution at 45°C for 1 min or until the tissue sections had a yellow background. Slides were then dehydrated, cleared and mounted as described in section 2.6.4.8.

Silver Solution	
Acetate Buffer pH 5.6	10 ml
ddH_2O	87 ml
1% Silver Nitrate (Fisher Scientific)	3 ml
Acetate Buffer pH 5.6	
0.2M Acetic Acid (Sigma)	4.8 ml
0.2M Sodium Acetate (Fisher Scientific)	45.2 ml
ddH_2O	50 ml
Reducer Solution	
Hydroquinone (Fluka)	1 g
Sodium Sulfite (Fisher Scientific)	5 g
ddH_2O	100 ml

Table 2.7 Constituents of the solutions required for Grimelius staining of enteroendocrine cells

2.6.4 Immunohistochemistry

IHC was performed for the visualisation of the presence and location of various proteins within the tissue sections. A generic protocol is described below; the specific conditions for each target are outlined in Table 2.8. PLL slides were dewaxed and rehydrated as previously described in section 2.6.1.

2.6.4.1 Antigen Retrieval

Antigens were unmasked by heating the tissue sections in 1X citrate buffer (2.94 g Sodium citrate tribasic dehydrate (Sigma) in 1 L dH_2O, pH 6) either in a boiling water bath, microwave or pressure cooker. For retrieval using the water bath method, adequate citrate buffer was preheated to

99.9°C in a glass coplin jar (R. A. Lamb) before the slides were immersed. Retrieval of antigens using the microwave was achieved by heating adequate buffer in a plastic container for 5 mins in a domestic microwave at 1000W. The slides were then immersed in the hot buffer using a plastic slide rack and further heated at full power (1000W) for 3 x 5 mins. For pressure cooker retrieval, adequate citrate buffer was heated in a pressure cooker without pressure in a domestic microwave for 5 mins at full power. Slides were then immersed in the solution in a plastic slide rack and heated under pressure until the yellow indicator rose. The microwave was then reduced to 300W and the solution heated for a further 15 mins. Special care was taken to ensure the slides did not boil dry and where necessary additional citrate buffer was added.

Following boiling, the slides were left to cool at RT (in citrate buffer) for 1 hr before washing in dH_2O or wash buffer. The wash buffers utilised were PBS or TBS/T (tris buffered saline/ 0.1% Tween, (NaCl 8.8 g, Tris-base 2.4 g in 1 L dH_2O (pH7.6), 1 ml Tween-20).

2.6.4.2 Blocking of endogenous peroxidises

Activity of endogenous peroxidases within tissue samples was blocked by treatment with hydrogen peroxide. Tissue sections were incubated in a 3% hydrogen peroxide solution in dH_20 (30% stock, Sigma) or in a commercial peroxidise blocking solution (Envision+ Kit, DAKO) at RT with agitation. The slides were then washed 3 x 5 mins in wash buffer at RT with agitation. Specific blocking and washing conditions can be found in Table 2.8.

2.6.4.3 Blocking of non-specific antibody binding

Non-specific binding of antibodies was blocked by incubating the tissue sections in a serum that is derived from a species that is different from the species that the primary antibody was raised in. A hydrophobic barrier pen (ImmEdge, Vector Labs) was utilised to draw an outline around the tissue sections. The serum was diluted to an appropriate concentration in wash buffer (see Table 2.8) and added to each slide and left to incubate at RT for 30 mins. Following the incubation period, the serum block was removed without washing the slides and the primary antibody was added.

2.6.4.4 Primary antibody incubation

The tissue sections were then incubated with a primary antibody diluted to a working concentration in blocking serum (see Table 2.8). The slides were incubated at either RT for 1 hr or O/N at 4°C, in a humidified slide chamber. To remove unbound residual primary antibody the slides were washed 3 x 5 mins in wash buffer at RT with agitation, before incubating with the secondary antibody.

2.6.4.5 Secondary antibody incubation

Secondary antibodies were either a biotinylated antibody diluted to a working concentration in blocking serum or a HRP-conjugated antibody from the Envision+ kit (DAKO). Secondary antibodies were applied to the slides, and incubated for an optimised amount of time at RT (see Table 2.8 for specific conditions). Slides were then washed 3 x 5 mins in wash buffer at RT with agitation.

2.6.4.6 Signal amplification

When a biotinylated secondary antibody was used, an additional signal amplification step was required. A Vectastain Avidin-Biotin Complex (ABC) kit (Vector labs) allows the binding of a HRP to the biotin of the secondary antibody. The ABC reagents were prepared according to the manufacturer's instructions, 30 mins prior to use and left at RT. The tissue sections were then incubated in the ABC reagent for 30 mins at RT in a humidified chamber before washing 3 x 5 mins in wash buffer.

2.6.4.7 Visualisation of antibody binding

Detection of the antigen was achieved by the 3,3'-diaminobenzidine (DAB) method for colourimetric detection producing a brown coloured stain. The sections were incubated at RT with DAB reagents (DAKO), prepared according to the manufacturers' instructions (1 drop DAB chromogen per 1ml DAB substrate buffer) for around 5 - 10 mins until a brown stain was observed. The sections were then washed in 2 x 5 mins in wash buffer and 1 x 5 mins in dH_20.

2.6.4.8 Counterstaining, dehydration and mounting of slides

Sections were counterstained with Mayer's Haemulum (R. A. Lamb) for 45 secs followed by thorough washing in running tap water for 5 mins.

The sections were then dehydrated by washing in increasing concentrations of alcohol baths (1 × 5 mins 70% EtOH, 1 × 5 mins 95% EtOH, 2 × 5 mins 100% EtOH). The slides were then cleared in 2 x 5 min incubations in xylene. The slides were then removed from the xylene, mounted in DPX mounting medium (Thermo Scientific) and appropriately sized coverslips were applied. The slides were left to air dry in a fume hood.

Primary Antibody	Manufacturer	Antigen Retrieval	Non-specific Signal Block	Wash Buffer	Primary Antibody Conditions	Secondary Antibody	Signal Aplification Step
Anti-BrdU	BD Biosciences #347580	20 mins, 99.9°C in water bath	**Peroxidase**: Envision + block (DAKO), 20 mins at RT. **Serum**: 1% BSA in PBS	PBS	1:150, O/N at 4°C	Envision+ HRP-conjugated anti-mouse (DAKO), 1 hr at RT	N/A
Anti-Ki67	Abcam #16667	30 mins, 99.9°C in water bath	**Peroxidase**: 0.5% H_2O_2, 20 mins, RT. **Serum**: 20% NGS in TBS/T, 20 mins, RT.	TBS/T	1:50, O/N at 4°C	Biotinylated goat anti-rabbit (DAKO) 1:200, 30 mins at RT	ABC Kit (Vetcor Labs)
Anti-Cleaved Caspase 3 (Asp175)	Cell Signalling #9661	10 mins at pressure using pressure cooker	**Peroxidase**: 3% H_2O_2, 10 mins at RT. **Serum**: 5% NGS in TBS/T, 1 hr at RT	TBS/T	1:200, 48 hrs at 4°C	Biotinylated goat anti-rabbit (DAKO) 1:200, 30 mins at RT	ABC Kit (Vetcor Labs)
Anti-Lysozyme	Thermo Scientific #RB-372-A1	4 x 5 mins in microwave	**Peroxidase**: 1.5% H_2O_2, 10 mins, RT. **Serum:** 10% NGS in TBS/T, 30 mins, RT	TBS/T	1:200, 1hr at RT	Envision+ HRP-conjugated anti-rabbit (DAKO), 1 hr at RT	N/A

Table 2.8 Outline of antibodies and conditions used for immunohistochemistry (IHC)

Key: RT - room temperature, BSA - bovine serum albumin, PBS - phosphate buffered saline, O/N - overnight, NGS - normal goat serum, TBS/T - tris buffered saline with 0.1%

2.7 Cell Counting

Quantification of histological sections was performed on an Olympus BX43 light microscope fitted with a Leica Mc170 HD camera and with the aid of Leica Application Suite (Version 4.6.1, Build 324) software, or Zeiss Axio Scan.Z1 slide scanner and ZEN image analysis software. Scoring was performed from areas that were not crosscut and free from other staining artifacts. For all comparisons, at least three biological replicates per cohort were analysed which allowed statistical analysis.

2.7.1 Crypt Size

Crypt size was scored by counting the total number of epithelial cells in a single line from the base to the top of the crypt. For the *AhCre* mouse model 25 whole crypts were scored, whereas 50 half crypts were scored from *VillinCreER*^{T2} mice.

2.7.2 Mitotic index

Mitotic cells were identified on H&E stained tissue sections based on their morphological appearance. The number of mitotic figures was scored per crypt from 25 whole crypts (*AhCre*) or 50 half crypts (*VillinCreER*^{T2}). The average (mean) number of mitoses per animal was calculated and then the mean across the cohorts was determined. Standard error of mean (SEM) was calculated by Graphpad Prism6 software. Significance of any differences was determined using Mann Whitney U statistical test (see section 2.11.1).

Ki67 and BrdU positively stained sections were scored as a proxy of proliferation. For both mouse models, Ki67 positive cells were counted from 25 whole crypts and analysed the same way as mitoses. The number of BrdU positive cells were scored from 50 half crypts from the base of the crypt to the villus tip, which enabled positional data to be collected to assess cell migration. The sum of BrdU positive cells at each cell position (position #1 = crypt base) was calculated per mouse. The average number of cells at each position was calculated per cohort and the cumulative frequencies were determined. Statistical differences were determined using Kolmogorov-Smirnov test (see section 2.11.2).

2.7.3 Apoptotic index

Apoptotic bodies were identified from H&E stained tissue sections based on their morphological appearance. Scoring was conducted in the same way as per the scoring of mitotic cells.

Caspase-3 stained sections were scored for apoptotic cells to confirm histological based scoring. The number of CC3 positive stained cells per crypt was counted from 25 whole crypts per

animal for both *AhCre* and *VillinCreER^{T2}* models. The mean values, SEM and significance were conducted as described in section 2.11.

2.7.4 Scoring of specific cell types

Numbers of enteroendocrine, goblet and Paneth cells were counted from grimelius silver, alcian blue and lysozyme stained tissue sections respectively. Goblet cells were counted from 25 whole crypts per section for both *AhCre* and *VillinCreER^{T2}* models, while enteroendocrine cells were scored from 50 half crypts for *AhCre* mice or 25 full crypts for *VillinCreER^{T2}* mice. Means, SEM and statistical differences were achieved as described in section 2.11. Paneth cells were scored from 50 half crypts per mouse for both models. Paneth cells were scored from the base of the crypt to the villus tip, which allowed positional data to be collected and analysed as per BrdU positivity (see section 2.7.2).

2.7.5 Counting in wildtype and aberrant crypts (*Apc$^{fl/fl}$* crypts)

Positive cells in wildtype crypts were counted from the base of the crypt up to the defined crypt-villus junction. *Apc$^{fl/fl}$* mice do not have defined crypt compartments, so the numbers of cells in the aberrant proliferative region were counted in a single line up to a visible crypt-villus junction.

2.8 *In situ* hybridisation

In situ hybridization was used on gut PLL sections in order to evaluate the location and expression of *Olfm4* mRNA. *In situ* hybridisation utilises digoxigenin (DIG) labelled anti-sense RNA probes complementary to the target mRNA sequence. Successful binding of the probe is visualised by the presence of a purple stain, produced by an enzyme substrate reaction. BM purple is a chromogenic substrate for the alkaline phosphatase enzyme on an anti-DIG alkaline phosphatase-conjugated antibody. Previously published probes for *Olfm4* were kindly provided by Han Clevers' group (van der Flier *et al.* 2009a) cloned into a pBluescript vector flanked by a promoter sequence for T3 and T7 RNA polymerase.

Due to probe sensitivity, all glassware used in this protocol was treated at 200°C O/N in a baking oven. All dH_2O was treated with diethylpyrocarbonate (DEPC, Sigma) and autoclaved.

2.8.1 Transformation of competent cells with cDNA vectors

For long-term use the probes were amplified by transfection into competent *Escherichia coli* (*E.coli*) cells. JM109 *E.coli* cells (50 µl, Promega) were incubated on ice for 30 mins with 1 µg plasmid DNA. The cells were then heat shocked at 42°C for 45 secs before placing back on ice for a further 2 mins. To the cells, 1 ml SOC medium (Invitrogen) was added and incubated in a shaking incubator at 37°C for 2 hrs. Agar plates containing ampicillin were made by dissolving four LB agar pellets (Q BioGene) in 500 ml dH_20 heated to 50°C and then autoclaved twice. When cool enough 500

µl of ampicillin (50 mg/ml) was added and poured in to petri dishes. To one agar plate 750 µl of the culture was added and 250 µl to another. The plates were incubated O/N at 37°C.

A single colony was selected from a plate using a sterile pipette tip and was streaked onto a fresh agar plate containing ampicillin. This plate was incubated O/N at 37°C. From this plate a further 4 colonies were isolated and cultured O/N at 37°C in 10 ml LB broth medium (10 capsules of LB broth (Fischer Scientific) dissolved in 500 ml dH_2O heated to 50°C and then autoclaved) containing ampicillin in a shaking incubator. Plasmid DNA was extracted from the culture using a Qiagen Mini-prep kit for an analytical digest (see section 2.8.2) or by using a Qiagen Midi-prep kit to enable large scale plasmid DNA extraction for probe synthesis (see section 2.8.3).

Plasmid stocks were produced by Madeleine Young.

2.8.2 Plasmid DNA extraction and probe linearisation

Analytical digests were performed on the plasmid containing the *Olfm4* probe using NotI and Sac1 restriction enzymes (New England Biolabs) following the restriction digest protocol outlined in Table 2.9. Extracted plasmid DNA was resuspended in 200 µl 10 mM Tris (pH 8) and quantified using a NanoDrop machine. The fragment size was analysed on a 4% agarose gel (approximate size 700 base pairs). Linearised plasmid DNA (200 µg) was isolated from a phenol/chloroform extraction by making the volume of plasmid DNA up to 500 ml with 10 mM Tris (pH 8) with an equal volume of phenol. The solution was then inverted for 5 mins at RT and then centrifuged at 13000 rpm for 10 mins. The upper aqueous phase was carefully added to a clean microtube and an equal volume of chloroform was added and inverted for a further 10 mins at RT. The mixture was then centrifuged at 13000 rpm for 10 mins. The aqueous phase was added to a clean microtube and DNA was precipitated by incubating at -20°C O/N in 0.1 volume of 3 M NaOAc (pH 5.2) and 2.5 volumes of 100% EtOH. The solution was then centrifuged at 13000 rpm for 20 mins at 4°C. The supernatant was discarded and the pellet was washed twice in 70% EtOH and allowed to air dry. The pellet was resuspended in 40 µl of 10 mM Tris (pH 8) and DNA was quantified using a NanoDrop machine. The linear DNA was then used as a template for probe transcription and labelling. These procedures were performed by Madeleine Young.

2.8.3 DIG labelling of probes

Linearised plasmid DNA (1 µg/µl) acted as a template for the transcription of DIG-labelled riboprobes using T3 and T7 RNA polymerases. The transcription labelling reaction were set as outlined in Table 2.11 and incubated for 2 hrs at 37°C. Then 2 µl of DNaseI (Ambion) was added and incubated for a further 15 mins at 37°C to digest the DNA template.

To precipitate out the DIG-labelled riboprobe, 2µl of 3 M NaOAc (pH 5.3) and 50 µl EtOH were added and incubated O/N at -20°C. This was then centrifuged at 15000 rpm for 20 mins at 4°C. The pellet was then washed twice in 70% EtOH and air dried before resuspending in 100 µl DEPC H_2O. The probes were aliquoted and stored at -80°C until needed.

2.8.4 Probe hybridisation

PLL sections were dewaxed (2 x 10 mins xylene) and rehydrated (2 x 1 min 100% EtOH, 30 secs in 95%, 85%, 70%, 50% and 30% EtOH). The slides were then transferred to 1X saline for 5 mins then washed in 1X PBS in DEPC H_2O for 5 mins. Endogenous alkaline phosphatase activity was blocked by incubating the slides in 250 ml of 6% hydrogen peroxide (diluted from 30% stock, Sigma, in 10X PBS in DEPC H_2O) for 30 mins. The slides were then washed 2 x 5 mins in PBS. The slides were then refixed in RNase free 4% paraformaldehyde (Sigma) for 20 mins on ice and then washed 2 x 5 mins in PBS. The sections were then incubated in proteinase K for 5 mins (20 mg/ml proteinase K in 1 M Tris (pH 8), 0.5 M EDTA (pH 8) in DEPC H_2O), washed 2 x 5 mins PBS and post-fixed in 4% paraformaldehyde for 5 mins to prevent the tissue from disintegrating. The slides were then washed for 2 mins in DEPC H_2O. Then the slides were incubated in acetic anhydride solution (2 M Acetic anhydride in 0.1 M triethanolamine hydrochloride) for 10 mins with agitation and washed 2 x 5 mins PBS and once in 1X saline. The slides were then dehydrated in increasing EtOH baths (30% EtOH for 30 secs, 70% EtOH for 5 mins, 30 secs in 85% and 95% EtOH, 2 x 30 secs in 100% EtOH) and allowed to air dry for 30 - 60 mins ready for probing. The *Olfm4* probe was diluted 1:100 in hybridisation buffer (5X saline sodium citrate buffer (SSC, Sigma), 50% formamide (Sigma), 5% Sodium dodecyl sulphate (SDS), 1 mg/ml heparin, 1 mg/ml calf liver tRNA) and heated to 80°C for 3 mins. The slides were placed in dark moisture chambers (containing 2.5 ml 20X SSC pH 7 (Sigma), 5 ml formamide and 2.5 ml DEPC H_2O) and incubated with 100 µl of the probe O/N at 65°C. Cover slips and parafilm were placed on top of each slide to prevent dehydration.

2.8.5 Post-hybridisation treatment

Following probe hybridisation, the slides were washed once in pre-warmed 200 ml of 5X SSC (pH 5) at 65°C for 15 mins. Then the slides were incubated twice in pre-warmed solution I (Table 2.10) at 65°C for 30 mins and 3 x 10 mins washes at RT in solution II (Table 2.10). The slides were then incubated at 37°C for 45 mins in solution II with 4 µl of 10 mg/ml RNase H. Following this the slides were washed once more in solution II at RT for 5 mins and then incubated 2 times in solution III (Table 2.10) for 30 mins at 65°C. The slides were then washed 2 x 10 mins in PBS/T at RT and then preblocked in 100 µl of 10% sheep serum in PBS/T in a dark, moist chamber at RT for 2 - 3 hrs. The anti-DIG alkaline phosphatase conjugated antibody (Roche) was prepared by heating in 1% heat-inactivated sheep

serum in PBS/T containing 3 mg/ml mouse intestinal powder at 70°C for 30 mins. 100 µl of prepared antibody was added to each slide and incubated O/N at 4°C in a dark, moist chamber.

2.8.6 Signal detection

The sections were washed 3 x 5 mins in PBS/T and then a further 3 x 30 mins in PBS/T. The slides were then preconditioned to inhibit endogenous alkaline phosphatase activity by washing 3 x 5 mins in NTMT buffer (10 ml of 5 M NaCl, 50 ml of 1 M Tris HCl (pH 9.5), 25 ml of 1 M $MgCl_2$, 0.5 ml of 0.1% Tween-20 and 0.5ml of 2 M Levamisole (Sigma) made up to 500 ml with DEPC H_2O) at RT. A hydrophobic barrier was drawn around the tissue and 1 ml of the substrate, BM purple, was added to each slide and incubated in the dark at 4°C for 24 - 72 hrs until a strong colour developed. Once a sufficient colour was present the slides were then washed in PBS/T for 10 mins and then H_2O for 30 mins. The sections were then counterstained with eosin (Sigma) and excess stain removed by washing in running H_2O. The slides were then dipped in xylene to clear and then allowed to air dry before mounting in DPX medium.

Restriction Digest	
RNase free H_20	to 200 µl
Plasmid DNA	30 µg
Restriction Enzyme	10 µl
Buffer (10X, NEB)	20 µl
BSA (1X, NEB)	1 µl

Table 2.9 Constituents required to perform a restriction digest on plasmid DNA

DIG RNA labelling mix	
Transcription buffer (10X, Roche)	1 µl
DIG RNA labellimg mix (10 mM, Roche)	2 µl
RNA polymerase (Roche)	2 µl
Rnase inhibitor (Promega)	1 µl
DEPC H_20	12 µl
Linearised plasmid DNA (1 µg/µl)	1 µl

Table 2.11 Constituents of the DIG-labelling mix to produce a DIG-labelled riboprobe

Post-hybridisation solutions	
Solution I	
Formamide (Sigma)	200 ml
20X SSC (pH 5, Sigma)	100 ml
10% SDS (Sigma)	40 ml
DEPC H_20	60 ml
Solution II	
5 M NaCl	100 ml
1 M Tris HCl (pH 7.5)	10 ml
Tween 20 (Sigma)	1 ml
DEPC H_20	to 1000 ml
Solution III	
Formamide (Sigma)	200 ml
20X SSC (pH 5, Sigma)	40 ml
DEPC H_20	160 ml

Table 2.10 Constituents for the solutions required for post hybridisation treatment riboprobe

2.9 Quantitative Reverse Transcription Polymerase Chain Reaction (qRT-PCR) RNA isolation

qRT-PCR was used to evaluate the relative expression levels of genes in small intestinal tissue. RNA was extracted using Trizol, from frozen intestinal sections or epithelial cell extracts isolated by a Weiser preparation (discussed in section 2.5.7). Extracted RNA was used as a template for cDNA (complementary DNA) synthesis. Care was taken during RNA isolation to ensure all consumables and equipment used was RNase-free. Bench tops and pipettes were treated with RNaseZAP (Sigma). A minimum of 3 mice per experimental cohort were assessed for gene expression changes.

2.9.1 Tissue homogenisation

Intestinal tissue or epithelial cell extracts were removed from storage and placed on dry ice to prevent defrosting. The tissues were placed in 1ml Trizol (Ambion) in homogenising lysing matrix D tubes (MP Biomedicals). Whole tissues were homogenised using a Precellys 24 homogeniser (Bertin Technologies) at 6000 rpm for 2 cycles of 45 secs, epithelial cell extracts were only homogenised for 15 secs.

2.9.2 RNA extraction and purification

All samples were kept on ice during RNA isolation to prevent tissue degradation. Following homogenisation, the samples were left to settle on ice to disperse bubbles. The samples were then centrifuged at 13000 rpm for 10 mins at RT to pellet insoluble material. Subsequently the supernatant was transferred to RNase/DNase free 1.5 ml microcentrifuge tubes and 200 µl of chilled chloroform (Sigma) was added. Each sample was shaken vigorously prior to incubation on ice for 15 mins. The samples were then centrifuged at 13000 rpm for 15 mins at 4°C, separating the aqueous phase from the organic phase. The aqueous upper phase was transferred to clean microcentrifuge tubes containing 500 µl of isopropanol (Fischer Scientific). Care was taken to ensure none of the organic phase was retained. The samples were then mixed and left to incubate O/N at 4°C to precipitate out the RNA. After incubation, the samples were centrifuged at 13000 rpm for 15 mins at RT. The supernatant was discarded and the pellet was washed with 500 µl chilled 70% EtOH, and then centrifuged at 13000 rpm for 5 mins at RT. The supernatant was discarded and the pellet allowed to air dry for 10 mins. The pellets were resuspended in 50 µl of RNase free H_2O by heating to 65°C for 10 mins. The RNA was quantified using a NanoDrop 2000 (Thermo Scientific).

2.9.3 DNase treatment

Contaminating DNA from purified RNA samples was removed by using a TURBO DNA-*free*™ kit (Ambion). To each sample 0.1 volume 10X TURBO DNase buffer and 1 µl TURBO DNase was added,

mixed gently and incubated at 37°C for 30 mins. 0.1 volume of DNase inactivation reagent was added to the RNA samples and incubated for 5 mins at RT with mixing. All samples were centrifuged at 13000 rpm for 1.5 mins and the supernatant was transferred to clean 1.5 ml microcentrifuge tubes. The RNA was quantified using a 1 µl sample on the NanoDrop 2000 (Thermo Scientific).

2.9.4 cDNA Synthesis

The DNA free RNA was utilised as a template for cDNA synthesis using Superscript III reverse transcriptase (Invitrogen). In thin-walled 12 well strip tubes (Grenier, Bio-One), 4 µg of RNA was added with the constituents of the cDNA mix (see Table 2.12) and heated to 65°C for 5 mins. The samples were quenched on ice for 1 min. To each sample, 11 µl of reverse transcription enzyme mix (see Table 2.12) was added and collected by brief centrifugation. Controls were also prepared in exactly the same way but using water instead of cDNA. The samples were incubated in a PTC-100 thermocycler (MJ Research) at 25°C for 5 mins, 50°C for 1 hr and 70°C for 15 mins. cDNA samples were stored at -20°C until needed.

2.9.5 Gene expression analysis

All qRT-PCR reactions were run on the QunatoStudio7 Flex real-time PCR system (Applied Biosystems). Each reaction was carried out in duplicate or triplicate with a minimum of 3 biological replicates and a control well containing no cDNA. The housekeeping gene *β-actin* (*Actb*) was run alongside the experiment to normalise the expression levels of target genes. The data was collected using StepOne software (Applied Biosystems).

2.9.5.1 Sybr Green gene expression analysis

Equal volumes (10 µl) of forward and reverse primers were diluted in dH_2O to produce a primer mix (10 mM final concentration per reaction). The primer sequences can be found in Table 2.13. Once the cDNA had defrosted on ice, 1 µl of each cDNA sample was loaded per well into thin-walled 96 well or 384 well PCR plates (Applied Biosystems). To each well, 9.5 µl of master mix was added (5 µl SYBR green fast master mix (Applied Biosystems), 0.5 µl primer mix and 4 µl dH_2O). The plate was sealed with MicroAmp optically clear sealing film lids (Applied Biosystems) and briefly centrifuged to collect the contents. The qRT-PCR was run using the following cycling conditions: 95°C for 20 secs, followed by 40 cycles of 95°C for 1 sec, 60°C for 20 secs.

2.9.5.2 TaqMan gene expression analysis

For some genes of interest a TaqMan assay was used. To each well 1 µl of cDNA was loaded per well into thin-walled 96 well or 384 well PCR plates. Then 9.5 µl of master mix was added per sample (5 µl TaqMan universal master mix II (Applied Biosystems), 0.5 µl of a pre-designed TaqMan

probe and 4 µl dH_2O). Taqman probe details are found in Table 2.13. The plate was then sealed with MicroAmp optically clear sealing film lids and briefly centrifuged to collect the contents. The qRT-PCR was run using the following cycling conditions: 50°C for 2 mins, 95°C for 10 mins, followed by 40 cycles of 95°C for 15 secs, 60°C for 1 min.

2.9.5.3 Analysis of qRT-PCR data

StepOne Software (Applied Biosystems) automatically collected data from all qRT-PCR reactions. Samples with reproducible cycle time (CT) values were analysed manually to produce an average CT for the gene of interest, which was subsequently normalised to the housekeeping gene *β-actin*, this produced a ΔCT value. The ΔΔCT value was then calculated for each biological sample by normalising to the average ΔCT of the control cohort (in this instance $Apc^{+/+}$ mice on control diet). This was achieved by subtracting the individual biological sample ΔCT from the average ΔCT of the control cohort. From the ΔΔCT values the fold change in gene expression was calculated using the equation, fold change = $2^{\Delta\Delta CT}$. The fold change per cohort in relation to the $Apc^{+/+}$ control group was graphically represented with the SEM using GraphPad Prism6. Statistical differences between cohorts were determined using a Mann Whitney U test.

cDNA Mix (per reaction)	
DNase free RNA	4 µg
dH_2O	Made up to 23 µl
dNTPs (10 mM, Promega)	2 µl
Random Primers (500 µg/ml, Promega)	1 µl
Reverse Transcription Enzyme Mixture (per reaction)	
5x First Strand Buffer (Invitrogen)	8 µl
MDTT (Invitrogen)	2 µl
SuperScriptt III (Invitrogen)	1 µl

Table 2.12 Recipe for cDNA synthesis

SYBR green	Forward Primer 5' - 3'	Reverse Primer 5' - 3'
Lysozyme1	TTCTGAAAAGGAATGGAATGG	TTTGTAGCTCGTGTGTTATAATTGC
Muc2	TCGCCCAAGTCGACACTCA	GCAAATAGCCATAGTACAGTTACACAGC
Synaptophysin	TTCGTGAAGGTGCTGCAGTG	TCTCCGGTGTAGCTGCCG
Bmi1	AAGCTTGTCTATTGAGTTCTTTGA	TCTCAAGTGCATCACAGTCATT
Lrig1	TTCCTCACCGGTGAGACTGG	CCATCACTGTGCCAACACTT
Rnf43	TCCACCTCATTCGCCAGC	GAAGGCCCCAACAGATAGGC
Tnfrsf19	CGCTGGTGAACCGCTTTC	CAGGCAGTCCCCGCAG
Msi1	CCTGGTTACACCTACCAGTTCC	AGAGCCTGTCCCTCGAACTAC
CD133	ATCGGGGAAACGAAGAAGTT	ACAGCCGGAAGTAACAGCAC
CyclinD1	ACGATTTCATCGAACACTTCCT	GGTCACACTTGATGACTCTGGA
Axin2	GCAGCTCAGCAAAAAGGGAAAT	TACATGGGGAGCACTGTCTCGT
c-Myc	CTAGTGCTGCATGAGGAGACAC	GTAGTTGTGCTGGTGAGTGGAG
EphB2	AAACCCTGATGGACTCTACGAC	TTGTTCTGGCTTGACTCAAAGA
EphB3	TAACGCTGTGGAGGTCTCTGTA	CCTTGCTTTGCTTTGTAACTCC
Tcf7	CAGCTCCCCCATACTGTGAG	TGCTGTCTATATCCGCAGGAA
Mif1	GGTTCCACCTTCGCTTGAGT	ACAGAACACTACGTGGAGCG
Sox9	CAGCAAGACTCTGGGCAAG	TCCACGAAGGGTCTCTTCTC
Sox17	GATGAACGCCTTTATGGTGTG	TACTTGTAGTTGGGGTGGTCCT
Tiam1	CTTTCTGAAGTCTGTGCATTCG	AATCGATGGTAAACCTGTTTCG
Wif1	AACAAGTGCCAGTGTCGAGAGG	GCCTTTTTAAGTGAAGGCGTGTG
CD44	ATCGCGGTCAATAGTAGGAGAA	AAATGCACCATTTCCTGAGACT
ß-actin	TGTTACCAACTGGGACGACA	GGGGTGTTGAAGGTCTCAAA
Taqman	**Assay ID**	**Supplier**
Lgr5	Mm00438890_m1	Applied Biosystems
Olfm4	Mm01320260_m1	Applied Biosystems
Ascl2	Mm01268891_g1	Applied Biosystems
ß-actin	4352933E	Applied Biosystems

Table 2.13 Outline of primer details used for qRT-PCR analysis by SYBR green and Taqman assays

2.10 Intestinal organoid culture

Intestinal organoid culture was utilised to access the functional output of malignant ISCs. The intestinal organoids culture method described below has been adapted, to increase efficiency, from the original method outlined by Sato *et al.* (2009).

2.10.1 Extraction of intestinal *Apc*$^{fl/fl}$ crypts

The first 20 cm of small intestine from *VillinCreER*^{T2} *Apc*$^{fl/fl}$ mice was dissected out and flushed with 25 ml of cold HBSS (Gibco) containing 1X penicillin/streptomycin (Gibco) and 50 µl of 250 µg/ml

fungizone (Invitrogen). The intestine was then opened longitudinally and firmly scraped with a glass coverslip in order to remove the villi compartment. The scraped intestine was then cut into 0.5 mm pieces and placed in 25 ml cold HBSS containing 1X penicillin/streptomycin and 50 µl of fungizone. The solution was gently shaken before being transferred into a primary tissue culture hood where subsequent steps were performed under sterile conditions. The antibiotic containing solution was removed and the intestinal pieces were washed four times in HBSS, with gentle shaking between each wash. The intestine was then incubated for 5 mins at RT with 10 ml of 8 mM EDTA (Fluka) in HBSS. The solution was shaken vigorously to remove more of the villi and then the supernatant was discarded. The intestine was incubated for a further 30 mins in 10 ml of 8 mM EDTA but on ice. Again, the solution was shaken vigorously, but the supernatant fraction was removed and retained as this contained crypts. This fraction was immediately diluted 1:1 in DMEM/F12 (Gibco) containing 1X glutamax (Gibco). 10 ml HBSS was added to the intestine, shaken vigorously and the supernatant added to the first fraction. This was repeated once more. The combined fractions containing crypts were centrifuged at 600 rpm for 5 mins to remove any single cells. The pellet was then resuspended in 10 ml HBSS and centrifuged at 800 rpm for 3 mins. The pellet was then resuspended in 10 ml DMEM/F12 and passed through a 70 µm cell strainer (Falcon) to remove any clumps. The crypt suspension was kept on ice.

2.10.2 Counting and seeding crypts

The number of crypts was counted from three 10 µl crypt suspension aliquots using a Olympus CKX41 brightfield microscope with an Olympus SC100 camera. The appropriate volume of crypt suspension required to seed 200 crypts per well was calculated. This volume was aliquoted into an appropriate tube and centrifuged at 1000 rpm for 3 mins. The supernatant was removed and 20 µl of DMEM/F12 was added to resuspend the crypts prior to further dilution in the appropriate volume of matrigel (Phenol-free, growth factor reduced matrigel, VWR) and seeded into pre-warmed Nunclon U-bottom plates (Thermo Scientific). In 24 well plates 50 µl of matrigel/crypt suspension was seeded, and 96 well plates were seeded with 10 µl of matrigel/crypt suspension.

2.10.3 Organoid growth media

The organoid growth media was made up as in Table 2.14 and 100 µl was added to each well of a 96 well plate and 500 µl was added to each well of a 24 well plate, once the matrigel had set. The plates were returned to the incubator immediately. The media was changed every 2 - 4 days.

Organoid Culture Medium	Volume	Supplier
Stock Media		
DMEM/F12	469 ml	Gibco
Glutamax (100X)	5 ml	Gibco
Hepes Buffer (1 M)	5 ml	Gibco
Penicillin/Streptomycin (100X)	5 ml	Gibco
N2 Supplement (100X)	5ml	Gibco
B27 Supplement (50X)	10 ml	Gibco
Fungizone (250 µg/ml)	1ml	Gibco
Then filter sterilise and aliquot		
Working Media		
Stock Media	25 ml	
Gentamycin (50 mg/ml)	25 µl	Sigma
Human recombinant EGF (5 µg/ml)	25 µl	Sigma
Human recombinant Noggin (10 µg/ml)	200 µl	PeproTech
Then filter sterilse and add to wells		

Table 2.14 Recipe for organoid culture medium for *Apc*$^{fl/fl}$ organoids including all growth factors

2.10.4 Passaging organoids to single cells

Each well of a 96 well plate was scraped with a 1 ml pipette tip to disrupt the matrigel on the bottom of the plate. The media-matrigel-organoid solution was collected and 100 µl 1X PBS (Gibco) was added to wash the well and collect any leftover organoid material. The organoid solution was centrifuged at 12000 rpm for 5 mins at 14°C. The supernatant was removed and 300 µl of TrypLE (Gibco) was added and incubated for 10 mins at 37°C. Once fully incubated, 300 µl of foetal bovine serum (Sera Laboratories International Ltd) was added and the solution was manually triturated to dissociate the organoids to single cells. Advanced DMEM/F12 (15 ml, Gibco) was added to the solution and then strained through a 40 µm cell strainer (Falcon). The single cell suspension was then centrifuged at 1200 rpm for 5 mins and all but 1 ml of the supernatant was discarded. The cell pellet was gently resuspended in the remaining 1 ml of media and equal volumes (10 µl) of cell suspension were mixed with Trypan blue (colours dead cells blue, Gibco). Viable cells (10 µl) were counted using a haemocytometer and the appropriate volume of cell suspension to seed 8000 cells per well was calculated. The volume was aliquoted and centrifuged at 1200 rpm for 5 mins. The supernatant was removed and 20 µl of advanced DMEM/F12 was added to resuspend the single cells prior to further dilution in the appropriate volume of matrigel. The single-cell matrigel solution was seeded into pre-warmed 96 well Nunclon U-bottom plates with 10 µl per well. Once the matrigel was set, 100 µl of

media (as described in section 2.10.3) was applied to each well. For the first 3 days, the ROCK inhibitor Y27632 (Sigma) was added to each well at a concentration of 10 µl/ml of media. After 3 days the media was changed to the standard *Apc$^{fl/fl}$* media.

2.10.5 Organoid formation efficiency assay

2.10.5.1 A readout of 'stemness'

Intestinal crypts were harvested from *VillinCreER^{T2} Apc$^{fl/fl}$* mice fed for 2 weeks on either the AIN76A diet or 10% freeze-dried BRB diet 3 days after induction with tamoxifen. A minimum of 20 wells of a 96 well plate were seeded at 200 crypts/well in 10 µl matrigel per well. Media was added to each well and changed every 2 days. The plates were read at day 1 and day 7 using the Gelcount (Oxford Optronix) machine and analysed to produce a readout for the proportion of seeded crypts that grew into organoids.

2.10.5.2 Ex vivo application of BRB-derived Anthocyanin extract

To access the efficiency of *Apc* deficient cells to form organoids in the continual presence of BRBs, a BRB-derived anthocyanin extract was utilised. The extract was kindly provided to us by our collaborators, Li-Shu Wang's group from the Medical College of Wisconsin, USA. The anthocyanins were extracted from whole BRBs; the extraction method has been extensively described by Wang *et al.* (2009). The BRB-derived anthoycanin syrup was provided at a concentration 160.4 µM/g and kept at -20°C until required.

2.10.5.3 CellTiter-Glo® Luminescent Cell Viability Assay

To determine an appropriate concentration of AC extract to use in subsequent organoid experiments, a CellTiter-Glo® 3D luminescent cell viability assay was performed. *Apc$^{fl/fl}$* organoids were passaged to single cell as described in section 2.10.4 and reseeded in matrigel at 8000 cells/well in Corning® white 96 well plates with clear flat bottoms. A minimum of 3 wells were used per AC dose.

100 µl of intestinal organoid media containing 10 µl/ml of ROCK inhibitor was added to each well for the first 3 days. On day 4 post seeding, 100 µl of different concentrations of AC extract in organoid media, without ROCK inhibitor (described in detail in section 2.10.5.4) were added to the wells for 4 days.

CellTiter-Glo® 3D reagent was left to defrost at RT for 30 mins before use. The organoid plate was also left at RT for 30 mins. The AC media was removed from the wells and placed into wells of a new 96 well plate. 50 µl of media was replaced into the respective well and 50 µl of CellTiter-Glo® reagent was added to each well. The plate lid was returned and then wrapped in tin foil. The plate was incubated with CellTiter-Glo® reagent for 30 mins in a shaking incubator at 200 rpm. Following

incubation, luminescence was read on the CLARIOstar plate reader (BMG Labteck). An IC_{50} from the CellTiter-Glo® Luminescent assay was determined using the software, XLFit add-on for Microsoft Excel.

2.10.5.4 Preparation of BRB-derived Anthocyanin (AC) extract

For the initial CellTiter-Glo® Luminescent Cell Viability assay, the maximum concentration of AC extract utilised was 500 µg/ml, however this did not produce a complete graph. Therefore the experiment was repeated with higher concentrations of AC media, maximum concentration was 16000 µg/ml.

The anthocyanin solution (160.4 µM/g) was diluted in filter-sterilised dH_2O to produce a concentration of 500 mg/ml (0.1 g in 200 µl dH_2O) or 1000 mg/ml (0.05 g in 50 µl dH_2O). The AC solutions were then diluted 1:10 in filter sterilised dH_2O to 50 mg/ml or 100 mg/ml and were then filter sterilised using a 10 ml syringe (BD Plastipak) and 0.22 µm filter unit (Millipore). Serial dilutions from each stock were produced as outlined in Table 2.15. To achieve final concentrations ranging between 0 - 500 µg/ml and 0 - 16000 µg/ml, each dilution was then mixed with appropriate volumes of organoid media see Table 2.15.

2.10.5.5 A readout of the effects of ex vivo application of BRBs on organoid forming efficiency

Intestines from *VillinCreER^{T2} Apc$^{fl/fl}$* mice were harvested and crypts were isolated as described in section 2.10.1. Wells were seeded at 200 crypts/ well in 10 µl matrigel in 96 well plates. Fresh media containing AC extracts spanning serial concentrations between 0 – 500 µg/ml were added to 4 wells per mouse (100 µl), and changed twice a week. The AC plates were read at day 1 and day 7 and the data analysed for the proportion of seeded crypts that grew into organoids and for the organoid size. Four biological replicates were used. Mann Whitney U tests were used to determine statistical significance.

2.10.5.6 A readout of the effects of ex vivo application of BRBs on the self-renewal efficiency of Apc deficient cells to form organoids

To determine the effect of *ex vivo* application of BRB-derived ACs on the self-renewal ability of *Apc$^{fl/fl}$* cells, organoids at day 7 after treatment with the respective doses of AC (0 – 500 µg/ml) from section 2.10.5.5, were passaged to single cells. The cells were then reseeded in matrigel at 8000 cells per well and fresh AC media was applied at the same concentration previously exposed to. The media was changed twice in a week. A plate read was taken at day 7 and analysed using the Gelcount software to evaluate the proportion of organoids that formed from single cells and the average organoid size. Statistical significance was determined using Mann Whitney U test.

To make a final 500 µg/ml solution	
500 mg/ml solution was made	
0.1 g of AC extract was dissolved in 200 µl of dH2O	
Then 1:10 dilution in dH_2O to get 50 mg/ml, then filter sterilised	
Serial dilutions were performed in dH_2O to produce AC concentrations of:	
Concentration	**Volume**
25 mg/ml	50 µl of 50 mg/ml stock in 50 µl of dH_2O
12.5 mg/ml	50 µl of 25 mg/ml stock in 50 µl of dH_2O
6.25 mg/ml	50 µl of 12.5 mg/ml stock in 50 µl of dH_2O
3.12 mg/ml	etc…
1.56 mg/ml	
0.78 mg/ml	
0.39 mg/ml	
0.159 mg/ml	
0.098 mg/ml	
0.048 mg/ml	
0 mg/ml	
1:100 dilution of each concentration in organoid media	
Final concentration	**Volume**
500 µg/ml	4 µl of 50 mg/ml stock in 396 µl media
250 µg/ml	4 µl of 25 mg/ml stock in 396 µl media
62.5 µg/ml	4 µl of 6.25 mg/ml stock in 396 µl media
31.25 µg/ml	4 µl of 3.12 mg/ml stock in 396 µl media
15.62 µg/ml	4 µl of 1.56 mg/ml stock in 396 µl media
7.81 µg/ml	4 µl of 0.78 mg/ml stock in 396 µl media
3.9 µg/ml	4 µl of 0.39 mg/ml stock in 396 µl media
1.95 µg/ml	4 µl of 0.159 mg/ml stock in 396 µl media
0.97 µg/ml	4 µl of 0.098 mg/ml stock in 396 µl media
0.48 µg/ml	4 µl of 0.048 mg/ml stock in 396 µl media
0 µg/ml	4 µl of dH_2O in 396 µl media

To make a final 16000 µg/ml solution	
1000 mg/ml solution was made	
0.05 g of AC extract was dissolved in 50 µl dH_2O	
1:10 dilution in dH_2O to get 100 mg/ml, then filter sterilised	
Serial dilutions were performed in dH_2O to produce AC concentrations of:	
Concentration	**Volume**
50 mg/ml	50 µl of 100 mg/ml stock in 50 µl of dH_2O
25 mg/ml	51 µl of 50 mg/ml stock in 50 µl of dH_2O
12.5 mg/ml	52 µl of 25 mg/ml stock in 50 µl of dH_2O
6.25 mg/ml	etc…
3.12 mg/ml	
0 mg/ml	
1:100 dilution of each serial dilution concentration in organoid media	
Final Concentration	**Volume**
1000 µg/ml	4 µl of 100 mg/ml stock in 396 µl media
500 µg/ml	4 µl of 50 mg/ml stock in 396 µl media
250 µg/ml	4 µl of 25 mg/ml stock in 396 µl media
125 µg/ml	4 µl of 12.5 mg/ml stock in 396 µl media
62.5 µg/ml	4 µl of 6.25 mg/ml stock in 396 µl media
31.25 µg/ml	4 µl of 3.12 mg/ml stock in 396 µl media
15.62 µg/ml	4 µl of 1.56 mg/ml stock in 396 µl media
0 µg/ml	4 µl of dH_2O in 396 µl media
The higher concentrations were produced by mixing different volumes of the 100 mg/ml stock in organoid media	
Final Concentration	**Volume**
16000 µg/ml	64 µl of 100 mg/ml stock in 336 µl media
8000 µg/ml	32 µl of 100 mg/ml stock in 368 µl media
4000 µg/ml	16 µl of 100 mg/ml stock in 384 µl media
2000 µg/ml	8 µl of 100 mg/ml stock in 392 µl media

Table 2.15 Outline of the preparation of BRB-derived anthocyanin (AC) concentrations

2.11 Data and Statistical Analysis

All data was represented graphically using GraphPad Prism6. The same programme performed all statistical analysis and calculated the cohort means and SEM.

2.11.1 Mann Whitney U test

To detect statistical differences between non-parametric data sets the Mann Whitney U two-tailed test was performed unless otherwise stated. For analysis of acute loss of *Apc* using the *AhCre* mouse model the Mann Whitney U one-tailed test was used due to a small n number (number of mice per cohort). Significant differences were accepted when p values were less than or equal to (≤) 0.05.

2.11.2 Kolmogorov-Smirnov test

Distributions of cells in crypts or aberrant areas were recorded in a specific manner using Microsoft Office Excel. Cells were scored from the base of the intestinal crypt (position #1), along the crypt-villus axis in a single line until the tip of the villi. Positively stained cells were recorded as 1 and negatively stained cells were recorded as 0 over 50 half crypts per biological replicate. The sum of cells at each position within the crypt-villus structure were calculated and averaged per cohort. The cumulative frequency for each cohort was then calculated and graphically represented as an XY plot in GraphPad Prism6. To determine whether the distribution between two datasets was significantly different a Kolmogorov-Smirnov test was performed. Statistically significant differences were determined when p values were less than or equal to (≤) 0.05.

2.11.3 Kaplan Meier survival analysis

A survival curve was generated using GraphPad Prism6. Statistical analysis was conducted using the Log-rank (Mantel-Cox) test and Gehan-Breslow-Wilcoxon test for significance. A significant difference between data sets was accepted when p values ≤ 0.05.

3 Investigating the effect of black raspberries on normal and Wnt-activated murine small intestine

3.1 Introduction

Wnt signalling is a key pathway in intestinal homeostasis. Numerous studies suggest that deregulation of this pathway through the loss of the APC tumour suppressor is an initiating event in the development of human intestinal tumourigenesis, and mutations in *APC* are present in approximately 80% of CRC cases (Powell *et al.* 1992; Leslie *et al.* 2002). *In vivo* murine models of Wnt-driven CRC, in addition to providing insights regarding tumourigenesis, also provide useful tools for identifying and investigating the effect of novel therapeutic and chemopreventative strategies for intestinal tumourigenesis.

It has long been known that our diet is strongly associated with cancer risk, such that certain dietary constituents are associated with increased risk of developing CRC (red/ processed meats, lack of dietary fibre) while others have a reduced risk (fruits and vegetables) (WCRF/AICR 2011). Despite this we have a very limited understanding of the mechanisms that underpin these associations. The potential chemopreventative effects of BRBs have been extensively investigated, and have been shown to have a range of anti-tumourigenic effects at both the initiation and progression stages of CRC development in both animal and human studies (Bi *et al.* 2010; Wang *et al.* 2013b; Wang *et al.* 2013c). Despite the promising results of BRB treatment in *in vitro* and *in vivo* models of murine and human CRC, one fundamental question has not been addressed, 'what effect do BRBs have on the normal and malignant ISC populations?' as the ISCs are thought to be the origin of CRC (Baker *et al.* 2009).

This chapter aimed to characterise, by histological and gene expression analysis, the effects BRBs had on the phenotype of normal small intestine ($Apc^{+/+}$ mouse) and at the earliest stage of intestinal cancer initiation ($Apc^{fl/fl}$ mouse). In order to achieve this two different mouse models were utilised: the *AhCre* and $VillinCreER^{T2}$ systems to drive recombination of *Apc* within the mouse intestinal epithelium. Cre recombinase under the control of the *Ah* promoter is expressed in the crypt epithelium excluding the Paneth cells. *AhCre* mice were fed *ad libitum* on a standard diet (RM3(E) standard diet = control diet) or a 10% freeze-dried BRB powder in AIN76A powder) 2 weeks prior to induction. The AIN76A diet, basal matched to BRB diet was not available at the time of this experiment so mice assigned to the control cohorts remained on the standard in house diet. Homozygous deletion of *Apc* was achieved by injection with βNF. The *Villin* promoter drives Cre expression in the entire intestinal epithelium including the Paneth cells. $VillinCreER^{T2}$ mice were started on an AIN76A pellet or a 10% BRB powder supplemented in an AIN76A pelleted diet (*ad libitum*) 2 weeks prior to induction. Recombination of the *Apc* allele was achieved by tamoxifen injection. In both models, *Apc* loss resulted

in dysregulated β-catenin localisation, expansion of the stem cell population, perturbed differentiation, migration, proliferation and apoptosis (Sansom *et al.* 2004; Andreu *et al.* 2005) suggesting that perturbation of the ISC compartment plays a vital role in tumourigenesis. Due to these phenotypes, particular attention was paid to the effects of BRBs on cell differentiation, ISC markers and Wnt target genes as a readout to evaluate the effect BRBs had on the ISCs.

3.2 Results

3.2.1 Examining homeostasis and the consequence of acute loss of *Apc* driven by *AhCre* in the context of BRB diet

To understand how BRBs mediate their chemopreventative effects, the effect of BRBs on homeostasis of the normal and *Apc* deficient murine small intestine was investigated. Age matched (136 days old) *AhCre* $Apc^{+/+}$ and *AhCre* $Apc^{fl/fl}$ mice were started on the control or 10% freeze-dried BRB diets. After two weeks of feeding on their respective diet, mice (150 days old) were induced by IP injection of βNF and then culled 5 days later before harvesting of their intestine and organs. Mice remained on their respective diets throughout the experiment. Tissue was dissected as previously described (section 2.5) and the intestines were rolled into 'swiss-roll' like structures and quick fixed in formalin, sectioned to 5 microns, and mounted onto slides in preparation for H&E staining and IHC. Cell scoring was counted from 25 full or 50 half crypts as outlined in Section 2.7. Table 3.1 and Table 3.2 represents all the parameters investigated and results obtained in this chapter.

Any immediate changes to crypt architecture as a result of BRB exposure were investigated by scoring the number of cells per crypt in H&E stained sections (Figure 3.1A). Feeding of BRBs had no effect on the number of cells per crypt in $Apc^{+/+}$ mice when compared to the wildtype control ($Apc^{+/+}$ control = 45.59 ± 1.86 (SEM) vs $Apc^{+/+}$ BRB = 43.43 ± 1.23; Figure 3.1B, Table 3.1). Cre-mediated *Apc* loss in the murine small intestine resulted in a significant increase in the number of cells per crypt ($Apc^{+/+}$ control = 45.59 ± 1.86 vs $Apc^{fl/fl}$ control= 135.7 ± 3.83; Figure 3.1B, Table 3.1) as previously reported and consistent with efficient Cre induced deletion of *Apc* (Sansom *et al.* 2004). Unexpectedly, BRB treatment amplified this phenotype with a further increase in the number of cells in the aberrant $Apc^{fl/fl}$ crypt ($Apc^{fl/fl}$ control = 135.7 ± 3.83 vs $Apc^{fl/fl}$ BRB = 153.7 ± 1.73; Figure 3.1B, Table 3.1).

To gain further insight into this architectural change the role of BRBs in crypt homeostasis was examined. Cell proliferation was determined by using three complimentary approaches: counting of mitotic bodies in H&E stained intestinal sections, Ki67 immunostaining and BrdU incorporation (Figure S 8.1 and Figure S 8.2). Based on analysis of mitotic bodies, BRBs had no significant effect on cell division in wildtype ($Apc^{+/+}$ control = 1.69 ± 0.20 vs $Apc^{+/+}$ BRB = 2.37 ± 0.24) or *Apc* deficient crypts ($Apc^{fl/fl}$ control = 4.63 ± 0.095 vs $Apc^{fl/fl}$ BRB = 6.87 ± 0.66; Figure 3.2A, Table 3.1). This data was

supported by analysis of the marker Ki67, which is a marker of all active phases of the cell cycle except G_0 and is used as a proxy measure of proliferation. There was no difference in scoring of Ki67 positive cells between control and BRB treated wildtype samples (*Apc*$^{+/+}$ control = 34.83 ± 0.69 vs *Apc*$^{+/+}$ BRB = 37.08 ± 1.49; Figure 3.2B, Table 3.1) or between control and BRB treated *Apc* samples (*Apc*$^{fl/fl}$ control = 123.7 ± 9.61 vs *Apc*$^{fl/fl}$ BRB = 127.5 ± 7.21; Figure 3.2B, Table 3.1). As expected the number of mitotic figures (*Apc*$^{+/+}$ control = 1.69 ± 0.20 vs *Apc*$^{fl/fl}$ control = 4.63 ± 0.95; Figure 3.2A, Table 3.1) and Ki67 positive cells (*Apc*$^{+/+}$ control = 34.83 ± 0.69 vs *Apc*$^{fl/fl}$ control = 123.7 ± 9.61; Figure 3.2B. Table 3.1) were increased by 2.7 fold and 3.5 fold respectively following *Apc* deletion compared to wildtype. However, analysis of BrdU, a thymidine analogue incorporated into newly synthesised DNA strands (Duque and Rakic 2011), suggested that BRBs influenced the cell cycle. *Apc*$^{fl/fl}$ mice were administered with BrdU 2 and 24 hrs prior to culling. There was no statistical difference in the number of BrdU positive cells in control fed *Apc*$^{fl/fl}$ mice over 24 hrs (2 hr *Apc*$^{fl/fl}$ control = 40.68 ± 3.33 vs 24 hr *Apc*$^{fl/fl}$ control = 33.94 ± 5.68; p value = 0.2000 one-tailed Mann Whitney U test; Figure 3.2C). However, BRB exposed mice had an increased number of BrdU positive cells over 24 hrs (2 hr *Apc*$^{fl/fl}$ BRB = 49.49 ± 5.10 vs 24 hr *Apc*$^{fl/fl}$ BRB = 71.05 ± 0.75; p value = 0.0286 one-tailed Mann Whitney U test; Figure 3.2C). When analysing the number of BrdU positive cells in the context of BRB treatment, there was no statistical difference between *Apc*$^{fl/fl}$ control diet and BRB treated mice at the 2 hr time point (2 hr *Apc*$^{fl/fl}$ control = 40.68 ± 3.33 vs 2 hr *Apc*$^{fl/fl}$ BRB = 49.49 ± 5.01, Figure 3.2C, Table 3.1), but there was a significant 2 fold increase at 24 hrs (24 hr *Apc*$^{fl/fl}$ control = 33.94 ± 5.68 vs 24 hr *Apc*$^{fl/fl}$ BRB = 71.05 ± 0.75; Figure 3.2C, Table 3.1). The 2 fold increase in BrdU positive cells at 24 hrs corresponded with a restoration of cell migration along the crypt-villus axis, which is supressed in *Apc* deficient intestine (Sansom *et al.* 2004). BrdU positive cells moved 10 cell positions (at the 50% cumulative frequency) over 24 hrs in the *Apc*$^{fl/fl}$ control fed diet (Figure 3.2D), consistent with previously published studies by Méniel *et al.* (2013). BRBs reinstated migration along the *Apc*$^{fl/fl}$ crypt-villus axis as BrdU-positive cells moved 25 cell positions over 24 hrs (Figure 3.2E), 15 cell positions further than the control fed mice.

Changes in proliferation and migration are associated with changes in cell death upon acute *Apc* loss driven by the *AhCre* transgene (Sansom *et al.* 2004). To assess changes in apoptosis in the context of BRBs, the number of apoptotic bodies was scored from H&E (Figure S 8.1) and cleaved-caspase 3 (CC3) stained intestinal sections (Figure 3.3A). Overall, exposure to BRBs was found to increase the amount of cell death in wildtype and *Apc*$^{fl/fl}$ mice. Quantification of apoptotic bodies revealed a significant 3.6 fold increase in the number of apoptotic bodies in BRB exposed wildtype crypts relative to wildtype control (*Apc*$^{+/+}$ control = 0.23 ± 0.08 vs *Apc*$^{+/+}$ BRB = 0.83 ± 0.17; Figure 3.3B, Table 3.1). Following acute loss of *Apc*, the number of apoptotic bodies was significantly increased (*Apc*$^{+/+}$ control = 0.23 ± 0.08 vs *Apc*$^{fl/fl}$ control = 2.06 ± 0.33, Figure 3.3B, Table 3.1) as previously

reported. There was a non-significant 2.1 fold increase in apoptotic bodies in BRB treated $Apc^{fl/fl}$ relative to $Apc^{fl/fl}$ control fed mice ($Apc^{fl/fl}$ control = 2.06 ± 0.33 vs $Apc^{fl/fl}$ BRB = 4.37 ± **1.25**; Figure 3.3B, Table 3.1). There was a large variation in apoptotic body counts within the BRB-treated *Apc*-deleted samples which meant the study was underpowered for this particular measurement. The power of a statistical test refers to the chance that the result will be statistically significant when it should, such that the alternative hypothesis is actually true and not due to chance. The power of any statistical test relies upon certain interrelated factors; a study with a low power has a reduced chance of identifying a true effect. In the instance of apoptosis in BRB fed $Apc^{fl/fl}$ mice, the statistical power was 58.6% for a sample size of 3 at a 95% confidence interval. The probability that this result would be statistically significant if the cohort size was increased to 6 would be over 80% (Lenth 2001). Consequently, other markers of apoptosis were applied to the samples.

CC3 is a marker of the sequential activation of the caspase cascade in apoptosis. Quantification of CC3 positive cells from CC3 IHC (Figure 3.3A) revealed no difference between control and BRB wildtype samples ($Apc^{+/+}$ control = 0.86 ± 0.28 vs $Apc^{+/+}$ BRB = 1.35 ± 0.37, Figure 3.3C, Table 3.1). *Apc* loss within the crypt cells resulted in a significant increase (6.7 fold) in the number of CC3 positive cells relative to wildtype ($Apc^{+/+}$ control = 0.86 ± 0.28 vs $Apc^{fl/fl}$ control = 5.78 ± 0.50). There was also a statistically significant difference between control treated and BRB treated *Apc* samples with a further increase (2.7 fold) in the number of CC3 positive cells ($Apc^{fl/fl}$ control = 5.78 ± 0.50 vs $Apc^{fl/fl}$ BRB = 15.61 ± 2.45; Figure 3.3C, Table 3.1).

Together, these data demonstrate that short-term exposure to freeze-dried BRBs had little effect on normal gut homeostasis with only small increases in mitosis and apoptosis. However, BRBs play a significant role in the *Apc* deficient epithelia with potential anti-tumourigenic effects on apoptosis and migration alongside potential pro-tumourigenic increases in proliferation and crypt size. Due to the short-term nature of this model we were unable to assess the net outcome of these changes in the context of chemoprevention.

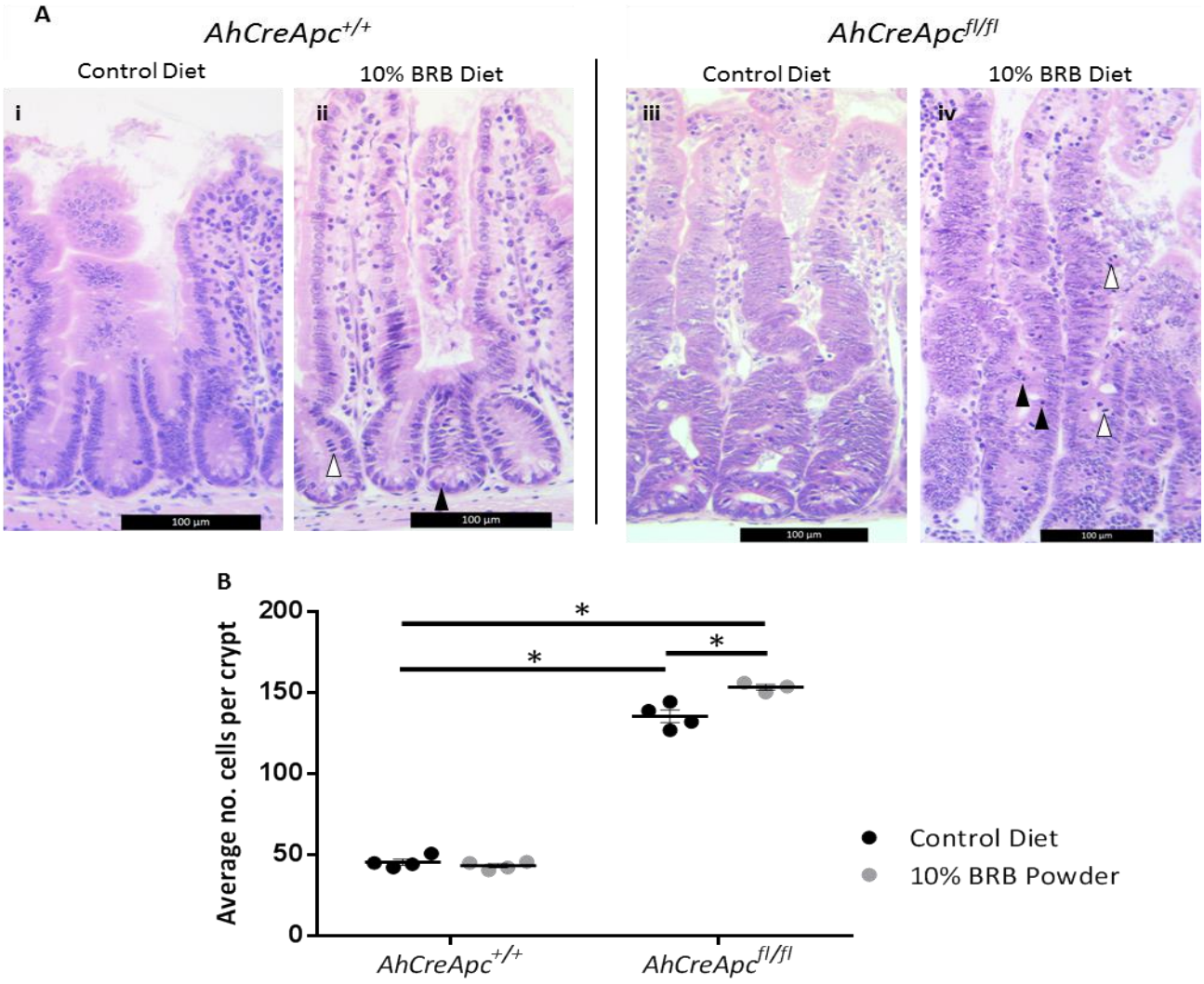

Figure 3.1 Feeding of 10% BRBs had no effect on the gross architecture of the normal murine small intestine but further increased crypt size following *Apc* loss

(A) H&E stained intestinal tissue sections highlight the intestinal epithelial cells. Mitotic cells are depicted by white arrows and apoptotic bodies are marked with black arrows. (B) Scoring of epithelial cells reported no effect of BRB on the number of cells per crypt in wildtype mice. *Apc* loss significantly altered the cellular phenotype of the small intestine (A iii) characterised by a marked increase in cell number and proliferative compartment. Exposure of *Apc* deficient intestine to BRBs resulted in a significantly larger crypt (A iv) than control. * P value ≤ 0.05, n ≥ 3, one-tailed Mann Whitney U test. Error bars represent SEM. Scale bars represent 100 µm.

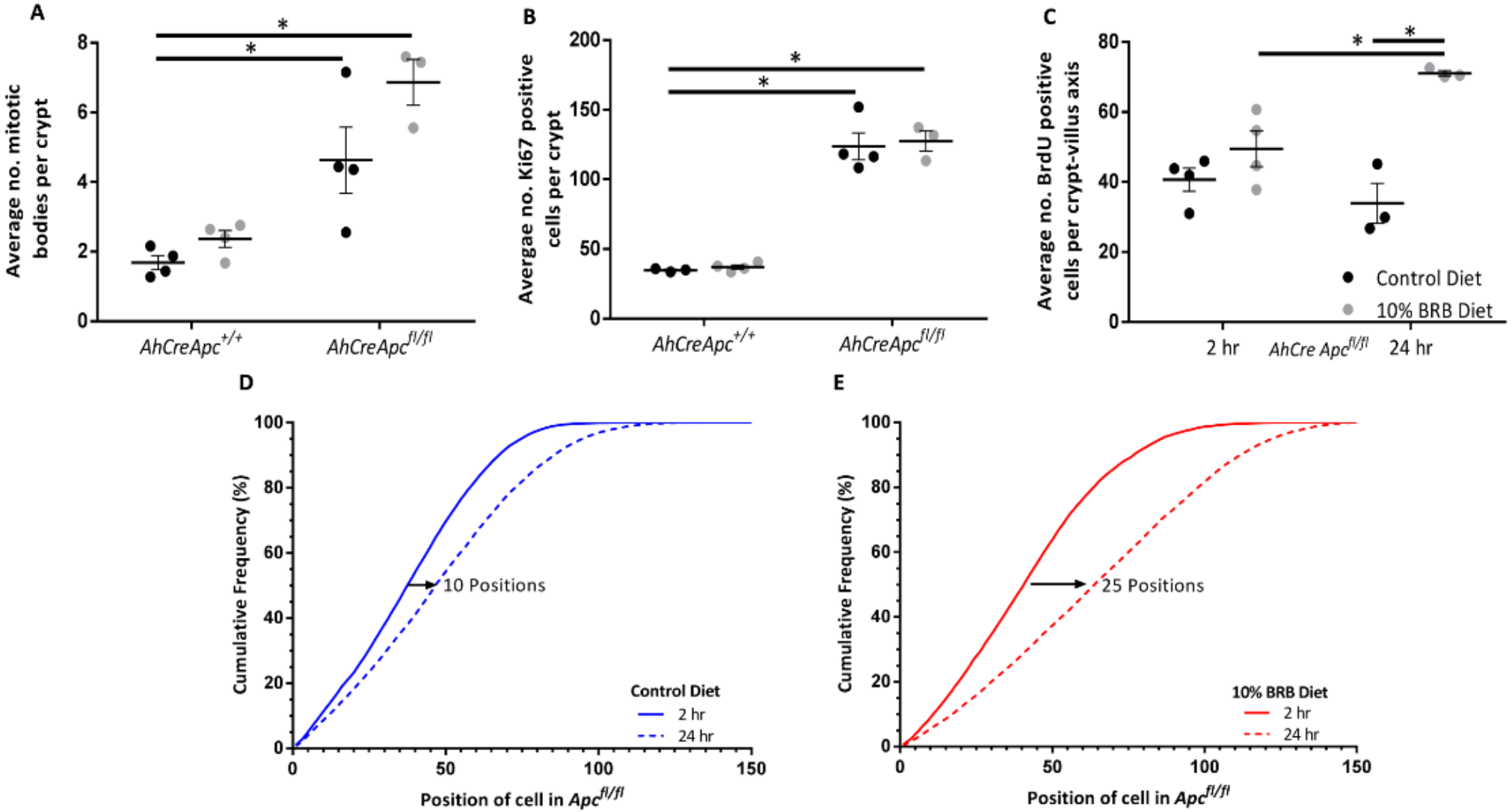

Figure 3.2 The chemopreventative effects of 10% BRBs characterised by scoring of histological mitosis, Ki67 and BrdU from AhCre *Apc*$^{+/+}$ and *AhCre Apc*$^{fl/fl}$ small intestine

(A) Scoring of mitotic figures and (B) Ki67 positive cells revealed that BRBs had no effect on mitosis in wildtype or *Apc*$^{fl/fl}$ small intestine. (C) Feeding of BRB in *Apc*$^{fl/fl}$ mice resulted in a significant increase in BrdU positive cells per half crypt at 24 hrs. (D) Acute loss of *Apc* perturbed cell migration. BrdU positive cells moved 10 cell positions (at 50% cumulative frequency) in *Apc*$^{fl/fl}$ mice fed the control diet, over 24 hrs. (E) BRBs reinstated migration of BrdU positive cells in *Apc*$^{fl/fl}$ mice as cells moved 25 cell positions (at 50% cumulative frequency) over 24 hrs 15 positions more than *Apc*$^{fl/fl}$ controls. * P value ≤ 0.05, n ≥ 3, one-tailed Mann Whitney U test (A, B, C) or Kolmogorov-Smirnov test (D and E). Error bars represent SEM.

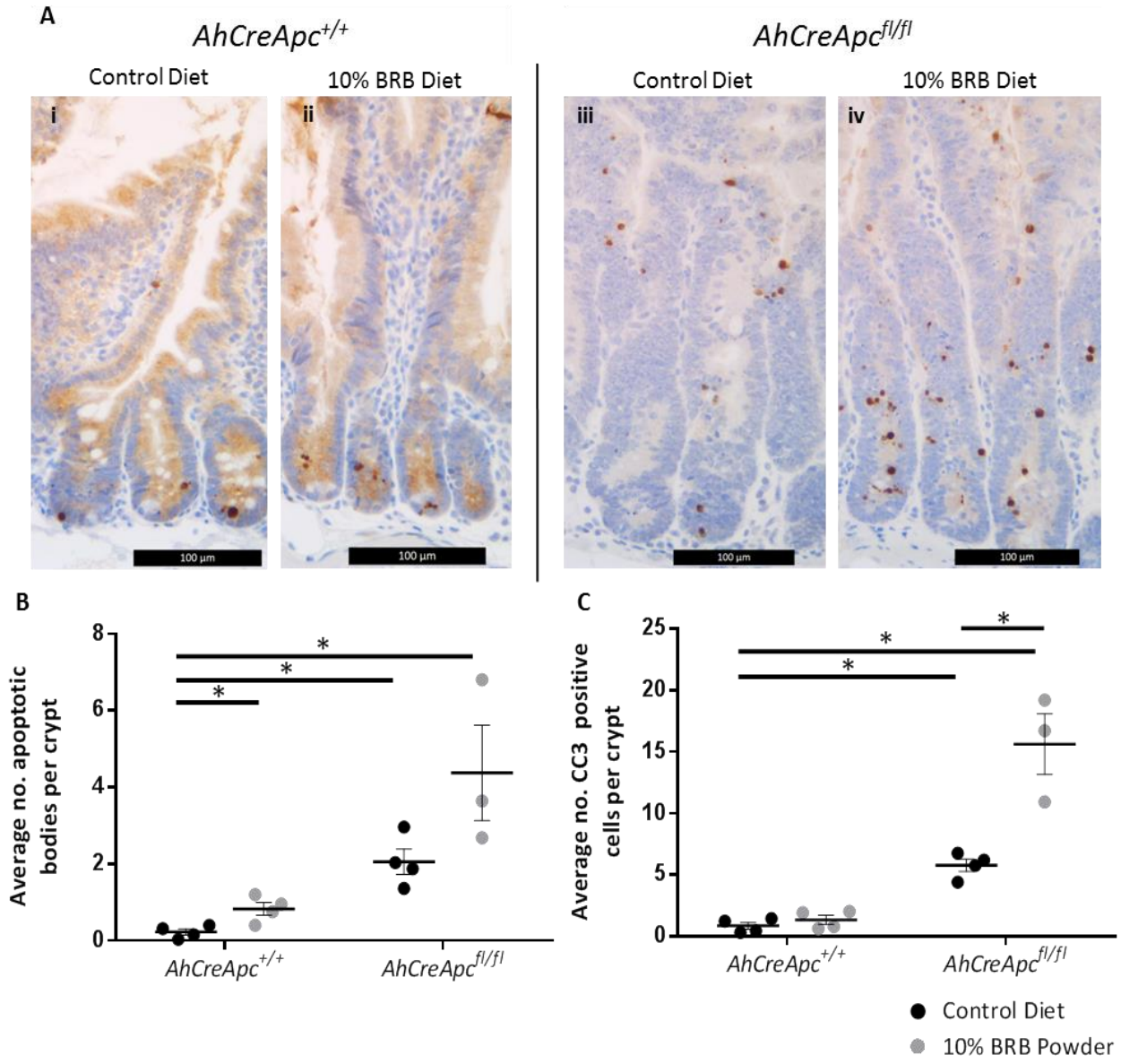

Figure 3.3 The chemopreventative effects of 10% BRBs, characterised by scoring of histological apoptotic figures and CC3 immunohistochemistry from *AhCre Apc*$^{+/+}$ and *AhCre Apc*$^{fl/fl}$ small intestine

(A) Representative images of CC3 staining in wildtype and *Apc*$^{fl/fl}$ crypt exposed to control and BRB diet. (B) Scoring of apoptotic bodies revealed that BRBs significantly increased cell death in wildtype but not *Apc*$^{fl/fl}$ small intestine. (C) However, scoring of CC3 positive cells per crypt showed that BRBs did not affect the number of CC3 cells in wildtype mice but significantly increased CC3 positivity in *Apc*$^{fl/fl}$ mice. * P value ≤ 0.05, n ≥ 3, one-tailed Mann Whitney U test. Error bars represent SEM. Scale bars represent 100 µm.

3.2.2 Evaluating the effect of BRBs on differentiation in gut homeostasis and *Apc* loss driven by *AhCre*

Cell differentiation is a regulated process crucial in the maintenance and function of the intestine. Previous studies using *AhCre Apc*$^{fl/fl}$ mice as a model of CRC have demonstrated an alteration in the number and position of the differentiated cell lineages, whereby this phenotype is assumed to be associated with CRC (Sansom *et al.* 2004). In order to see if these phenotypes could be attenuated by 2 week feeding with a BRB diet, IHC and gene expression analysis for markers of the differentiated intestinal cell populations was performed.

The chemopreventative effects of BRBs on intestinal cell differentiation were evaluated by scoring the number of enteroendocrine cells (Figure 3.4A), goblet cells (Figure 3.5A) and Paneth cells (Figure 3.6A) from stained wildtype and *Apc*$^{fl/fl}$ intestinal sections and gene expression analysis by qRT-PCR. In BRB exposed wildtype mice the number of enteroendocrine cells was increased while goblet and Paneth cells were unaltered. Specifically, BRB exposure significantly increased the number of enteroendocrine cells by 1.3 fold (*Apc*$^{+/+}$ control = 1.26 ± 0.04 vs *Apc*$^{+/+}$ BRB = 1.70 ± 0.12; Figure 3.4B, Table 3.1) and gene expression of *Synaptophysin* by 3.9 fold in wildtype mice relative to control (Figure 3.4C, Table 3.2). Synaptophysin is a membrane glycoprotein on small synaptic-like microvesicles (Wiedenmann *et al.* 1986) expressed within enteroendocrine cells and thus is a proxy marker for this cell type (Schwitalla *et al.* 2013). BRB exposure did not significantly alter the number or expression of goblet cells in wildtype mice relative to control (*Apc*$^{+/+}$ control = 18.33 ± 0.13 vs *Apc*$^{+/+}$ BRB = 17.37 ± 0.27; Figure 3.5B, Table 3.1). *Muc2* which encodes a mucin secreted by the goblet cells, revealed BRBs had no significant effect on *Muc2* expression in *Apc*$^{+/+}$ mice (Figure 3.5C, Table 3.2). Whilst IHC quantification demonstrated Paneth cells were not altered in wildtype mice exposed to BRBs (*Apc*$^{+/+}$ control = 1.78 ± 0.13 vs *Apc*$^{+/+}$ BRB = 1.77 ± 0.16; Figure 3.6C, Table 3.1), gene expression analysis of the Paneth cell marker *Lysozyme1* revealed a 4 fold decrease in expression in wildtype mice exposed to BRBs compared to the control (*Apc*$^{+/+}$ control = 1 ± 0.18 vs *Apc*$^{+/+}$ BRB = 0.26 ± 0.11; Figure 3.6D, Table 3.2). The disparity between Paneth cell count and gene expression data could be indicative of changes at the transcriptional level.

It has been previously reported that loss of *Apc* perturbed differentiation in the intestinal crypts, such that enteroendocrine and goblet cells were lost whilst Paneth cells increased in number (Sansom *et al.* 2004). Consistent with these changes, loss of *Apc* significantly decreased the percent of enteroendocrine cells (*Apc*$^{+/+}$ control = 1.26 ± 0.04 vs *Apc*$^{fl/fl}$ control = 0.91 ± 0.07; Figure 3.4B, Table 3.1) and goblet cells per crypt (*Apc*$^{+/+}$ control = 18.33 ± 0.52 vs *Apc*$^{fl/fl}$ control = 4.33 ± 0.25; Figure 3.5B, Table 3.1). However, gene expression data for *Synaptophysin* and *Muc2* were not significantly altered following *Apc* loss relative to wildtype (Figure 3.4C and Figure 3.5C respectively, Table 3.2). The

number of Paneth cells were increased following acute loss of *Apc* ($Apc^{+/+}$ control = 1.78 ± 0.13 vs $Apc^{fl/fl}$ control= 5.86 ± 1.02; Figure 3.6C, Table 3.1). Consistent with Paneth cell scoring, loss of *Apc* resulted in a significant increase in *Lysozyme1* expression (by 2.7 fold) relative to the wildtype control ($Apc^{+/+}$ control = 1 ± 0.18 vs $Apc^{fl/fl}$ control = 2.72 ± 0.69; Figure 3.6D, Table 3.2).

Analysis of the cell types revealed that BRBs partially reinstated differentiation in *Apc* deficient crypts. BRB feeding increased the number of enteroendocrine ($Apc^{fl/fl}$ control = 0.91 ± 0.07 vs $Apc^{fl/fl}$ BRB = 1.26 ± 0.09; Figure 3.4B, Table 3.1) and goblet cells ($Apc^{fl/fl}$ control = 4.33 ± 0.25 vs $Apc^{fl/fl}$ BRB = 7.82 ± 0.24; Figure 3.5B, Table 3.1) by 1.3 fold and 1.8 fold respectively, relative to the $Apc^{fl/fl}$ control. However, gene expression data did not corroborate these findings as *Synaptophysin* ($Apc^{fl/fl}$ control = 1.11 ± 0.18 vs $Apc^{fl/fl}$ BRB = 1.87 ± 0.59; Figure 3.4C, Table 3.2) and *Muc2* ($Apc^{fl/fl}$ control = 0.88 ± 0.24 vs $Apc^{fl/fl}$ BRB = 0.40 ± 0.22; Figure 3.5C, Table 3.2) gene expressions were not significantly altered. The lack of significance in these tests suggests that the study was underpowered for these particular markers which could be addressed by increasing the cohort size in a subsequent study. BRB treatment resulted in a significant decrease (56%) in the number of Paneth cells in *Apc* deficient intestine relative to $Apc^{fl/fl}$ control ($Apc^{fl/fl}$ control = 5.86 ± 1.02 vs $Apc^{fl/fl}$ BRB= 2.57 ± 0.21; Figure 3.6C, Table 3.1). Consistent with this, BRBs significantly decreased *Lysozyme1* gene expression, by 4 fold, in $Apc^{fl/fl}$ mice compared to $Apc^{fl/fl}$ control ($Apc^{fl/fl}$ control = 2.72 ± 0.69 vs $Apc^{fl/fl}$ BRB= 0.67 ± 0.14; Figure 3.6D, Table 3.2). Previous studies have reported that in addition to an increased number of Paneth cells, acute loss of *Apc* perturbed the positioning of Paneth cells such that they were no longer confined to the crypt base (Sansom *et al.* 2004). Therefore, Paneth cell position was next evaluated. Paneth cell position was not altered in wildtype mice exposed to BRBs where they remained confined to the crypt base akin to wildtype controls ($Apc^{+/+}$ control = red line vs $Apc^{+/+}$ BRB = blue line, n = 4, p value = >0.999, Kolmogorov-Smirnov test, Figure 3.6B). In support of previous work, loss of *Apc* significantly mis-localised Paneth cells throughout the crypt-villus structure ($Apc^{+/+}$ control = red line vs $Apc^{fl/fl}$ control = orange line, n = 4, p value = <0.0001, Kolmogorov-Smirnov test, Figure 3.6B). BRBs were able to partially restore Paneth cell position in *Apc* deficient crypts. Although the Paneth cells were still mis-localised they were significantly lower down the crypt-villus axis compared to the $Apc^{fl/fl}$ controls ($Apc^{fl/fl}$ control = orange line vs n = 4, $Apc^{fl/fl}$ BRB = green line, n = 3, p value = <0.0001, Kolmogorov-Smirnov test, Figure 3.6B).

Taken together, these data show that a 2 week feeding of 10% BRB powder was sufficient to attenuate the crypt-progenitor phenotype observed following acute *Apc* loss, by partially reinstating differentiation and cell positioning within the crypts. A summary of these findings can be found in Table 3.3.

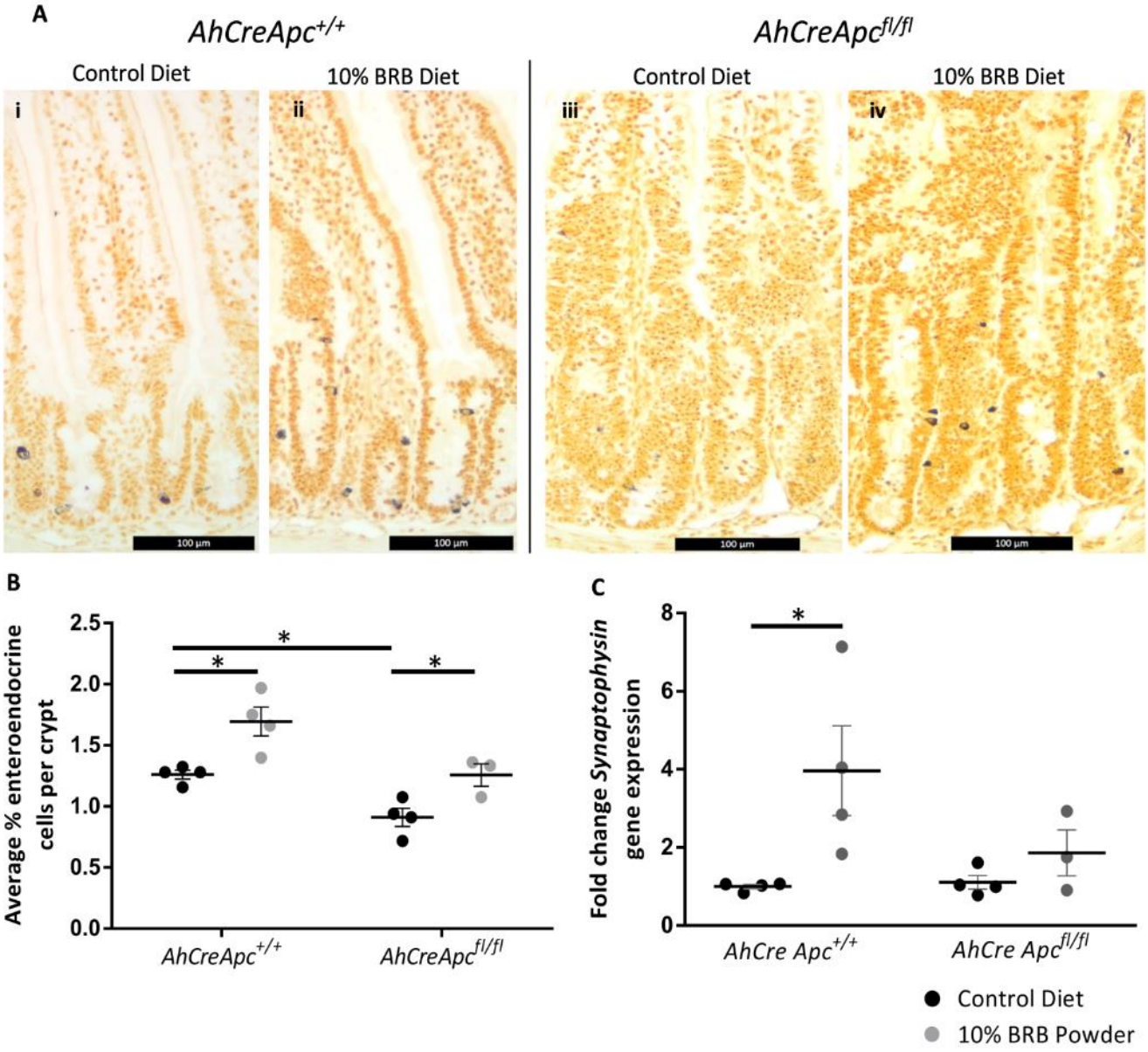

Figure 3.4 Two-week feeding of 10% BRBs increased enteroendocrine cells in wildtype and *Apc* deficient small intestine

(A) Grimelius silver stained intestinal tissue sections highlight enteroendocrine cells marked by black deposits. (B) Scoring of black deposits revealed that BRBs significantly increased the number of enteroendocrine cells in wildtype and *AhCre Apc*$^{fl/fl}$ small intestine. (C) Gene expression analysis of the enteroendocrine marker *Synaptophysin* resulted in a significant increase in gene expression in wildtype but not *Apc*$^{fl/fl}$ intestine exposed to BRB. * P value ≤ 0.05, n ≥ 3, one-tailed Mann Whitney U test. Error bars represent SEM. Scale bars represent 100 µm.

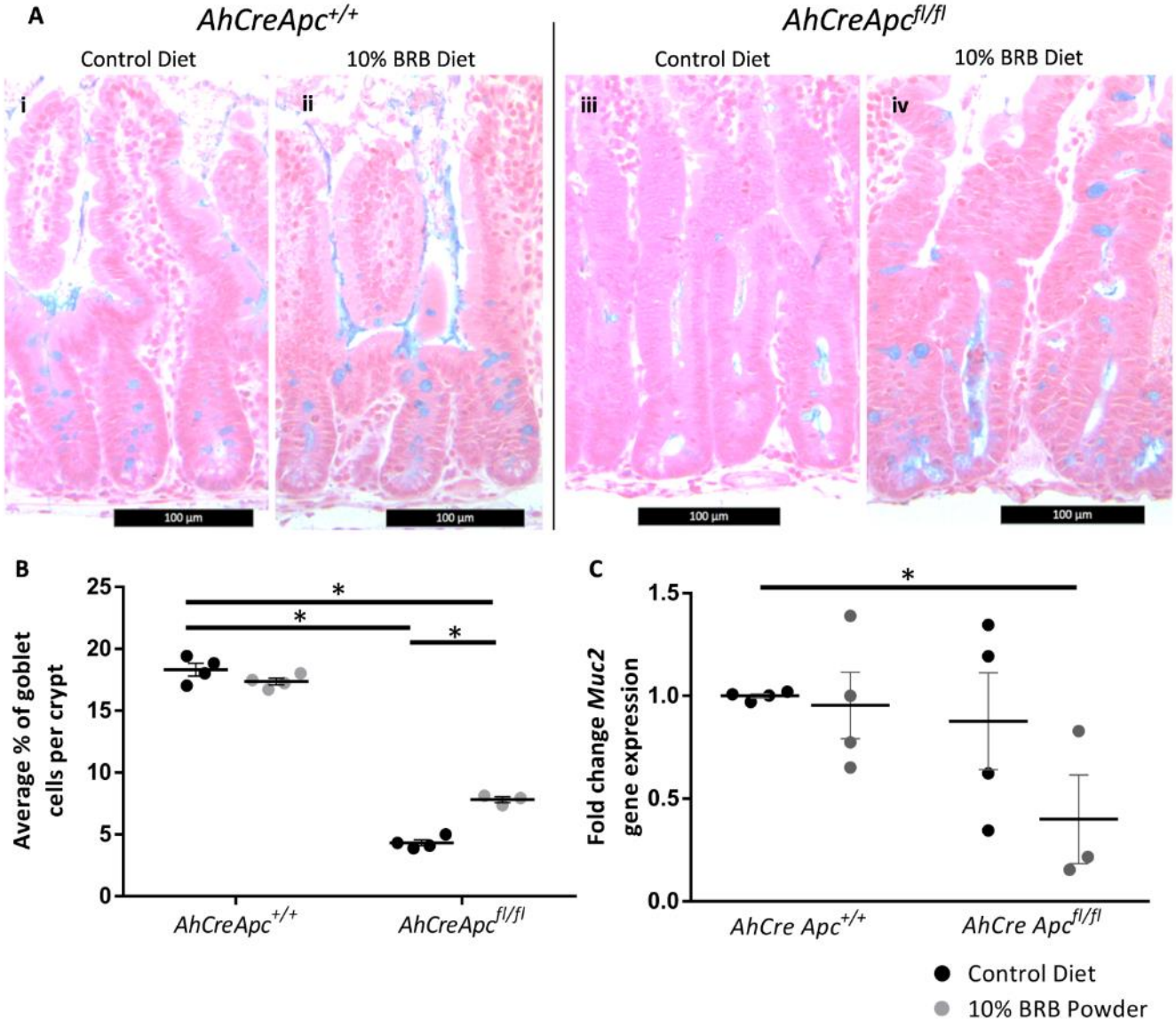

Figure 3.5 Two-week feeding of 10% BRBs increased the number of goblet cells in *Apc* deficient small intestine

(A) Alcian blue stained intestinal tissue sections show goblet cells in blue. (B) BRBs had no effect on the number of goblet cells in wildtype intestine but significantly increased the average % of goblet cells in the aberrant crypt region, following acute loss of *Apc* in the intestine driven by the *AhCre* transgene. (C) Gene expression analysis of the goblet cell marker *Muc2* was not altered in wildtype or $Apc^{fl/fl}$ small intestine in the context of BRBs. * P value ≤ 0.05, n ≥ 3, one-tailed Mann Whitney U test. Error bars represent SEM. Scale bars represent 100 µm.

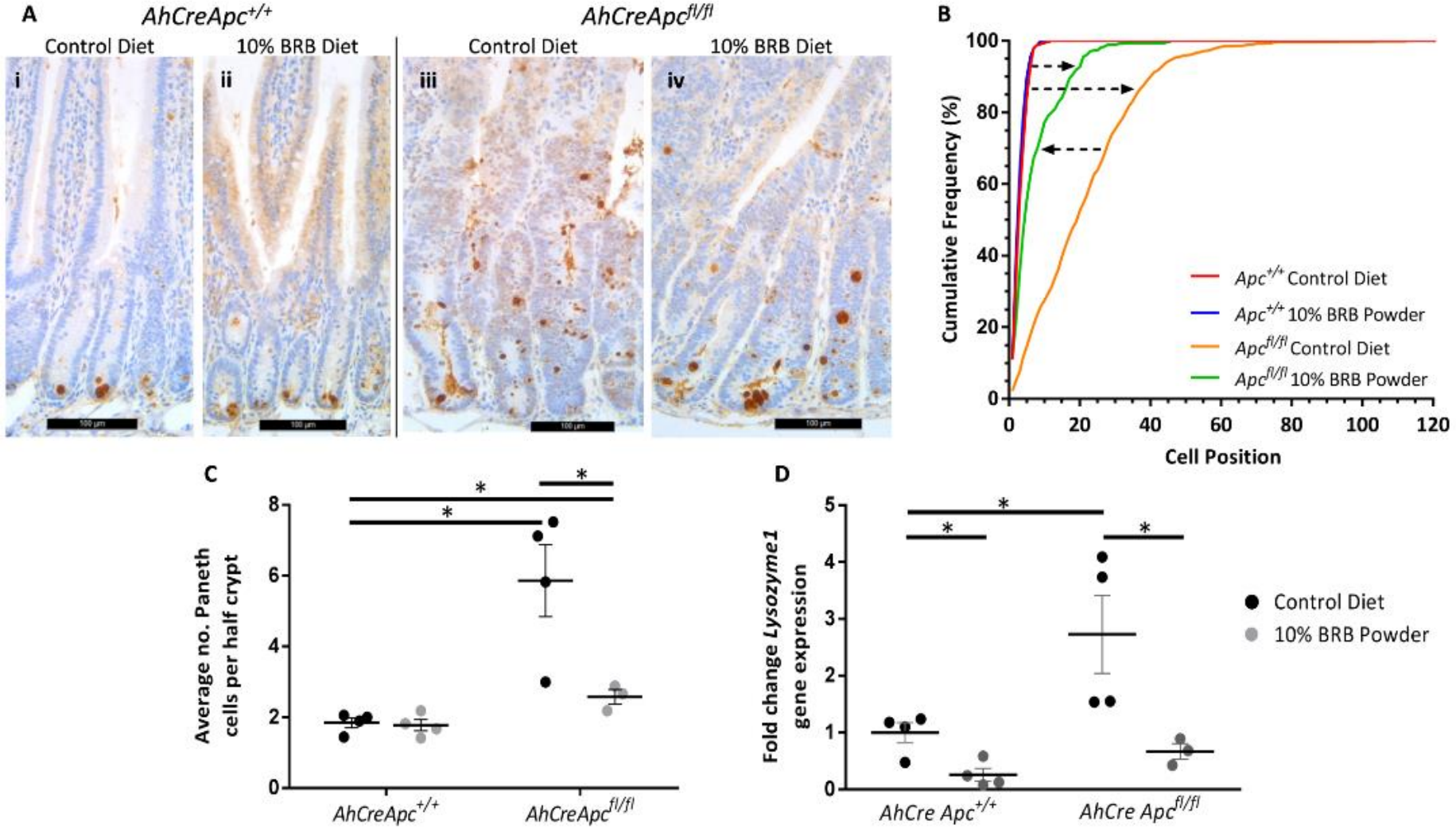

Figure 3.6 Two-week feeding of 10% BRBs attenuated the perturbed differentiation of Paneth cells following acute loss of *Apc* in the murine small intestine

(A) Lysozyme immunohistochemistry marks Paneth cells with brown staining. Paneth cells are increased in number in *AhCre Apc*$^{fl/fl}$ crypts and no longer found exclusively at the crypt base (iii). BRBs had no effect on the number of Paneth cells in the wildtype crypt (C) and they were found at the base of the crypt as expected (B, blue line). Acute loss of *Apc* resulted in a significant increase in Paneth cell number (C) where the cells were mis-localised throughout the crypt (B, orange line). BRB treatment significantly reduced the number of Paneth cells in *Apc*$^{fl/fl}$ mice (C) and attenuated their perturbed positioning bringing them closer to the crypt base (B, green line). (D) Gene expression analysis showed that BRB feeding significantly decreased expression of the Paneth cell marker *Lysozyme1* in both wildtype and *Apc*$^{fl/fl}$ intestine. * P value ≤ 0.05, n ≥ 3, one-tailed Mann Whitney U test (C and D) or Kolmogorov-Smirnov test (B). Error bars represent SEM. Scale bars represent 100 µm.

3.2.3 10% BRB diet altered ISC gene expression in wildtype and *Apc$^{fl/fl}$* small intestine

As previously outlined in sections 1.5 and 1.8 the ISCs (specifically the Lgr5^{+} population) are pivotal in the regeneration of the intestinal tissue and are thought to be the origin of CSCs (Barker *et al.* 2009). Potentially, an expansion of the ISC population could result in an increased number of cells of origin and thus augment tumourigenesis. Previous animal, cell line and human based studies of the chemopreventative effects of BRBs have not addressed the effects of BRBs on ISCs or CSCs. Therefore, this thesis sought to investigate the effects of BRBs on the normal and malignant ISC populations. A number of putative ISC markers were analysed in control and BRB fed *AhCre Apc$^{+/+}$* and *Apc$^{fl/fl}$* samples by qRT-PCR analysis. Results for all markers can be found in Table 3.2. Only statistically significant changes as a result of BRB exposure are graphically represented (Figure 3.7). Loss of *Apc* resulted in a significant increase in all ISC associated genes analysed (Table 3.2), consistent with an expansion in the ISC compartment (Sansom *et al.* 2004). The majority of these markers followed a similar trend of further up-regulation in *Apc$^{fl/fl}$* mice when exposed to BRBs, but these changes were not found to be significant (Table 3.2).

Overall, feeding of BRBs reduced the expression of putative stem cell markers in wildtype and *Apc* deficient intestine, with the exception of *Ascl2* which increased in BRB exposed *Apc$^{fl/fl}$* intestine. In wildtype intestine, *Lgr5* and *Olfm4* gene expressions were significantly down-regulated by 3.5 and 4.7 fold respectively, by BRB exposure relative to wildtype controls (*Lgr5 Apc$^{+/+}$* control = 1 ± 0.05 vs *Apc$^{+/+}$* BRB = 0.28 ± 0.11; Figure 3.7A, Table 3.2; *Olfm4 Apc$^{+/+}$* control = 1 ± 0.08 vs *Apc$^{+/+}$* BRB = 0.21 ± 0.03; Figure 3.7A, Table 3.2). *Ascl2* gene expression was non-significantly decreased by 2.3 fold in BRB treated wildtype mice compared to wildtype control (*Apc$^{+/+}$* control = 1 ± 0.10 vs *Apc$^{+/+}$* BRB = 0.44 ± 0.20; Figure 3.7A, Table 3.2).

Exposure of *Apc* deficient mice to BRBs resulted in a non-significant down-regulation in *Lgr5* expression (*Apc$^{fl/fl}$* control = 4.99 ± **1.18** vs *Apc$^{fl/fl}$* BRB= 2.17 ± 0.69; Figure 3.7A, Table 3.2). There was large variation in gene expression of *Lgr5* in the *Apc$^{fl/fl}$* control cohort which were not explained by differences in sex. A second study with a larger cohort size will be required to determine the relevance of these findings. Additionally, *Olfm4* gene expression was significantly decreased in *Apc* deficient intestine following BRB treatment, relative to *Apc$^{fl/fl}$* control (*Apc$^{fl/fl}$* control = 4.97 ± 0.88 vs *Apc$^{fl/fl}$* BRB = 1.14 ± 0.45; Figure 3.7A, Table 3.2). Contradictory to *Lgr5* and *Olfm4* data, *Ascl2* gene expression was further up-regulated in *Apc* deficient mice following BRB treatment (*Apc$^{fl/fl}$* control = 7.08 ± 0.37 vs *Apc$^{fl/fl}$* BRB = 13.05 ± 1.35; Figure 3.7A, Table 3.2).

To further evaluate the effect of BRBs on *Olfm4* expression in both wildtype and *Apc$^{fl/fl}$* intestine, *in situ* hybridisation was performed. In wildtype small intestine, *in situ* hybridisation revealed *Olfm4* was expressed at the base of the crypt (Figure 3.7B i). When evaluating the effects of

BRBs in wildtype mice, the expression of *Olfm4* was still restricted to the crypt base, but the probe signal appeared weaker (Figure 3.7B ii). Acute loss of *Apc* resulted in an expansion of the *Olfm4* positive zone (Figure 3.7B iii), consistent with an increased stem cell zone and expansion in the proliferative area (Sansom *et al.* 2004). BRB treatment did not limit the zone of *Olfm4* expression in the *Apc* deficient crypt, but the probe signal appeared reduced compared to the $Apc^{fl/fl}$ control (Figure 3.7B iv). This suggested that there was a reduction in *Olfm4* expression and thus a potential reduction in the malignant ISC population. Due to tissue disruption by proteinase K in the *in situ* hybridisation technique, it was not possible to count the number of cells stained for *Olfm4* using this approach. Importantly, this method is not quantitative, and potential differences can only be determined through representative images. Nonetheless, the apparent reduction in probe signal of *Olfm4* in both the wildtype and $Apc^{fl/fl}$ intestine supported the significant decrease in *Olfm4* gene expression revealed by qRT-PCR analysis (Figure 3.7A). Together, the *Olfm4* data showed a reduction in stem cell marker expression in the context of BRB feeding. However, from this it was not possible to determine whether feeding of BRBs alter the number of stem cells. Alterations in ISC gene expression in wildtype and $Apc^{fl/fl}$ mice in the context of BRBs are summarised in Table 3.4.

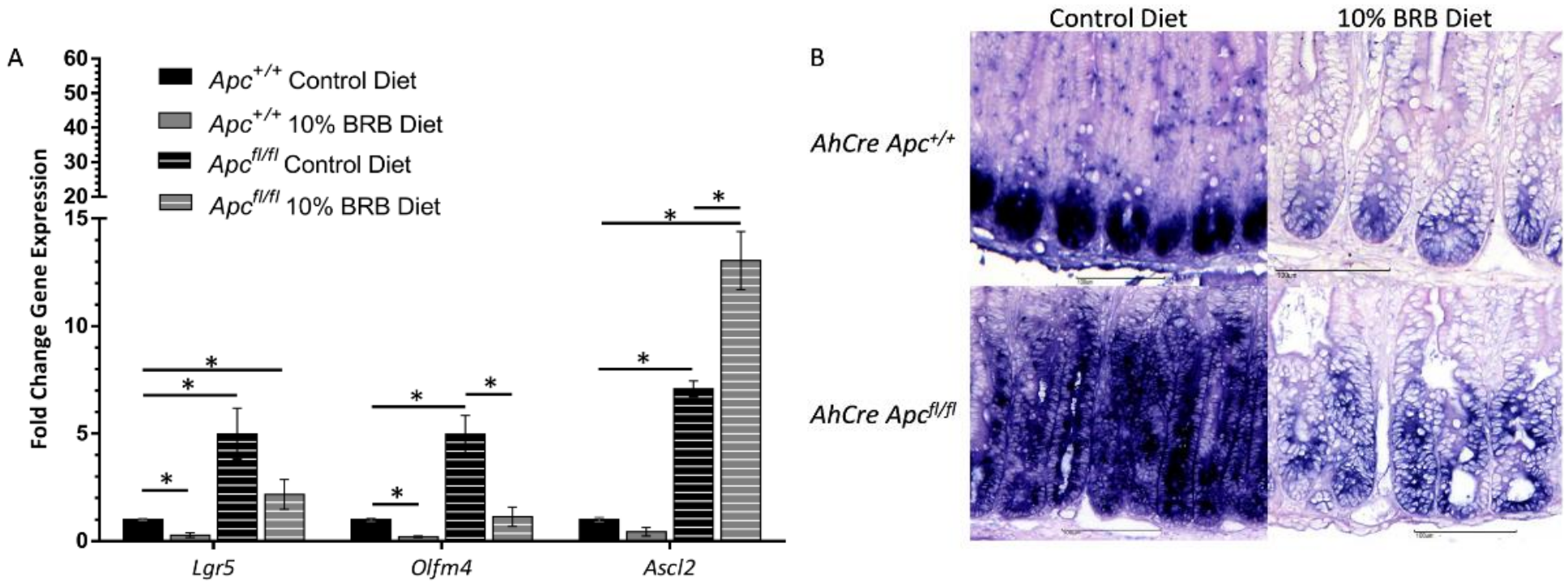

Figure 3.7 Feeding of 10% BRBs altered the expression of some ISC markers in normal and *Apc* deficient small intestine

(A) qRT-PCR gene expression analysis revealed that BRBs significantly decreased expression of *Lgr5* and *Olfm4* in wildtype intestine. Acute loss of *Apc* driven by *AhCre* recombination resulted in a significant up-regulation of all ISC markers, as expected with an increased crypt-progenitor phenotype. *Lgr5* and *Olfm4* gene expression was reduced in $Apc^{fl/fl}$ intestine exposed to the BRB diet, although this was only significant for *Olfm4*. *Ascl2* gene expression on the other hand appeared to significantly increase in $Apc^{fl/fl}$ intestine exposed to the BRB diet. (B) *In situ* hybridisation for the marker *Olfm4* revealed that expression of *Olfm4* was reduced in wildtype and *Apc* deficient intestine following BRB intervention, consistent with the gene expression data. * P value ≤ 0.05, n ≥ 3, one-tailed Mann Whitney U test. Error bars represent SEM. Scale bars represent 100 µm.

3.2.4 Evaluating the Wnt target genes in the context of BRBs in wildtype and *Apc*$^{fl/fl}$ small intestine

The Wnt signalling pathway is fundamental for embryonic development and maintenance of intestinal homeostasis (see section 1.6.1). CRC is thought to initiate from mutations in genes that encode proteins involved in the Wnt pathway, specifically in the ISC. It could be hypothesised that alterations in ISC markers could be as a consequence of, or related to, changes in Wnt signalling. Thus, expression levels of Wnt target genes were next determined. As with the previous section, only statistically significant changes as a result of BRB feeding are graphically represented (Figure 3.8), with all data presented in Table 3.2. As acute *Apc* loss within the intestine results in constitutively activated Wnt signalling, the majority of Wnt target genes were up-regulated in the *Apc* deficient intestine, as expected.

As summarised in section 1.6.1, β-catenin binds with TCF to activate transcription of Wnt target genes and thus, *Tcf7* gene expression can be used as a readout of Wnt activation. BRB treatment significantly increased *Tcf7* gene expression in both wildtype and *Apc*$^{fl/fl}$ intestine by approximately 3.3 fold each when compared to their appropriate controls (*Apc*$^{+/+}$ control = 1 ± 0.05 vs *Apc*$^{+/+}$ BRB = 3.32 ± 1.25; *Apc*$^{fl/fl}$ control = 3.28 ± 0.42 vs *Apc*$^{fl/fl}$ BRB = 11.16 ± 1.94; Figure 3.8, Table 3.2). This suggests that BRBs enhanced transcription of Wnt signalling targets in both wildtype and *Apc* deficient intestine.

Two proteins involved in regulating proliferation and the cell cycle in normal intestine are CyclinD1 and EphB receptors (Gregorieff *et al.* 2005; Holmberg *et al.* 2006). CyclinD1 is involved in the regulation of the cell cycle, specifically in the transition from G1 to S phase, while the EphB2 receptor promotes proliferation in the normal intestinal epithelium (Holmberg *et al.* 2006). Expression analysis for *CyclinD1* and *EphB2* revealed that BRB exposure significantly reduced the expression levels of these genes in wildtype intestine by 3 and 2 fold respectively relative to wildtype controls (*CyclinD1* = *Apc*$^{+/+}$ control = 1 ± 0.07 vs *Apc*$^{+/+}$ BRB = 0.34 ± 0.10. *EphB2* = *Apc*$^{+/+}$ control = 1 ± 0.04 vs *Apc*$^{+/+}$ BRB = 0.53 ± 0.15; Figure 3.8, Table 3.2). This suggests that in a wildtype setting, BRBs inhibited markers of proliferation at the transcriptional level, despite having no effect on proliferation at the cellular level (Figure 3.2). The expression levels of *CyclinD1* and *EphB2* were also assessed in the *Apc* deficient intestine in the context of BRBs. BRBs did not significantly affect the expression of *CyclinD1* in *Apc* deficient intestine relative to *Apc*$^{fl/fl}$ control (*Apc*$^{fl/fl}$ control = 3.91 ± 0.47 vs *Apc*$^{fl/fl}$ BRB = 4.49 ± 2.20; Figure 3.8, Table 3.2). It has been previously reported that EphB2 has a dual function in the intestine such that it acts as tumour suppressor in colon tumourigenesis (Batlle *et al.* 2005). However, *EphB2* expression was significantly increased by 4.5 fold following *Apc* loss, but this is consistent with studies by Holik *et al.* (2014). BRBs did not significantly affect *EphB2* expression in *Apc*$^{fl/fl}$ mice, although

expression appeared to reduce by 2 fold compared to $Apc^{fl/fl}$ control ($Apc^{fl/fl}$ control = 4.46 ± 1.21 vs $Apc^{fl/fl}$ BRB = 1.99 ± 0.42; Figure 3.8, Table 3.2). In addition to EphB2, the macrophage migration inhibitory factor (MIF) which is a pro-inflammatory cytokine (Lue *et al.* 2002) has been reported to control cell proliferation, differentiation, angiogenesis, tumour progression and metastasis in intestinal tumourigenesis (Chesney *et al.* 1999; Sun *et al.* 2005), Specifically, increased MIF expression has been linked to enhanced proliferation of murine colon cancer cells and a loss of differentiation (He *et al.* 2004). The gene expression of *Mif1* non-significantly increased by 3 fold in BRB treated wildtype mice relative to wildtype control ($Apc^{+/+}$ control = 1 ± 0.13 vs $Apc^{+/+}$ BRB = 3.04 ± 0.75; Figure 3.8, Table 3.2). Despite reports that *Mif1* expression increases with increased tissue dysplasia (Wilson *et al.* 2005), acute loss of *Apc* did not result in a significant up-regulation of *Mif1* gene expression ($Apc^{+/+}$ control = 1 ± 0. 13 vs $Apc^{fl/fl}$ control= 2.55 ± 0.77; Figure 3.8, Table 3.2). BRB treatment resulted in a significant 5 fold increase in *Mif1* gene expression in $Apc^{fl/fl}$ mice compared to the $Apc^{fl/fl}$ control ($Apc^{fl/fl}$ control = 2.55 ± 0.77 vs $Apc^{fl/fl}$ BRB = 13.36 ± 5.50; Figure 3.8, Table 3.2). This suggests that BRBs may have some pro-carcinogenic effects in the intestine.

Sox proteins are regulators of cell fate specification and differentiation within the intestine. Some Sox proteins are antagonists of Wnt signalling while others act as Wnt agonists. Sox9 is thought to be a negative regulator of the Wnt signalling pathway as conditional deletion of *Sox9* in the murine intestine prevented Paneth cell differentiation and resulted in the up-regulation of several Wnt target genes such as *CyclinD1*, leading to intestinal hyperplasia (Bastide *et al.* 2007; Mori-Akiyama *et al.* 2007). *Sox17* has also been identified as a negative regulator of the Wnt signalling pathway (Sinner *et al.* 2007). It is present in normal intestinal epithelium but it is commonly silenced in intestinal neoplasia and CRC (Fu *et al.* 2010). Gene expression analysis revealed that in wildtype mice *Sox9* expression was non-significantly increased by 3 fold ($Apc^{+/+}$ control = 1 ± 0.15 vs $Apc^{+/+}$ BRB = 3.24 ± 0.92; Figure 3.8, Table 3.2), while *Sox17* expression was significantly up-regulated by 12 fold in the context of BRB feeding. ($Apc^{+/+}$ control = 1 ± 0.13 vs $Apc^{+/+}$ BRB = 11.96 ± 5.67; Figure 3.8, Table 3.2). Both genes were up-regulated following *Apc* loss as expected. BRB treatment further increased *Sox9* gene expression in $Apc^{fl/fl}$ mice in comparison to the $Apc^{fl/fl}$ control ($Apc^{fl/fl}$ control = 4.56 ± 0.79 vs $Apc^{fl/fl}$ BRB = 18.37 ± 4.98; Figure 3.8, Table 3.2). However, *Sox17* expression was not significantly altered by BRBs in $Apc^{fl/fl}$ mice ($Apc^{fl/fl}$ control = 119.8 ± 20.54 vs $Apc^{fl/fl}$ BRB = 90.65 ± 39.26; Figure 3.8, Table 3.2).

Taken together, these results suggest that at the transcriptional level BRBs reduced markers of proliferation while up-regulating transcription of Wnt repressor genes in wildtype mice. Hypothetically, this could suggest one of two possibilities. Firstly is that BRBs may reduce the number of stem cells and thus, may reduce the number of cells that have the potential to be transformed. The second being that the presence of BRBs may minimise the impact of mutations that do occur by

limiting the expansion capability of mutated cells. In conjunction with this, it appears that BRBs play a role in repressing Wnt signalling at the earlier stages of Wnt-driven tumourigenesis, despite having a potential pro-tumourigenic effect on *Mif1* expression. A summary of these finding are shown in Table 3.5.

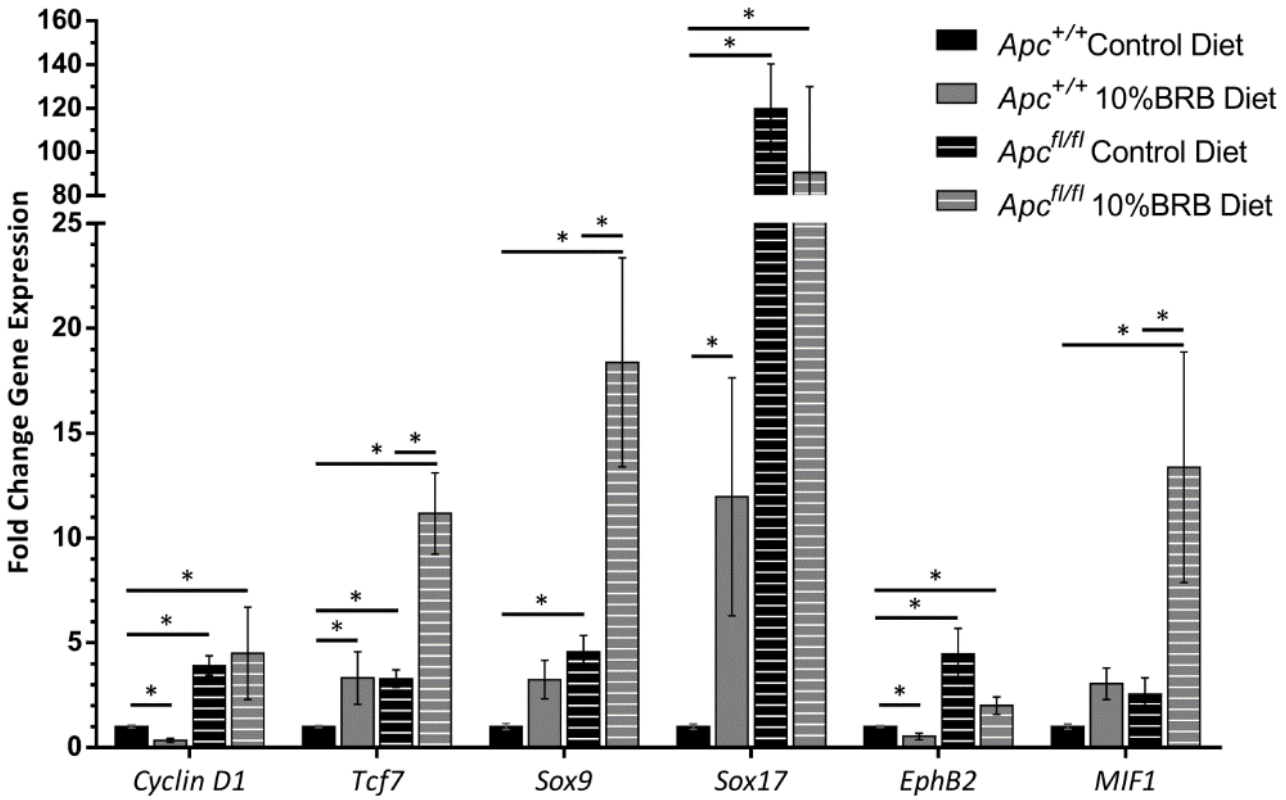

Figure 3.8 Alterations in Wnt target gene expression in *AhCre Apc*$^{+/+}$ and *Apc*$^{fl/fl}$ small intestine in the context of 10% BRB diet

qRT-PCR was performed on RNA extracted from frozen intestinal sections from *AhCre Apc*$^{+/+}$ and *Apc*$^{fl/fl}$ mice. In wildtype mice fed on the 10% BRB diet, gene expressions of *CyclinD1* and *EphB2* were significantly reduced compared to the wildtype control, while *Tcf7* and *Sox17* expressions increased. *Sox9* and *Mif1* were not significantly altered. Acute loss of *Apc* resulted in a significant increase in expression of all genes except *Mif1*. BRB fed *Apc*$^{fl/fl}$ mice had a further increase in expression of *Tcf7*, *Sox9* and *Mif1. CyclinD1, Sox17* and *EphB2* were not statistically altered. * P value ≤ 0.05, n ≥ 3, one-tailed Mann Whitney U test. Error bars represent SEM.

3.2.5 Assessing whether BRB treatment rescued the phenotype induced by acute *Apc* loss driven by the *AhCre* transgene

The ultimate goal of most therapeutic strategies is to restore disease phenotypes to a normal setting. Therefore, this thesis set out to determine whether the 10% freeze-dried BRB diet normalised the aberrant crypt-progenitor phenotype, characteristic of acute *Apc* loss, to a normal level. Histological analysis, IHC counts and gene expression data for cell population markers, stem cell markers and Wnt target genes were compared from control treated wildtype mice and *AhCre* $Apc^{fl/fl}$ BRB treated mice. Complete rescue to a normal phenotype is indicated by no significant difference (p value ≥ 0.05) between wildtype controls and BRB fed $Apc^{fl/fl}$ mice as determined by Mann Whitney U statistical tests. The results and p values for all parameters can be found in Table 3.1 and Table 3.2.

Acute loss of *Apc* driven by the *AhCre* promoter resulted in a significant increase in mitosis and apoptosis (Figure 3.2C and Figure 3.3C respectively) consistent with previous studies (Sansom *et al.* 2004). BRB treatment in this mouse model did not restore cell proliferation or cell death to normal levels, but a further increase in CC3 number in $Apc^{fl/fl}$ mice could be anti-tumourigenic. In addition, BRBs re-established cell migration in the aberrant crypts that arrested upon *Apc* loss (Figure 3.2E). The crypt-progenitor phenotype is characteristic of altered cell differentiation such that enteroendocrine and goblet cells are significantly reduced in number (Figure 3.4 and Figure 3.5 respectively, Table 3.1) and Paneth cells were mis-localised and dramatically increased (Figure 3.6B and C respectively), to support an increased stem cell zone (Sansom *et al.* 2004). When comparing BRB treated $Apc^{fl/fl}$ with wildtype controls, the BRB treatment restored enteroendocrine and Paneth cell phenotypes to within the normal wildtype range (Figure 3.4B and Figure 3.6C, Table 3.1). Similarly, *Synaptophysin* and *Lysoyme1* gene expression were rescued by BRB treatment (Figure 3.4C and Figure 3.6D, Table 3.2), however *Synaptophysin* expression was not altered upon acute *Apc* loss. In addition, BRBs were only partly able to reinstate Paneth cell position. Despite positioned significantly lower in the aberrant crypt compared to the $Apc^{fl/fl}$ control (Figure 3.6B green line vs orange line), Paneth cells were still mis-located in comparison to the wildtype control (Figure 3.6B red line vs green line). For goblet cells, an intermediate phenotype was observed between wildtype control and BRB treated $Apc^{fl/fl}$ measurements, suggesting partial rescue of the *Apc* phenotype by the BRB treatment (Figure 3.5B, Table 3.1). In contrast, gene expression for *Muc2* was not returned to normal wildtype levels by BRBs. Taken together, these readouts for differentiation indicate that BRBs restored, at least in part, the majority of differentiated cell populations to within normal homeostatic levels.

It is evident that BRBs affect stem cell dynamics as seen by the significant alteration in the gene expression of the stem cell markers *Lgr5*, *Olfm4* and *Ascl2* in the aberrant *Apc* deficient crypt compared to $Apc^{fl/fl}$ controls (Figure 3.7, Table 3.2). Although BRBs appeared to reduce expression of

Lgr5 and *Olfm4* in *Apc*$^{fl/fl}$ only the *Olfm4* data was significant (Figure 3.7A). No statistical difference (p value = 0.3143, one-tailed Mann Whitney U test) between *Olfm4* levels in wildtype control and BRB *Apc*$^{fl/fl}$ mice highlights the extent of rescue, such that *Olfm4* was returned to within normal levels.

The expression levels of the Wnt target genes *CyclinD1, Tcf7, Sox9, Sox17, EphB2* and *Mif1* were not returned to within normal levels of wildtype mice. As described in section 3.2.3, the expression levels of *Tcf7, Sox9* and *Mif1* were significantly increased in BRB fed *Apc*$^{fl/fl}$ mice (Figure 3.8, Table 3.2). It could be hypothesised that enhanced expression of Wnt targets could be pro-tumourigenic due to the role Wnt signalling plays in stem cell and progenitor cell fate. However, some of these targets can act as Wnt repressors and so the significance of these increases are discussed in section 3.3. These findings are summarised in Table 3.3, Table 3.4 and Table 3.5.

AhCre Mouse Model								
Cell type/marker	***Apc*$^{+/+}$ Control vs *Apc*$^{+/+}$ BRB n = 3/4**		***Apc*$^{+/+}$ Control vs *Apc*$^{fl/fl}$ control n = 3/4**		***Apc*$^{+/+}$ Control vs *Apc*$^{fl/fl}$ *BRB* n = 3/4**		***Apc*$^{fl/fl}$ Control vs *Apc*$^{fl/fl}$ BRB n = 3/4**	
	Average Number (± SEM)	**P value**	**Average Number (± SEM)**	**P value**	**Average Number (± SEM)**	**P value**	**Average Number (± SEM)**	**P value**
Cell number	45.59 ± 1.86 vs 43.43 ± 1.23	0.4429	45.59 ± 1.86 vs 135.7 ± 3.83	**0.0143**	45.59 ± 1.86 vs 153.7 ± 1.73	**0.0286**	135.7 ± 3.83 vs 153.7 ± 1.73	**0.0286**
Mitosis	1.69 ± 0.20 vs 2.37 ± 0.24	0.0571	1.69 ± 0.20 vs 4.63 ± 0.95	**0.0143**	1.69 ± 0.20 vs 6.87 ± 0.66	**0.0286**	4.63 ± 0.95 vs 6.87 ± 0.66	0.0571
Ki67	34.83 ± 0.69 vs 37.08 ± 1.49	0.1143	34.83 ± 0.69 vs 123.7 ± 9.61	**0.0286**	34.83 ± 0.69 vs 127.5 ± 7.21	**0.0500**	123.7 ± 9.61 vs 127.5 ± 7.21	0.4286
BrdU 2 hrs	N/D		N/D		N/D		40.68 ± 3.33 vs 49.49 ± 5.10	0.1714
BrdU 24 hrs	N/D		N/D		N/D		33.94 ± 5.69 vs 71.05 ± 0.75	**0.0500**
Apoptosis	0.23 ± 0.08 vs 0.83 ± 0.17	**0.0286**	0.23 ± 0.08 vs 2.06 ± 0.33	**0.0143**	0.23 ± 0.08 vs 4.37 ± 1.25	**0.0286**	2.06 ± 0.33 vs 4.37 ± 1.25	0.0571
CC3	0.86 ± 0.28 vs 1.35 ± 0.37	0.1714	0.86 ± 0.28 vs 5.78 ± 0.50	**0.0143**	0.86 ± 0.28 vs 15.61 ± 2.45	**0.0286**	5.78 ± 0.50 vs 15.61 ± 2.45	**0.0286**
Enteroendocrine cells	1.26 ± 0.04 vs 1.70 ± 0.12	**0.0143**	1.26 ± 0.04 vs 0.91 ± 0.07	**0.0143**	1.26 ± 0.04 vs 1.26 ± 0.09	0.3143	0.91 ± 0.07 vs 1.26 ± 0.09	**0.0286**
Goblet cells	18.33 ± 0.52 vs 17.37 ± 0.27	0.1714	18.33 ± 0.52 vs 4.33 ± 0.25	**0.0143**	18.33 ± 0.52 vs 7.82 ± 0.24	**0.0286**	4.33 ± 0.25 vs 7.82 ± 0.24	**0.0286**
Paneth cells	1.78 ± 0.13 vs 1.77 ± 0.16	0.4429	1.78 ± 0.13 vs 5.86 ± 1.02	**0.0143**	1.78 ± 0.13 vs 2.57 ± 0.21	**0.0286**	5.86 ± 1.02 vs 2.57 ± 0.21	**0.0286**

Table 3.1 Raw data counts from histological and IHC stained *AhCre Apc*$^{+/+}$ and *Apc*$^{fl/fl}$ intestinal sections exposed to control and 10% freeze-dried BRB powdered diets

Cohorts consisted of 3 – 4 mice. Significance of results (p value = ≤ 0.05) was determined using one-tailed Mann Whitney U statistical test. SEM = standard error of mean; N/D = no data.

	Gene	*Apc*$^{+/+}$ Control vs *Apc*$^{+/+}$ BRB n = 3/4		*Apc*$^{+/+}$ Control vs *Apc*$^{fl/fl}$ control n = 3/4		*Apc*$^{+/+}$ Control vs *Apc*$^{fl/fl}$ *BRB* n = 3/4		*Apc*$^{fl/fl}$ Control vs *Apc*$^{fl/fl}$ BRB n = 3/4	
		Average Fold Change (± SEM)	P value	Average Fold Change (± SEM)	P value	Average Fold Change (± SEM)	P value	Average Fold Change (± SEM)	P value
Cell Type Markers	*Lysozyme1*	1 ± 0.18 vs 0.26 ± 0.11	**0.0286**	1 ± 0.18 vs 2.72 ± 0.67	**0.0143**	1 ± 0.18 vs 0.67 ± 0.14	0.2286	2.72 ± 0.69 vs 0.67 ± 0.14	**0.0286**
	Muc2	1 ± 0.01 vs 0.95 ± 0.16	0.2429	1 ± 0.01 vs 0.88 ± 0.24	0.5000	1 ± 0.01 vs 0.40 ± 0.22	**0.0286**	0.88 ± 0.24 vs 0.40 ± 0.22	0.1143
	Synaptophysin	1 ± 0.06 vs 3.97 ± 1.15	**0.0143**	1 ± 0.06 vs 1.11 ± 0.18	0.4429	1 ± 0.06 vs 1.87 ± 0.59	0.2000	1.11 ± 0.18 vs 1.87 ± 0.59	0.2000
Active Cycling Stem Cell Markers	*Lgr5*	1 ± 0.05 vs 0.28 ± 0.11	**0.0143**	1 ± 0.05 vs 4.99 ± 1.18	**0.0143**	1 ± 0.05 vs2.17 ± 0.69	**0.0286**	4.99 ± 1.18 vs 2.17 ± 0.69	0.1143
	Olfm4	1 ± 0.08 vs 0.21 ± 0.03	**0.0286**	1 ± 0.08 vs 4.97 ± 0.88	**0.0143**	1 ± 0.08 vs1.14 ± 0.45	0.3143	4.97 ± 0.88 vs 1.14 ± 0.45	**0.0286**
	Ascl2	1 ± 0.10 vs 0.44 ± 0.20	0.0571	1 ± 0.10 vs 7.08 ± 0.37	**0.0143**	1 ± 0.10 vs 13.05 ± 1.35	**0.0286**	7.08 ± 0.37 vs 13.05 ± 1.35	**0.0286**
	Rnf43	1 ± 0.07 vs 0.62 ± 0.32	0.1714	1 ± 0.07 vs 3.76 ± 1.59	**0.0143**	1 ± 0.07 vs 4.21 ± 1.51	**0.0286**	3.76 ± 1.59 vs 4.21 ± 1.51	0.4286
	Tnfrsf19	1 ± 0.15 vs 2.81 ± 1.02	0.1	1 ± 0.15 vs 20.87 ± 3.86	**0.0143**	1 ± 0.15 vs 66.71 ± 36.19	**0.0286**	20.87 ± 3.86 vs 66.71 ± 36.19	0.2
	Msi1	1.04 ± 0.13 vs 1.3 ± 0.44	0.3429	1.04 ± 0.13 vs 11.41 ± 2.73	**0.0143**	1.04 ± 0.13 vs 13.97 ± 0.38	**0.0286**	11.41 ± 2.73 vs 13.97 ± 0.38	0.3143
	CD133	1 ± 0.04 vs 0.78 ± 0.18	0.1143	1 ± 0.04 vs 2.39 ± 0.82	**0.0143**	1 ± 0.04 vs 5.98 ± 1.48	**0.0286**	2.39 ± 0.82 vs 5.98 ± 1.48	0.1143
+4 Stem Cell Markers	*Bmi1*	1.09 ± 0.22 vs 3.49 ± 1.25	0.1714	1.09 ± 0.22 vs 3.05 ± 0.90	0.0571	1.09 ± 0.22 vs 7.55 ± 2.19	**0.0286**	3.05 ± 0.90 vs 7.55 ± 2.19	0.1143
	Lrig1	1 ± 0.10 vs 1.19 ± 0.46	0.3500	1 ± 0.01 vs 1.41 ± 0.34	0.1143	1 ± 0.10 vs 2.51 ± 1.07	0.3500	1.41 ± 0.34 vs 2.51 ± 1.07	0.3143
Wnt target Genes	*CyclinD1*	1 ± 0.07 vs 0.34 ± 0.10	**0.0143**	1 ± 0.07 vs 3.91 ± 0.47	**0.0143**	1 ± 0.07 vs 4.49 ± 2.20	0.3143	3.91 ± 0.47 vs 4.49 ± 2.20	0.3143
	Axin2	1 ± 0.05 vs 2.11 ± 0.64	0.1000	1 ± 0.05 vs 6.78 ± 0.99	**0.0143**	1 ± 0.05 vs 15.56 ± 5.93	**0.0286**	6.78 ± 0.99 vs 15.56 ± 5.93	0.2000
	c-myc	1 ± 0.11 vs 1.90 ± 0.41	0.1000	1 ± 0.11 vs 9.81 ± 0.74	**0.0143**	1 ± 0.11 vs 17.29 ± 8.93	**0.0286**	9.81 ± 0.74 vs 17.29 ± 8.93	0.5000
	EphB2	1 ± 0.04 vs 0.53 ± 0.15	**0.0143**	1 ± 0.04 vs 4.46 ± 1.21	**0.0143**	1 ± 0.04 vs 1.99 ± 0.42	**0.0286**	4.46 ± 1.21 vs 1.99 ± 0.42	0.1143
	EphB3	1 ± 0.15 vs 1.05 ± 0.20	0.3429	1 ± 0.15 vs 7.28 ± 1.35	**0.0143**	1 ± 0.15 vs 10.12 ± 1.80	**0.0286**	7.28 ± 1.35 vs 10.12 ± 1.80	0.2000
	Tcf7	1 ± 0.05 vs 3.32 ± 1.25	**0.0143**	1 ± 0.05 vs 3.28 ± 0.42	**0.0143**	1 ± 0.05 vs 11.16 ± 1.94	**0.0286**	3.28 ± 0.42 vs 11.16 ± 1.94	**0.0286**
	Mif1	1 ± 0.13 vs 3.04 ± 0.75	0.1000	1 ± 0.13 vs 2.55 ± 0.77	0.1000	1 ± 0.13 vs 13.36 vs 5.50	**0.0286**	2.55 ± 0.77 vs 13.36 vs 5.50	**0.0286**
	Sox9	1 ± 0.15 vs 3.24 ± 0.92	0.1000	1 ± 0.15 vs 4.56 ± 0.79	**0.0143**	1 ± 0.15 vs 18.37 ± 4.98	**0.0286**	4.56 ± 0.79 vs 18.37 ± 4.98	**0.0286**
	Sox17	1 ± 0.13 vs 11.96 ± 5.67	**0.0286**	1 ± 0.13 vs 119.8 ± 20.54	**0.0143**	1 ± 0.13 vs 90.65 ± 39.26	**0.0286**	119.8 ± 20.54 vs 90.65 ± 39.26	0.4286
	Tiam1	1 ± 0.06 vs 1.25 ± 0.53	0.4286	1 ± 0.04 vs 5.04 ± 0.47	**0.0143**	1 ± 0.06 vs 8.49 ± 4.61	0.3143	5.04 ± 0.47 vs 8.49 ± 4.61	0.3143
	Wif1	1 ± 0.07 vs 2.14 ± 0.88	0.5000	1 ± 0.07 vs 4.95 ± 0.80	**0.0143**	1 ± 0.07 vs 3.41 ± 1.04	**0.0286**	4.95 ± 0.80 vs 3.41 ± 1.04	0.2000
	CD44	1 ± 0.10 vs 1.20 ± 0.16	0.1000	1 ± 0.10 vs 7.15 ± 1.18	**0.0143**	1 ± 0.10 vs 10.23 ± 2.99	**0.0286**	7.15 ± 1.18 vs 10.23 ± 2.99	0.3143

Table 3.2 Raw fold change in gene expression of cell type, stem cell and Wnt target gene markers in *AhCre Apc*$^{+/+}$ and *Apc*$^{fl/fl}$ intestinal tissue exposed to control and 10% freeze-dried BRB diets

Cohorts consisted of 3 – 4 mice. Significance of results (p value = ≤ 0.05) was determined using one-tailed Mann Whitney U statistical test. SEM = standard error of mean.

	AhCre Mouse Model			
	Apc $^{+/+}$ **Control vs *Apc*** $^{+/+}$ **BRB**	***Apc*** $^{+/+}$ **Control vs *Apc*** $^{fl/fl}$ ***Control***	***Apc*** $^{+/+}$ **Control vs *Apc*** $^{fl/fl}$ **BRB**	***Apc*** $^{fl/fl}$ **Control vs *Apc*** $^{fl/fl}$ **BRB**
	Effect of BRBs on normal intestine	Effect of acute loss of *Apc*	Rescue of *Apc* $^{fl/fl}$ to wildtype?	Effect of BRBs on pre-malignant intestine
Cell number	↔	↑	↑	↑
Mitosis	↑	↑	↑	↑
Ki67	↔	↑	↑	↔
BrdU no. 2 hrs	N/D	N/D	N/D	↑
BrdU no. 24 hrs	N/D	N/D	N/D	↑
BrdU migration	N/D	Moved 10 positions	N/D	Moved 25 positions
Apoptosis	↑	↑	↑	↑
CC3	↔	↑	↑	↑
Enteroendocrine no.	↑	↓	↔	↑
Goblet cell no.	↔	↓	↓	↑
Paneth cell	↔	↑	↑	↓
Paneth cell position	↔	Mislocalised	Mislocalised	Mislocalised but closer to crypt base
Lysozyme1	↓	↑	↔	↓
Synaptophysin	↑	↔	↑	↑
Muc2	↔	↔	↓	↓

	VillinCreER ^{T2} *Mouse Model*			
	Apc $^{+/+}$ **Control vs *Apc*** $^{+/+}$ **BRB**	***Apc*** $^{+/+}$ **Control vs *Apc*** $^{fl/fl}$ ***Control***	***Apc*** $^{+/+}$ **Control vs *Apc*** $^{fl/fl}$ **BRB**	***Apc*** $^{fl/fl}$ **Control vs *Apc*** $^{fl/fl}$ **BRB**
	Effect of BRBs on normal intestine	Effect of acute loss of *Apc*	Rescue of *Apc* $^{fl/fl}$ to wildtype?	Effect of BRBs on pre-malignant intestine
Cell number	↔	↑	↑	↔
Mitosis	↓	↑	↑	↓
Ki67	↔	↑	↑	↔
BrdU no. 2 hrs	↔	↑	↑	↔
BrdU no. 24 hrs	N/D	N/D	N/D	N/D
BrdU migration	N/D	N/D	N/D	N/D
Apoptosis	↔	↑	↑	↑
CC3	↑	↑	↑	↑
Enteroendocrine no.	↑	↓	↓	↑
Goblet cell no.	↔	↓	↓	↑
Paneth cell	↔	↑	↑	↑
Paneth cell position	↔	Mislocalised	Mislocalised	Mislocalised
Lysozyme1	↓	↑	↔	↓
Synaptophysin	↔	↔	↔	↑
Muc2	↔	↓	↓	↔

Table 3.3 Summary of observed changes in histological and IHC markers in *AhCre* and *VillinCreER*^{T2} *Apc*$^{+/+}$ and *Apc*$^{fl/fl}$ intestinal sections following intervention with control and 10% freeze-dried BRB diets

↔ = no change; ↓large blue arrow = significant decrease; ↓small blue arrow = non-significant decrease; ↑ large red arrow = significant increase; ↑small red arrow = non-significant increase; N/D = no data.

		AhCre Mouse Model			
		Apc $^{+/+}$ **Control vs** ***Apc*** $^{+/+}$ **BRB**	***Apc*** $^{+/+}$ **Control vs** ***Apc*** $^{fl/fl}$ ***Control***	***Apc*** $^{+/+}$ **Control vs** ***Apc*** $^{fl/fl}$ **BRB**	***Apc*** $^{fl/fl}$ **Control vs** ***Apc*** $^{fl/fl}$ **BRB**
		Effect of BRBs on normal intestine	Effect of acute loss of *Apc*	Rescue of *Apc* $^{fl/fl}$ to wildtype?	Effect of BRBs on pre-malignant intestine
Active Cycling Stem cell markers	***Lgr5***	↓	↑	↑	↓
	Olfm4	↓	↑	↔	↓
	Ascl2	↓	↑	↑	↑
	Rnf43	↓	↑	↑	↑
	Tnfrsf19	↑	↑	↑	↑
	Msi1	↑	↑	↑	↑
	CD133	↓	↑	↑	↑
+4 Stem Cell Markers	***Bmi1***	↑	↑	↑	↑
	Lrig1	↑	↑	↑	↑

		VillinCreER ^{T2}			
		Apc $^{+/+}$ **Control vs** ***Apc*** $^{+/+}$ **BRB**	***Apc*** $^{+/+}$ **Control vs** ***Apc*** $^{fl/fl}$ ***Control***	***Apc*** $^{+/+}$ **Control vs** ***Apc*** $^{fl/fl}$ **BRB**	***Apc*** $^{fl/fl}$ **Control vs** ***Apc*** $^{fl/fl}$ **BRB**
		Effect of BRBs on normal intestine	Effect of acute loss of *Apc*	Rescue of *Apc* $^{fl/fl}$ to wildtype?	Effect of BRBs on pre-malignant intestine
Active Cycling Stem cell markers	***Lgr5***	↔	↑	↑	↑
	Olfm4	↔	↔	↑	↑
	Ascl2	↔	↑	↑	↑
	Rnf43	↓	↑	↑	↑
	Tnfrsf19	↓	↑	↑	↑
	Msi1	↔	↑	↑	↔
	CD133	N/D	N/D	N/D	N/D
+4 Stem Cell Markers	***Bmi1***	↑	↑	↑	↑
	Lrig1	↓	↑	↑	↔

Table 3.4 Summary of observed changes in gene expression of intestinal stem cell markers in *AhCre* and *VillinCreER*^{T2} *Apc*$^{+/+}$ and *Apc*$^{fl/fl}$ intestinal tissue following intervention with control and 10% freeze-dried BRB diets

↔ = no change; ↓large blue arrow = significant decrease; ↓small blue arrow = non-significant decrease; ↑ large red arrow = significant increase; ↑small red arrow = non-significant increase; N/D = no data.

		AhCre Mouse Model			
		Apc $^{+/+}$ Control vs *Apc* $^{+/+}$ BRB	*Apc* $^{+/+}$ Control vs *Apc* $^{fl/fl}$ *Control*	*Apc* $^{+/+}$ Control vs *Apc* $^{fl/fl}$ BRB	*Apc* $^{fl/fl}$ Control vs *Apc* $^{fl/fl}$ BRB
		Effect of BRBs on normal intestine	Effect of acute loss of *Apc*	Rescue of *Apc* $^{fl/fl}$ to wildtype?	Effect of BRBs on pre-malignant intestine
Wnt target genes	*CyclinD1*	↓	↑	↑	↑
	Axin2	↑	↑	↑	↑
	c-myc	↑	↑	↑	↑
	EphB2	↓	↑	↑	↓
	EphB3	↔	↑	↑	↑
	Tcf7	↑	↑	↑	↑
	Mif1	↑	↑	↑	↑
	Sox9	↑	↑	↑	↑
	Sox17	↑	↑	↑	↓
	Tiam1	↑	↑	↑	↑
	Wif1	↑	↑	↑	↓
	CD44	↑	↑	↑	↑

		VillinCreER ^{T2} *Mouse Model*			
		Apc $^{+/+}$ Control vs *Apc* $^{+/+}$ BRB	*Apc* $^{+/+}$ Control vs *Apc* $^{fl/fl}$ *Control*	*Apc* $^{+/+}$ Control vs *Apc* $^{fl/fl}$ BRB	*Apc* $^{fl/fl}$ Control vs *Apc* $^{fl/fl}$ BRB
		Effect of BRBs on normal intestine	Effect of acute loss of *Apc*	Rescue of *Apc* $^{fl/fl}$ to wildtype?	Effect of BRBs on pre-malignant intestine
Wnt target genes	*CyclinD1*	↔	↔	↔	↔
	Axin2	↔	↑	↑	↑
	c-myc	↔	↑	↑	↓
	EphB2	↔	↑	↑	↔
	EphB3	↓	↑	↑	↔
	Tcf7	↔	↑	↑	↓
	Mif1	↔	↑	↑	↑
	Sox9	↑	↑	↑	↑
	Sox17	N/D	N/D	N/D	N/D
	Tiam1	N/D	N/D	N/D	N/D
	Wif1	N/D	N/D	N/D	N/D
	CD44	N/D	N/D	N/D	N/D

Table 3.5 Summary of observed changes in gene expression of Wnt target gene markers in *AhCre* and *VillinCreER*^{T2} *Apc*$^{+/+}$ and *Apc*$^{fl/fl}$ intestinal tissue following intervention with control and 10% freeze-dried BRB diets

↔ = no change; ↓large blue arrow = significant decrease; ↓small blue arrow = non-significant decrease; ↑ large red arrow = significant increase; ↑small red arrow = non-significant increase; N/D = no data.

3.2.6 Examining homeostasis and the consequence of acute loss of *Apc* driven by the *VillinCreER^{T2}* transgene in the context of BRB diet

The findings in the *AhCre* mouse models suggested that BRBs have anti-tumourigenic properties at the early stages of intestinal tumourigenesis. To further evaluate on these findings, the *VillinCreER^{T2} Apc$^{+/+}$* and *Apc$^{fl/fl}$* mouse models were used. This model differs from the *AhCre* model such that, upon induction, *Apc* is lost from the entire intestinal epithelium (crypt and villus) including the Paneth cells, in contrast to the *AhCre* transgene which recombines only in the crypt epithelium excluding the Paneth cells. Despite the differences in sites of expression of these Cre lines, the phenotypes are similar (Andreu *et al.* 2005).

The phenotype of both control and experimental mice were characterised using the same endpoints as the *AhCre* mouse model, with the following differences. Aged matched 12 - 13 weeks old, (45 - 52 days younger than *AhCre* mice) *VillinCreER^{T2} Apc$^{+/+}$* and *VillinCreER^{T2} Apc$^{fl/fl}$* mice were fed *ad libitum* on either the control diet, AIN76A pellets (rather than the standard mouse chow used in the *AhCre* study) or a 10% freeze-dried BRB powder supplemented in AIN76A pellets. A pelleted diet rather than a powdered version was used for logistical reasons. The powdered diet was wasteful as it dropped from the feeding troughs and mixed with the bedding, which also lowered the cleanliness of the cages. *VillinCreER^{T2}* mice were sacrificed at day 4 post induction, rather than day 5, as previous studies found that at this time point, *Apc* loss resulted in a dramatic enlargement of the crypt compartment, accompanied with an increase in proliferation, apoptosis and a diminished cell migration. These mice also presented with symptoms of severe illness within 4 days and were culled to prevent further suffering (Andreu *et al.* 2005). The method of Cre activation was also different; Cre expression (ISC and progenitor compartment) in *AhCre* mice required the presence of βNF while Cre expression under the *Villin* promoter (entire intestinal epithelium) was driven by tamoxifen injection. Tamoxifen can be less well tolerated in mice than βNF, and so for this reason *VillinCreER^{T2}* mice were injected with a reduced dose of tamoxifen at 3 x 60 mg/kg rather than 80 mg/kg as with βNF. The different inducing concentration could affect the recombination efficiency and affect gene loss in certain cell types differently (Parry *et al.* 2013). RNA was extracted from isolated epithelial cells rather than from whole frozen tissue for gene expression analyses, which leaves a purer extract of epithelial cells without the underlying muscle and stromal cells. Table 3.6 and Table 3.7 represents the data of the findings of the short-term effects of 10% freeze-dried BRB diet on the normal intestine, in *Apc* deficient intestine and the effects of acute loss of *Apc* in the context of the *VillinCreER^{T2}* mouse model.

In wildtype mice the key findings were:

- 10% BRB diet reduced proliferation and increased cell death whilst maintaining the size of the crypt (Figure S 8.3 and Figure S 8.4).
- Paneth and goblet cells were not affected by BRB diet however, the number of enteroendocrine cells was increased (Figure S 8.5, Figure S 8.6 and Figure S 8.7).
- The ISC populations were not altered as determined by qRT-PCR gene expression analysis (Figure S 8.8).

The key findings in *VillinCreER*^{T2} *Apc*$^{fl/fl}$ mice were:

- BRB diet inhibited proliferation and increased cell death (Figure S 8.3 and Figure S 8.4).
- BRBs partially rescued enteroendocrine and goblet cell differentiation but Paneth cell differentiation remained augmented and mis-localised (Figure S 8.5, Figure S 8.6 and Figure S 8.7).
- Expression of putative stem cell markers were increased in BRB exposed *Apc*$^{fl/fl}$ deficient crypts (Figure S 8.8).
- *Sox9* gene expression was up-regulated in *Apc* deficient intestine as a result of BRB intervention (Figure S 8.9).

A summary of these findings can be found in Table 3.3, Table 3.4 and Table 3.5.

VillinCreER^{T2} Mouse Model								
Cell type/marker	***Apc$^{+/+}$* Control vs *Apc$^{+/+}$* BRB n = 5**		***Apc$^{+/+}$* Control vs *Apc$^{fl/fl}$* control n = 5**		***Apc$^{+/+}$* Control vs *Apc$^{fl/fl}$* BRB n = 4/5**		***Apc$^{fl/fl}$* Control vs *Apc$^{fl/fl}$* BRB n = 4/5**	
	Average Number (± SEM)	**P value**	**Average Number (± SEM)**	**P value**	**Average Number (± SEM)**	**P value**	**Average Number (± SEM)**	**P value**
Cell number	24.64 ± 0.78 vs 24.13 ± 0.43	0.8413	24.64 ± 0.78 vs 61.57 ± 4.93	**0.0079**	24.64 ± 0.78 vs 66.68 ± 2.12	**0.0079**	61.57 ± 4.93 vs 66.68 ± 2.12	0.3095
Mitosis	2.28 ± 0.12 vs 1.92 ± 0.26	**0.0159**	2.28 ± 0.12 vs 8.44 ± 1.15	**0.0079**	2.28 ± 0.12 vs 5.56 ± 1.42	**0.0079**	8.44 ± 1.15 vs 5.56 ± 1.42	**0.0159**
Ki67	42.55 ± 1.97 vs 44.34 ± 1.33	0.5476	42.55 ± 1.97 vs 84.72 ± 2.14	**0.0079**	42.55 ± 1.97 vs 82.91 ± 3.46	**0.0079**	84.72 ± 2.14 vs 82.91 ± 3.46	0.7381
BrdU 2 hrs	9.82 ± 0.72 vs 9.94 ± 0.62	>0.9999	9.82 ± 0.72 vs 33.40 ± 0.85	**0.0079**	9.82 ± 0.72 vs 32.36 ± 1.66	**0.0079**	9.82 ± 0.72 vs 32.36 ± 1.66	0.7381
BrdU 24 hrs	N/D		N/D		N/D		N/D	
Apoptosis	1.05 ± 0.33 vs 0.80 ± 0.08	>0.9999	1.05 ± 0.33 vs 2.98 ± 0.47	**0.0317**	1.05 ± 0.33 vs 5.52 ± 0.45	**0.0079**	2.98 ± 0.47 vs 5.52 ± 0.45	**0.0159**
CC3	2.21 ± 0.26 vs 3.24 ± 0.21	**0.0159**	2.21 ± 0.26 vs 5.96 ± 0.75	**0.0079**	2.21 ± 0.26 vs 14.18 ± 0.58	**0.0079**	5.96 ± 0.75 vs 14.18 ± 0.58	**0.0079**
Enteroendocrine cells	4.74 ± 0.18 vs 5.35 ± 0.12	**0.0476**	4.74 ± 0.18 vs 2.72 ± 0.10	**0.0079**	4.74 ± 0.18 vs 4.10 ± 0.33	**0.0794**	2.72 ± 0.10 vs 4.10 ± 0.33	**0.0079**
Goblet cells	28.41 ± 1.34 vs 28.55 ± 1.42	0.8413	28.41 ± 1.34 vs 5.78 ± 0.52	**0.0079**	28.41 ± 1.34 vs 11.26 ± 0.90	**0.0079**	5.78 ± 0.52 vs 11.26 ± 0.90	**0.0079**
Paneth cells	2.05 ± 0.14 vs 2.22 ± 0.11	0.2778	2.05 ± 0.14 vs 5.08 ± 0.54	**0.0079**	2.05 ± 0.14 vs 7.00 ± 1.36	**0.0079**	5.08 ± 0.54 vs 7.00 ± 1.36	0.4206

Table 3.6 Raw data counts from histological and IHC stained *VillinCreER^{T2} Apc$^{+/+}$* and *Apc$^{fl/fl}$* intestinal sections exposed to control and 10% freeze-dried BRB powdered diets

Cohorts consisted of 4 – 5 mice. Significance of results (p value = ≤ 0.05) was determined using two-tailed Mann Whitney U statistical test. SEM = standard error of mean; N/D = no data.

		VillinCreER^{T2} Mouse Model							
	Gene	***Apc$^{+/+}$* Control vs *Apc$^{+/+}$* BRB n = 4/5**		***Apc$^{+/+}$* Control vs *Apc$^{fl/fl}$* control n = 4/5**		***Apc$^{+/+}$* Control vs *Apc$^{fl/fl}$* BRB n = 4/5**		***Apc$^{fl/fl}$* Control vs *Apc$^{fl/fl}$* BRB n = 4/5**	
		Average Fold Change (± SEM)	**P value**	**Average Fold Change (± SEM)**	**P value**	**Average Fold Change (± SEM)**	**P value**	**Average Fold Change (± SEM)**	**P value**
Cell Type Markers	*Lysozyme1*	1 ± 0.04 vs 0.55 ± 0.26	0.1508	1 ± 0.04 vs 1.21 ± 0.24	0.5476	1 ± 0.04 vs 1.03 ± 0.36	0.8254	1.21 ± 0.24 vs 1.03 ± 0.36	0.9048
	Muc2	1 ± 0.03 vs 0.95 ± 0.22	0.6905	1 ± 0.03 vs 0.21 ± 0.06	**0.0079**	1 ± 0.03 vs 0.16 ± 0.03	**0.0079**	0.21 ± 0.06 vs 0.16 ± 0.03	0.8413
	Synaptophysin	1 ± 0.01 vs 0.98 ± 0.05	0.8413	1 ± 0.01 vs 1 ± 0.13	0.6905	1 ± 0.01 vs 1.21 ± 0.17	0.6667	1 ± 0.13 vs 1.21 ± 0.17	0.3095
Active Cycling Stem Cell Markers	*Lgr5*	1 ± 0.04 vs 0.84 ± 0.10	0.2222	1 ± 0.04 vs 6.85 ± 1.48	**0.0079**	1 ± 0.04 vs 17.86 ± 3.90	**0.0159**	6.85 ± 1.48 vs 17.86 ± 3.90	**0.0317**
	Olfm4	1 ± 0.15 vs 0.77 ± 0.18	0.4206	1 ± 0.15 vs 1.03 ± 0.15	0.8413	1 ± 0.15 vs 2.48 ± 0.17	**0.0159**	1.03 ± 0.15 vs 2.48 ± 0.17	**0.0159**
	Ascl2	1 ± 0.02 vs 0.80 ± 0.12	0.0952	1 ± 0.02 vs 5.99 ± 0.77	**0.0079**	1 ± 0.02 vs 7.91 ± 0.53	**0.0159**	5.99 ± 0.77 vs 7.91 ± 0.53	0.1905
	Rnf43	1 ± 0.02 vs 0.79 ± 0.14	0.2222	1 ± 0.02 vs 4.44 ± 0.30	**0.0079**	1 ± 0.02 vs 6.38 ± 0.95	**0.0079**	4.44 ± 0.30 vs 6.38 ± 0.95	0.1508
	Tnfrsf19	1 ± 0.01 vs 0.78 ± 0.15	0.1508	1 ± 0.01 vs 25.88 ± 5.22	**0.0079**	1 ± 0.01 vs 41.08 ± 5.55	**0.0079**	25.88 ± 5.22 vs 41.08 ± 5.55	0.1508
	Msi1	1 ± 0.02 vs 0.92 ± 0.18	0.8413	1 ± 0.02 vs 5.25 ± 1.21	**0.0079**	1 ± 0.02 vs 5.50 ± 0.61	**0.0079**	5.25 ± 1.21 vs 5.50 ± 0.61	0.5476
	CD133	N/D		N/D		N/D		N/D	
+4 Stem Cell Markers	*Bmi1*	1 ± 0.04 vs 1.20 ± 0.13	0.1508	1 ± 0.04 vs 2 ± 0.33	**0.0079**	1 ± 0.04 vs 2.51 ± 0.34	**0.0079**	2 ± 0.33 vs 2.51 ± 0.34	0.3095
	Lrig1	1 ± 0.01 vs 0.83 ± 0.13	0.1508	1 ± 0.01 vs 1.32 ± 0.26	0.6905	1 ± 0.01 vs 1.41 ± 0.19	0.1508	1.32 ± 0.26 vs 1.41 ± 0.19	0.6905
Wnt target Genes	*CyclinD1*	1 ± 0.07 vs 0.93 ± 0.17	>0.9999	1 ± 0.07 vs 0.85 ± 0.23	0.6905	1 ± 0.07 vs 0.91 ± 0.10	0.3968	0.85 ± 0.23 vs 0.91 ± 0.10	0.7302
	Axin2	1 ± 0.02 vs 0.86 ± 0.12	0.2222	1 ± 0.02 vs 4.07 ± 0.65	**0.0079**	1 ± 0.02 vs 6.28 ± 0.76	**0.0079**	4.07 ± 0.65 vs 6.28 ± 0.76	0.0556
	c-myc	1 ± 0.02 vs 1.10 ± 0.22	0.1508	1 ± 0.02 vs 5.75 ± 1.68	**0.0079**	1 ± 0.02 vs 4.90 ± 0.73	**0.0079**	5.75 ± 1.68 vs 4.90 ± 0.73	>0.9999
	EphB2	1 ± 0.02 vs 1.01 ± 0.12	0.6905	1 ± 0.02 vs 2.15 ± 0.55	0.2222	1 ± 0.02 vs 2.55 ± 0.26	**0.0079**	2.15 ± 0.55 vs 2.55 ± 0.26	0.8413
	EphB3	1 ± 0.05 vs 0.64 ± 0.11	**0.0317**	1 ± 0.05 vs 4.60 ± 1.27	**0.0079**	1 ± 0.05 vs 5.01 ± 1.11	**0.0159**	4.60 ± 1.27 vs 5.01 ± 1.11	0.9048
	Tcf7	1 ± 0.03 vs 1.14 ± 0.37	0.6857	1 ± 0.03 vs 9.15 ± 2.72	**0.0159**	1 ± 0.03 vs 5.75 ± 0.84	**0.0286**	9.15 ± 2.72 vs 5.75 ± 0.84	0.5556
	Mif1	1 ± 0.04 vs 1.19 ± 0.32	>0.9999	1 ± 0.04 vs 7.06 ± 2.41	**0.0159**	1 ± 0.04 vs 8.72 ± 2.55	**0.0286**	7.06 ± 2.41 vs 8.72 ± 2.55	0.5556
	Sox9	1 ± 0.05 vs 1.55 ± 0.33	0.3429	1 ± 0.05 vs 1.74 ± 0.29	**0.0317**	1 ± 0.05 vs 4.61 ± 0.84	**0.0286**	1.74 ± 0.29 vs 4.61 ± 0.84	**0.0317**
	Sox17	N/D		N/D		N/D		N/D	
	Tiam1	N/D		N/D		N/D		N/D	
	Wif1	N/D		N/D		N/D		N/D	
	CD44	N/D		N/D		N/D		N/D	

Table 3.7 Raw fold change in gene expression of cell type, stem cell and Wnt target gene markers in *VillinCreER^{T2} Apc$^{+/+}$* and *Apc$^{fl/fl}$* intestinal tissue exposed to control and 10% freeze-dried BRB diets

Cohorts consisted of 4 – 5 mice. Significance of results (p value = ≤ 0.05) was determined using two-tailed Mann Whitney U statistical test. SEM = standard error of mean; N/D = no data.

3.3 Discussion

Wnt signalling is a key pathway in intestinal homeostasis and deregulation of this pathway through the loss of the APC tumour suppressor is a key event in the initiation and development of intestinal tumourigenesis. It is also widely known that diet plays a significant role in the aetiology of many human diseases, in particular colorectal tumourigenesis. Previous studies have indicated a protective role for bioactive phytochemicals, such as the polyphenols (anthocyanins), found in high levels in BRBs (Stoner 2009), but despite this there has been little research on the effect of BRBs on the normal and malignant ISC populations, the cells thought to be the 'cell of origin' of many cancers. Taking into consideration this previous work, it was hypothesised that BRBs may be an attractive chemopreventative therapeutic by suppressing Wnt-driven tumourigenesis through alteration of the Wnt signature and an altered ISC compartment. However, before the potential benefits of BRB at the earliest stages of tumourigenesis could be addressed, it was important to first evaluate their effect, if any, on intestinal homeostasis.

3.3.1 Evaluating the effect of BRBs on intestinal homeostasis

A key aim of this work was determine whether the addition of BRB to the diet had an impact on normal intestinal homeostasis. This was investigated in two mouse models, *AhCre* $Apc^{+/+}$ and *VillinCreER*^{T2} $Apc^{+/+}$. To control for the effects of Cre expression or response to induction agents both models were appropriately induced (enabling subsequent comparison to be made with mice co ntaining a loxP flanked *Apc*). Overall, short-term feeding of BRBs had no major detrimental effects on intestinal homeostasis in either model. However, there were some significant differences in data obtained from the two models, which could reflect the experimental design as discussed below.

These differences are likley attributable to external factors in relation to the diet as the cohorts of BRB fed mice were compared to appropriately treated control mice. 1) The control diet used in the *AhCre* studies was not basal matched to the BRB diet. It is possible that this could either, exaggerate the effects of BRB treatment, or the phenotypic differences could be attributable to other components of the BRB diet. 2) The animal studies for the *AhCre* powdered BRB experiment was started in 2008, whereas the *VillinCreER*^{T2} studies began in 2013. Due to time elapsed between these experiments it was necessary to buy a new diet as the shelf life of BRB diets range between 3 - 6 months depending on storage conditions. The production of the diets in different years could result in different chemopreventive potential of the two diets, possibly due to differences in polyphenol content (Wang 2006). If this is the case, it could be argued that the pelleted BRB diet used in the *VillinCreER*^{T2} experiments may have less polyphenol content and thus did not elicit the same effect on Wnt signalling and stem cell dynamics. 3) Although all animals were maintained on an outbred

background, the mice used in the *AhCre* studies were from different colonies and backgrounds. This could also explain the large variations between individual animals within cohorts. 4) The number of animals in each cohort utilised in these studies was relatively low (n = 3 - 5). Previous work using genetic models indicated that this number would be sufficient to confidently detect changes in the intestine. In a dietary study, where changes might be more subtle, this number might be too small to consistently detect changes in both models.

While feeding of BRBs resulted in no perturbations in the gross histology of the small intestine in either wildtype model, cell death was consistently increased. Differentiation was not grossly altered as evidenced by the normal representation of the majority of cell types. However, the number of enteroendocrine cells was increased, again in both models. The enteroendocrine cells are often described as the chemo sensors of the intestinal epithelium and dietary modifications have previously been shown to affect this population of cells (Moran-Ramos *et al.* 2012; Gribble and Reimann 2016). For example, the small intestines of rats fed a high-fat diet (HFD), which has been shown to enhance tumourigenesis (Beyaz *et al.* 2016), were lacking subpopulations of enteroendocrine cells which were responsible for inhibition of food intake and gastric acid production (Sakar *et al.* 2014). This could alter the hormone balance and ultimately limit the effectiveness of homeostasis and signalling pathways that would normally restrain eating. Although the specific populations of enteroendocrine cells were not determined in this thesis, it could be hypothesised that this population of cells were up-regulated in response to a change in dietary composition. This subsequently maintained the normal number of cells per crypt structure by counteracting the increase in cell death, and maintained the normal homeostatic and motility functions of the gut. Furthermore, the BRB-induced increase in cell death may change the cancer risk in these models. Cell death is the mechanism by which damaged or abnormal cells are lost from the tissue. Cancer cells employ several mechanisms to evade this process (Fernald and Kurokawa 2013) and so agents which can limit a cancer cells resistance to apoptosis will have valuable benefits. Although the studies described herein have not determined which cells underwent apoptosis, it could be hypothesised that cell death occurring in the stem cell population or progenitor cells would lower the tumourigenic potential should a mutation occur. In addition, it could also be that BRBs increase the sensitivity of these cells to damage which results in more apoptosis. It has been previously shown that a different dietary compound, curcumin the active component in turmeric and its derivatives sensitise resistant CSCs to chemo and radio therapies (Ramasamy *et al.* 2015). It may be possible that BRBs work in a similar way to sensitise cells to death. A decrease in cell proliferation was observed in the *VillinCreER*^{T2} model but not in the *AhCre* model. This could be in accordance with the increase in cell death, such that BRBs limit the risk of mutations being retained within the normal intestine by reducing the number of highly proliferative daughters. BRB feeding also

reduced the expression of important stem cell markers in the *AhCre* mouse while expression of these three genes were not altered in the *VillinCreER^{T2}* mouse. This could infer that BRBs limit the activity or reduce the number of the active stem cells, while not detrimentally altering gut architecture or function. It was also found that BRBs alter Wnt signalling but to a lesser extent in the *VillinCreER^{T2}* model.

Overall, the data suggested that BRB intervention induced relatively small changes and did not grossly disturb the normal homeostatic function of normal intestinal tissue. The consistent changes between these models are likely to be a true reflection of the effect of BRBs on wildtype intestine, while the differences observed between models require further investigation to determine the actual extent of the effect. It is also important to note that while mice are an excellent platform to study the links between diet, genetics and cancer they are not human. There are a number of genetically modified murine models that are powerful and useful tools for studying the mechanism of human disease and homeostasis however, the inherent physiological differences between mouse and man limits the use of animal studies to suitably predict human responses.

Taken together, these findings indicate that BRBs are well tolerated and maintain intestinal homeostasis. Thus, if BRBs were used for chemopreventative strategies in CRC, there should be no adverse effects on the normal intestinal tissue in the short-term. While this holds promise, there are differences between mouse and man so further work will be required.

3.3.2 Evaluating the effect of BRBs on acute loss of *Apc* in the intestine

Another key aim of this work was to evaluate the effects of BRB in the diet at the earliest stages of colorectal tumourigenesis. Previous studies have reported that oral consumption of BRBs are well tolerated by humans and have been shown to have protective effects at the early stages of oral dysplasia (Shumway *et al*. 2008; Mallery *et al.* 2014). However, animal and human based studies of the intestine have only studied the beneficial effects of BRBs at later stages of tumour formation (Bi *et al.* 2010; Wang *et al.* 2014). Based on these data, it was predicted that, in the models presented here, BRBs would exert protective effects at the earliest stages of tumourigenesis. Moreover, due to the evidence that ISCs are the 'cell of origin' of CRC (Barker *et al.* 2009), it is also crucial to understand how diet influences the ISCs, which has not currrently been addressed in BRB studies. The earliest stages of intestinal cancer have been well documented in the context of homozygous deletion of *Apc* in the intestinal epithelium as described previously (Sansom *et al.* 2004; Andreu *et al.* 2005). This thesis supports the phenotype typical of *Apc* loss. The present study was conducted, therefore, to determine whether BRBs were able to prevent the phenotype typical of acute *Apc* loss within the intestinal epithelium, to determine whether BRBs influence ISCs, and to what extent the phenotype was rescued in relation to wildtype mice.

Two mouse models, *AhCre Apc*$^{fl/fl}$ and *VillinCreER*^{T2} *Apc*$^{fl/fl}$, were utilised to investigate the chemopreventative effects of BRBs at the earliest stages of tumourigenesis with particular focus on the ISC population. The mouse models used resulted in homozygous recombination of the *Apc* allele, when injected with the relevant inducing agent. The major difference was *Ah*-drives recombination in the ISC and progenitor compartment, while *Villin* drove Cre in the entire intestinal epithelium including the Paneth cells.

Both the *AhCre Apc*$^{fl/fl}$ and *VillinCreER*^{T2} *Apc*$^{fl/fl}$ models showed changes indicating that ISC function or number may be altered by BRBs. One model (*VillinCreER*^{T2} *Apc*$^{fl/fl}$) showed a decrease in proliferation with an increased expression of ISC associated genes, with a concordant up-regulation in Wnt target genes. The other model (*AhCre Apc*$^{fl/fl}$) showed an increased cell cycle and migratory pattern, with decreased expression of ISC markers but an increase in Wnt targets. Additionally, both models showed that short-term feeding of BRBs partially attenuated the crypt-progenitor phenotype by reinstating differentiation and inducing cell death, processes which are associated with tumour inhibition. Enhanced cell death by BRB administration is consistent with previously published work that showed BRBs or its AC derivatives induced cell death in preneoplastic oesophageal tissue (Wang *et al.* 2009) and in premalignant oral lesions in humans (Mallery *et al*. 2008; Mallery *et al.* 2014). Additionally, increased cell death by BRBs has been reported in cell lines of rat esophageal epithelial cells (Zikri *et al.* 2009), human cell lines of oral SCC (Rodrigo *et al.* 2006), cervical cancer (Zhang *et al.* 2011) and CRC (Wang *et al.* 2013b), in animal models and humans of Wnt-driven CRC and FAP (Wang *et al.* 2013c; Wang *et al.* 2014). Although the majority of these studies investigated the role of BRBs in cancer settings rather than premalignant tissue, they provide compelling evidence that BRBs have pro-apoptotic properties in tumourigenesis. Taken together, these data indicate that BRBs may limit the risk of developing CRC by reducing the number of proliferative daughter cells.

Aside from the difference in diet regime as outlined in the wildtype discussion (Section 3.3.1), it is likely that the expression of Cre recombinase in different cell types influenced the data obtained. Although the consequences of Wnt deregulation in the differentiated region of the villus in the *VillinCreER*^{T2} *Apc*$^{fl/fl}$ model has not been characterised in this thesis, it has been previously reported that the crypt and villus react differently to Wnt/ β-catenin signalling. The immediate consequence of acute *Apc* loss in the crypt compartment resulted in severe changes, whereas *Apc* loss in the villus compartment, resulted in cells becoming resistant to morphological change and proliferation despite activation of the Wnt/ β-catenin signalling pathway (Andreu *et al.* 2005). The number of *Apc* deficient cells in the *VillinCreER*^{T2} model outweighs the number of *Apc* deficient cells in the *AhCre* model, thus it could be argued that any changes in the crypt compartment of *VillinCreER*^{T2} mice will be heavily influenced or even masked by the villus compartment. In addition, RNA and gene expression data in

the *VillinCreER*^{T2} model was extracted from whole epithelial cell extracts consisting of both the crypt and villus compartments and so may not be a true representation of the effects of BRB within the proliferative and stem cell zones due to loss of *Apc* within the villus.

BRBs partially restored enteroendocrine and goblet cell differentiation in both animal models utilised in this thesis. This is in contrast to previously published work that observed no alteration in goblet cell differentiation (Bi *et al.* 2010). However, the work published by Bi *et al.* (2010) evaluated the effect of BRBs on differentation in two tumour bearing murine models rather than the premaligant tissue described here. Furthermore, this body of work did not investigate other cell type populations and so did not provide an overall examination of intestinal differentation in the context of BRBs and *Apc* loss. *Apc* deficiency abrogated cell migration, such that mutated cells were retained within the crypt and not shed from the epithelium, potentially enabling tumour formation. Although only investigated in one model (*AhCre Apc*$^{fl/fl}$) due to time constraints, BRBs improved migration along the crypt-villus axis. This suggested that BRBs may elicit chemopreventative effects by enabling cell migration such that *Apc* deficient cells capable of initiating tumour formation are lost from the epithelium. In accordance with this,

Aside from regulating cell proliferation within intestinal crypts, EphB2 also functions to coordinate migration such that it maintains the normal crypt-villus architecture (Batlle *et al.* 2002). BRB feeding in *AhCre Apc*$^{fl/fl}$ mice resulted in a two-fold decrease in *EphB2* gene expression. A potential loss of genes that usually control cell position within the crypt-villus cells could result in cells usually confined to the certain areas localising to different regions and thus initiating migration along the crypt-villus axis, which in the context of Apc deficiency could eliminate transformed cells. However, this will need to be explored in more detail with a larger cohort size. The caveat to this experiment is that it did not provide insight in to the mechanism of how BRBs reinstall migration. Homeostasis and normal functioning of the small intestine is maintained by shedding of cells at the villus tip at the same rate as cell division at the crypt base. This is to ensure that the gut barrier is maintained at all times to prevent the entry of harmful microorganisms and toxins. In instances of inflammation which can predispose to cancer, the rate of cell shedding can exceed the rate at which new cells are generated (Guan *et al.* 2011a; Kiesslich *et al.* 2012). Previous studies have investigated this phenomenon to better understand the mechanisms involved in cell migration and found that cell shedding occurred in parallel to apoptosis in the context of an inflammatory response, specifically as a result of administration of the lipopolysaccharide (LPS) in mice (Williams *et al.* 2013). Thus it could be assumed that certain stimuli, in this instance presence of BRBs, resulted in epithelial cell apoptosis and warrant migration to repair the temporary gap formed when apoptotic cells are shed into the lumen. However, it was not possible to investigate this at the present time and so scoring of CC3 positive in the villus

tip for apoptotic and shed cells will need to be analysed in subsequent studies following the methods outlined by Williams *et al.* (2013). Additionally, it may be possible that, in the context of the *AhCre* model, *Apc* loss arrested the cell cycle at the G2/M checkpoint, which has been previously seen in the liver following Wnt activation (Feng *et al.* 2012). BRBs may initiate the transition to mitosis which could explain why BRB exposed *Apc* deficient crypts are larger and have more BrdU positive cells than the control treated crypts despite an increase in cell death. In support of this notion, it has recently been shown that the velocity of villus cell migration is tightly coupled to the rate of crypt cell production and in such mitotic pressure is the driving force for cell migration (Parker *et al.* 2017). In this instance, it is likely that BRBs increase proliferation to drive migration and thus shedding of *Apc* deficient cells to prevent initiation and progression of intestinal tumourigenesis. Future work will need to evaluate markers of the cell cycle to determine if BRBs initiate cell cycle progression in the context of *Apc* deficiency.

This thesis used proxy readouts (gene expression, cell types and migrations) to measure the effect of BRBs on ISC dynamics and Wnt signalling. However, these studies did not determine the intrinsic effect on a malignant stem cell population. Previous studies have proposed that ISCs are the cell of origin of CRC, as deletion of *Apc* specifically within the $Lgr5^+$ ISCs propagated tumour formation by repopulating the entire crypt and villus epithelium with *Apc* deficient cells (Barker *et al.* 2009). Although not well understood, diet-induced physiological cues are likely to influence ISC biology (Mihaylova *et al.* 2014). The effect of dietary components on the malignant ISC populations is at the core of cancer research and studies are beginning to provide insight on the mechanisms involved in dietary induced stem cell dynamics. Recent studies have shown that the $Lgr5^+$ stem cells are extremely sensitive to dietary factors. Natural polyphenols such as curcumin and long-chain polyunsaturated fatty acids (PUFAs) have been found, in animal models, to synergistically promote targeted apoptosis in DNA damaged $Lgr5^+$ stem cells and reduce nuclear β-catenin levels in ACF at the pretumour stage (Kim *et al.* 2016a). Epidemiological studies report a link between obesity and high fat diets to a heightened risk of developing intestinal cancer (Wu *et al.* 2016). A recent study found that high fat diet augmented the self-renewal ability of ISCs and enhanced the stemness and tumourigenic ability of progenitor cells. In addition, high fat diet resulted in more adenomas and carcinomas, possibly due to the fact there were more ISCs as a result of the diet (Beyaz *et al.* 2016). Due to the association of high fruit and fibre diets to reduced CRC risk, it could be predicted that BRBs have the opposite effects on stem cells than that of high fat diets.

The potential chemopreventative effects of BRBs may be explained by a reduction in gene expression of the active ISC markers in the *AhCre* system. Although this reduction in stem cell marker expression is not consistent with an increased proliferative index or Wnt target gene expression, it

may be possible that ISCs respond differently to other cells within the epithelium that are altered as a result of BRB exposure, as highlighted by the results from the *VillinCreER^{T2}* model. Gene expression of the main stem cell markers, *Lgr5* and *Olfm4*, were decreased in the *AhCre* model but up-regulated in the *VillinCreER^{T2}* model. This could imply that either, in the *AhCre* model the number of stem cells are reduced following BRB treatment, or the same number of stem cells exist but their expression is down-regulated or in the context of the *VillinCreER^{T2}* model, the number and/ or activity of malignant ISCs is enhanced. *Ascl2* is commonly up-regulated in the early stages of intestinal neoplasia. Previous studies have suggested a role of *Ascl2* in promoting proliferation and migration (Jubb *et al.* 2006). Thus, although *Ascl2* co-localises with *Lgr5* in the ISCs (van der Flier *et al.* 2009b), its up-regualtion in *Apc* deficient crypts exposed to BRB may be correlated with an increased proliferative and migration status, rather than an ISC signature. Additionally, BRBs have been shown to exert chemopreventative effects by alterating epigentic biomarkers and demethylating tumour supressor genes commonly silenced in CRC (Wang *et al.* 2011; Wang *et al.* 2013c). *Ascl2* is imprinted at the early stages of intestinal development (Tunster *et al.* 2016), and although it is not epigenetically imprinted in the adult murine intestine (van der Flier *et al.* 2009b), it may be possible that the nutri-epigentic effects of BRBs influence *Ascl2* gene expression.

BRBs induced alterations in expression of Wnt target genes in both models, with *Sox9* being consistently up-regulated. *Olfm4* and *Sox9* have been reported to have an antagonist effect on the Wnt signalling pathway (Bastide *et al.* 2007; Liu *et al.* 2016). In the context of Olfm4 as a Wnt repressor, it could be assumed that a reduction in *Olfm4* expression as a result of BRB treatment could limit the antagonistic effect on Wnt signalling and thus promote tumourigenesis. However, the "just right" model proposes that a specific level of Wnt activity is required for tumourigenesis and levels of Wnt signalling below or above this threshold compromises tumour development (Albuquerque *et al.* 2002). Thus, a reduction of *Olfm4* (and its repressive role) and an increase in Wnt target gene expression by BRBs could potentially increase Wnt signalling such that there is 'too much Wnt' incompatible for tumour initiation. Furthermore, *Olfm4* is also a direct target of the Notch signalling pathway and inhibition of Notch results in CBC loss, enhanced differentiation and apoptosis. *Olfm4* expression has been found to be dependent on Notch signalling, which maintains progenitor cells, and thus it could therefore be predicted that BRBs repress Notch signalling thereby reducing *Olfm4* gene expression and subsequently increasing the number of differentiated cells (VanDussen *et al.* 2012). It is evident that there is cross talk between Wnt and Notch signalling pathways and repression of one pathway could down-regulate the other. However, targets of the Notch signalling pathway will need to be investigated to evaluate the effects of BRBs on Notch's involvement in loss or gain of stem cell marker expression.

While this thesis has already outlined the logistical difference in control diet and potential influence of different BRB diet from different years, it is important to determine which model is most likely to represent true changes in the ISC population.

1) It is possible that the inconsistent stem cell marker expression levels between the two models may represent differential recombination efficiency within the ISC compartment. Directly comparing the effect of BRBs on the ISCs requires the same level of recombination within the two mouse models. It has been previously reported that in order to achieve similar recombination within the ISCs, both *AhCre* and *VillinCreER^{T2}* models required 3 x IP injections with 80 mg/kg over 24 hours of βNF and tamoxifen respectively (Parry *et al.* 2013). In the *VillinCreER^{T2}* model utilised herein, mice received 3 x IP 60 mg/kg tamoxifen as recent experiments using *VillinCreER^{T2} Apc$^{fl/fl}$* mice injected with 3 x 80 mg/kg tamoxifen presented with signs of illness much earlier than previously reported by Andreu *et al.* (2005). Thus, to enable mice to reach the desired endpoint (day 4 post induction) a lower dose of tamoxifen was administered. It is therefore possible that *Apc* recombination within the ISCs was less efficient in the *VillinCreER^{T2}* model than in the *AhCre* system, rendering it a less reliable system for modelling the effects of BRB on Wnt activated ISC populations.

2) As previous studies have outlined that the two models described here induce recombination in the ISC population (irrespective of recombination rate), the mechanisms underlying the different ISC response to BRB diet could be linked to the fact that the two Cre systems differentially drive recombination within other cell types. Cre expression under the control of the *VillinCreER^{T2}* transgene drives recombination in differentiated cells, most notably Paneth cells which constitute the ISC niche, whereas this population of cells is spared in the *AhCre* model (El Marjou *et al.* 2004; Ireland *et al.* 2004). The 'cancer stem cell' hypothesis proposes that only a subpopulation of cells i.e. stem cells, are capable of initiating and progressing tumourigenesis (Tan *et al.* 2006). It is also important to note that tumours are thought to arise from mutations which arise within a single ISC, rather than from mutations which occur globally through the tissue (Barker *et al.* 2009). In order to evaluate the real effect of BRB diet on ISCs in a tumour relevant model it is beneficial to analyse *Apc* loss in the ISCs alone, such that other cell types do not interfere with the stem cell dynamics that would normally occur following injury or mutation, especially if those cells influence the stem cell niche. In this instance, as the *VillinCreER^{T2}* model deletes *Apc* in the Paneth cell, the resulting Wnt-over activation within the ISC niche could negatively influence malignant ISC dynamics. This could therefore portray an enhanced stem cell marker expression that would have a

deleterious impact on the intestine and could potentiate tumourigenesis. This is in contrast to the *AhCre* model, in which the Paneth cells are spared from *Apc* gene ablation, and therefore may better recapitulate the events leading to tumourigenesis, and thus better reflects actual stem cell marker alterations. Despite our assumption that increased Wnt activation drives tumourigenesis, there is growing evidence that over-activation of Wnt signalling can have a tumour protective effect within the intestine (Albuquerque *et al.* 2002; Méniel *et al.* 2013). In this instance, expression of some Wnt target genes were upregualted in both the BRB fed *AhCre* and *VillinCreER^{T2}* models, which could infer that BRBs elicit an enhanced Wnt response to hinder tumourigenesis.

3) There has been a lot of controversy over the published ISC markers (Tian *et al.* 2011; Barker *et al.* 2012; Muñoz *et al.* 2012) as many markers do not have functional roles in the maintenance of the ISC population. As some ISC marker genes are also Wnt target genes, it is important to remember that changes in expression levels within the whole intestinal epithelium may not represent changes to the functional stem cell population, rather indicate a response to Wnt activation within differentiated epithelial cells. Within the context of global *Apc* deletion, identification of the ISC population becomes even more challenging, and so the difference in the results observed between *AhCre* and *VillinCreER^{T2}* may be the direct result of Wnt-activation on a different number of cells or a different cell population (such as the Paneth cells), and not the result of an expansion/ reduction of the functional ISC compartment. In addition, it is also possible that, in the instance of the *VillinCreER^{T2}* model, differentiated cell populations have dedifferentiated and reverted to have stem-cell like properties (Schwitalla *et al.* 2013). It is not possible from this data to distinguish whether such changes reflect a dedifferentiated population reacquiring Lgr5^{+} expression or a direct effect on ISC marker expression. The *AhCre* system does not result in Wnt-activated differentiated cells and so is unlikely that these differentiated populations will revert to stem-like cells.

Taking into consideration the discussion above, it is likely that the *AhCre* system is a more reliable model than the *VillinCreER^{T2}* model used here to examine ISC changes especially in the context of dietary intervention. Future work will need to investigate the effect of BRBs on the ISC population more specifically. However, taken together, these observations provide some evidence that BRBs mediate chemopreventative and anti-tumourigenic properties at the earliest stages of cancer initiation.

3.4 Summary and Future Directions

In summary, three major conclusions can be drawn from the data presented in this chapter. First, 2 week feeding of 10% freeze-dried BRBs had no harmful effect on the normal intestine. Secondly, BRBs exerted chemopreventive effects by partially reinstating the cell differentiation pathways that are severely perturbed following acute *Apc* loss, induced cell death and reinstated migration. Thus, BRBs attenuated the premalignant intestine phenotype. And finally, BRBs altered the expression of the stem cell compartment and Wnt target genes.

The data presented here suggests two things:

1) The numbers of stem cells are altered after BRB feeding and/ or
2) BRBs effect the expression and thus potentially affect the functional output of the ISCs..

Therefore, it is important to determine the number of ISCs present per crypt following feeding of BRBs. The lack of reliable and adequate antibodies targeting stem cell markers has hindered the progression of ISC research and understanding the important interactions between ISCs and carcinogenesis. The recently developed RNAscope® *in situ* hybridisation technology enables sensitive and reliable identification of stem cell-specific gene expression at a single RNA transcript level (Wang *et al.* 2012). Studies have reliably identified distinct ISC populations (Yan *et al.* 2012) and alterations in stem cell expression in different grade human colorectal tumours through the use of RNAscope® technology (Baker *et al.* 2015). This technique has vastly improved our ability to identify the intestinal stem cells and would reliably identify and enable quantification of the number of stem cells in control and BRB treated tissue.

It is also important to note that qRT-PCR gene expression analysis is a powerful tool used to investigate transcriptional behaviour by quantifying the number of mRNA transcripts present for a given gene. However, due to post transcriptional regulation, mRNA quantification does not necessarily correlate to protein activity. The gene expression data presented in this chapter provides some evidence that Wnt signalling is further enhanced in Wnt-activated crypts following acute *Apc* loss. This could support the 'just-right' hypothesis such that a certain level of Wnt activation is required for tumour growth and levels either side of the threshold hinders tumourigenesis (Albuquerque *et al.* 2002). To test this hypothesis it would be beneficial to analyse the effect of BRBs on proteins involved in Wnt signalling. Western blotting or global gene expression analysis through the use of RNA-sequencing may provide an extensive and more informative readout of gene and protein changes that occur in this experimental setup. It wold also be useful to perform gene and protein analysis for markers of the cell cycle to ascertain whether BRBs influence cycle cell dynamics. Additionally, due to the complicated cross talk between several signalling pathways, it would also be useful to investigate

the effect of BRBs on the Notch and Hedgehog signalling pathways, due to their involvement in the stem cell niche (Moore and Lemischka 2006; Umar 2010; Clevers *et al.* 2014).

Taken together, these findings provide evidence of the therapeutic potential of BRBs as a chemopreventative strategy at the earliest stages of tumourigenesis.

4 Functional analysis of potential tumour initiating cells exposed to BRB

4.1 Introduction

The work outlined in chapter 3 described how crypt dynamics and gene expressions were altered following feeding of 10% freeze-dried BRB diet in two murine models of Wnt deregulation in the intestine. Acute *Apc* loss in the intestine is characterised by increased stem-like cells and a lack of differentiation and migration (Sansom *et al.* 2004). *Apc* mutations can lead to an expansion of the ISC compartment and thus result in more cells with the potential to instigate tumourigenesis. It was found that BRBs partially reinstated cell differentiation and migration immediately following gene ablation of *Apc* and altered ISC marker gene expression. Specifically, in the *AhCre* $Apc^{fl/fl}$ mouse model, BRBs decreased *Olfm4* and to some extent *Lgr5* gene expression. Hypothetically, these observations could reflect a decrease in the number of stem cells present or activity of the stem cells within the *Apc* deficient cell population. However, as outlined in chapter 3, *Olfm4* and *Lgr5* were used as markers of gene expression and may not represent functional changes in the stem cell compartment. Additionally, the data from gene expression and *in situ* hybridisation did not permit the determination of the number of stem cells present per crypt.

This chapter aimed to evaluate the effect of BRBs on the stemness and self-renewal properties of *Apc* deficient cells. In order to achieve this, the *ex vivo* three dimensional (3D) culture system was utilised to grow intestinal organoids from intestinal crypts or ISCs. These cultures produce self-renewing intestinal organoids that can be expanded indefinitely in culture (Sato *et al.* 2009). The ability of intestinal organoids to develop in 3D simulates the physiology, shape and dynamics of the *in vivo* intestinal epithelium (Young and Reed 2016). The increased physiological relevance of this technique has led to advances in our understanding of the normal and malignant ISC and is becoming routinely used for translational research and drug discovery (Hollins and Parry 2016). It has been shown in wildtype organoids, that formation and self-renewal efficiency provide a good readout of the functional capacity of the ISC compartment (Young 2013). In an $Apc^{fl/fl}$ model however, it is not known whether only ISCs are capable of forming organoids and, *Apc* deficient organoids do not functionally differentiate. This indicates that organoid formation in an $Apc^{fl/fl}$ model may not be a direct readout of the number of ISCs but may give an insight into the capacity of cells to initiate tumour formation. Self-renewal however, is a hallmark of ISCs and so may be more accurate readout of stem cell capacity within a Wnt deregulated intestine. Thus in this chapter, *ex vivo* culture of *Apc* deficient crypts and single cells enabled us to obtain a

functional readout of ISC and tumour forming capacity after exposure to BRBs by determining the efficiency of organoid formation and self-renewal.

4.2 Results

4.2.1 BRBs have no overt effect on organoid formation efficiency of *Apc* deficient crypts

To determine whether BRBs had any overt effect on the functional output and number of *Apc* deficient cells, a stem cell functionality assay was performed to quantify the organoid forming efficiency in the context of BRBs. *VillinCreER^{T2} Apc$^{fl/fl}$* mice were randomly assigned to two cohorts: AIN76A diet (control) or 10% BRB diet, n = 4 mice per group. Mice were fed for 2 weeks on either the AIN76A pelleted diet or 10% freeze-dried BRB powder supplemented in AIN76A pellets, before Cre-induced *Apc* gene ablation and remained on their respective diets until culled at day 3 post induction. Acute *Apc* loss was driven by IP tamoxifen induction of Cre recombinase under the control of the *VillinCreER^{T2}* promoter. This induced *Apc* loss specifically in the intestinal epithelium including in the Paneth cells. On day 3 post induction, mice were culled and the intestine was harvested as described in section 2.10.1 and prepared using the crypt culture method (Section 2.10). Crypts were cultured without the Wnt activator R-spondin to select for organoids derived from *Apc* deficient ISCs. The number of organoids formed was counted using the Gelcount, Oxford Optronix plate reader at day 1 and day 7 post crypt seeding. This crypt culture method has been shown to result in the development of cyst-like organoids forming at days 1 - 2, characteristic of *Apc* loss (Sato *et al.* 2009). This crypt culture method enabled the quantification of organoid forming efficiency of *Apc$^{fl/fl}$* intestinal crypts as a proxy readout for the potential number of cells capable of initiating tumourigenesis (Yilmaz *et al.* 2012; Beyaz *et al.* 2016). Organoid forming efficiency refers to the percentage of seeded crypts/cells that have formed functional organoids over 7 days. Any alterations to crypt dynamics, as a result of feeding on BRBs, would have been established *in vivo* prior to seeding *ex vivo*. Using this methodology it was possible to determine whether prior exposure to BRBs had any effect on the overall size and number of organoids that formed.

Feeding of BRBs had no effect on the organoid forming efficiency of *Apc$^{fl/fl}$* crypts compared to the control (Figure 4.1A and C, Table 4.1A). Crypts pre-exposed to both control and BRB diet grew into organoids over 7 days, increasing in size as described by Sato *et al.* (2009), (Figure 4.1B, Table 4.1A). Pre-treated BRBs *Apc$^{fl/fl}$* organoids were 15% larger than control treated organoids at day 7, but this was not found to be statistically significant (Figure 4.1B, Table 4.1A). Taken together, this data indicated that exposure of the normal intestinal

epithelia to BRBs did not overtly alter the organoid forming behaviour and growth capacity of these cells following *Apc* deletion and removal of BRBs once cultured.

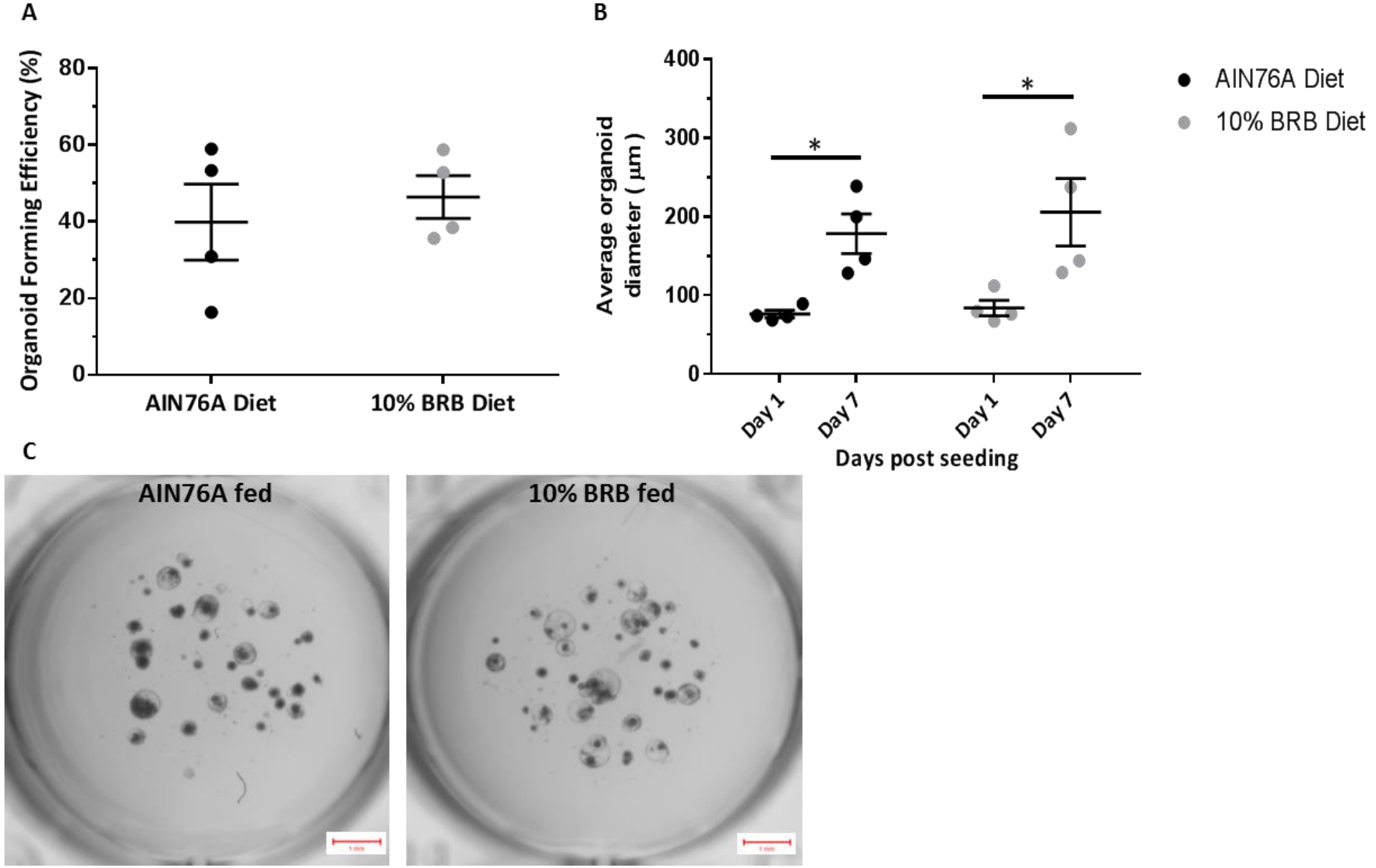

Figure 4.1 Effect of *in vivo* exposure to 10% freeze-dried BRB diet on *Apc* deficient crypts ability to form organoids *ex vivo*

(A) Feeding of BRB diet had no overt effect on the ability of $Apc^{fl/fl}$ crypts to form organoids when compared to control. (B) Control and BRB pre-exposed organoids increased in size over 7 days as described by Sato *et al.* (2009). BRB diet had no overt effect on the size of organoids at day 1 or day 7 post crypt seeding relative to the respective control time points. (C) Representative image of the number and size of organoids that formed from $Apc^{fl/fl}$ crypts exposed to control and BRB diet *in vivo*. A and B) Error bars represent SEM, C) scale bars represent 1 mm.

4.2.2 *Apc* deficient organoids are sensitive to increasing concentration of BRBs

In the previous section *Apc* deficient organoids derived from BRB exposed intestines were selected and maintained in the absence of BRBs. Thus, the previously reported BRB mediated *in vivo* down-regulation of ISC is likely to be lost and any selective pressure applied may fail to manifest or be rapidly lost in the *ex vivo* culture. Therefore, the next experiment set out to evaluate the effects of continual exposure to BRBs on *Apc* deficient organoids.

It was not possible to dissolve freeze-dried BRB powder in the intestinal culture medium, so an anthocyanin (AC) extract (containing cyanidin-3-O-glucoside, cyanidin-3-O-xylosylrutinoside and cyanidin-3-O-rutinoside) extracted from fresh BRBs was utilised, as these are, at least in part, responsible for the chemopreventative effects of BRBs (Wang *et al.* 2013b). The BRB-derived AC solution was provided by our collaborators (Li-Shu Wang, Medical College of Wisconsin, USA). Previous studies from this group have used BRB-derived ACs in cell culture work and showed that 0.5, 5, and 25 µg/ml of AC solution suppressed the activity of DNA methylation proteins in 3 human CRC cell lines that are commonly unregulated in cancer. Additionally, they reported that BRB-derived ACs inhibited proliferation and enhanced apoptosis of these cells (Wang *et al.* 2013b). Human cell lines have several benefits, they are a good platform for screening and characterising cancer therapeutics, they retain many genetic, epigenetic and gene expression features of cancers, they are easy to handle and manipulate (Vargo-Gogola and Rosen 2007) and they enable analysis of homogenous populations within a tumour (Vargo-Gogola and Rosen 2007; van Staveren *et al.* 2009). However, cell lines do have their limitations which question their relevance in future studies. The drawbacks of cell lines are that they are generally established from aggressive and metastatic tumours which restrict their use in cancer progression studies and early drug interventions (Ferreira *et al.* 2013). Cell culture is not a true representation of the environment of the primary tumour (Vargo-Gogola and Rosen 2007) and can often lead to alterations in cell morphology, gene expression and pathways (van Staveren *et al.* 2009). *In vivo* tumours are comprised of heterogeneous cell populations; this natural heterogeneity is lost in *in vitro* cultures (Vargo-Gogola and Rosen 2007). The use of organoids as a model of cancer has been a major breakthrough in research and is now a widely used tool for studying basic and clinical biology. Although 3D organoid models have some limitations such that, the lack of a native microenvironment impedes analysis of stem cell interactions with their typical niche, they recapitulate a number of biological interactions *in vivo.* They are near-physiological models for studying stem cells, they enable analysis of cell-cell and cell-matrix interactions and contain heterogeneous populations of the original tissue. The organoid

modelling system has bridged the gap between *in vitro* culture studies and *in vivo* animal models. As the work by Wang *et al.* studied the effects of ACs in human cell lines (Wang *et al.* 2013b), and as the concentration of active components might vary between preparations, it was important to determine an appropriate range of concentrations to use on murine *Apc* deficient intestinal organoids and to evaluate the effect of these concentrations of BRB-derived ACs on murine intestinal crypt dynamics.

The CellTiter-Glo® luminescent cell viability assay was utilised to determine the IC_{50} of the AC solution for murine organoids (IC_{50} refers to the concentration of AC required to reduce organoid viability by half). This assay determines the number of viable cells or organoids based on their ATP output, which indicates the presence of metabolically active organoids. The luminescence signal was read using the CLARIOstar plate reader and Xlfit software was utilised to calculate the IC_{50} value. Based on a previous study (Wang *et al.* 2013b) a BRB-derived AC stock solution (160.4 µM/g) was utilised to generate serial concentrations ranging from 0 µg/ml (no AC extract) to 500 µg/ml. As the concentrations used proved too low to reach 100% cell death, the data was extrapolated using the XLfit software to give an estimated IC_{50} of 11.6 mg/ml (Figure 4.2A). This indicated that 500 µg/ml of BRB-derived ACs were not sufficiently toxic to the organoids to cause complete cell death. In addition, it was apparent that organoid sensitivity to ACs manifested at concentrations above 15.6 µg/ml, as cell viability started to decrease in a dose-dependent manner. To establish a complete cell viability readout, the concentration of AC extract was increased to 16 mg/ml to cover the 11.6 mg/ml concentration determined by the IC_{50}. Concentrations between 15.6 µg/ml and 16 mg/ml produced a graph which plateaued at the bottom allowing an IC_{50} of 1.4 mg/ml to be determined (Figure 4.2B). In addition, this data also indicated that organoid viability decreased in a dose-dependent manner, as changes in viability began to decline at AC concentrations between 15.6 - 500 µg/ml.

Together, these results indicated that concentrations of AC extract between 15.6 and 500 µg/ml shows some but not complete toxicity and therefore, have some potential chemopreventative effects by reducing the viability of *Apc* deficient organoids.

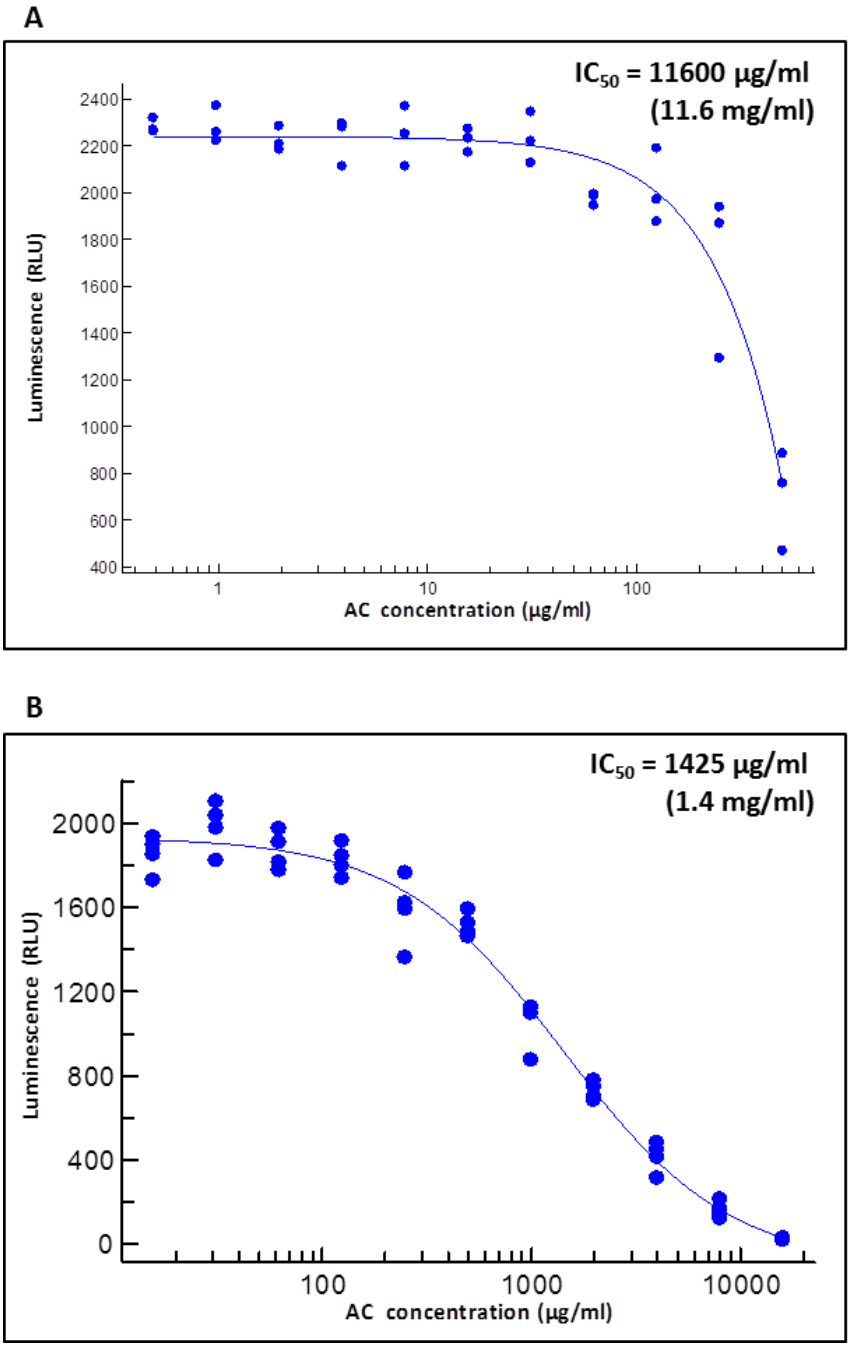

Figure 4.2 IC_{50} curves for BRB-derived anthocyanins (ACs)

IC_{50} curves show that *Apc*$^{fl/fl}$ organoids are sensitive to increasing concentrations of BRB anthocyanins. (A) Concentration of AC extract ranged from 0.48 - 500 µg/ml and (B) 15.6 µg/ml - 16 mg/ml. High concentrations of AC extract are toxic to *Apc* deficient cells as cell viability is reduced in a dose-dependent manner. IC_{50} values were determined by Xlfit software from the CellTiter-Glo cell proliferation assay after four days of incubation with the AC extracts. Each data point was calculated from 3 or 4 well replicates.

4.2.3 BRB-derived anthocyanins reduce the self-renewal ability of *Apc*$^{fl/fl}$ deficient cells

The CellTiter-Glo luminescent cell viability assay revealed that concentrations of BRB-derived ACs, 15.6 – 500 µg/ml, where sufficient to reduce organoid viability and were not associated with high toxicity. For this reason, concentrations between 0 µg/ml and 500 µg/ml of BRB-derived ACs were used to determine the effect of continual treatment of ACs on organoid forming efficiency and on the self-renewal capability of *Apc* deficient cells *ex vivo*.

Crypts isolated from *Apc*$^{fl/fl}$ murine small intestine were seeded at 200 crypts per well and then incubated with media containing AC extract. There were four wells per dose of AC extract, except the 3.9 µg/ml dose which had 3 wells. Four biological replicates were performed for each dose. Analysis of the organoid forming efficiency indicated that 1 week exposure to a range of AC concentrations had no overt effect on the efficiency of *Apc* deficient crypts to form organoids when compared to control (0 µg/ml, no AC extract) (Figure 4.3A and C, Table 4.1B). However, there appeared to be a linear relationship of decreased organoid formation efficiency at AC concentrations above 15.6 µg/ml. This is in accordance with the reduction in organoid viability previously observed at these concentrations. In addition to organoid forming efficiency, the overall organoid size in the context of BRB-derived ACs was also evaluated. Results indicated that 1 week exposure to 500 µg/ml AC media resulted in a significantly smaller organoid compared to the control group (Figure 4.3B and C, Table 4.1B). Concentrations above 15.6 µg/ml followed a linear trend of reduced organoid size, in accordance with reduced viability and organoid forming efficiency.

To determine whether *ex vivo* application of the AC extracts had any effect on the self-renewal capabilities of *Apc* deficient cells, *Apc*$^{fl/fl}$ organoids exposed to AC extracts for 1 week were subsequently passaged to single cell as described in section 2.10.4. Growth medium containing the same concentration of AC as previously treated with was added to the respective single cells. The results showed that treatment with 500 µg/ml AC extract significantly reduced the number of organoids that formed by 12 fold compared to control (Figure 4.4 Organoid formation efficiency (self-renewal efficiency) and size following exposure of *Apc* deficient single cells to BRB-derived ACs.A and C, Table 4.1B). As with organoids before passage, AC concentrations above 15.6 µg/ml appeared to reduce the ability of organoid formation in a linear fashion. Overall, ACs had no overt effect on organoid size when compared to the control. But, consistent with the organoid forming efficiency, the size of organoids treated with AC doses above 15.6 µg/ml appeared to be smaller (Figure 4.4B and C, Table 4.1B).

In summary, exposing *Apc* deficient crypts to ACs *ex vivo* had no overt effect on the percentage of cells capable of forming an organoid. In contrast, maintaining these organoids in the presence of AC significantly slowed their growth and resulted in fewer cells capable of self-renewing.

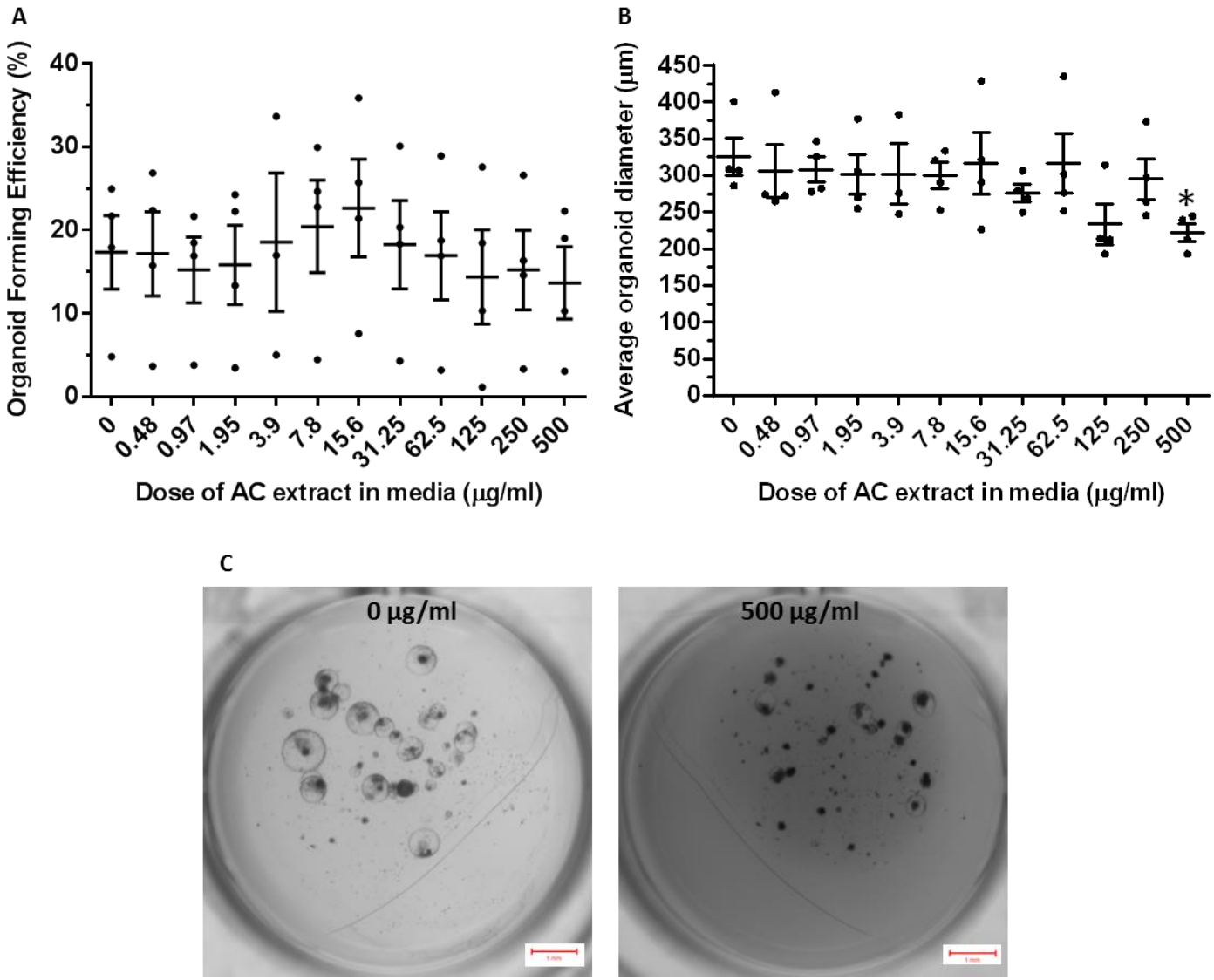

Figure 4.3 Organoid formation efficiency and size following exposure of *Apc* deficient crypts to BRB-derived ACs

(A) Scatter-plot diagram showing organoid forming efficiency of $Apc^{fl/fl}$ crypts in the presence of BRB-derived ACs. ACs had no significant effect on the efficiency of crypts to form organoids however, concentrations above 15.6 µg/ml appeared to be reduce efficiency linearly. (B) Scatter-plot diagram showing 500 µg/ml of AC reduced the average diameter of *Apc* deficient organoids when compared to control. Similarly, concentrations between 15.6 – 250 µg/ml appeared to reduce organoids diameter in a linear trend. (C) Representative image of the number of organoids that formed following exposure to 0 µg/ml and 500 µg/ml of AC extract. * P value ≤ 0.05, n ≥ 3, two-tailed Mann Whitney U test. Error bars represent SEM. Scale bars represent 1 mm.

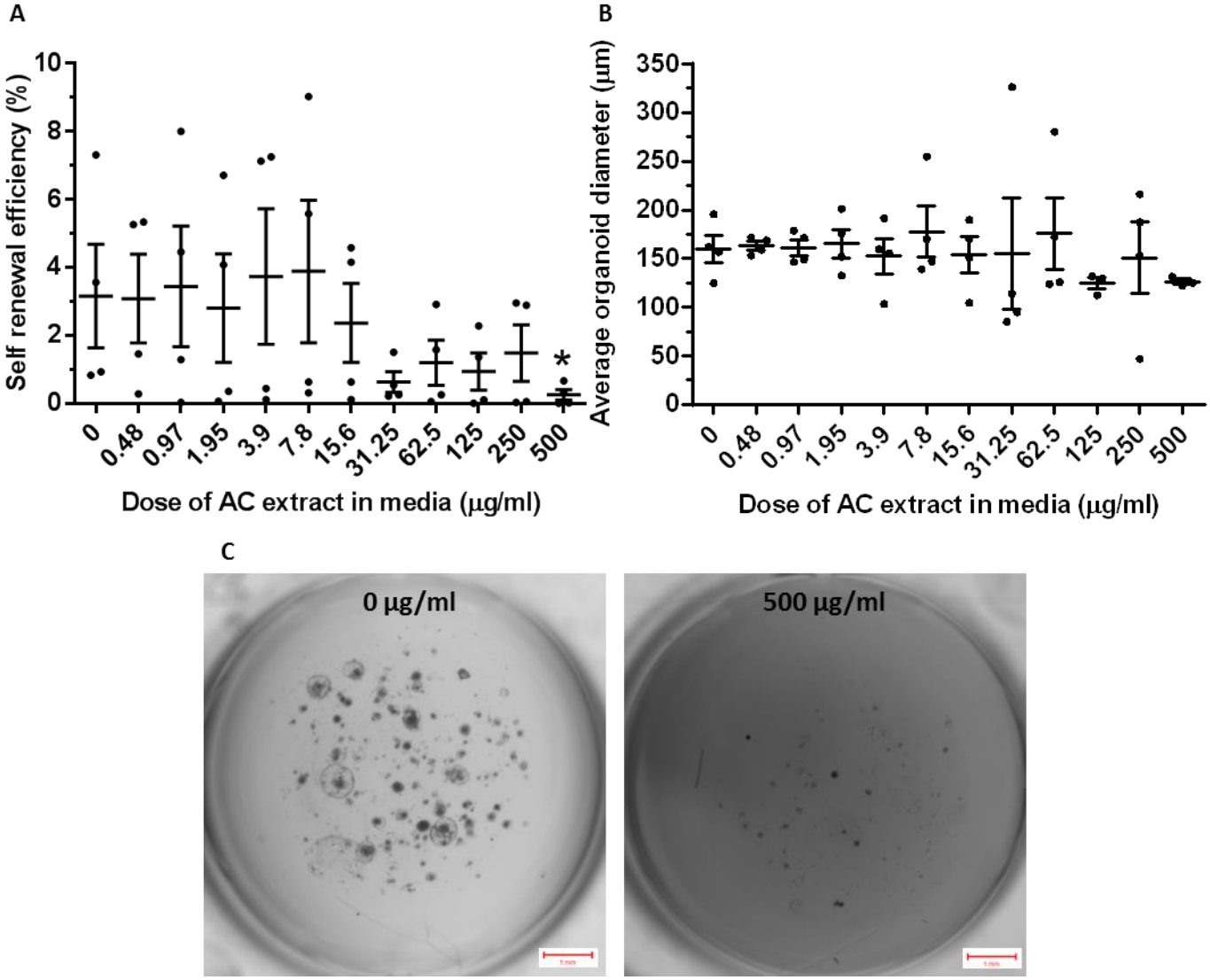

Figure 4.4 Organoid formation efficiency (self-renewal efficiency) and size following exposure of *Apc* deficient single cells to BRB-derived ACs.

(A) Scatter-plot diagram showing the self-renewal efficiency of $Apc^{fl/fl}$ single cells to form organoids in the presence of *ex vivo* application of BRB-derived ACs was decreased at concentrations above 15.6 µg/ml. The 500 µg/ml extract significantly reduced the number of organoids that formed compared to control 0 µg/ml. (B) Scatter-plot diagram showing the average diameter of *Apc* deficient organoids was not significantly altered by ACs when compared to the control. (C) Representative image of the number of organoids that formed from single cells following exposure to 0 µg/ml and 500 µg/ml of AC extract.* P value ≤ 0.05, n ≥ 3, two-tailed Mann Whitney U test. Error bars represent SEM. Scale bars represent 1 mm.

A

Apc$^{fl/fl}$ Organoids with prior exposure to diets in vivo			
	Organoid Forming Efficency (%)	***n***	***P Value***
Control Diet vs BRB Diet	39.85 ± 9.90 vs 46.38 ± 5.57	4 vs 4	0.8286
	Average Organoid Diameter (µM)	***n***	***P Value***
Control Day 1 vs Control Day 7	76.20 ± 4.53 vs 178.02 ± 25.18	4 vs 4	**0.0286**
BRB Day 1 vs BRB Day 7	83.73 ± 9.75 vs 205.4 ± 42.77	4 vs 4	**0.0286**
Control Day 1 vs BRB Day 1	76.20 ± 4.53 vs 83.73 ± 9.75	4 vs 4	0.6571
Control Day 7 vs BRB Day 7	178.02 ± 25.18 vs 205.4 ± 42.77	4 vs 4	0.8286

B

	Apc$^{fl/fl}$ organoids with ex vivo exposure to BRB-derived AC extract						
	AC dose	***Organoid Forming Efficency (%) (± SEM)***	***n***	***P Value***	***Average Organoid Diameter (µM) (± SEM)***	***n***	***P Value***
Initial Seeding (Pre Passage)	*0 µg/ml vs 0.48 µg/ml*	17.35 ± 4.42 vs 17.17 ± 5.05	4 vs 4	> 0.9999	325.6 ± 25.6 vs 305.9 ± 35.75	4 vs 4	0.3429
	0 µg/ml vs 0.97 µg/ml	17.35 ± 4.42 vs 15.22 ± 3.93	4 vs 3	0.4857	325.6 ± 25.6 vs 308.1 ± 16.76	4 vs 3	0.6571
	0 µg/ml vs 1.95 µg/ml	17.35 ± 4.42 vs 15.83 ± 4.76	4 vs 4	0.8286	325.6 ± 25.6 vs 301.8 ± 27.29	4 vs 4	0.3429
	0 µg/ml vs 3.9 µg/ml	17.35 ± 4.42 vs 18.56 ± 8.32	4 vs 4	> 0.9999	325.6 ± 25.6 vs 302.1 ± 41.23	4 vs 4	0.4000
	0 µg/ml vs 7.8 µg/ml	17.35 ± 4.42 vs 20.46 ± 5.55	4 vs 4	0.6571	325.6 ± 25.6 vs 299.4 ± 17.93	4 vs 4	0.8286
	0 µg/ml vs 15.6 µg/ml	17.35 ± 4.42 vs 22.66 ± 5.87	4 vs 4	0.4857	325.6 ± 25.6 vs 316.8 ± 42.23	4 vs 4	> 0.9999
	0 µg/ml vs 31.25 µg/ml	17.35 ± 4.42 vs 18.27 ± 5.32	4 vs 4	> 0.9999	325.6 ± 25.6 vs 276.1 ± 11.88	4 vs 4	0.0571
	0 µg/ml vs 62.5 µg/ml	17.35 ± 4.42 vs 16.94 ± 5.29	4 vs 4	0.8286	325.6 ± 25.6 vs 316.3 ± 40.9	4 vs 4	0.4857
	0 µg/ml vs 125 µg/ml	17.35 ± 4.42 vs 14.38 ± 5.65	4 vs 4	0.8286	325.6 ± 25.6 vs 233.4 ± 27.31	4 vs 4	0.2000
	0 µg/ml vs 250 µg/ml	17.35 ± 4.42 vs 15.22 ± 4.77	4 vs 4	0.6571	325.6 ± 25.6 vs 294.9 ± 28.2	4 vs 4	0.3429
	0 µg/ml vs 500µg/ml	17.35 ± 4.42 vs 13.66 ± 4.34	4 vs 4	0.6571	325.6 ± 25.6 vs 222.5 ± 12.03	4 vs 4	**0.0286**
Post Passage to Single Cell	*0 µg/ml vs 0.48 µg/ml*	3.156 ± 1.52 vs 3.08 ± 1.30	4 vs 4	> 0.9999	159.8 ± 14.48 vs 163.2 ± 4.24	4 vs 4	0.8286
	0 µg/ml vs 0.97 µg/ml	3.156 ± 1.52 vs 3.441 ± 1.78	4 vs 4	0.8286	159.8 ± 14.48 vs 161.4 ± 8.02	4 vs 4	> 0.9999
	0 µg/ml vs 1.95 µg/ml	3.156 ± 1.52 vs 2.8 ± 1.59	4 vs 4	0.6571	159.8 ± 14.48 vs 165.4 ± 14.85	4 vs 4	0.8286
	0 µg/ml vs 3.9 µg/ml	3.156 ± 1.52 vs 3.73 ± 1.99	4 vs 4	0.6571	159.8 ± 14.48 vs 152.5 ± 18.2	4 vs 4	0.6571
	0 µg/ml vs 7.8 µg/ml	3.156 ± 1.52 vs 3.88 ± 2.09	4 vs 4	0.8286	159.8 ± 14.48 vs 177.8 ± 26.48	4 vs 4	0.8286
	0 µg/ml vs 15.6 µg/ml	3.156 ± 1.52 vs 2.36 ± 1.61	4 vs 4	0.6571	159.8 ± 14.48 vs 153.8 ± 18.25	4 vs 4	0.8286
	0 µg/ml vs 31.25 µg/ml	3.156 ± 1.52 vs 0.625 ± 0.30	4 vs 4	0.1143	159.8 ± 14.48 vs 155.1 ± 57.34	4 vs 4	0.3429
	0 µg/ml vs 62.5 µg/ml	3.156 ± 1.52 vs 1.197 ± 0.66	4 vs 4	0.3429	159.8 ± 14.48 vs 175.6 ± 36.7	4 vs 4	> 0.9999
	0 µg/ml vs 125 µg/ml	3.156 ± 1.52 vs 0.93 ± 0.54	4 vs 4	0.3429	159.8 ± 14.48 vs 124.7 ± 6.12	4 vs 4	0.2286
	0 µg/ml vs 250 µg/ml	3.156 ± 1.52 vs 1.478 ± 0.83	4 vs 4	0.3429	159.8 ± 14.48 vs 151 ± 36.94	4 vs 4	> 0.9999
	0 µg/ml vs 500µg/ml	3.156 ± 1.52 vs 0.25 ± 0.15	4 vs 4	**0.0286**	159.8 ± 14.48 vs 126.4 ± 2.70	4 vs 4	0.2286

Table 4.1 Organoid forming efficiency (%) and average organoid diameter (µm) of *Apc* deficient cells following (A) *in vivo* exposure to AIN76A or 10% freeze-dried BRB diet and (B) exposure to BRB-derived anthocyanins (AC) *ex vivo*

Significant differences (p value ≤ 0.05) were determined using two-tailed Mann Whitney U statistical test. SEM = standard error of mean.

4.3 Discussion

The previous chapter aimed to characterise the chemopreventative effects of BRBs on normal intestinal epithelium and in suppressing Wnt-driven tumourigenesis at the earliest stages of cancer initiation. It was found that BRBs partially attenuated the 'crypt-progenitor' phenotype distinctive of acute *Apc* loss in the intestinal epithelium and altered the expression of ISC markers in two mouse models of early Wnt deregulation. The expression levels of the ISC markers were contradictory to one another such that ISC markers decreased in the *AhCre* model and increased in the *VillinCreER^{T2}* mouse model, possible reasons for this were discussed in chapter 3. Additionally, it was not possible to directly evaluate the functional ability of malignant ISCs following BRB treatment. Therefore, chapter 4 attempted to determine the functionality of malignant *Apc* deficient cells and stem cells *ex vivo*, in the context of BRB intervention. While it is important to consider how *in vivo* and *ex vivo* BRB intervention relates to human doses, the fundamental aim of this chapter was to evaluate what effect BRBs have on intestinal stem and crypt dynamics, as this has not been investigated before.

4.3.1 Organoid forming efficiency of *Apc$^{fl/fl}$* crypts is not affected by BRBs

A defining feature of CSCs is their capability to self-renew and support tumour growth at the initiation and progression stages (Clevers 2016). It has been proposed that stemness can be explained by four properties: it can be categorical, such that ISCs function as stem cells irrespective of their environment; it can be dispositonal, a stem cells capacity only emerges when it is in the correct environment; it could be relational, the microenvironment induces stem cell capacity in a cell that's normally a non-stem cell; and finally it could be systemic, a property that is regulated by a system such as a tissue rather than a single cell (Clevers 2016; Laplane 2016). Which framework best describes the function of ISCs is still up for debate but Laplane has provided more clarity over the definitions and concepts of stem cell biology which can be applied to experiments.

Although unable to determine which framework best fits the organoid forming experiments discussed herein, it was possible to evaluate the potential of isolated *Apc* deficient crypts to form organoid bodies *ex vivo* after *in vivo* exposure to BRBs. This provided insight into the effects of BRB on tumour initiating ability. Alterations to the ISC compartment as a result of feeding on 10% freeze-dried BRBs would have established *in vivo* prior to *Apc* gene ablation. Therefore, any changes in the abilty of crypts to form organoids *ex vivo* would be a consequence of dietary effects on the ISCs. It was shown here that BRBs do not affect the potential of *Apc$^{fl/fl}$* crypts to form organoids, thus not overtly affecting the abiltity to form tumours. The limitations with this experiment were that firstly, the organoids that develop could be forming from either Wnt-activated ISCs or from Wnt-activated cells. Wnt-activated cells from the proliferative zone can have stem cell-like properties but they are not 'true' ISCs. Previous

studies have utilised cKit as a marker to distinguish the proliferative and differentiation zones of colonic wildtype crypts (Rothenberg *et al.* 2012; Wang *et al.* 2013a). To circumvent this problem, *Apc* deficient intestinal cells could be FACs sorted based on their expression of Lgr5 and cKit, such that expression of $Lgr5^{hi}$ $cKit^{lo}$ marks ISCs and $Lgr5^{lo}$ $cKit^{hi}$ marks the proliferative region. Organoid formation from these seperated populations would allow a better representation of the stemness capacity of cell populations specifically, as very few organoids should form from $Lgr5^{lo}$ $cKit^{hi}$ populations. Additionally, it could be assumed that if Lgr5 and cKit are sufficient markers for these distinct populations, analysing the raw number of FACs sorted $Lgr5^{hi}$ $cKit^{lo}$ and $Lgr5^{lo}$ $cKit^{hi}$ populations as a proportion of total cells would provide an insight into the cell type responsible for organoid formation, in the context of BRBs. However, a potential drawback of these methodologies is the plasticity of *Apc* deficient intestinal tissue. As stem cells may be defined by their environmental niche, non-stem cells could be capable of gaining stem cell-like properties when exposed to specific conditions. Studies have recently determined that cKit also marks deep crypt secretory cells such as goblet cells in the colon and Paneth cells in the small intestine. Studies have shown that these deep secretory cells, in a wildtype setting, are fundamental for maintenance of ISCs and highlighted the role of $cKit^{+}$ cells in supporting $Lgr5^{+}$ stem cell driven colonic organoid formation (Rothenberg *et al.* 2012; Sasaki *et al.* 2016). Due to the role of $cKit^{+}$ cells in governing stem cell dynamics, cells expressing $Lgr5^{lo}$ $cKit^{hi}$ may enable cells to aquire stem like-properties capable of organoid formation. Therefore, other markers of the proliferative and differentiation zones may also be required to purify the cell populations.

Another drawback to this technique is that in order for it to be a true representation of stemness and tumour initiating capacity, the ability of organoids to self-renew needed to be evaluated. In order to assess this the organoids were subsequently passaged to single cells using trypLE, and a definitive number of unsorted single cells were seeded per well. Whilst possible, sorting cells for specific stem cell markers such as Lgr5 prior to seeding would impose a pre-selection bias of stemness and tumourigenic potential, so cells were not sorted for this reason. Unfortunately 2/4 control preparations and 1/4 BRB preparations presented with signs of fungal infection a couple days after re-seeding and so a readout of self-renewal efficiency was not possible. Despite this, the relevance of differences, if any, in the self-renewal efficiency of *Apc* deficient single cells as a result of BRB exposure could be disputed as the cells/ organoids will not have been exposed to BRBs for 2 weeks by the end of the experiment. Therefore, to determine a more accurate reflection of ISC self-renewal after BRB treatment it was necessary to expose organoids to BRBs throughout the duration of the *ex vivo* assay.

4.3.2 BRB-derived ACs limit the self-renewal efficiency of *Apc*$^{fl/fl}$ cells

As previously outlined, in order to achieve a better representation of the effect of BRBs on the self-renewal efficiency of ISCs, *Apc*$^{fl/fl}$ cells would need to be continual exposed to BRBs. Anthocyanins have been shown, in part, to be responsible for the chemopreventative effects of BRBs in cancer (Wang *et al.* 2009). As other studies have utilised BRB-derived ACs in cell culture studies (Wang *et al.* 2009; Wang *et al.* 2013b) and due to the diffculties in dissolving freeze-dried BRB powder in organoid media, it was decided to use ACs in the subsequent self-renewal assays.

Characterising the responsiveness of each model system to novel therapeutics is important and can be achieved through the use of the CellTiter-Glo® luminescent cell viability assay. Presented herein, initial assays with 4 day exposure to ACs up to concentrations of 500 µg/ml resulted in the reduction of cell viability. However, these concentrations were not sufficient to completely reduce the activity of all the *Apc* deficient organoids, as shown by an incomplete dose-response curve (Figure 4.2A). The IC_{50} generated from this graph was approximately 11.6 mg/ml and despite the fact that the Xlfit software was able to fit a dose-response curve to the data, how meaningful this IC_{50} is still needs to be determined. As the data did not have a bottom plateau which would define '0', it would not be possible to accurately define '50'. To overcome this problem, the concentration of AC used in a subsequent assay was increased to 16 mg/ml. This assay did provide a complete dose-response curve with an IC_{50} value of 1.4 mg/ml. These data implied that higher doses of AC are toxic as the ATP luminescence signal at 16 mg/ml produced a near zero reading. However, it may be possible that the signal at this dose may have been quenched by the purple colour of the media. Promega have reported that luminescence intensity can differ dependent on the type of culture media that was used. For example, medium containing no phenol red had a ~5% increase in luminescence compared to medium containing standard phenol red concentrations. Additionally, media containing twice the normal concentration of phenol red had a ~2% decrease in luminescence (Promega 2015). In order to determine whether this signal was quenched it would be beneficial to repeat this assay including control wells containing matrigel with no organoids with the highest doses of AC media to determine background luminescence signals. In addition, as the CellTiter-Glo® assay was set up as per manufacturers' instructions, equal volume of CellTitre-Glo® reagent was mixed with equal volume of AC organoid media, future experiments could mix equal volumes of CellTitre-Glo® reagent with organoid growth medium without any ACs. Lastly, it would be very useful to determine the effects of BRBs on wildtype organoids. In order to relate this to human studies, it is important to make sure that BRBs and their AC derivatives have no adverse effect on normal intestinal tissue. Performing cell viability and self-renewal assays on wildtype organoids would reveal whether or not the cytotoxic effects of ACs are specific to *Apc* deficient organoids. Our group have previously reported that growing

wildtype organoids from single cells, even with the addition of Wnt3a, EGF, Noggin, Rspo1 and the ROCK inhibitor Y-27632, resulted in a very low organoid forming efficiency (<0.03%) (Young 2013). Sato *et al.* managed to grow wildtype organoids from sorted single $Lgr5^{hi}$ cells, but this required the addition of the Notch-agonist peptide, Jagged1 (Li *et al.* 1998), to the growth factor medium, but the organoid forming efficiency was still low (6%) (Sato *et al.* 2009). At the time of the cell viability and self-renewal assays discussed herein, Jagged1 was not available in the lab and so growing organoids from wildtype single cells was not possible. It would be beneficial to repeat these assays using wildtype preparations with Jagged1 peptide in the future.

The lack of significance in the self-renewal assay using AC doses 15.6 – 250 µg/ml could be attributed to the statistical power of the test and there were a number of variables that could determine this. Firstly, the number of wells used per dose of AC was 3 or 4 and the number of organoids that grew was very variable between wells and biological replicates. Previous work by Young established that in order to provide an accurate readout of stemness (in the context of wildtype organoids), the absolute minimum number of wells required was 6 and numbers below this provided varied results (Young 2013). Despite this, these self-renewal results indicated that 500 µg/ml AC reduced the ability of cells to propagate into organoids thereby potentially limiting the stemness/ tumour initiating ability of *Apc* deficient cells.

4.4 Summary and Future Directions

In summary, the data presented in this chapter indicated that BRB-derived ACs do not overtly affect the capacity of an already established malignant ISC to form organoids but do limit the efficiency of these ISCs/ *Apc* deficient cells to self-renew. These preliminary findings are novel in the context of BRB chemoprevention of CRC and these studies warrant a more in-depth analysis of the effects of BRBs and ACs on malignant ISC populations.

A reduction in the ability of malignant $Apc^{fl/fl}$ cells to self-renewal holds great promise for the use of BRBs as a CRC preventative strategy that targets the CSC populations. However, it is important to elucidate whether BRBs reduce the stemness of non-malignant ISCs and so further investigation into the effect of *ex vivo* application of ACs on wildtype ISC is necessary. In addition, the self-renewal assays showed that higher doses of AC extract reduced the ability of *Apc* deficient cells to re-establish into new organoids. As with chapter 3, these studies do not provide insight in to whether BRBs reduce the number of ISCs or simply reduce their stem cell potential. It could be hypothesised that the reduction in organoid formation is a result of having fewer stem cells present following BRB treatment. To test this hypothesis it would be beneficial to use *the* $Lgr5CreER^{T2}$-$EGFP^{+}$ mouse model. Induction of this mouse using tamoxifen drives recombination specifically within the ISCs and consequently these cells are identified by GFP (green fluorescent protein) fluorescence. Crypt preparations from

Lgr5CreER^{T2}*-EGFP*$^{+}$ *Apc*$^{+/+}$ and *Apc*$^{fl/fl}$ mice could be analysed by flow cytometry to assess the level of GFP signal, as a readout for the number of ISCs or utilise the methods outlined by Wang *et al.* to sort cells based on their stem cell and proliferative markers (Wang *et al.* 2013a). It would also be useful to assess proliferation and apoptosis rates of intestinal organoids following exposure to ACs, as it is likely that reduced cell viability is linked to these molecular processes. It would be beneficial to determine whether the reduction in organoid viability is due to AC-induced cell death or AC-induced metabolic changes that limit the ability of organoids to proliferate. In addition, performing gene expression analysis for stem cell and Wnt target genes in organoids exposed to AC concentrations would provide insightful data on the impact of BRBs on normal and malignant stem cells. These experiments will provide a more in depth analysis on the effects of BRB-derived ACs on wildtype and *Apc* deficient cells in a system that closely resembles the *in vivo* setting.

5 Investigating the long-term effects of 10% BRBs on wildtype intestine and *Apc* loss-driven intestinal tumourigenesis

5.1 Introduction

Work described in chapters 3 and 4 suggested that short-term exposure to BRBs had chemopreventative effects at the earliest stages of intestinal tumourigenesis, in part, by attenuating the phenotype of acute *Apc* loss in the intestine and reducing the capacity of malignant ISCs to self-renew. In addition, it was shown that short-term exposure to BRBs had no major detrimental effects on normal gut homeostasis. Previous studies have shown that BRBs reduced intestinal tumours by 45% in an animal model of Wnt-driven tumourigenesis (Bi *et al.* 2010) and were sufficient in regressing rectal polyps in patients with FAP disease (Wang *et al.* 2014). These studies present evidence for the use of freeze-dried BRBs as a therapeutic strategy for intestinal tissues with *Apc* mutations. Mechanistic experiments from these studies highlighted that tumour development was supressed by inhibition of the Wnt/ β-catenin signalling pathway, and by altering epigenetic marks in FAP polyps. Despite these promising results, these published studies did not examine the potential effect of BRBs on the intestinal and cancer stem cell populations. As the ISCs are considered a 'cell of origin' of CRC (Barker *et al.* 2009), it is necessary to understand the interactions between BRBs and stem cells.

This chapter describes the effect of long-term feeding on BRBs. The longer-term effect of BRBs on both normal and malignant ISCs was examined. This was achieved by utilising the *Lgr5CreER^{T2}* mouse model, which was previously used to demonstrate that ISCs are the cell of origin for murine CRC (Barker *et al.* 2009). In this model Cre is expressed solely in the active ISCs. Combining this model with the *Apc$^{fl/fl}$* allele enables us to evaluate the human disease situation more closely. Cohorts of *Lgr5CreER ^{T2} Apc$^{+/+}$* (wildtype *Apc* allele with *Lgr5CreER ^{T2}* transgene = equivalent to a wildtype control) and *Lgr5CreER^{T2} Apc$^{fl/fl}$* (homozygously floxed *Apc* allele with *Lgr5CreER^{T2}* transgene) mice were randomly assigned into two groups and fed *ad libitum* on a control diet (AIN76A pellets) or a 10% freeze-dried BRB powder supplemented in AIN76A pellets for an initial period of two weeks. After two weeks of feeding on their respective diet, all mice were induced by IP injections of tamoxifen over four consecutive days. This resulted in recombination of the *Apc* allele in the ISCs of mice bearing the loxP flanked *Apc* allele (i.e. *Lgr5CreER^{T2} Apc$^{fl/fl}$* mice). Mice were then aged for a maximum of 190 days post induction (wildtype) or until they became symptomatic of disease and had to be sacrificed, and the appropriate tissues were dissected. Mice remained on their respective diets throughout the experiment.

5.2 Results

5.2.1 Long-term feeding of BRBs does not influence body weight

Due to the links between obesity and intestinal tumourigenesis (Beyaz *et al.* 2016) mice were weighed to determine whether long-term feeding of 10% freeze-dried BRBs influenced body weight. Aged matched (11 - 14 weeks) wildtype and *Apc*$^{fl/fl}$ mice were randomly assigned to control or BRB treated cohorts (wildtype n = 6 and *Apc*$^{fl/fl}$ control diet n = 11, BRB diet n = 10). All experimental mice were weighed weekly with the initial measurement taken before starting on the AIN76A or BRB diets (represented as 100% body weight at -14 days, Figure 5.1). All four cohorts were IP injected with tamoxifen, which controlled for any weight change induced by tamoxifen administration.

Long-term feeding on BRB diet did not alter the average % body weight of wildtype mice relative to control (AIN76A). However, both wildtype cohorts appeared to increase in weight with increased age. Two week feeding (-14 to 0 days post induction (PI)) on either the AIN76A or BRB diet did not alter the body weight of wildtype mice (Figure 5.1A). After a further 16 and 30 days on their respective diets (30 and 44 days in total), the body weight of wildtype mice was still not significantly altered. At 80 days PI (94 days on diets); wildtype mice fed both diets were significantly heavier than at 30 days post induction (Figure 5.1A). An increase in body weight would be expected with increasing age. At 180 days PI (194 days on diets), the body weight of wildtype mice fed the AIN76A or BRB diet were not altered when compared to their weights at 80 days PI. Despite a gradual increase in body weight over the duration of the experiment, long-term feeding of BRBs did not affect the average body weight of wildtype mice in relation to the AIN76A fed mice at each time point. Adult mice were a minimum of 11 weeks of age before starting on their respective diet. Several studies have shown that with increasing age mice continue to increase in body weight, but the rate of weight gain decreases the older the mouse becomes (Robertson 1926; Gall and Kyle 1968). Although mice on control and BRB diet were slightly heavier at 180 days PI (minimum 38 weeks of age) than they were at 80 days PI (minimum 22 weeks of age), the lack of significance in weight change is likely to reflect the start of the plateau in weight gain.

Long-term feeding on a BRB diet did not alter the average % body weight of *Apc*$^{fl/fl}$ mice when compared to *Apc*$^{fl/fl}$ AIN76A fed mice. However, AIN76A mice appeared to increase in weight initially and lost weight quicker than BRB exposed mice when symptomatic of disease. *Apc*$^{fl/fl}$ mouse body weight was not altered after being on the control and BRB diets for 2 weeks (Figure 5.1B). Up to 16 days PI (30 days on diets) control and BRB fed *Apc*$^{fl/fl}$ mice were heavier by 6% (control: 0 days PI = 99%, n = 11 vs 16 days PI = 105%, n = 8, p value =

0.0091, Mann Whitney U test, Figure 5.1B) and 4% respectively, but this change was only found to be significant for control mice. *Apc*$^{fl/fl}$ mice on the control diet started to present with signs of illness, possibly from tumour burden as a result of loss of *Apc*, at 20 days PI (Figure 5.1). In accordance with onset of intestinal disease, the body weight of control fed *Apc*$^{fl/fl}$ mice which had survived to 30 days PI (44 days on diet) were significantly reduced by approximately 7% (16 days PI = 105%, n = 8 vs 30 days PI = 98%, n = 6, p value = 0.0080, Mann Whitney U test, Figure 5.1B). While BRB treated *Apc*$^{fl/fl}$ mice at 30 days PI had lost 3% of their body weight on average, it was not found to be significant and suggested that BRBs have a protective effect against disease onset. The final weight measurement taken for *Apc*$^{fl/fl}$ mice was just before sacrifice, when mice presented with symptoms of illness including loss of weight (no more than 25% of original body weight), paling of feet and tail, piloerection and abdominal pinching and hunching. *Apc*$^{fl/fl}$ mice fed on the control and BRB diets had significantly reduced in weight at the time of sacrifice by 12% and 20% respectively when compared to their body weights at 30 days PI (control diet: 30 days PI = 98%, n = 6 vs death = 86%, n = 7, p value = 0.035. BRB diet: 30 days PI = 102%, n = 8, vs death = 82%, n = 10, p value = < 0.0001, Mann Whitney U test, Figure 5.1B). It is apparent that the reduction in body weight is due to illness and not as a result of feeding on the specific diets. This is supported by the wildtype data in Figure 5.1A that indicated at all-time points there was no significant change in the weight profile between control and BRB fed mice. However, as the average body weight of BRB treated *Apc*$^{fl/fl}$ mice were marginally higher than the control mice at the each time point it suggested that body weight of BRB treated *Apc*$^{fl/fl}$ mice was maintained for longer, and subsequently lost slower when mice become symptomatic of disease.

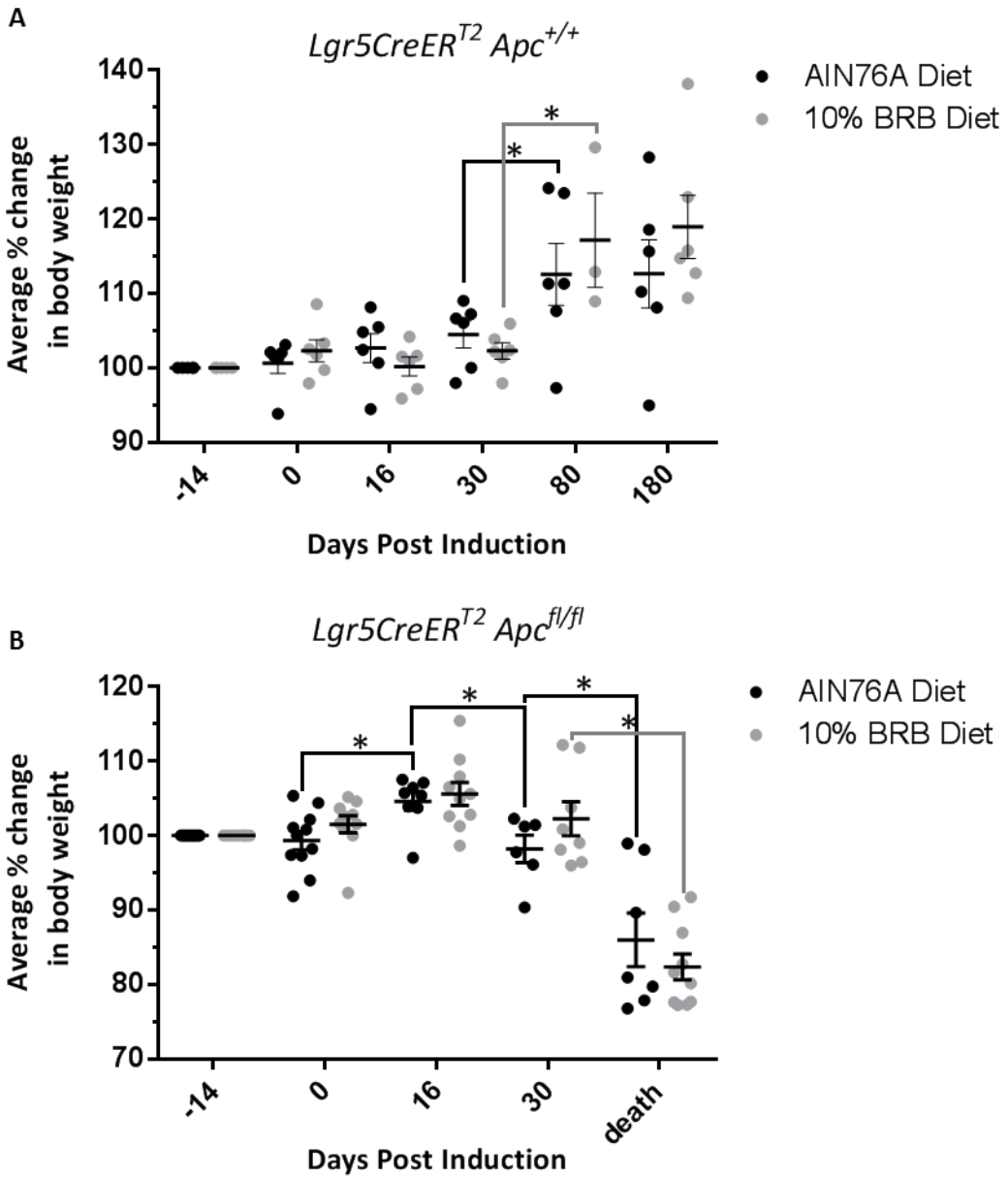

Figure 5.1 Average % change in body weight of *Lgr5CreER^{T2} Apc$^{+/+}$ and Apc$^{fl/fl}$* mice in the context of BRB diet

All mice were started on their respective diets 2 weeks (-14 days) before induction with tamoxifen (0). (A) The average weight of wildtype mice (*Apc$^{+/+}$*) was not altered by feeding on AIN76A (control) or 10% freeze-dried BRB diet for 30 days post induction (44 days on diets in total). After a further 50 days on the diet (80 days post induction) AIN76A and BRB fed mice weighed significantly more, consistent with gaining weight with increased age. At 180 days post induction (194 days on diets) both AIN76A and BRB fed mice had not significantly increased in body weight compared to 80 days post induction. There was no significant difference in weight between AIN76A and BRB fed wildtype mice at any time point. This suggested that long-term feeding of BRBs does not adversely affect body weight. (B) The average weight of *Apc$^{fl/fl}$* mice was not altered following 2 week feeding on their respective diet. *Apc$^{fl/fl}$* mice fed the AIN76A diet increased in body weight following a further 16 days on the diet, while BRB exposed mouse body weight was not significantly altered. At 30 days post induction (44 days on diet), body weight of AIN76A mice significantly decreased in accordance with onset of illness, but BRB fed mice maintained their weight. At time of death, both AIN76A and BRB fed mice weighed significantly less than at 30 days post induction. n.b. measurements for *Apc$^{fl/fl}$* do not include all mice measured initially as not all *Apc$^{fl/fl}$* mice survived to these time points. * P value ≤ 0.05, n = 6 - 11, two-tailed Mann Whitney U test. Error bars represent SEM.

5.2.2 Long-term feeding of 10% BRBs significantly increased survival of mice following deletion of *Apc* in ISCs

Long-term feeding on BRB diet did not affect the lifespan of wildtype mice but significantly prolonged the life of tumour bearing $Apc^{fl/fl}$ mice.

At 190 days post tamoxifen induction, $Lgr5CreER^{T2}$ $Apc^{+/+}$ BRB fed mice (n = 6) and 5/6 $Lgr5CreER^{T2}$ $Apc^{+/+}$ control mice showed no signs of ill health and so were culled (p value = 0.3173, Log-rank (Mantel-Cox) test and Gehan-Breslow-Wilcoxon test, Figure 5.2). One wildtype control mouse was sacrificed at 134 days post induction when it showed evidence of paling feet and abdominal hunching. Upon dissection it presented with abnormal looking kidneys, they were discoloured, rough and dehydrated in appearance. Since Cre expression under the *Lgr5* promoter is not expressed in the kidney upon induction with the relevant inducing agent, the decline in health of this wildtype control could be attributed to the normal process of ageing. $Lgr5CreER^{T2}$ $Apc^{fl/fl}$ mice fed on the control and BRB diets started showing symptoms of ill health at 20 and 28 days post induction, respectively. Survival analysis revealed that feeding of BRBs prior to deletion of *Apc* within the ISCs, and continued feeding post induction, significantly increased the lifespan of tumour bearing mice by 22 days compared to the $Apc^{fl/fl}$ controls ($Apc^{fl/fl}$ control median survival = 32 days, $Apc^{fl/fl}$ BRB median survival = 54 days, n = 15, p value = 0.0343 Log-rank (Mantel-Cox) test, p value = 0.0032 Gehan-Breslow-Wilcoxon test, Figure 5.2). The small and large intestine was harvested from the mice at time of culling. The intestinal sections were fixed ready for counting of histological markers. Due to this approach of tissue preparation it was not possible to determine tumour burden. This is because the $Lgr5CreER^{T2}$ $Apc^{fl/fl}$ model develops a 'blanket' of adenomas at the stomach end of the small intestine, making it very difficult to identify discrete tumours. As previous studies using mouse models of *Apc* driven tumourigenesis have shown BRBs to reduce tumour burden, it could be hypothesised that mice survived longer as a result of a lessened tumour burden.

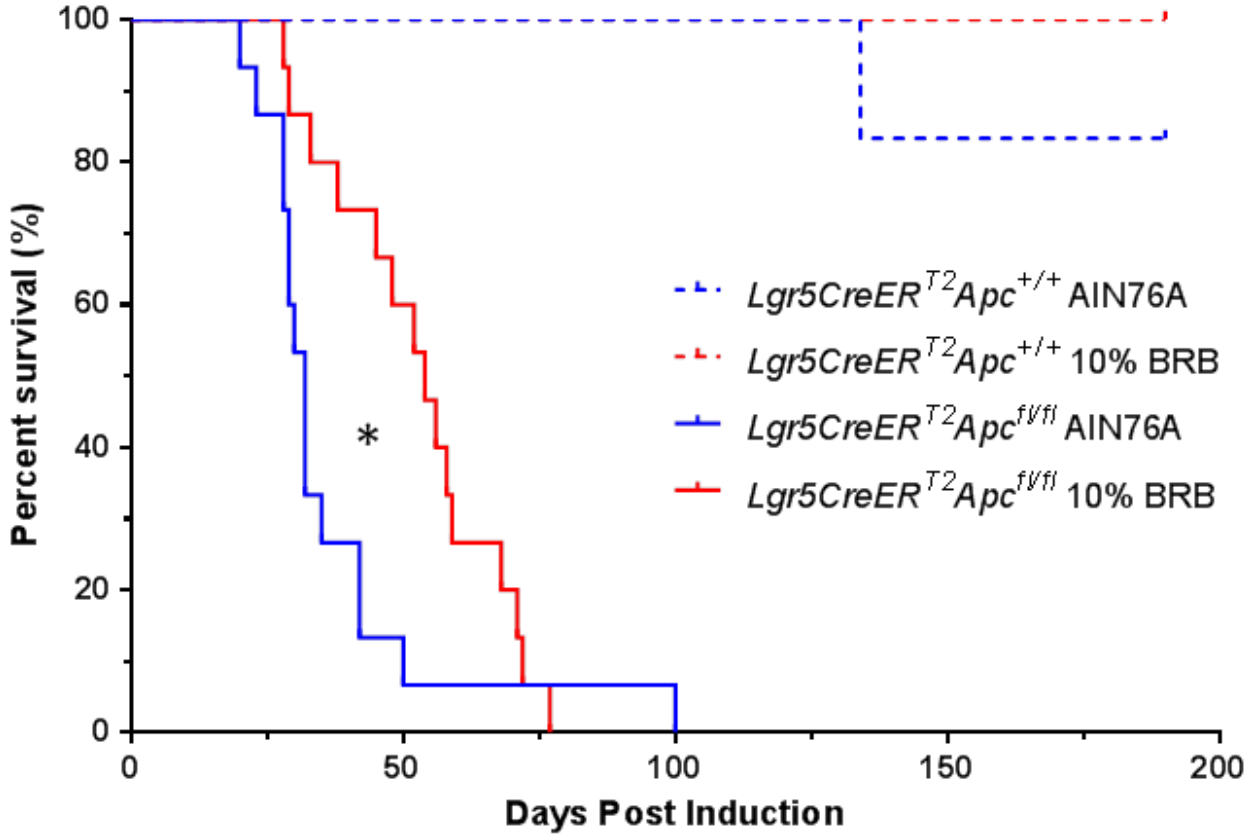

Figure 5.2 Overall survival curve of *Lgr5CreER^{T2} Apc$^{+/+}$* (dashed lines) and *Apc$^{fl/fl}$* mice (solid lines) on the AIN76A (blue) and 10% freeze-dried BRB diet (red) post induction with tamoxifen

Wildtype mice did not present with signs of ill health so were culled at 190 days post induction. There was no statistical difference in wildtype survival, p value = 0.3173, n = 6 vs 6, Log-Rank statistical test. The median lifespan of *Apc$^{fl/fl}$* mice was increased by 22 days post induction by feeding on the 10% BRB diet compared to the AIN76A diet, * p value = 0.0343, n = 15 vs 15, Long-rank statistical test.

5.3 Discussion

5.3.1 Evaluating the effect of long-term BRB feeding on body weight

A key aim of the work was to determine whether long-term feeding of BRBs had any detrimental effect on the health of animals. This can be evaluated by measuring weight gain or loss over the length of the experiment. This was investigated in both a non-tumour bearing (*Lgr5CreER^{T2} Apc$^{+/+}$*) and intestinal *Apc$^{fl/fl}$* driven tumour setting (*Lgr5CreER^{T2} Apc$^{fl/fl}$*) in the context of control and BRB diet.

The body weights of wildtype and *Apc$^{fl/fl}$* mice were not affected by long-term feeding on BRBs in relation to the AIN76A fed controls. This is consistent with studies that have shown in a model of rat oesophagoduodenal anastomosis which mimics the development of human oesophageal adenocarcinomas, BRB feeding did not alter the weight of animals in relation control animals (Aiyer *et al.* 2014). The limitation of this study is that the rats were only administered BRBs for 4 weeks and so longer-term exposure in this model could have different results. In addition, in a study of carcinogen induced oesophageal cancer in rats fed 10% BRBs over a period of 30 weeks, weights of animals was not altered on BRBs until the last 3 weeks of the study when rats on BRBs had lower body weights compared to vehicle treated rats (Kresty *et al.* 2001). However, the authors have not addressed why these animals lost weight. In relation to the study described herein, the work described by Kresty *et al.* (2001) in models of oesophageal tumourigenesis was performed for a longer duration than the work here using the *Lgr5CreER^{T2} Apc$^{fl/fl}$* model of intestinal tumourigenesis. Despite this it would not be possible to evaluate the effect of BRBs in *Lgr5CreER^{T2} Apc$^{fl/fl}$* mouse model as the phenotype of intestinal tumour burden occurred quicker than the phenotype of oesophageal tumourigenesis in rats. However, in the context of the results described in this chapter it can be concluded that BRBs do not adversely affect mouse weight.

On average, mice fed the BRB-enriched diet had similar body weights to their respective controls; however this experiment did not evaluate whether feeding patterns were altered. Although the addition of BRB powder to the AIN76A diet occurred at the expense of sucrose it is possible that the sugar content between the two diets were slightly different, as BRB anthocyanidins contain sugar moieties. In order to have a better understanding of the associations that underpins the chemopreventive effects of freeze-dried BRBs in CRC it may be beneficial to analyse dietary intake among cohorts and perform metabolomics studies to evaluate whether biomarkers and glucose and hormone levels are altered as a result of BRB feeding.

5.3.2 Long-term feeding on BRBs prolongs life of tumour bearing mice

The second aim of this work was to determine, if any, the long-term effect of BRBs on non-tumour and tumour mice. All but one wildtype mouse fed both the AIN76A and 10% freeze-dried BRB diet presented with no signs of illness at 190 days post induction. The experiment was terminated at this time point due to time restrictions. While feeding on BRBs did not alter the lifespan of wildtype mice, it improved the survival of *Apc*$^{fl/fl}$ mice which developed macroscopic stem-cell derived Wnt-driven adenomas. This is the first time that exposure to BRBs has been reported to increase the survival of a Wnt-driven tumourigenic mouse model, and thus supports the use of BRBs as a novel therapeutic strategy in preventing and managing CRC.

Despite this promising result, the work described in this chapter did not provide an insight into how BRBs improved survival. Previously published work has shown that 12-week feeding of 10% BRB diet in two distinctive models of intestinal and CRC cancer, reduced tumour burden and multiplicity by targeting several pathways. It was found in one model of *Apc* inactivation, that BRBs inhibited intestinal tumourigenesis by supressing Wnt/ β-catenin signalling, and in the other model of inflammation-driven colon tumourigenesis by dampening down chronic inflammation (Bi *et al.* 2010). From this study it is evident that BRBs reduced tumour incidence and this is also supported by various other studies in rodent models of oesophageal cancer (Kresty *et al.* 2001), chemically induced colon cancer (Harris *et al.* 2001) and regression of polyps in FAP patients (Wang *et al.* 2014). Despite the reduction in tumour burden these studies propose different mechanisms of action (i.e. epigenetic alterations, suppression of various signalling pathways such as Wnt, regulation of inflammatory processes, oxidative stress etc.) and in some clinical studies report some non-responders to BRB treatment. This could be attributed to the natural heterogeneity among patients and within tumours. In addition, the method of BRB administration and concentration varied across studies and could be a possible reason for the different outcomes.

This thesis is the first to investigate the effects of BRB-enriched diet on ISCs, specifically in the context of gene loss. Unlike in human disease, the *Lgr5CreER*^{T2} *Apc*$^{fl/fl}$ mouse model does not require a second hit of *Apc* loss for tumour initiation. Using this model, it is evident that BRBs play a significant role in supressing initiation or growth of CRC, which is relevant at the ISC level.

5.4 Summary and Future Directions

In summary, two major conclusions can be made from the data presented in this chapter. Firstly, long-term feeding on BRBs is well tolerated and did not have any adverse effect on body weight in wildtype or tumour bearing mice. Secondly, 10% freeze-dried BRBs in the diet prolonged the life of tumour bearing mice that result from chronic loss of *Apc* in the ISCs.

Taken together, in combination with previously published data, these results indicated that BRBs display chemopreventative effects against colorectal tumourigenesis, at least in part, by influencing the normal and/ or malignant ISCs. This provides more evidence for the use of BRBs as a natural chemopreventive option. However, several interesting questions remain unanswered with regard to stem cell dynamics and dosing regimens and thus warrant further investigation.

As Wnt signalling has been attributed to the development of both human and murine CRC (Powell *et al.* 1992; Leslie *et al.* 2002) and previous studies have shown that BRBs supressed Wnt/ β-catenin signalling (Bi *et al.* 2010), it would also be beneficial to determine the effects of BRBs on the Wnt status in the *Lgr5CreER^{T2} Apc$^{fl/fl}$* mice. This could be achieved by analysing the number of cells that contain nuclear and cytoplasmic β-catenin using IHC. In addition to this, qRT-PCR gene expression analysis could be performed for Wnt target genes on normal adjacent tissue and tumour tissues that were frozen at time of dissection. As previously outlined, tumour number was not determined from *Apc$^{fl/fl}$* mice fed the AIN76A or BRB diets. It is important to evaluate whether BRB exposed mice survived longer as a result of a reduced tumour burden. A recent study by Phesse *et al.* estimated tumour burden of *Lgr5CreER^{T2} Apc$^{fl/fl}$* mice by measuring the area of adenomas on H&E stained histological cross sections of 'swiss-rolled' intestines and normalising to the length of the intestine per mouse (Phesse *et al.* 2014). In addition, it would also be beneficial to count the number of small intestinal lesions or ACF from H&E and β-catenin stained *Lgr5CreER^{T2} Apc$^{fl/fl}$* intestines at an earlier time point when tumours have manifested. To evaluate this, separate cohorts of *Lgr5CreER^{T2} Apc$^{fl/fl}$* fed the AIN76A and BRB diets were dissected at 20 days post induction. The intestinal sections have been stained for H&E and β-catenin IHC and are waiting to be analysed for tumour number. Therefore, the number of tumours in control and BRB fed mice could be determined using these techniques in the future.

Several studies have outlined the chemopreventative effects of BRBs, but the fundamental question of what effect BRBs have on the intestinal and cancer stem cells has not been investigated. Although this thesis has identified gene expression changes of ISC markers and a reduction in ISC self-renew capacity *ex vivo*, it is still necessary to determine the number of stem cells that are present following BRB treatment. As the *Lgr5CreER^{T2}* model drives GFP expression in Lgr5^{+} stem cells (Barker *et al.* 2007), immunohistochemistry for GFP could be performed on formalin-fixed paraffin-embedded intestinal tissue from *Lgr5CreER^{T2} Apc$^{+/+}$* and *Apc$^{fl/fl}$* mice 20 days post induction. This would enable quantification of the number of stem cells depicted by GFP positivity in the context of BRB treatment. If this is unsuccessful RNAscope® *in situ* hybridization technology for *Lgr5* in the same mouse models could be used or quantified by the amount of GFP fluorescence in control and BRB fed mice from FACs sorted intestinal epithelial cells, which would represent the percentage of Lgr5^{+} ISCs.

6 General Discussion

CRC is the fourth most common cancer type in the UK, but accounts for the second most deaths by cancer after lung cancer (CRUK 2014). With an ever-increasing ageing population, CRC incidence continues to rise despite improvements in survival rates. It is known that CRC develops through interplay of genetic, epigenetic and environmental factors but what is most surprising and not readily made aware of is that over half of new CRC cases could have been prevented by lifestyle changes (Hou *et al.* 2013). This highlights the importance of understanding and determining novel chemopreventative strategies that can delay, reverse or inhibit the process of carcinogenesis (Sporn 1976; Steward and Brown 2013).

Several studies have reported an association between diet and cancer risk, in particular in CRC. Diets high in fat have been linked to an increased risk whereas diets rich in fibre and fruit result in a reduced risk (WCRF/AICR 2011). The specific mechanisms that underpin these interactions are not well understood. Previous work has evaluated the use of several nutritional polyphenols as naturally occurring chemopreventive agents. The protective roles of the polyphenols found in BRBs have been extensively studied in cell lines, animal models and in human patients at the initiation and progression stages of CRC (Kula and Krauze-Baranowska 2016). Evidence from cell line studies and human CRC patients has shown that BRBs were responsible for epigenetically reactivating silenced Wnt pathway antagonists. Animal based studies (Bi *et al.* 2010), supported by human studies of CRC (Wang *et al.* 2011) and FAP disease (Wang *et al.* 2014) reported that BRBs were sufficient to inhibit tumourigenesis and regress FAP polyps, providing further evidence of the chemopreventative properties of dietary polyphenols. While this holds great promise for cancer prevention, these studies are limited as the effect of BRBs on both normal and malignant ISC populations have not been investigated.

The majority of CRCs are known to initiate from mutations that activate the Wnt signalling pathway, with the most common gene mutations occurring in the Wnt antagonist *APC*. For many years the cell of origin remained elusive however, in 2009 Clevers' group identified the intestinal CBCs as the cell of origin of intestinal cancer in murine models (Barker *et al.* 2009). This work emphasises the relationship between ISCs and carcinogenesis.

The aim of this thesis was to explore applications of BRB to address the following questions, in the context of normal and malignant ISCs:

1. Do BRBs adversely affect normal homeostasis of the murine adult intestine?
2. What are the chemopreventative effects of BRBs at the earliest stages of intestinal tumourigenesis following homozygous deletion of *Apc*?
3. What effect do BRBs have on long-term Wnt-driven tumourigenesis?

This chapter aimed to explore to what extent the above three objectives have been achieved and the contributions made by this thesis.

6.1 BRBs and intestinal homeostasis

Chapter 3 described work investigating the short-term effects of dietary BRB supplement on normal murine small intestinal homeostasis. Investigations revealed that 2 week feeding on 10% BRB powder, in two mouse models, did not perturb the gross structure of the small intestine. BRBs had no effect on the differentiated goblet and Paneth cell types. However, proliferation decreased while cell death and enteroendocrine differentiation increased in the context of BRBs. Although there is limited data on the effect of dietary polyphenols on strictly 'normal' tissues, it is known that the enteroendocrine cell population are specifically sensitive to dietary changes due to their role as chemo sensors within the gut (Moran-Ramos *et al.* 2012; Gribble and Reimann 2016). A recent study highlighted that the number of enteroendocrine cells in the intestine reduced in the context of high fat diet (HFD) (Beyaz *et al.* 2016). As HFDs have been associated with increased risk of developing cancer, it could be hypothesised that diets which maintain or enhance enteroendocrine differentiation promotes normal homeostasis and lowers the risk of cancer.

Intestinal homeostasis depends on a balance between asymmetric and symmetric ISC divisions and the ratio of stem or differentiated daughter cells that are produced (Stine and Matunis 2013). Thus, stem cells may play a vital role in how tissues adapt to diet-induced physiological states. Chapter 3 also evaluated the effect of BRBs on normal ISCs. Gene expression data of putative markers revealed that in one short-term wildtype model, *AhCre*, either ISC marker expression levels or total ISC number may be altered by BRBs, concordant with alterations in Wnt target genes, while no alteration in ISC expression was noted in the second model, *VillinCreER^{T2}*. These data indicated that BRBs may protect normal intestinal tissue from genetic insult by limiting the ISC capacity and number of highly proliferative daughter cells. However, these potential changes do not occur at the expense of survival, as long-term feeding of BRBs did not affect the lifespan or weight (and thus, health) of wildtype mice as described in chapter 5. Thus, a change in the ISC population did not have any adverse effect on intestinal homeostasis. This is supported by several studies which have shown that intestinal homeostasis is not perturbed following the complete loss of *Lgr5*-expressing cells (Tian *et al.* 2011; Yan *et al.* 2012). In addition, administration of BRBs has been reported to be well tolerated by humans in several clinical trials of oral, oesophageal and colorectal cancers (Stoner *et al.* 2005; Kresty *et al.* 2006; Shumway *et al.* 2008; Wang *et al.* 2011), with only mild disturbances including diarrhea and constipation which was resolved within a few days (Kresty *et al.* 2006; Wang *et al.* 2011). This indicates that any adverse effects of BRBs on normal tissue could be minimal if used as a cancer therapeutic which is supported by no change in weight of wildtype or *Apc* deficient mice as a result of BRB diet.

Despite this, some patients in a study of BRB intervention in Barrett's esophagus (BE) experienced weight gain (Kresty *et al.* 2006). This is in contrast to the results presented herein that show long-term feeding on BRBs in wildtype (~7 months) and Wnt-driven tumour bearing mice (average duration on BRB diet ~ 3 months) had no adverse effects on body weight when compared to mice fed a matched basal diet. The authors' reported that patients were not advised to modify their usual diet and suggested that the extra caloric intake from BRBs could be responsible for the weight gain (Kresty *et al.* 2006). However, the study explains that whilst compliance of berry consumption was documented, consumption of other food stuffs consumed was not recorded. Only 2 out of 10 patients who completed the trial reported considerable weight gain (14 lb), and so it could be possible that weight gain was related to consumption of other dietary components that the researchers were unaware of. Despite this, this result should not be disregarded, as it warrants further investigation and consideration for dietary interventions in patients as obesity is a major risk factor associated with the progression of many cancers.

The major caveat of the work described in chapter 3 is that the control diet used in the *AhCre* experiments was not basal matched to the BRB diet, due to availability of the AIN76A control diet at the time. However, there were several direct comparisons between the two short-term models which enable us to confidently conclude that BRBs enhanced cell death and enteroendocrine differentiation in wildtype mice, whilst not overtly affecting the intestinal homeostasis and ongoing health of the animal. Thus, further analysis of the proliferation, ISC and Wnt target gene changes are warranted in order to ascertain whether these alterations are truly the case of addition of BRBs to the diet. It is also important to note that the number of animals utilised in the short-term feeding experiments were relatively low. A cohort size of 3 animals had the ability to detect a statistical change at the power of 58.6% which may not be sufficient to detect subtle changes that are likely to occur in dietary intervention studies, therefore warranting larger cohort sizes in subsequent studies.

To my knowledge, this is the first study to investigate the effect of BRB intervention on wildtype murine intestine without any precancerous or tumour settings. Taken together, the data presented in this thesis indicated that BRBs have no major detrimental effects on the health of mice. This is important because, in human cancer patients the majority of tissue is normal, which means there should be minimal detrimental effect on normal tissue and reduced side effects if BRBs were used as a potential chemotherapeutic against cancer. However, these studies only evaluated the effect of BRBs on Wnt signalling, which presents the question 'what effect do BRBs have on other signalling pathways crucial for intestinal homeostasis?' To potentially resolve this issue, Western blotting, qRT-PCR and IHC analysis could be performed for targets involved in the Notch, Hedgehog and TGF-β/BMP signalling pathways. This work is also hindered by the lack of specific ISCs markers

which limits our ability to definitively characterise and identify the ISC populations. As stem cell dynamics may be altered in the context of BRBs it is fundamental that a mechanism of action is elucidated. Performing the stemness organoid forming and self-renewal assays in the presence of BRB-derived ACs will provide further insight into the effect of BRBs on the ISCs however, it will not aid in determining whether the number of stem cells are altered or provide information regarding stem cell-niche interactions. The newly developed RNAscope® technology enables the reliable detection of stem cells at the level of a single RNA transcript (Wang *et al.* 2012), and will allow quantification of the number of stem cells present in control and BRB fed wildtype mice. This line of analysis is currently being pursued within our laboratory on the two short-term wildtype models, control and BRB fed *AhCre Apc*$^{+/+}$ and *VillinCreER*^{T2} *Apc*$^{+/+}$ mice.

The data presented here suggests that BRBs may protect normal intestinal tissue from neoplastic changes in the future however, the relevance of the model system must be considered. Whilst murine models represent an invaluable tool for evaluating the links between genetics, diet, health and disease the differences between mouse and humans restricts their use to confidently predict human responses. The majority of clinical studies evaluating the effects of BRBs in humans have been in a premalignant or cancer setting; however in the phase I clinical study by Wang *et al.* biopsies of adjacent normal tissue was taken alongside colorectal adenocarcinomas from 20 patients before and after 1 – 9 weeks of BRB powder intervention (Wang *et al.* 2011). Although the adjacent normal tissue biopsies are not strictly wildtype, as they have been taken from CRC patients, it would be useful to determine the number of stem cells present following BRB administration[1], this could be achieved through the RNAscope®[2] technology of stem cell markers on paraffin embedded tissue sections. Additionally, characterisation of proliferation, apoptosis, differentiation and cell migration would also be beneficial to establish if BRB treatment in humans supports the data obtained from mouse models.

6.2 BRBs, *Apc* deficiency and intestinal stem cell interactions

Initial work described in this thesis (chapter 3) examined the effects of BRBs on the immediate loss of *Apc* in the murine small intestine. This was achieved by conditional deletion of both copies of the *Apc* gene within the crypt epithelium (excluding Paneth cells, *AhCre Apc*$^{fl/fl}$) and the entire intestinal epithelium (*VillinCreER*^{T2} *Apc*$^{fl/fl}$), which has been previously reported to cause aberrant Wnt

[1] Formalin-fixed paraffin-embedded blocks containing normal adjacent tissue biopsies from CRC patients before and after intervention with BRBs were kindly provided in collaboration with Dr Li-Shu Wang, Medical College of Wisconsin, USA.

[2] The normal adjacent tissue sections from CRC patients are currently undergoing RNAscope® *in situ* hybridisation for the putative stem cell markers *LGR5* and *OLFM4* in collaboration with Prof Owen Sansom's group, Beatson Institute, CRUK centre Glasgow, UK.

signalling, expansion of the crypt compartment, enhanced proliferation and apoptosis and abrogated differentiation and migration (Sansom *et al.* 2004; Andreu *et al.* 2005). The continual proliferation, lack of migration and cell sloughing leads to retention of mutant cells and tumour initiation. The restoration of apoptosis and increased differentiation by BRBs likely reduces the tumourigenicity of the mutant cells. This present study is the first to report partial rescue of the cellular differentiation pathways by BRBs in murine models of intestinal dysfunction. Work by Bi and colleagues reported that 12-week feeding of BRBs had no effect on goblet cell differentiation in two murine models of intestinal tumourigenesis (Bi *et al.* 2010). Clearly, there is some discrepency between the data reported here and that of the published data by Bi *et al.* (2010). The limitation of their study is that, firstly, differentiation was not broadly investigated, such that Paneth and enteroendocrine cells were not evaluated and secondly, the number of goblet cells was assessed from normal adjacent tissue and not from premaligant or tumour tissue. Thus, their data may be better compared to the wildtype data described in chapter 3, such that goblet cell differentiation was not altered by BRB in the normal intestine. Despite this, BRBs have been documented to have protective roles in modulating host immune differentiation of myeloid cells in chronic inflammation and tumour settings (Mace *et al*. 2014), thereby providing further evidence in support of the beneficial effects of BRBs in cancer prevention. The *AhCre* data supports the notion that BRBs protectively modulate cell differentiation. In addition, BRBs were also found to increase rate of migration of cells along the crypt-villus axis, and thus increase the likelihood of eliminating *Apc* deficient cells from the epithelium that are capable of initiating tumourigenesis. Due to time constraints migration was only evaluated in the *AhCre* experiments, however intestinal tissue sections from *VillinCreER^{T2} Apc$^{fl/fl}$* mice have been stained for BrdU IHC and are awaiting analysis.

Current cytotoxic therapies have shown promise in the treatment of CRC by reducing the size of tumours (Corrie *et al.* 2008). The bulk of a tumour is comprised of rapidly dividing cells that are targeted by chemo and radio therapies. One of the contributing factors to the shortcomings of current cancer therapies is the fundamental notion that CSCs have a slower cycling time and thus develops resistance to therapeutics, enabling the reestablishment of tumourigenesis, metastasis and relapse (Kim *et al.* 2016b). This limits the suitability of several cancer therapeutics and highlights two areas for improvement 1) the requirement for a better understanding of the mechanisms underlying malignant stem cell populations and 2) the need for novel therapeutic strategies which can target these populations without the adverse side effects associated with many current regimes. Chapters 3 and 4 highlighted that altering the diet, in this instance short-term feeding on BRBs *in vivo*, or exposure to BRB-derived anthocyanins *ex vivo*, is enough to alter stem cell dynamics. The expression of putative stem cell markers, *Lgr5* and *Olfm4,* were down-regulated when crypt dynamics were altered as a

consequence of acute *Apc* loss driven by the *Ah* transgene, in the context of BRB intervention. While *Apc* loss within the entire intestinal epithelium mediated by the *VillinCreER^{T2}* transgene resulted in the up-regulation of these markers in the context of BRBs. This highlighted how ISC response to BRB diet is influenced by the cell types which are *Apc* deficient, which is discussed in more detail later on. However, organoid studies revealed that whilst prior treatment with BRBs had no effect on the ability of *Apc* deficient crypts to form organoids, the ability of *Apc* deficient cells to form organoids following disruption to single cell was greatly inhibited by ACs. This indicates that ACs influence self-renewal and therefore ISC activity. This supports the *in vivo* data (*AhCre*) which showed a lower level of ISC marker expression as a result of the BRB diet. This is significant for three reasons. Firstly, this is the first study to evaluate the chemopreventative effect of BRBs against a malignant stem cell population. These data therefore represent the first evidence indicating that BRB-derived ACs prevented the self-renewal of Wnt-activated, and thus pro-tumourigenic, ISCs. Secondly, this suggests that BRB-derived ACs are sufficient to prevent malignant stem cell self-renew. And thus, BRBs may be a useful intervention that targets the CSC population. Finally, the correlation between the *ex vivo* data and the *in vivo* expression levels indicates that the self-renewal assay described here is a useful indication of ISC capacity.

Several naturally occurring dietary compounds have already been reported to target the stem cell population in disease settings. For example, resveratrol, found in the skin of grapes and several edible berries, has been shown to inhibit Wnt signalling and the proliferative nature of breast cancer stem-like cells (BCSCs) *in vitro* and *in vivo*, thereby limiting their ability to form mammospheres (Fu *et al.* 2014). Quercetin, found in many fruits, vegetables, leaves and grains, has been reported to reduce the self-renewal capacity of pancreatic cancer cells enriched in CSC markers to form spheroids, induced apoptosis and reduced expression of CSC and metastatic markers. Studies have reported that curcumin potentially targets CSCs by down-regulating Wnt signalling in breast (Kakarala *et al.* 2009), gastric, intestine, and colon cancer cells (Park *et al.* 2005), and inhibiting Wnt and Hedgehog pathways in medulloblastoma cancer cells (Elamin *et al.* 2010). Additionally, curcumin sensitised quiescent leukemic cells (Gardane *et al.* 2016) and previously resistant colorectal CSCs to conventional chemotherapeutics (Kanwar *et al.* 2011) and targeted therapies (Yu *et al*. 2009; Nautiyal *et al.* 2011). These naturally occurring dietary compounds show great potential for irradiating the CSC populations with far fewer toxic side effects. It is likely that the mechanism which underpins the chemotherapeutic effects of BRBs in limiting the self-renewal ability of malignant cells, is similar to those reported for other dietary compounds. This warrants further investigation into novel intervention strategies using dietary phytochemicals that target CSCs, specifically in the context of the BRB intervention.

One interpretation of the data presented herein is that the rate and site of recombination between the two short-term models has a critical impact on BRB response. Wnt-activation in all differentiated cells in particular Paneth cells had a profound effect on the ISC marker expression, which limits the use of the *VillinCreER*^{T2} model to accurately reflect true changes in ISC marker expression, especially in the context of BRB intervention. As briefly touched on, there remains controversy over the relevance of certain markers of the ISCs, as some markers are also targets in particular pathways. In the results described herein, it was found that the stem cell marker *Ascl2* was up-regulated in the *AhCre Apc*$^{fl/fl}$ mouse following BRB treatment, which is contradictory to the *Lgr5* and *Olfm4* patterns. While this could be interpreted as enhancing 'stemness', previous work in the group found that entopic overexpression of *Ascl2* in the *Apc*^{Min} mouse had no effect on tumour formation or survival in a Wnt dependent setting (Reed *et al.* 2012). Thus taking this into consideration, it is possible that an increase in *Ascl2* expression following BRB intervention does not contribute to tumourigenesis in Wnt-activated intestinal epithelial. Aside from being markers of the ISC population, Lgr5, Olfm4 and Ascl2 have functional roles in the intestine however, their roles still remain elusive. Several studies have reported that LGR5 functions as a receptor of R-spondins in stem cells, and thus is an activator of the Wnt signalling pathway (Carmon *et al.* 2012). In the context of the *AhCre* mouse model, a reduction in *Lgr5* gene expression could represent a decrease in the number of Lgr5 receptors, and potentially fewer stem cells. This could decrease the risk of Wnt-driven tumourigenesis by down-regulating the Wnt signalling pathway. OLFM4 has been reported to be a Wnt pathway antagonist, by competing with ligands for the frizzled receptors at the cell surface, especially in *APC* deficient intestinal tissue (Liu *et al.* 2016). Thus, down-regulation of *Olfm4* expression could result in reduced Olfm4 protein to negatively regulate the Wnt signalling pathway, which could potentiate intestinal tumourigenesis. However, *OLFM4* has also been documented as a target gene of the Wnt signalling pathway (Liu *et al.* 2016) and so its down-regulation in the *AhCre Apc*$^{fl/fl}$ model following BRB treatment may simply be related to decreased Wnt signals and stem cell potential. Ascl2 is a Wnt target and has been reported to be a 'Wnt-responsive master transcription factor' that governs Lgr5^{+} stem cell identity (Yan and Kuo 2015), as deletion of *Ascl2* in mice resulted in a loss of Lgr5^{+} ISCs (van der Flier *et al.* 2009b). Findings from Schuijers *et al.* report a mechanism whereby Ascl2 regulates its own expression via an autoactivatory loop dependent on previous Wnt/R-spondin thresholds. Cells which were subjected to a 'low-Wnt-signal' required a stronger Wnt signal to up-regulate *Ascl2* expression, whereas cells from a 'high-Wnt-signal' environment did not and thus Ascl2 can act as transcriptional switch for stemness (Schuijers *et al.* 2015). It could be predicted from these findings, that the previously high levels of Wnt activation and enhanced stem cell potential in *Apc*$^{fl/fl}$ crypts enhanced *Ascl2* transcription to try and maintain the reduction in active cycling stem cell

identity that occurs following BRB treament. Another prediction that can be made from the findings by Schuijers is that the intestinal epithelium maintains a state of plasticity such that queiscent stem cell populations, committed progenitors and mature differentated cells may be able to interconvert to a stem cell state when presented with an appropriate signal (Schuijers *et al.* 2015).

This thesis is the first to investigate the effects of BRB-enriched diet on ISCs, specifically in the context of gene loss. The organoid work however, is limited by its inability to fully recapitulate the *in vivo* microenvironment of mice and humans, and provide an insight into whether the number or function of malignant ISCs is affected by BRB intervention. Unlike in human disease, the *Lgr5CreER*^{T2} *Apc*$^{fl/fl}$ mouse model does not require a second hit of *Apc* loss for tumour initiation. Using this model, it suggests that BRBs play a significant role in supressing initiation or growth of CRC, which is relevant at the ISC level, as BRB intervention significantly prolonged the lifespan of mice bearing ISC derived tumours (chapter 5). Given that recent data in the literature has indicated that tumour and polyp incidence is reduced following BRB intervention in animal and human based studies (Bi *et al.* 2010; Wang *et al.* 2011; Wang *et al.* 2014), it could be hypothesised that, in the context of BRB feeding, the lifespan of tumour bearing mice is prolonged due to a reduced tumour burden. Although tumour burden has not been determined in this thesis, intestinal tissue sections at 20 days post induction have been stained with H&E and β-catenin IHC and are waiting to be analysed for tumour number and grade. The question that remains is, 'what is the net effect on the ISC population?' Knowledge of the ISC population and dynamics presents two potential hypotheses;

1) The BRB diet reduces the number of ISCs before induction such that initiation of tumourigenesis is reduced by limiting the number of cells which have the potential to form tumours when transformed (Figure 6.1A).
2) BRBs act to inhibit the proliferative and self-renewal nature of the transformed/ malignant ISCs (or CSCs) which give rise to intestinal lesions (Figure 6.1B).

Previous work by Beyaz *et al.* has shown that high-fat diet increased the number and self-renewal capacity of ISCs *in vivo*, enhancing their tumourigenic potential (Beyaz *et al.* 2016), so it is likely that BRBs may also interfere with stem cell dynamics. A separate study by Doug Winton's group have reported that certain oncogenic mutations, including heterozygous and homozygous loss of *Apc* within the ISC compartment, confer a competitive advantage to mutated stem cells over neighbouring stem cells. This advantage is conferred by the preferential division of these mutant stem cells to produce two ISC daughter cells instead of two TA cells, thereby skewing neutral drift. This skew to neutral drift increases the chances of the mutated clone becoming represented in every cell within the crypt, a process known as crypt fixation. By acting on the normal dynamics of stem cell

replacement (Lopez-Garcia *et al.* 2010; Snippert *et al.* 2010), $Apc^{+/-}$ clones had a slight advantage over wildtype cells, while $Apc^{-/-}$ mutant clones had a much greater selective fitness and were able to fix within the crypt, such that the mutant clones were retained whilst wildtype cells were lost from the crypt (Vermeulen *et al.* 2013). This led to a third hypothesis, such that it may be possible that exposure of malignant *Apc* ISCs to BRBs *in vivo* limits the competitive advantage of *Apc* loss such that the normal neutral drift within the intestinal crypt is restored, reducing the frequency at which oncogenic mutations are fixed within the crypt and able to initiate tumourigenesis (Figure 6.2). However, in order to investigate whether this hypothesis is correct, lineage tracing technology will need to be applied to the $AhCreER^{T2}$ $Apc^{fl/fl}$ mouse model containing a RFP reporter. For this experiment it is important that only an individual $Apc^{fl/fl}$*-RFP* clone is induced per crypt. Therefore, titrated doses of βNF (40 mg/kg) and tamoxifen (0.15 mg) would need to be administered following 2-week feeding on either the control diet or BRB diet. RFP clone sizes could then be quantified over time by scoring the amount of RFP within the crypt base circumference. The neutral drift model (clonal fitness of mutated stem cells in the context of BRB diet) can be determined through a Bayesian mathematical model as discussed by Vermeulen *et al.* (2013).

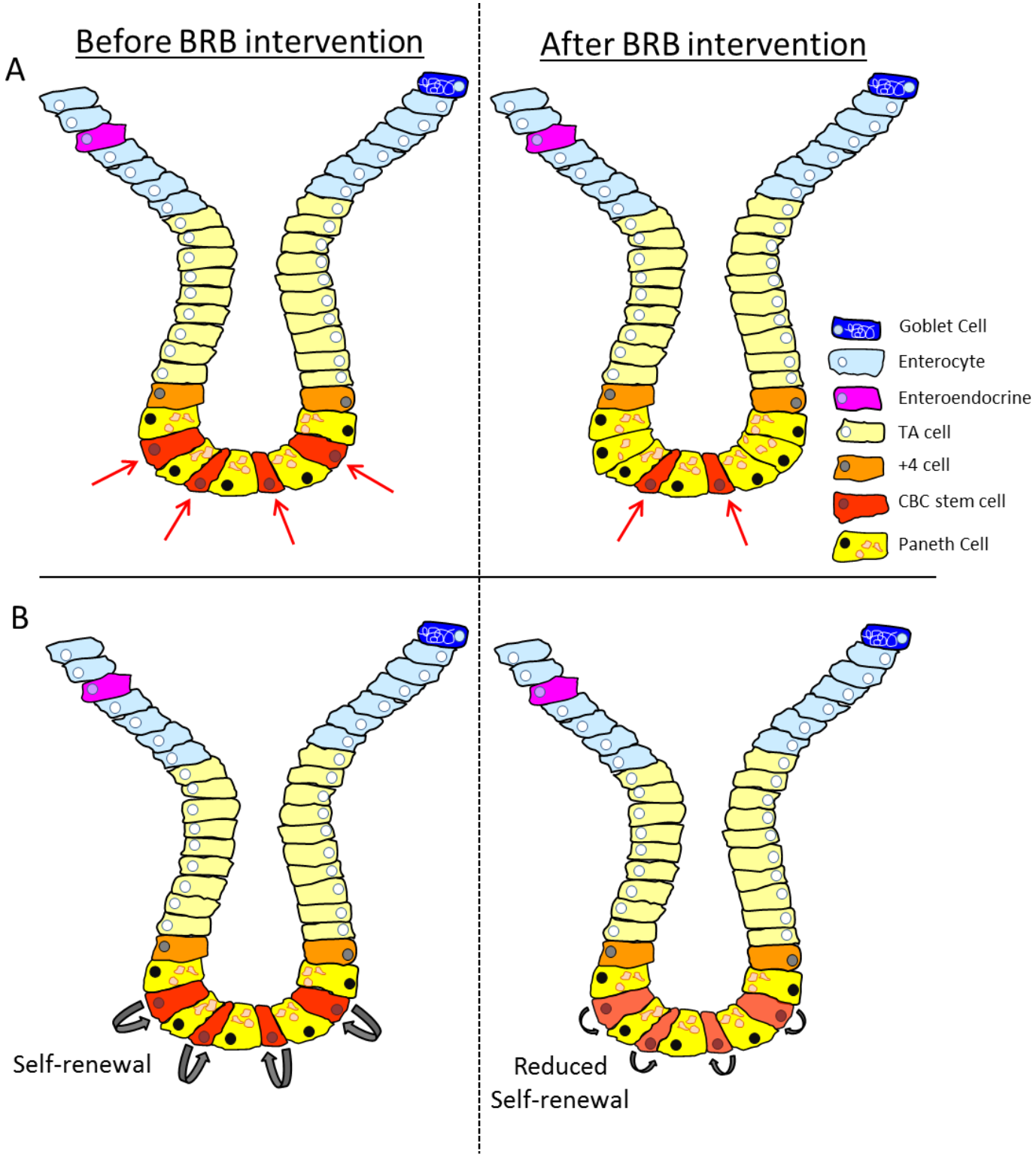

Figure 6.1 Schematic representation of the hypotheses generated from these studies on ISC dynamics in the context of BRB exposure

(A) The first hypothesis proposes that BRB intervention reduces the number of CBC ISCs in the crypt and thus, limits the number of potential targets of mutational insult. (B) The second hypothesis suggests that prior exposure of the intestinal epithelium to BRBs reduces the ability of ISCs to self-renewal. This would therefore limit the ability of malignant stem cells which initiate tumourigenesis. TA = transit-amplifying cells; CBC = crypt base columnar cell; ISC = intestinal stem cell; BRB = black raspberries.

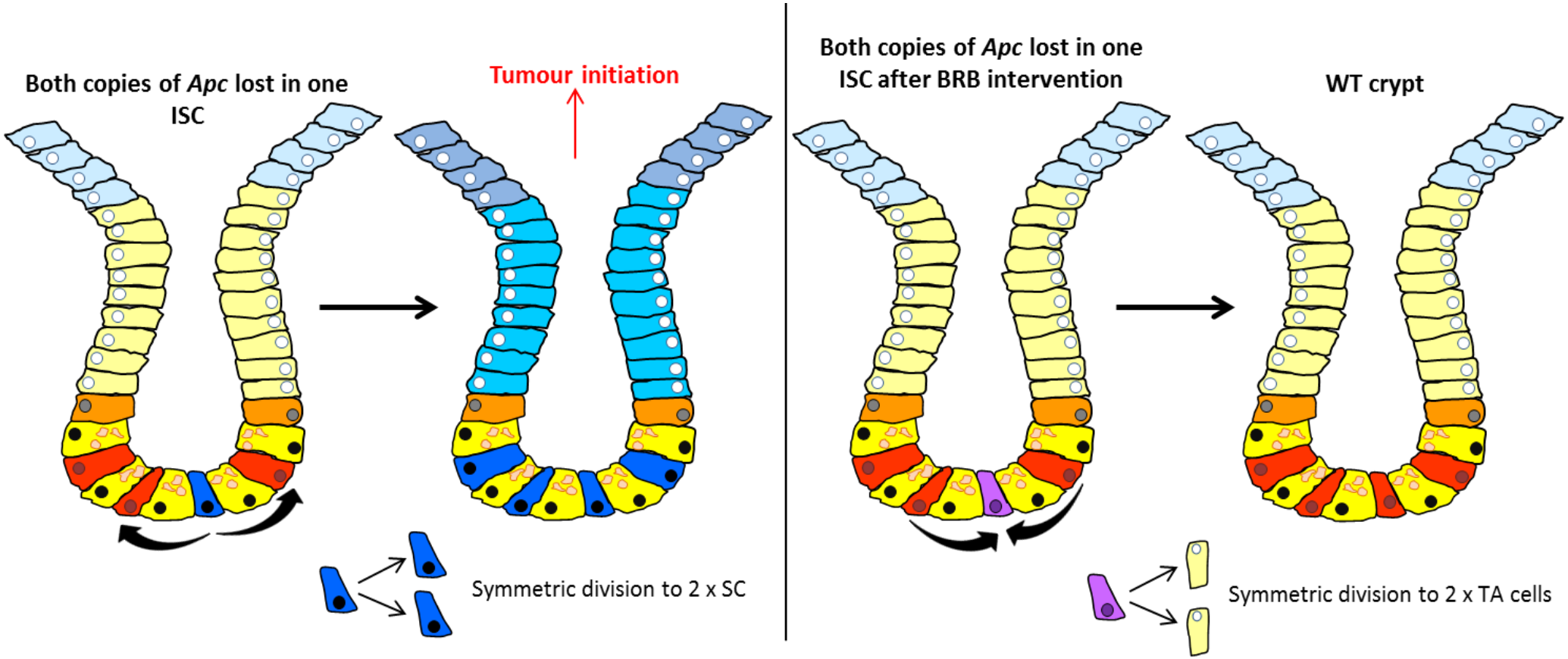

Figure 6.2 Schematic representation of the hypothesis that BRB intervention limits the competitive advantage of *Apc* deficient clones

According to work by Doug Winton's group homozygous loss of *Apc* within single ISCs confers a clonal advantage of the malignant stem cell (dark blue) over neighbouring WT stem cells (red). This drives ISC division to preferentially produce two malignant ISCs. Eventually the *Apc* deficient clone is fixed within a crypt with every cell (stem, TA and differentiated cells) having the *Apc* mutation (Vermeulen *et al.* 2013) and leads to the onset of tumourigenesis. This thesis proposes that exposure of a single *Apc* deficeint stem cell to BRBs (purple) reduces the competitive advantage conferred by *Apc* loss. This subsequently results in the loss of the malignant cell by pushing ISC division to produce two TA cells which will be lost by cell shedding from the villus tip. This therefore limits the likehood of malignant mutations from becoming fixed within a crypt and reduces the chance of cancer initiation. ISC = intestinal stem cell; BRB = black raspberry; WT = wildtype; SC = stem cell; TA = transit-amplifying cell.

6.3 Using mouse models and organoid culture to model BRB intervention in human CRC

The data presented here represent the first body of work exploring the chemopreventative as opposed to chemotherapeutic properties of BRBs. The term chemoprevention refers to the efforts of naturally occurring, synthetic or biological agents to delay, block or inhibit the process of carcinogenesis often by disrupting the molecular mechanisms that drive tumourigenesis (Steward and Brown 2013; Landis-Piwowar and Iyer 2014). The principle of chemoprevention is to 1) reduce the number of people that develop cancer and thus reduce the number of people that require treatment, 2) expand the window of opportunity to efficiently treat and detect lower grade tumours and 3) lessen the risk of relapse following treatment (Fleet 2014).

The role of diet in the aetiology of CRC has been studied in great detail but the precise mechanisms that underpin these associations are not well understood. Human studies are complicated and often limited as they cannot determine cause and effort relationships or identify the underlying mechanisms that make certain dietary components beneficial or detrimental to disease, making disease modelling essential. Preclinical animal models, which enable genetic manipulation of genes involved in carcinogenesis, were chosen for this study exploring the potential role of BRBs as a chemopreventative as the mouse anatomy, physiology and genetics share many important similarities to that of humans (Chinwalla *et al.* 2002; Mestas and Hughes 2004; Corpet and Pierre 2005; Shay *et al.* 2013) and common pathways involved in cancer are present in both species (Frese and Tuveson 2007). In addition, the animal models enabled the translation of data derived from previously described studies exploring the role of BRBs using a cell line based system into an *in vivo* model in the presence of an intact immune system and microbiome. Although these mouse models provide a more functionally relevant model than cell line work, the limitations due to the differences between mice and humans must be considered when trying to predict the effect of BRB supplement in humans. For example it has been found that human tumours are more heterogeneous than mouse tumours (McIntyre *et al.* 2015), which could reflect differences in lifespan, variations in diet and the microbiome (Nguyen *et al.* 2015). Due to the natural diversity and heterogeneity of human CRCs, understanding the molecular mechanisms of cancer and the cause and effect relationship of dietary interventions in this context is not possible from a single mouse model.

Mouse models which utilise Cre-mediated bialleic loss of *Apc* have proved invaluable tools for understanding the mechanisms that underpin early tumourigenesis and allow control over when dietary interventions are introduced with respect to gene mutations, which is beneficial when investigating preventative strategies. Therefore, these mouse models were utilised in this thesis. However, it must be considered that the majority of sporadic human CRCs do not occur from simultaneous loss of both *Apc* alleles, and so the effect of BRB diet on tumourigenesis could be

different in this context. In both sporadic and inherited CRC in humans, one allele of *Apc* is mutated (either sporadically or due to an inherited mutation), and at a later date the second allele is mutated. Generally, a chemopreventative would be successful in this scenario if it was capable of limiting the rate at which loss of heterozygosity (LOH) occurred. LOH refers to the loss of the functional copy of a gene in a situation where the other allele is already non-functional due to an inherited mutation. BRBs were shown here to increase migration and alter ISC dynamics in such a way that would likely decrease the likelihood of a clone which had lost its second allele of *Apc* being retained in the crypt, thereby reducing the rate at which LOH initiated tumourigenesis. However, to more accurately recapitulate the events that lead to tumourigenesis in humans, heterozygous mouse models of *Apc* loss (e.g. $Apc^{Min/+}$) could be used. This approach is limited by the long tumour latency and as such was beyond the scope of this study.

Another way in which the mouse models used here are limited in modelling human CRC is tumour location. CRC patients present with tumours within the large intestine whereas primary tumours in mouse models predominantly develop in the small intestine (Fleet 2014; Jackstadt and Sansom 2016). This contrasting tumour location pattern may result in discrepancies between disease development and response to BRB diet. For example the $Apc^{Min/+}$ model develop a large number of polyps in both the small and large intestine, with morbidity occurring as a result of tumour burden rather than advancement of the disease (metastasis is rarely reported in this model) (Moser *et al.* 1990). In contrast, human FAP disease and sporadic CRCs preferentially develop in the distal colon and are usually detected at later stages due to disease progression. In addition, human CRCs can take several years to emerge and progress to an advanced state. Although beneficial in terms of performing experiments, the latency of tumours from GEMM models is relatively short (Green and Hudson 2005) and may limit the use of animals to translate to human studies however, models of *Apc* heterozygosity could be used to evaluate the effect of BRBs on FAP and advanced CRC in future studies. Recent work by Tomasetti and Vogelstein has highlighted that while the number of human colonic stem cells division is 150 times more than that of the small intestine, stem cell division in the murine colon and small intestine are in fact the opposite to that of humans (Tomasetti and Vogelstein 2015). Taken together, with the similarities in tumour make-up and the pathways involved in tumourigenesis, GEMMs serve as vital tools to investigate the mechanisms of human disease. There are several colon-specific Cres (Hinoi *et al.* 2007; Robanus-Maandag *et al.* 2010; Tetteh *et al.* 2016b) that may overcome the issues with tumour burden and location within the intestine and aid the evaluation into later stage disease. While studies have shown that the tumours which arise in colon-specific Cre systems have very similar morphology to human cancers (Robanus-Maandag *et al.* 2010), the rates of stem cell division may not always reflect the dynamics of human stem cells, and so changes in murine ISC

dynamics as a result of BRB intervention may not directly translate to an equivalent change in humans. However, these models of colon-specific tumourigenesis could be utilised in future experiments of BRB intervention, especially in the context of BRB rectal suppository interventions to better predict the outcome of FAP and CRC patients as in Wang *et al.* (2014) and to further the studies described here.

Several studies have identified that stem cells can be influenced by extrinsic and environmental factors (Tomasetti and Vogelstein 2015; Wu *et al.* 2016). This thesis provides the first evidence that BRB diet influences ISC dynamics and prolongs the lifespan of mice bearing Wnt-driven ISC derived tumours. The results described herein also support previous preclinical and clinical studies that BRB diet is well tolerated and not associated with any serious side effects in normal tissue when used as a cancer preventative or therapeutic. In the context of BRB intervention, several preclinical mouse studies (Kresty *et al.* 2001; Wang *et al.* 2009; Bi *et al.* 2010) have been translated in to the clinic in human trials (Kresty *et al.* 2006; Wang *et al.* 2011; Wang *et al.* 2014). The promising results generated from these *in vivo* mouse studies in reducing tumour burden, latency and multiplicity have seen some positive results in human tumour response to BRBs in reducing tumour size and severity. This provides scope for advancing the preclinical studies outlined here to clinical trials. However, in some CRC and FAP patients BRB intervention was reported to have no effect, possibly due to tumour heterogeneity and differences between patients microbiome, and so this highlights the need for other models of human disease to accurately recapitulate and predict human response to drug and chemopreventative therapies.

Organoid culture (Sato *et al.* 2009), is proving to be a fundamental tool in human biology by bridging the gaps between 2D (two dimensional) cell culture studies and *in vivo* mouse and human studies (Fatehullah *et al.* 2016). This system allows the development of near-physiological tissue from mouse and human intestinal and CRC tissue (Sato *et al.* 2011b) and from human colonic stem cells (Jung *et al.* 2011). This makes organoids a more clinically relevant model that is likely to translate to *in vivo* studies unlike 2D culture systems. In addition, *ex vivo* culture of murine and human tissue has many advantages over animal models as it enables genetic alterations to be established easily and quickly from minimal starting material. The role of adult stem cells in homeostasis, tissue regeneration and disease, especially in the context of dietary intervention, can be investigated without influence from the local microenvironment as with the BRB organoid studies performed herein. The complex mechanisms which underlie human disease which cannot be investigated in mouse models can be studied from patient-derived tissue and novel interventions can be exploited to better predict individual patient outcomes to therapies (Huch and Koo 2015). As with any system there are always limitations. As the current method for culturing organoids takes a reductionist approach there is a lack

of native microenvironment, stroma, extracellular matrix, vasculature, immune system and microbiome which precludes ISC studies with their surrounding niche and in drug development studies (Fatehullah *et al.* 2016; Hollins and Parry 2016). However, the utility of mouse organoids to recapitulate the *in vivo* scenario is shown in this study where AC-reduced self-renewal of *Apc* deficient cells in intestinal organoid culture supported a down-regulation of ISC marker expression *in vivo*. This suggests that the combination of animal and organoid studies can complement each other in chemoprevention and mechanistic studies. In support of this, these two systems have also started to elucidate the mechanisms that link high-fat diet and CRC (Beyaz *et al.* 2016).

The need for organoids to replicate the environment of human disease is critical to aid our understanding of the mechanisms that underpin cancer and the involvement of our environment. Holistic representation of the intestinal environment through co-culturing would make murine and human organoids even more relevant (Sato *et al.* 2011b; Kabiri *et al.* 2014; Lindemans *et al.* 2015; VanDussen *et al.* 2015; Beyaz *et al.* 2016; Nozaki *et al.* 2016). Co-culturing systems combined with microfluidic techniques would closely mimic the *in vivo* interactions between the microenvironment and intestine or tumour tissue (Ramadan *et al.* 2013; Gracz *et al.* 2015), and these techniques could be implemented in future studies to better predict patient outcomes to BRB intervention and understand the true influence of diet on ISCs and their microenvironment. Additionally, in order for organoid culture to be more clinically relevant in the future, a system needs to be developed that replicates the *in vivo* human system, encompassing administration of dietary compounds to the apical surface whilst in the presence of an intact immune system, stem cell niche and microbiome. This is because the current system enables organoids to form such that the apical surface faces the inside of the 3D structure with the basal surface having direct contact with the matrigel and exogenous dietary compounds. BRB anthocyanins administered orally are absorbed from the intestinal lumen by the cells of the stomach and small and large intestines. While studies report that ACs are highly permeable across the gastrointestinal mucosa and can reside at high concentrations in the intestinal tissue some ACs, such as cyanidin-3-glucoside, have been reported to be absorbed by the gut and enter the systemic circulation (Fang 2014). However, AC concentrations in the blood are often lower than in intestinal tissue (Fang 2014). Several studies have suggested that pharmacologically relevant concentrations of ACs could be achieved within the intestinal tissue following exposure at the luminal surface and thus can exert chemopreventative and therapeutic effects locally (Fang 2014; Kamiloglu *et al.* 2015). Therefore, it may be beneficial in the future for dietary components to be injected into individual organoids (Ogaki *et al.* 2015) in order to understand the interactions of diet on ISCs and cancer in a clinically relevant multi-factorial setting.

6.4 Potential use of BRBs as a CRC preventative

Preclinical data from mouse models and organoid culture may not accurately reflect human response to dietary and drug interventions. However, several studies using mouse models have been directly translated into humans, including the use of curcumin in preventing colorectal neoplasia (Carroll *et al.* 2011), and aspirin in preventing hereditary CRC (Burn *et al.* 2011). While further work is required to determine the mechanisms that link environmental factors and CRC, the potential of BRBs to be implicated as a CRC preventative is indisputable, as daily administration of BRBs have shown to reduce colorectal tumour and polyp numbers and severity in humans (Wang *et al.* 2011; Wang *et al.* 2014). This thesis and previously published work have identified some of the pleiotropic effects of BRBs on cell death, differentiation, inflammation, epigenetic regulations, the metabolome and malignant ISC dynamics at the premalignant and malignant stages of intestinal tumourigenesis. This highlights their potential for therapeutic cancer intervention; however it also highlights the complexity of the involvement of extrinsic factors in carcinogenesis. Moreover, translation into the clinic has not been simple, with varied responses occurring among patients (Wang *et al.* 2011; Wang *et al.* 2014). This is likely to reflect the heterogeneity among individuals and within tumours, differences in molecular signalling and enzyme activity near the tumour and differences in patients' microbiota and metabolism (Kula and Krauze-Baranowska 2016).

It is important to note that chemoprevention is not trying to radicalise our lifestyle, but identify ways in which to adopt a healthier lifestyle and lessen the risks of developing cancer. Patient compliance (Ropka *et al.* 2010) is a rate limiting step in the success of chemopreventive strategies (that have substantial scientific evidence), and so it is important that such strategies are easy to adhere to. While it remains difficult to accurately estimate the beneficial amount of BRB consumption for individual patients, the purpose of chemoprevention in the context of this thesis was to evaluate whether prior exposure to BRBs was sufficient to limit tumourigenesis, rather than intervene with BRBs after cancer diagnosis like the studies by Wang *et al.* (2011), Wang *et al.* (2014) and Pan *et al.* (2015) where BRBs were administered after patients were diagnosed with CRC or FAP disease. Putting this aside, it is necessary that the regime is simple and doesn't require the consumption of hundreds of berries a day which is not a sustainable lifestyle change. In clinical studies, patients consumed 20 g of freeze-dried BRB powder in 100 ml water, three times a day. The total of 60 g of freeze-dried BRB powder has been reported to approximately equate to 1.3 lbs of fresh BRBs a day which is equivalent to a 7% rodent BRB powder diet (Wang *et al.* 2011). However, as freeze-dried BRB powder have been shown to have chemopreventative effects in murine cancers at concentrations of 5 – 10%, it is likely that BRB concentrations that span this range will be beneficial in humans.

BRB powder is widely available as a food supplement for human consumption from health shops. However, the concentration of dose widely advised is approximately 10 fold lower (Swanson Health Products 2017) than shown effective as a therapeutic in human studies of CRC (Wang *et al.* 2011; Wang *et al.* 2014) and lower still than the equivalent concentration shown herein to have a chemopreventative effect in mice (10% rodent diet approximately equates to 85 g of freeze-dried BRB powder). As with many food supplements the utility of this treatment and effective concentration range needs to be further investigated before public uptake.

The organoid studies described herein and cell culture and animal-based studies already published (Wang *et al.* 2009; Zikri *et al.* 2009; Wang *et al.* 2013b) have reported some of the chemopreventative and therapeutic effects of BRB-derived anthocyanins, cyanidin-3-O-glucoside, cyanidin-3-O-xylosylrutinoside and cyanidin-3-O-rutinoside, against cancer. Specifically, results reported in this thesis revealed that 500 µg/ml of BRB-derived ACs significantly reduced the ability of *Apc* deficient cells to self-renew. Approximately, 500 µg/ml of this BRB AC extract equated to 0.0147 g of freeze-dried BRB powder, which is approximately 4000 fold lower than the concentration of anthocyanins in 60 g/day BRB slurry administered in humans, and approximately 100 fold lower than the AC content in 1.4 g of BRB suppositories administered to FAP patients daily. However, it is important to note that in this thesis, the AC extract was added directly to the organoids rather than orally as reported by Wang *et al.* (2011); Wang *et al.* (2014) and Pan *et al.* (2015). Thus, higher doses of AC would need to be administered orally to get a desired concentratin of 500 µg/ml to the cells, after absorption and metabolism. Despite this, it is clear that AC doses of 500 µg/ml and rodent diets of 10% freeze-dried BRB powder have chemopreventative effects at different stages of intestinal tumourigenesis which highlights their potential use for cancer prevention and intervention. Whilst a precise concentration and dosing regime still needs to be determined for optimal cancer prevention and treatment, the combination of previously published data and results reported in this thesis highlight that diets of 10% BRB diet do have tissue specific effects. However, more research is required to determine a precise mechanism of action and to further predict patient response to BRB intervention. Future work could focus on identifying whether a single anthocyanin is responsible for the cancer inhibitory effects of BRBs or a combination. Additionally, it would also be beneficial to determine whether the consumption of several berry fruit powders have synergistic effects in preventing CRC.

In summary, BRB intervention in mice is well tolerated and has chemopreventative effects against CRC initiation and progression without causing gastric side effects within normal tissue. BRBs and their AC derivatives have pleiotropic effects in both mice and humans. This study represents the

first evidence that one of the mechanisms of action of the BRB diet in preventing CRC is through regulation of the ISC population.

7 Reference List

WCRF/AICR World Cancer Research Fund, American Institute for Cancer Research. *Continuous Update Project Colorectal Cancer 2011 Report. Food, nutrition, physical activity, and the prevention of colorectal cancer.* Washington DC: WCRF. 2011.

(1977). Report of the American Institute of Nutrition Ad Hoc Committee on Standards for Nutritional Studies. *The Journal of Nutrition* **107:**1340-1348.

(1980). Second report of the ad hoc committee for experimental animals. *Journal of Nutrition* **107:**1726.

Adachi, S., Nagao, T., To, S., Joe, A. K., Shimizu, M., Matsushima-Nishiwaki, R., Kozawa, O. *et al.* (2008). (−)-Epigallocatechin gallate causes internalization of the epidermal growth factor receptor in human colon cancer cells. *Carcinogenesis* **29:**1986-1993.

Ahmad, N., Cheng, P. and Mukhtar, H. (2000). Cell Cycle Dysregulation by Green Tea Polyphenol Epigallocatechin-3-Gallate. *Biochemical and Biophysical Research Communications* **275:**328-334.

Aiyer, H., Li, Y., Reuter, N. and Martin, R. (2014). Dietary black raspberry boosts cellular antioxidant defenses in reflux-induced esophagitis. *Cancer Research* **68:**5480.

Al-Hajj, M., Wicha, M. S., Benito-Hernandez, A., Morrison, S. J. and Clarke, M. F. (2003). Prospective identification of tumorigenic breast cancer cells. *Proceedings of the National Academy of Sciences* **100:**3983-3988.

Albuquerque, C., Breukel, C., van der Luijt, R., Fidalgo, P., Lage, P., Slors, F. J. M., Leitão, C. N. *et al.* (2002). The 'just-right' signaling model: APC somatic mutations are selected based on a specific level of activation of the β-catenin signaling cascade. *Human Molecular Genetics* **11:**1549-1560.

Allis, C. D. and Jenuwein, T. (2016). The molecular hallmarks of epigenetic control. *Nat Rev Genet* **17:**487-500.

Andreu, P., Colnot, S., Godard, C., Gad, S., Chafey, P., Niwa-Kawakita, M., Laurent-Puig, P. *et al.* (2005). Crypt-restricted proliferation and commitment to the Paneth cell lineage following Apc loss in the mouse intestine. *Development* **132:**1443-1451.

Artavanis-Tsakonas, S., Rand , M. D. and Lake, R. J. (1999). Notch Signaling: Cell Fate Control and Signal Integration in Development. *Science* **284:**770-776.

Baker, A.-M., Graham, T. A., Elia, G., Wright, N. A. and Rodriguez-Justo, M. (2015). Characterization of LGR5 stem cells in colorectal adenomas and carcinomas. *Scientific Reports* **5:**8654.

Barker, N. (2014). Adult intestinal stem cells: critical drivers of epithelial homeostasis and regeneration. *Nature Reviews Molecular Cell Biology* **15:**19–33.

Barker, N. and Clevers, H. (2007). Tracking Down the Stem Cells of the Intestine: Strategies to Identify Adult Stem Cells. *Gastroenterology* **133:**1755-1760.

Barker, N., Ridgway, R. A., van Es, J. H., van de Wetering, M., Begthel, H., van der Born, M., Danenberg, E. *et al.* (2009). Crypt stem cells as the cells-of-origin of intestinal cancer. *Nature* **457:**608-611.

Barker, N., van de Wetering, M. and Clevers, H. (2008). The intestinal stem cell. *Genes & Development* **22:**1856-1864.

Barker, N., van Es, J. H., Kuipers, J., Kujala, P., van den Born, M., Cozijnsen, M., Haegebarth, A. *et al.* (2007). Identification of stem cells in small intestine and colon by marker gene *Lgr5*. *Nature* **449:**1003-1007.

Barker, N., van Oudenaarden, A. and Clevers, H. (2012). Identifying the Stem Cell of the Intestinal Crypt: Strategies and Pitfalls. *Cell Stem Cell* **11:**452-460.

Barnard, J. A., Beauchamp, R. D., Coffey, R. J. and Moses, H. L. (1989). Regulation of intestinal epithelial cell growth by transforming growth factor type beta. *Proceedings of the National Academy of Sciences* **86:**1578-1582.

Bastide, P., Darido, C., Pannequin, J., Kist, R., Robine, S., Marty-Double, C., Bibeau, F. *et al.* (2007). Sox9 regulates cell proliferation and is required for Paneth cell differentiation in the intestinal epithelium. *The Journal of Cell Biology* **178:**635-648.

Batlle, E., Bacani, J., Begthel, H., Jonkeer, S., Gregorieff, A., van de Born, M., Malats, N. *et al.* (2005). EphB receptor activity suppresses colorectal cancer progression. *Nature* **435:**1126-1130.

Batlle, E., Henderson, J. T., Beghtel, H., van den Born, M. M. W., Sancho, E., Huls, G., Meeldijk, J. *et al.* (2002). β-Catenin and TCF Mediate Cell Positioning in the Intestinal Epithelium by Controlling the Expression of EphB/EphrinB. *Cell* **111**:251-263.

Behrens, J., von Kries, J. P., Kühl, M., Bruhn, L., Wedlich, D., Grosschedl, R. and Birchmeier, W. (1996). Functional interaction of beta-catenin with the transcription factor LEF-1. *Nature* **382:**638-642.

Beumer, J. and Clevers, H. (2016). Regulation and plasticity of intestinal stem cells during homeostasis and regeneration. *Development* **143:**3639.

Bevins, C. L. and Salzman, N. H. (2011). Paneth cells, antimicrobial peptides and maintenance of intestinal homeostasis. *Nature Reviews Microbiology* **9:**356-368.

Beyaz, S., Mana, M. D., Roper, J., Kedrin, D., Saadatpour, A., Hong, S.-J., Bauer-Rowe, K. E. *et al.* (2016). High-fat diet enhances stemness and tumorigenicity of intestinal progenitors. *Nature* **531:**53-58.

Bi, X., Fang, W., Wang, L.-S., Stoner, G. D. and Yang, W. (2010). Black Raspberries Inhibit Intestinal Tumorigenesis in *Apc1638*+/- and *Muc2*-/- Mouse Models of Colorectal Cancer. *Cancer Prevention Research* **3:**1443-1450.

Bilchik , A. J., Graeme, P., Curley , A., S., Strasberg , S., Saltz , L., Adam, R. *et al.* (2005). Neoadjuvant Chemotherapy for Metastatic Colon Cancer: A Cautionary Note. *Journal of Clinical Oncology* **23:**9073-9078.

Bjerknes, M. and Cheng, H. (1999). Clonal analysis of mouse intestinal epithelial progenitors. *Gastroenterology* **116:**7-14.

Blanke, C. D. (2009). Dual-Antibody Therapy in Advanced ColorectalCancer: Gather Ye Rosebuds While Ye May. *Journal of Clinical Oncology* **27:**655-658.

Bokemeyer, C., Bondarenko, I., Makhson, A., Hartmann, J. T., Aparicio, J., de Braud, F., Donea, S. *et al.* (2009). Fluorouracil, Leucovorin, and Oxaliplatin With and Without Cetuximab in the First-Line Treatment of Metastatic Colorectal Cancer. *Journal of Clinical Oncology* **27:**663-671.

Bravo, L. (1998). Polyphenols: chemistry, dietary sources, metabolism, and nutritional significance. *Nutrition Reviews* **56:**317–333.

Bu, H., He, X., Zhang, Z., Yin, Q., Yu, H. and Li, Y. (2014). A TPGS-incorporating nanoemulsion of paclitaxel circumvents drug resistance in breast cancer. *International Journal of Pharmaceutics* **471:**206-213.

Buczacki, S. J. A., Zecchini, H. I., Nicholson, A. M., Russell, R., Vermeulen, L., Kemp, R. and Winton, D. J. (2013). Intestinal label-retaining cells are secretory precursors expressing Lgr5. *Nature* **495:**65-69.

Burn, J., Gerdes, A.-M., Macrae, F., Mecklin, J.-P., Moeslein, G., Olschwang, S., Eccles, D. *et al.* (2011). Long-term effect of aspirin on cancer risk in carriers of hereditary colorectal cancer: an analysis from the CAPP2 randomised controlled trial. *Lancet* **378:**2081-2087.

Cancer Research UK 2014. http://www.cancerresearchuk.org/health-professional/cancer-statistics/statistics-by-cancer-type/bowel-cancer. Acessed online October 2016.

Carmon, K. S., Lin, Q., Gong, X., Thomas, A. and Liu, Q. (2012). LGR5 Interacts and Cointernalizes with Wnt Receptors To Modulate Wnt/β-Catenin Signaling. *Molecular and Cellular Biology* **32:**2054-2064.

Carroll, R. E., Benya, R. V., Turgeon, D. K., Vareed, S., Neuman, M., Rodriguez, L., Kakarala, M. *et al.* (2011). Phase IIA Clinical Trial of Curcumin for the Prevention of Colorectal Neoplasia. *Cancer prevention research (Philadelphia, Pa.)* **4:**354-364.

Chan, A. T. and Giovannucci, E. L. (2010). Primary Prevention of Colorectal Cancer. *Gastroenterology* **138:**2029-2043.e2010.

Chen, H.-J., Hsu, L.-S., Shia, Y.-T., Lin, M.-W. and Lin, C.-M. (2012). The β-catenin/TCF complex as a novel target of resveratrol in the Wnt/β-catenin signaling pathway. *Biochemical Pharmacology* **84:**1143-1153.

Cheng, H. and Leblond, C. P. (1974). Origin, differentiation and renewal of the four main epithelial cell types in the mouse small intestine V. Unitarian theory of the origin of the four epithelial cell types. *American Journal of Anatomy* **141:**537-561.

Chesney, J., Metz, C., Bacher, M., Peng, T., Meinhardt, A. and Bucala, R. (1999). An essential role for macrophage migration inhibitory factor (MIF) in angiogenesis and the growth of a murine lymphoma. *Molecular Medicine* **5:**181-191.

Chinwalla, A. T., Cook, L. L., Delehaunty, K. D., Fewell, G. A., Fulton, L. A., Fulton, R. S., Graves, T. A. *et al.* (2002). Initial sequencing and comparative analysis of the mouse genome. *Nature* **420:**520-562.

Clevers, H. (2016). Cancer therapy: Defining stemness. *Nature* **534:**176-177.

Clevers, H., Loh, K. M. and Nusse, R. (2014). An integral program for tissue renewal and regeneration: Wnt signaling and stem cell control. *Science* **346:**1248012.

Clevers, H. and van de Wetering, M. (1997). TCF/LEF factor earn their wings. *Trends in Genetics* **13:**485-489.

Cordenunsi, B. R., Oliveira do Nascimento, J. R., Genovese, M. I. and Lajolo, F. M. (2002). Influence of Cultivar on Quality Parameters and Chemical Composition of Strawberry Fruits Grown in Brazil. *Journal of Agricultural and Food Chemistry* **50:**2581-2586.

Corpet, D. E. and Pierre, F. (2005). How good are rodent models of carcinogenesis in predicting efficacy in humans? A systematic review and meta-analysis of colon chemoprevention in rats, mice and men. *European Journal of Cancer* **41:**1911-1922.

Corrie, P. G. (2008). Cytotoxic chemotherapy: clinical aspects. *Medicine* **36**: 24-28.

Creamer, B. (1967). The turnover of the epithelium of the small intestine. *British Medical Bulletin* **23:**226-230.

CRUK. (2014). [Online]. Available at: http://www.cancerresearchuk.org/health-professional/cancer-statistics/statistics-by-cancer-type/bowel-cancer#heading-Zero [Accessed: February 2017].

Dalerba, P., Dylla, S. J., Park, I. K., Liu, R., Wang, X., Cho, R. W., Hoey, T. *et al.* (2007). Phenotypic characterization of human colorectal cancer stem cells. *Proc Natl Acad Sci USA* **104**.

Date, S. and Sato, T. (2015). Mini-Gut Organoids:Reconstitution of the Stem Cell Niche. *The Annual Review of Cell and Developmental Biology* **31:**269–289.

Deighton, N., Brennan, R. and Davies, H. V. (2000). Antioxidant properties of domesticated and wild *Rubus* species. *Journal of the Science of Food and Agriculture* **80:**1307–1313.

Denev, P. N., Kratchanov, C. G., Ciz, M., Lojek, A. and Kratchanova, M. G. (2012). Bioavailability and Antioxidant Activity of Black Chokeberry (Aronia melanocarpa) Polyphenols: in vitro and in vivo Evidences and Possible Mechanisms of Action: A Review. *Comprehensive Reviews in Food Science and Food Safety* **11:**471-489.

de Sousa e Melo, F., Kurtova, A. V., Harnoss, J. M., Kljavin, N., Hoeck, J. D., Hung, J., Anderson, J. E. *et al.* (2017). A distinct role for Lgr5^{+} stem cells in primary and metastatic colon cancer. *Nature* **543:**676–680.

Dignass, A. U. and Sturm, A. (2001). Peptide growth factors in the intestine. *European Journal of Gastroenterology & Hepatology* **13:**763–770.

Dihlmann, S. and von Knebel Doeberitz, M. (2005). Wnt/β-catenin-pathway as a molecular target for future anti-cancer therapeutics. *International Journal of Cancer* **113:**515-524.

Diplock, A. T., Charleux, J. L., Crozier-Willi, G., Kok, F. J., Rice-Evans, C., Roberfroid, M., Stahl, W. *et al.* (1998). Functional food science and defence against reactive oxidative species. *British Journal of Nutrition* **80:**S77-S112.

Drake, R. L., Vogl, A. W. and Mitchell, A. W. M. (2005). G*ray's anatomy for students*. Third ed. Philadelphia: Elsevier/Churchill Livingstone. p312-320.

Duque, A. and Rakic, P. (2011). Different effects of BrdU and (3)H-Thymidine incorporation into DNA on cell proliferation, position and fate. *The Journal of neuroscience : the official journal of the Society for Neuroscience* **31:**15205-15217.

Durand, A., Donahue, B., Peignon, G., Letourneur, F., Cagnard, N., Slomianny, C., Perret, C. *et al.* (2012). Functional intestinal stem cells after Paneth cell ablation induced by the loss of transcription factor Math1 (Atoh1). *Proceedings of the National Academy of Sciences of the United States of America* **109:**8965-8970.

Duval, A., Rolland, S., Tubacher, E., Bui, H., Thomas, G. and Hamelin, R. (2000). The human T-cell transcription factor-4 gene: structure, extensive characterization of alternative splicings, and mutational analysis in colorectal cancer cell lines. *Cancer Research* **60:**3872-3879.

El Marjou, F., Janssen, K. J., Chang, B. H.-J., Li, M., Hindie, V., Chan, L., Louvard, D. *et al.* (2004). Tissue-Specific and Inducible Cre-Mediated Recombination in the Gut Epithelium. *Genesis* **39:**186 –193.

Elamin, M. H., Shinwari, Z., Hendrayani, S. F., Al-Hindi, H., Al-Shail, E., Khafaga, Y., Al-kofide, A. *et al.* (2010). Curcumin inhibits the sonic hedgehog signaling pathway and triggers apoptosis in medulloblastoma cells. *Molecular Carcinogenesis* **49:**302-314.

Fang, J. (2014). Bioavailability of anthocyanins. *Drug Metabolism Reviews* **46:**508-520.

Farin, H. F., Van Es, J. H. and Clevers, H. (2012). Redundant Sources of Wnt Regulate Intestinal Stem Cells and Promote Formation of Paneth Cells. *Gastroenterology* **143:**1518-1529.e1517.

Fatehullah, A., Tan, S. H. and Barker, N. (2016). Organoids as an in vitro model of human development and disease. *Nat Cell Biol* **18:**246-254.

Fearon, E. R. and Vogelstein, B. (1990). A genetic model for colorectal tumorigenesis. *Cell* **61:**759-767.

Feng, G. J., Cotta, W., Wei, X. Q., Poetz, O., Evans, R., Jardé, T., Reed, K. *et al.* (2012). Conditional Disruption of Axin1 Leads to Development of Liver Tumors in Mice. *Gastroenterology* **143:**1650-1659.

Ferlay, J., Soerjomataram, I., Dikshit, R., Eser, S., Mathers, C., Rebelo, M., Parkin, D. M. *et al.* (2015). Cancer incidence and mortality worldwide: Sources, methods and major patterns in GLOBOCAN 2012. *International Journal of Cancer* **136:**E359-E386.

Fernald, K. and Kurokawa, M. (2013). Evading apoptosis in cancer. *Trends in Cell Biology* **23:**620-633.

Ferreira, D., Adega, F. and Chaves, R. (2013). The Importance of Cancer Cell Lines as in vitro Models in Cancer Methylome Analysis and Anticancer Drugs Testing.

Fleet, J. C. (2014). Animal models of gastrointestinal and liver diseases. New mouse models for studying dietary prevention of colorectal cancer. *American Journal of Physiology - Gastrointestinal and Liver Physiology* **307:**G249-G259.

Fletcher, A. G., Breward, C. J. W. and Jonathan Chapman, S. (2012). Mathematical modeling of monoclonal conversion in the colonic crypt. *Journal of Theoretical Biology* **300:**118-133.

Fodde, R., Edelmann, W., Yang, K., van Leeuwen, C., Carlson, C., Renault, B., Breukel, C. *et al.* (1994). A targeted chain-termination mutation in the mouse Apc gene results in multiple intestinal tumors. *Proceedings of the National Academy of Sciences of the United States of America* **91:**8969-8973.

Fox, J. G., Barthold, S., Davisson, M., Newcomer, C. E., Quimby, F. W. and Smith, A. (2006). The Mouse in Biomedical Research: Normative Biology, Husbandry, and Models.*American College of Laboratory Animal Medicine*. Elsevier Science, pp. 65-67.

Frese, K. K. and Tuveson, D. A. (2007). Maximizing mouse cancer models. *Nat Rev Cancer* **7:**654-658.

Fu, D.-Y., Wang, Z.-M., Li, C., Wang, B.-L., Shen, Z.-Z., Huang, W. and Shao, Z.-M. (2010). Sox17, the canonical Wnt antagonist, is epigenetically inactivated by promoter methylation in human breast cancer. *Breast Cancer Research and Treatment* **119:**601-612.

Fu, Y., Chang, H., Peng, X., Bai, Q., Yi, L., Zhou, Y., Zhu, J. *et al.* (2014). Resveratrol Inhibits Breast Cancer Stem-Like Cells and Induces Autophagy via Suppressing Wnt/β-Catenin Signaling Pathway. *PLOS ONE* **9:**e102535.

Gall, G. A. E. and Kyle, W. H. (1968). Growth of the Laboratory Mouse. *Theoretical and Applied Genetics* **38:**304-308.

Gardane, A., Poonawala, M. and Vaidya, A. (2016). Curcumin sensitizes quiescent leukemic cells to antimitotic drug 5-fluorouracil by inducing proliferative responses in them. *Journal of Cancer Metastasis and Treatment* **2**:245-252

Gerber, J. M., Smith, B. D., Ngwang, B., Zhang, H., Vala, M. S., Morsberger, L., S., G. *et al.* (2012). A clinically relevant population of leukemic CD34(+)CD38(-) cells in acute myeloid leukemia. *Blood* **119:**3571-3577.

Germann, M., Xu, H., Malaterre, J., Sampurno, S., Huyghe, M., Cheasley, D., Fre, S. *et al.* (2014). Tripartite interactions between Wnt signaling, Notch and Myb for stem/progenitor cell functions during intestinal tumorigenesis. *Stem Cell Research* **13:**355–366.

Giovannucci, E., Rimm, E. B., Ascherio, A., Stampfer, M. J., Colditz, G. A. and Willett, W. C. (1995). Alcohol, low-methionine--low-folate diets, and risk of colon cancer in men. *Journal of the National Cancer Institute* **87:**265-273.

Gracz, A. D., Williamson, I. A., Roche, K. C., Johnston, M. J., Wang, F., Wang, Y., Attayek, P. J. *et al.* (2015). A high throughput platform for stem cell-niche co-cultures and downstream gene expression analysis. *Nature cell biology* **17:**340-349.

Green, J. E. and Hudson, T. (2005). The promise of genetically engineered mice for cancer prevention studies. *Nat Rev Cancer* **5:**184-198.

Gregorieff, A., Pinto, D., Begthel, H., Destrée, O., Kielman, M. and Clevers, H. (2005). Expression pattern of Wnt signaling components in the adult intestine. *Gastroenterology* **129:**628-638.

Gribble, F. M. and Reimann, F. (2016). Enteroendocrine Cells: Chemosensors in the Intestinal Epithelium. *Annual Review of Physiology* **78:**277-299.

Guan, Y., Watson, A. J. M., Marchiando, A. M., Bradford, E., Shen, L., Turner, J. R. and Montrose, M. H. (2011a). Redistribution of the tight junction protein ZO-1 during physiological shedding of mouse intestinal epithelial cells. *American Journal of Physiology - Cell Physiology* **300:**C1404-C1414.

Guan, Z. Z., Xu, J. M., Luo, R. C., Feng, F. Y., Wang, L. W., Shen, L., Yu, S. Y. *et al.* (2011b). Efficacy and safety of bevacizumab plus chemotherapy in Chinese patients with metastatic colorectal cancer: a randomized phase III ARTIST trial. *Chinese Journal of Cancer* **30:**682–689.

Guinney, J., Dienstmann, R., Wang, X., de Reyniès, A., Schlicker, A., Soneson, C., Marisa, L. *et al.* (2015). The consensus molecular subtypes of colorectal cancer. *Nature medicine* **21**:1350-1356.

Hagan, S., Orr, M. C. M. and Doyle, B. (2013). Targeted therapies in colorectal cancer — an integrative view by PPPM. *EPMA Journal* **4:**3.

Haramis , A. P., Begthel, H., van den Born, M., van Es, J., Jonkheer, S., Offerhaus, G. J. and Clevers, H. (2004). De novo crypt formation and juvenile polyposis on BMP inhibition in mouse intestine. *Science* **303:**1684-1686.

Harris, G. K., Gupta, A., Nines, R. G., Kresty, L. A., Habib, S. G., Frankel, W. L., LaPerle, K. *et al.* (2001). Effects of lyophilized black raspberries on azoxymethane-induced colon cancer and 8-hydroxy-2'-deoxyguanosine levels in the fischer 344 rat. *Nutrition and Cancer* **40:**125-133.

He, X. C., Zhang, J., Tong, W. G., Tawfik, O., Ross, J., Scoville, D. H., Tian, Q. *et al.* (2004). BMP signaling inhibits intestinal stem cell self-renewal through suppression of Wnt- β -catenin signaling. *Nature Genetics* **36:**1117-1121.

Hinoi, T., Akyol, A., Theisen, B. K., Ferguson, D. O., Greenson, J. K., Williams, B. O., Cho, K. R. *et al.* (2007). Mouse Model of Colonic Adenoma-Carcinoma Progression Based on Somatic Apc Inactivation. *Cancer Research* **67:**9721.

Holik, A. Z., Young, M., Krzystyniak, J., Williams, G. T., Metzger, D., Shorning, B. Y. and Clarke, A. R. (2014). Brg1 Loss Attenuates Aberrant Wnt-Signalling and Prevents Wnt-Dependent Tumourigenesis in the Murine Small Intestine. *PLoS Genetics* **10:**e1004453.

Holmberg, J., Genander, M., Halford, M. M., Annerén, C., Sondell, M., Chumley, M. J., Silvany, R. E. *et al.* (2006). EphB Receptors Coordinate Migration and Proliferation in the Intestinal Stem Cell Niche. *Cell* **125:**1151-1163.

Hope, C., Kestutis, P., Marina, P., Moyer, M. P., Johal, K. S., Woo, J., Santoso, C. *et al.* (2008). Low concentrations of resveratrol inhibit Wnt signal throughput in colon-derived cells: Implications for colon cancer prevention. *Molecular nutrition & food research* **52:**S52-S61.

Hori, N., Iwasa, S., Hashimoto, H., Yanai, T., Kato, K., Hamaguchi, T., Yamada, Y. *et al.* (2013). Reasons for avoidance of bevacizumab with first-line FOLFOX for advanced colorectal cancer. *International Journal of Clinical Oncology* **18:**435-438.

Hou, N., Huo, D. and Dignam, J. J. (2013). Prevention of colorectal cancer and dietary management. *Chinese clinical oncology* **2:**13-13.

Huang, Y.-W., Gu, F., Dombkowski, A., Wang, L.-S. and Stoner, G. D. (2016). Black raspberries demethylate Sfrp4, a WNT pathway antagonist, in rat esophageal squamous cell papilloma. *Molecular Carcinogenesis* **55:**1867-1875.

Huch, M. and Koo, B.-K. (2015). Modeling mouse and human development using organoid cultures. *Development* **142:**3113.

Huderson, A. C., Myers, J. N., Niaz, M. S., Washington, M. K. and Ramesh, A. (2013). Chemoprevention of benzo(a)pyrene-induced colon polyps in Apc(Min) mice by resveratrol. *The Journal of nutritional biochemistry* **24:**713-724.

Hurwitz, H., Fehrenbacher, L., Novotny, W., Cartwright, T., Hainsworth, J., Heim, W., Berlin, J. *et al.* (2004). Bevacizumab plus irinotecan, fluorouracil, and leucovorin for metastatic colorectal cancer. *The New England Journal of Medicine* **350:**2335-2342.

Ireland, H., Kemp, R., Houghton, C., Howard, L., Clarke, A. R., Sansom, O. J. and Winton, D. J. (2004). Inducible cre-mediated control of gene expression in the murine gastrointestinal tract: effect of loss of β-catenin. *Gastroenterology* **126:**1236-1246.

Itzkovitz, S., Lyubimova, A., Blat, I. C., Maynard, M., van Es, J., Lees, J., Jacks, T. *et al.* (2012). Single-molecule transcript counting of stem-cell markers in the mouse intestine. *Nat Cell Biol* **14:**106-114.

Jackstadt, R. and Sansom, O. J. (2016). Mouse models of intestinal cancer. *The Journal of Pathology* **238:**141-151.

Jarde, T., Evans, R. J., McQuillan, K. L., Parry, L., Feng, G. J., Alvares, B., Clarke, A. R. *et al.* (2013). In vivo and in vitro models for the therapeutic targeting of Wnt signaling using a Tet-O[Delta]N89[beta]-catenin system. *Oncogene* **32:**883-893.

Jessup, J. M., Stewart, A., Greene, F. L. and Minsky, B. D. (2005). Adjuvant Chemotherapy for Stage III Colon Cancer Implications of Race/Ethnicity, Age, and Differentiation. *The Journal of American Medical Association* **294:**2703-2711.

Jinek, M., Chylinski, K., Fonfara, I., Hauer, M., Doudna, J. A., and Charpentier, E. (2012). A Programmable Dual-RNA–Guided DNA Endonuclease in Adaptive Bacterial Immunity. *Science* **337**: 816-821.

Johnson, J. (2009). Effect of Black Raspberry Extracts on Colon Cancer Cell Proliferation. Thesis Master of Science, The Ohio State University.

Johnson, R. L. and Fleet, J. C. (2013). Animal Models of Colorectal Cancer. *Cancer metastasis reviews* **32:**39-61.

Johnston, P. G. (2014). Identification of Clinically Relevant Molecular Subtypes in Colorectal Cancer: The Dawning of a New Era. *The Oncologist* **19:**568-573.

Jonker, D. J., O'Callaghan, C. J., Karapetis, C. S., Zalcberg, J. R., Tu, D., Au, H. J., Berry, S. R. *et al.* (2007). Cetuximab for the treatment of colorectal cancer. *The New England Journal of Medicine* **357:**2040-2048.

Jubb, A. M., Chalasani, S., Frantz, G. D., Smits, R., Grabsch, H. I., Kavi, V., Maughan, N. J. *et al.* (2006). Achaete-scute like 2 (ascl2) is a target of Wnt signalling and is upregulated in intestinal neoplasia. *Oncogene* **25:**3445-3457.

Jung, P., Sato, T., Merlos-Suarez, A., Barriga, F. M., Iglesias, M., Rossell, D., Auer, H. *et al.* (2011). Isolation and in vitro expansion of human colonic stem cells. *Nat Med* **17:**1225-1227.

Kabiri, Z., Greicius, G., Madan, B., Biechele, S., Zhong, Z., Zaribafzadeh, H., Edison *et al.* (2014). Stroma provides an intestinal stem cell niche in the absence of epithelial Wnts. *Development* **141:**2206.

Kaestner, K. H., Silberg, D. G., Traber, P. G. and Schütz, G. (1997). The mesenchymal winged helix transcription factor Fkh6 is required for the control of gastrointestinal proliferation and differentiation. *Genes and Development* **11:**1583-1595.

Kakarala, M., Brenner, D. E., Korkaya, H., Cheng, C., Tazi, K., Ginestier, C., Liu, S. *et al.* (2009). Targeting breast stem cells with the cancer preventive compounds curcumin and piperine. *Breast Cancer Res Treat* **122**.

Kamiloglu, S., Capanoglu, E., Grootaert, C. and Van Camp, J. (2015). Anthocyanin Absorption and Metabolism by Human Intestinal Caco-2 Cells—A Review. *International Journal of Molecular Sciences* **16:**21555-21574.

Kanwar, S. S., Yu, Y., Nautiyal, J., Patel, B. B., Padhye, S., Sarkar, F. H. and Majumdar, A. P. N. (2011). Difluorinated-curcumin (CDF): a novel curcumin analog is a potent inhibitor of colon cancer stem-like cells. *Pharm Res* **28**:827.

Kayahara, T., Sawada, M., Takaishi, S., Fukui, H., Seno, H., Fukuzawa, H., Suzuki, K. *et al.* (2003). Candidate markers for stem and early progenitor cells, Musashi-1 and Hes1, are expressed in crypt base columnar cells of mouse small intestine. *FEBS Letters* **535:**131-135.

Kiesslich, R., Duckworth, C. A., Moussata, D., Gloeckner, A., Lim, L. G., Goetz, M., Pritchard, D. M. *et al.* (2012). Local barrier dysfunction identified by confocal laser endomicroscopy predicts relapse in inflammatory bowel disease. *Gut* **61:**1146-1153.

Kim, E., Davidson, L. A., Zoh, R. S., Hensel, M. E., Salinas, M. L., Patil, B. S., Jayaprakasha, G. K. *et al.* (2016a). Rapidly cycling Lgr5+ stem cells are exquisitely sensitive to extrinsic dietary factors that modulate colon cancer risk. *Cell Death Dis* **7:**e2460.

Kim, K. A., Kakitani, M., Zhao, J., Oshima, T., Tang, T., Binnerts, M., Liu, Y. *et al.* (2005). Mitogenic influence of human R-spondin1 on the intestinal epithelium. *Science* **309:**1256-1259.

Kim, K. A., Wagle, M., Tran, K., Zhan, X., Dixon, M. A., Liu, S., Gros, D. *et al.* (2008). R-Spondin family members regulate the Wnt pathway by a common mechanism. *Molecular biology of the cell* **19:**2588-2596.

Kim, Y. J., Siegler, E. L., Siriwon, N. and Wang, P. (2016b). Therapeutic strategies for targeting cancer stem cells. *Journal of Cancer Metastasis and Treatment* **2:**233-242.

Kohn, A. D. and Moon, R. T. (2005). Wnt and calcium signaling: beta-catenin-independent pathways. *Cell Calcium* **38:**439-446.

Komiya, Y. and Habas, R. (2008). Wnt signal transduction pathways. *Organogenesis* **4:**68-75.

Kong, J., Chia, L., Goh, N., Chia, T. and Brouillard, R. (2003). Analysis and biological activities of anthocyanins. *Phytochemistry* **64:**933.

Koo, B.-K., Spit, M., Jordens, I., Low, T. Y., Stange, D. E., van de Wetering, M., van Es, J. H. *et al.* (2012). Tumour suppressor RNF43 is a stem-cell E3 ligase that induces endocytosis of Wnt receptors. *Nature* **488:**665-669.

Korinek, V., Barker, N., Moerer, P., van Donselaar, E., Huls, G., Peters, P. J. and Clevers, H. (1998). Depletion of epithelial stem-cell compartments in the small intestine of mice lacking Tcf-4. *Nature Genetics* **19:**379-383.

Kosinski, C., Stange, D. E., Xu, C., Chan, A. S., Ho, C., Yuen, S. T., Mifflin, R. C. *et al.* (2010). Indian hedgehog regulates intestinal stem cell fate through epithelial-mesenchymal interactions during development. *Gastroenterology* **139:**893-903.

Kresty, L. A., Frankel, W. L., Hammond, C. D., Baird, M. E., Mele, J. M., Stoner, G. D. and Fromkes, J. J. (2006). Transitioning From Preclinical to Clinical Chemopreventive Assessments of Lyophilized Black Raspberries: Interim Results Show Berries Modulate Markers of Oxidative Stress in Barrett's Esophagus Patients. *Nutrition and Cancer* **54:**148-156.

Kresty, L. A., Fromkes, J. J., Frankel, W. L., Hammond, C. D., Seeram, N. P., Baird, M. and Stoner, G. D. (2016a). A phase I pilot study evaluating the beneficial effects of black raspberries in patients with Barrett's esophagus. *Oncotarget; Advance Online Publications: Page 2*.

Kresty, L. A., Mallery, S. R. and Stoner, G. D. (2016b). Black raspberries in cancer clinical trials: Past, present and future. *Journal of berry research* **6:**251-261.

Kresty, L. A., Morse, M. A., Morgan, C., Carlton, P. S., Lu, J., Gupta, A., Blackwood, M. *et al.* (2001). Chemoprevention of Esophageal Tumorigenesis by Dietary Administration of Lyophilized Black Raspberries. *Cancer Research* **61:**6112.

Kuhnert, F., Davis, C. R., Wang, H. T., Chu, P., Lee, M., Yuan, J., Nusse, R. *et al.* (2004). Essential requirement for Wnt signaling in proliferation of adult small intestine and colon revealed by adenoviral expression of Dickkopf-1. *Proceedings of the National Academy of Sciences of the United States of America* **101:**266-271.

Kula, M. and Krauze-Baranowska, M. (2016). Rubus occidentalis: The black raspberry—its potential in the prevention of cancer. *Nutrition and Cancer* **68:**18-28.

Landis-Piwowar, K. R. and Iyer, N. R. (2014). Cancer Chemoprevention: Current State of the Art. *Cancer Growth and Metastasis* **7:**19-25.

Lapidot, T., Sirard, C., Vormoor, J., Murdoch, B., Hoang, T., Caceres-Cortes, J., Minden, M. *et al.* (1994). A cell initiating human acute myeloid leukaemia after transplantation into SCID mice. *Nature* **367:**645-648.

Laplane, L. (2016). Cancer Stem Cells: Philosophy and Therapies. *Harvard University Press* Abstract only.

Lechner, J. F., Reen, R. K., Dombkowski, A. A., Cukovic, D., Salagrama, S., Wang, L. S. and Stoner, G. D. (2008). Effects of a black raspberry diet on gene expression in the rat esophagus. *Nutrition Cancer* **1:**61-69.

Lee, J.-H., Oh, M., Seok, J. H., Kim, S., Lee, D. B., Bae, G., Bae, H.-I. *et al.* (2016). Antiviral Effects of Black Raspberry (*Rubus coreanus*) Seed and Its Gallic Acid against Influenza Virus Infection. *Viruses* **8:**157.

Leslie, A., Carey, F. A., Pratt, N. R. and Steele, R. J. C. (2002). The Colorectal Adenoma-Carcinoma Sequence. *British Journal of Surgery* **89:**845-860.

Li, L., Milner, L. A., Deng, Y., Iwata, M., Banta, A., Graf, L., Marcovina, S. *et al.* (1998). The human homolog of rat Jagged1 expressed by marrow stroma inhibits differentiation of 32D cells through interaction with Notch1. *Immunity* **8:**43-55.

Li, N., Yousefi, M., Nakauka-Ddamba, A., Jain, R., Tobias, J., Epstein, Jonathan A., Jensen, Shane T. *et al.* (2014). Single-Cell Analysis of Proxy Reporter Allele-Marked Epithelial Cells Establishes Intestinal Stem Cell Hierarchy. *Stem Cell Reports* **3:**876-891.

Li, T. and Perez-Soler, R. (2009). Skin toxicities associated with epidermal growth factor receptor inhibitors. *Targeted Oncology* **4:**107–119.

Lindemans, C. A., Calafiore, M., Mertelsmann, A. M., O'Connor, M. H., Dudakov, J. A., Jenq, R. R., Velardi, E. *et al.* (2015). Interleukin-22 Promotes Intestinal Stem Cell-Mediated Epithelial Regeneration. *Nature* **528:**560-564.

Liu, G., Yuan, X., Zeng, Z., Tunici, P., Ng, H., Abdulkadir, I. R., Lu, L. *et al.* (2006). Analysis of gene expression and chemoresistance of CD133+ cancer stem cells in glioblastoma. *Molecular Cancer* **5:**67.

Liu, W., Li, H., Hong, S. H., Piszczek, G. P., Chen, W. and Rodgers, G. P. (2016). Olfactomedin 4 deletion induces colon adenocarcinoma in Apc(Min/+) mice. *Oncogene* **35:**5237-5247.

Livet, J., Weissman, T.A., Kang, H., Draft, R.W., Lu, J., Bennis, R.A., Sanes, J.R. and Lichtman, J.W. (2007). Transgenic strategies for combinatorial expression of fluorescent proteins in the nervous system. *Nature* **450**: 56–62.

Lobo, N. A., Shimono, Y., Qian, D. and Clarke, M. F. (2007). The biology of cancer stem cells. *Annual Review of Cell and Developmental Biology* **23:**675-699.

Loeffler, M., Birke, A., Winton, D. and Potten, C. (1993). Somatic Mutation, Monoclonality and Stochastic Models of Stem Cell Organization in the Intestinal Crypt. *Journal of Theoretical Biology* **160:**471-491.

Logan, C. Y. and Nusse, R. (2004). The Wnt signaling pathway in development and disease. *Annual Review of Cell and Developmental Biology* **20:**781-810.

Lopez-Garcia, C., Klein, A. M., Simons, B. D. and Winton, D. J. (2010). Intestinal Stem Cell Replacement Follows a Pattern of Neutral Drift. *Science* **330:**822.

Lue, H., Kleemann, R., Calandra, T., Roger, T. and Bernhagen, J. (2002). Macrophage migration inhibitory factor (MIF): mechanisms of action and role in disease. *Microbes and Infection* **4:**449-460.

Ma, S., Chan, K. W., Hu, L., Lee, T. K., Wo, J. Y., Ng, I. O., Zheng, B. J. *et al.* (2007). Identification and characterization of tumorigenic liver cancer stem/progenitor cells. *Gastroenterology* **132:**2542-2556.

Mace, T. A., King, S. A., Ameen, Z., Elnaggar, O., Young, G., Riedl, K. M., Schwartz, S. J. *et al.* (2014). Bioactive compounds or metabolites from black raspberries modulate T lymphocyte proliferation, myeloid cell differentiation and Jak/STAT signaling. *Cancer immunology, immunotherapy : CII* **63:**889-900.

Madison, B. B., McKenna, L. B., Dolson, D., Epstein, D. J. and Kaestner, K. H. (2009). FoxF1 and FoxL1 Link Hedgehog Signaling and the Control of Epithelial Proliferation in the Developing Stomach and Intestine. *The Journal of Biological Chemistry* **284:**5936–5944.

Mallery, S. R., Tong, M., Shumway, B. S., Curran, A. E., Larsen, P. E., Ness, G. M., Kennedy, K. S. *et al.* (2014). Topical Application of a Mucoadhesive Freeze-Dried Black Raspberry Gel Induces Clinical and Histologic Regression and Reduces Loss of Heterozygosity Events in Premalignant Oral Intraepithelial Lesions.: Results from a Multi-Centered, Placebo Controlled Clinical Trial. *Clinical cancer research : an official journal of the American Association for Cancer Research* **20:**1910-1924.

Mallery, S. R., Zwick, J. C., Pei, P., Tong, M., Larsen, P. E., Shumway, B. S., Lu, B. *et al.* (2008). Topical Application of a Bioadhesive Black Raspberry Gel Modulates Gene Expression and Reduces Cyclooxygenase 2 Protein in Human Premalignant Oral Lesions. *Cancer research* **68:**4945-4957.

Manach, C., Scalbert, A., Morand, C., Remesy, C. and Jimenez, L. (2004). Polyphenols: food sources and bioavailability. *The American Journal of Clinical Nutrition* **79:**727–747.

Marsh, V., Winton, D. J., Williams, G. T., Dubois, N., Trumpp, A., Sansom, O. J. and Clarke, A. R. (2008). Epithelial Pten is dispensible for intestinal homeostasis but supresses adenoma development and progression after *Apc* mutation. *Nature Genetics* **40:**1436-1444.

Marshman, E., Booth, C. and Potten, C. S. (2002). The intestinal epithelial stem cell. *Bioessays* **24:**91-98.

Martinez, M., Hope, C., Planutis, K., Planutiene, M., Pontello, A., Duarte, B., Albers, C. G. *et al.* (2010). Dietary grape-derived resveratrol for colon cancer prevention. *Journal of Clinical Oncology (Meeting Abstracts)* **28:**3622.

Massagué, J., Blain, S. W. and Lo, R. S. (2000). TGFbeta signaling in growth control, cancer, and heritable disorders. *Cell* **103:**295-309.

Mazza, G. (2007). Anthocyanins and heart health. *Ann. Ist. Super. Sanità* **43:**369-374.

McCullough, M. L., Robertson, A. S., Rodriguez, C., Jacobs, E. J., Chao, A., Carolyn, J., Calle, E. E. *et al.* (2003). Calcium, vitamin D, dairy products, and risk of colorectal cancer in the Cancer Prevention Study II Nutrition Cohort (United States). *Cancer Causes Control* **14:**1-12.

McGhie, T. K., Hall, H. K., Ainge, G. D. and Mowat, A. D. eds. (2002). *Breeding Rubus Cultivars for High Anthocyanin Content and High Antioxidant Capacity*. International Society for Horticultural Science (ISHS), Leuven, Belgium.

McIntyre, R. E., Buczacki, S. J. A., Arends, M. J. and Adams, D. J. (2015). Mouse models of colorectal cancer as preclinical models. *Bioessays* **37:**909-920.

Medema, J. P. and Vermeulen, L. (2011). Microenvironmental regulation of stem cells in intestinal homeostasis and cancer. *Nature Reviews Molecular Cell Biology* **474:**318–326.

Mestas, J. and Hughes, C. C. W. (2004). Of Mice and Not Men: Differences between Mouse and Human Immunology. *The Journal of Immunology* **172:**2731.

Middleton, J., E., Kandaswami, C. and Theoharides, T. C. (2000). The effects of plant flavonoids on mammalian cells: implications for inflammation, heart disease, and cancer. *Pharmacological Reviews* **52:**673–751.

Mihaylova, M. M., Sabatini, D. M. and Yilmaz, Ö. H. (2014). Dietary and Metabolic Control of Stem Cell Function in Physiology and Cancer. *Cell stem cell* **14:**292-305.

Millen, A. E., Subar, A. F., Graubard, B. I., Peters, U., Hayes, R. B., Weissfeld, J. L., Yokochi, L. A. *et al.* (2007). Fruit and vegetable intake and prevalence of colorectal adenoma in a cancer screening trial. *American Journal of Clinical Nutrition* **86:**1754-1764.

Moiseeva, E. P., Almeida, G. M., Jones, G. D. D. and Manson, M. M. (2007). Extended treatment with physiologic concentrations of dietary phytochemicals results in altered gene expression, reduced growth, and apoptosis of cancer cells. *Molecular Cancer Therapeutics* **6:**3071.

Montgomery, R. K., Carlone, D. L., Richmond, C. A., Farilla, L., Kranendonk, M. E. G., Henderson, D. E., Baffour-Awuah, N. Y. *et al.* (2011). Mouse telomerase reverse transcriptase (mTert) expression marks slowly cycling intestinal stem cells. *Proceedings of the National Academy of Sciences* **108:**179-184.

Moore, K. A. and Lemischka, I. R. (2006). Stem Cells and Their Niches. *Science* **311:**1880.

Moran-Ramos, S., Tovar, A. R. and Torres, N. (2012). Diet: Friend or Foe of Enteroendocrine Cells—How It Interacts with Enteroendocrine Cells. *Advances in Nutrition* **3:**8-20.

Morin, P. J., Sparks, A. B., Korinek, V., Barker, N., Clevers, H., Vogelstein, B. and Kinzler, K. W. (1997). Activation of beta-catenin-Tcf signaling in colon cancer by mutations in beta-catenin or APC. *Science* **275:**1787-1790.

Mori–Akiyama, Y., van den Born, M., van Es, J. H., Hamilton, S. R., Adams, H. P., Zhang, J., Clevers, H. *et al.* (2007). SOX9 Is Required for the Differentiation of Paneth Cells in the Intestinal Epithelium. *Gastroenterology* **133:**539-546.

Moser, A. R., Dove, W. R., Roth, K. A. and Gordonll, J. I. (1992). The Min (multiple intestinal neoplasia) mutation: its effect on gut epithelial cell differentiation and interaction with a modifier system. *The Journal of Cell Biology* **116:**1517-1526.

Moser, A. R., Pitot, H. C. and Dove, W. F. (1990). A dominant mutation that predisposes to multiple intestinal neoplasia in the mouse. *Science* **247:**322.

Moyer, R. A., Hummer, K. E., Finn, C. E., Frei, B. and Wrolstad, R. E. (2002). Anthocyanins, Phenolics, and Antioxidant Capacity in Diverse Small Fruits: Vaccinium, Rubus, and Ribes. *Journal of Agricultural and Food Chemistry* **50:**519-525.

Muller, P. A., Caswell, P. T., Doyle, B., *et al.* (2009). Mutant *p53* drives invasion by promoting integrin recycling. *Cell* **139**:1327–1341.

Munoz, N. M., Upton, M., Rojas, A., *et al.* (2006). Transforming growth factor beta receptor type II inactivation induces the malignant transformation of intestinal neoplasms initiated by Apc mutation. *Cancer research* **66**:9837–9844.

Muñoz, J., Stange, D. E., Schepers, A. G., van de Wetering, M., Koo, B.-K., Itzkovitz, S., Volckmann, R. *et al.* (2012). The Lgr5 intestinal stem cell signature: robust expression of proposed quiescent '+4' cell markers. *The EMBO Journal* **31:**3079-3091.

Määttä-Riihinen, K. R., Kamal-Eldin, A., Mattila, P. H., González-Paramás, A. M. and Törrönen, A. R. (2004). Distribution and Contents of Phenolic Compounds in Eighteen Scandinavian Berry Species. *Journal of Agricultural and Food Chemistry* **52:**4477-4486.

Méniel, V., Song, F., Phesse, T., Young, M., Poetz, O., Parry, L., Jenkins, J. R. *et al.* (2013). Cited1 Deficiency Suppresses Intestinal Tumorigenesis. *PLOS Genetics* **9:**e1003638.

Müller, M. F., Ibrahim, A. E. K., and Arends, M. J.(2016). Molecular pathological classification of colorectal cancer. *Virchows Arch* **469**:125–134.

Nautiyal, J., Kanwar, S. S., Yu, Y. and Majumdar, A. P. (2011). Combination of dasatinib and curcumin eliminates chemo-resistant colon cancer cells. *J Mol Signal* **6:**7.

Nguyen, T. L. A., Vieira-Silva, S., Liston, A. and Raes, J. (2015). How informative is the mouse for human gut microbiota research? *Disease Models & Mechanisms* **8:**1-16.

Nijveldt, R. J., van Nood, E., van Hoorn, D. E., Boelens, P. G., van Norren, K. and van Leeuwen, P. A. (2001). Flavonoids: a review of probable mechanisms of action and potential applications. *The American Journal of Clinical Nutrition* **74:**418–425.

Nozaki, K., Mochizuki, W., Matsumoto, Y., Matsumoto, T., Fukuda, M., Mizutani, T., Watanabe, M. *et al.* (2016). Co-culture with intestinal epithelial organoids allows efficient expansion and motility analysis of intraepithelial lymphocytes. *Journal of Gastroenterology* **51:**206-213.

Ogaki, S., Morooka, M., Otera, K. and Kume, S. (2015). A cost-effective system for differentiation of intestinal epithelium from human induced pluripotent stem cells. *Scientific Reports* **5:**17297.

Ogawa, K., Sakakibara, H., Iwata, R., Ishii, T., Sato, T., Goda, T., Shimoi, K. *et al.* (2008). Anthocyanin Composition and Antioxidant Activity of the Crowberry (Empetrum nigrum) and Other Berries. *Journal of Agricultural and Food Chemistry* **56:**4457-4462.

Oh, S., Gwak, J., Park, S. and Yang, C. S. (2014). Green tea polyphenol EGCG suppresses Wnt/β-catenin signaling by promoting GSK-3β- and PP2A-independent β-catenin phosphorylation/degradation. *BioFactors (Oxford, England)* **40:**586-595.

Ohhara, Y., Fukuda, N., Takeuchi, S., Honma, R., Shimizu, Y., Kinoshita, I. and Dosaka-Akita, H. (2016). Role of targeted therapy in metastatic colorectal cancer. *World Journal of Gastrointestinal Oncology* **8:**642–655.

Onuma, K., Ochiai, M., Orihashi, K., Takahashi, M., Imai, T., Nakagama, H. and Hippo, Y. (2013). Genetic reconstitution of tumorigenesis in primary intestinal cells. *Proceedings of the National Academy of Sciences* **110:**11127-11132.

Ootani, A., Li, X., Sangiorgi, E., Ho, Q. T., Ueno, H., Toda, S., Sugihara, H. *et al.* (2009). Sustained in vitro intestinal epithelial culture within a Wnt-dependent stem cell niche. *Nat Med* **15:**701-706.

Orford, K. W. and Scadden, D. T. (2008). Deconstructing stem cell self-renewal: genetic insights into cell-cycle regulation. *Nat Rev Genet* **9:**115-128.

O'Brien, C. A., Pollett, A., Gallinger, S. and Dick, J. E. (2007). A human colon cancer cell capable of initiating tumour growth in immunodeficient mice. *Nature* **445:**106-110.

Pan, P., Skaer, C. W., Stirdivant, S. M., Young, M. R., Stoner, G. D., Lechner, J. F., Huang, Y.-W. *et al.* (2015). Beneficial regulation of metabolic profiles by black raspberries in human colorectal cancer patients. *Cancer prevention research (Philadelphia, Pa.)* **8:**743-750.

Park, C. H., Hahm, E. R., Park, S., Kim, H. K. and Yang, C. H. (2005). The inhibitory mechanism of curcumin and its derivative against beta-catenin/Tcf signaling. *FEBS Lett* **579:**2965–2971.

Parker, A., Maclaren, O. J., Fletcher, A. G., Muraro, D., Kreuzaler, P. A., Byrne, H. M., Maini, P. K., Watson, A. J., Pin, C. (2017). Cell proliferation within small intestinal crypts is the principal driving force for cell migration on villi. *FASEB J* **31**:636-649.

Parkin, D. M., Boyd, L. and Walker, L. C. (2011). The fraction of cancer attributable to lifestyle and environmental factors in the UK in 2010. *Britsih Journal of Cancer* **105:**S77-S81.

Parry, L., Young, M., El Marjou, F. and Clarke, A. R. (2013). Evidence for a Crucial Role of Paneth Cells in Mediating the Intestinal Response to Injury. *Stem Cells* **31:**776-785.

Paul, B., Barnes, S., Demark-Wahnefried, W., Morrow, C., Salvador, C., Skibola, C. and Tollefsbol, T. O. (2015). Influences of diet and the gut microbiome on epigenetic modulation in cancer and other diseases. *Clinical Epigenetics* **7:**112.

Peiffer, D. S., Zimmerman, N. P., Wang, L.-S., Ransom, B. W. S., Carmella, S. G., Kuo, C.-T., Siddiqui, J. *et al.* (2014). Chemoprevention of Esophageal Cancer with Black Raspberries, Their Component Anthocyanins, and a Major Anthocyanin Metabolite, Protocatechuic Acid. *Cancer Prevention Research* **7:**574.

Pellegrinet, L., Rodilla, V., Liu, Z., Chen, S., Koch, U., Espinosa, L., Kaestner, K. H. *et al.* (2011). Dll1- and Dll4-mediated Notch signaling is required for homeostasis of intestinal stem cells. *Gastroenterology* **140:**1230–1240.e1237.

Perreault, N. and Beaulieu, J.-F. (1996). Use of the Dissociating Enzyme Thermolysin to Generate Viable Human Normal Intestinal Epithelial Cell Cultures. *Experimental cell research* **224:**354–364.

Peters, U., Sinha, R., Chatterjee, N., Subar, A. F., Ziegler, R. G., Kulldorff, M., Bresalier, R. *et al.* (2003). Dietary fibre and colorectal adenoma in a colorectal cancer early detection programme. *Lancet* **361:**1491-1495.

Phesse, T. J., Buchert, M., Stuart, S., Flanagan, D. J., Faux, M., Afshar-Sterle, S., Walker, F. *et al.* (2014). Partial inhibition of gp130-Jak-Stat3 signaling prevents Wnt–β-catenin–mediated intestinal tumor growth and regeneration. *Science Signaling* **7:**ra92.

Pinto, D., Gregorieff, A., Begthel, H. and Clevers, H. (2003). Canonical Wnt signals are essential for homeostasis of the intestinal epithelium. *Genes and Development* **17:**1709-1713.

Potten, C. S., Hume, W. J., Reid, P. and Cairns, J. (1978). The segregation of DNA in epithelial stem cells. *Cell* **15:**899-906.

Potten, C. S., Kovacs, L. and Hamilton, E. (1974). Continuous labelling studies on mouse skin and intestine. *Cell Proliferation* **7:**271-283.

Potten, C. S., Owen, G. and Booth, D. (2002). Intestinal stem cells protect their genome by selective segregation of template DNA strands. *Journal of Cell Science* **115:**2381.

Powell, A. E., Wang, Y., Li, Y., Poulin, E. J., Means, A. L., Washington, M. K., Higginbotham, J. N. *et al.* (2012). The Pan-ErbB Negative Regulator Lrig1 Is an Intestinal Stem Cell Marker that Functions as a Tumor Suppressor. *Cell* **149:**146-158.

Powell, S. M., Zilz, N., Beazer-Barclay, Y., Bryan, T. M., Hamilton, S. R., Thibodeau, S. N., Vogelstein, B. *et al.* (1992). APC mutations occur early during colorectal tumorigenesis. *Nature* **359:**235-237.

Prior, R. L., Cao, G., Martin, A., Sofic, E., McEwen, J., O'Brien, C., Lischner, N. *et al.* (1998). Antioxidant Capacity As Influenced by Total Phenolic and Anthocyanin Content, Maturity, and Variety of Vaccinium Species. *Journal of Agricultural and Food Chemistry* **46:**2686-2693.

Promega. (2015). CellTiter-Glo ® Luminescent Cell Viability Assay: Technical Bulletin. USA.

Ramadan, Q., Jafarpoorchekab, H., Huang, C., Silacci, P., Carrara, S., Koklu, G., Ghaye, J. *et al.* (2013). NutriChip: nutrition analysis meets microfluidics. *Lab on a Chip* **13:**196-203.

Ramasamy, T. S., Ayob, A. Z., Myint, H. H. L., Thiagarajah, S. and Amini, F. (2015). Targeting colorectal cancer stem cells using curcumin and curcumin analogues: insights into the mechanism of the therapeutic efficacy. *Cancer Cell International* **15:**96.

Reed, K. R., Tunster, S. J., Young, M., Carrico, A., John, R. M. and Clarke, A. R. (2012). Entopic overexpression of Ascl2 does not accelerate tumourigenesis in ApcMin mice. *Gut* **61:**1435-1438.

Resnick, M. B., Routhier, J., Konkin, T., Sabo, E. and Pricolo, V. E. (2004). Epidermal growth factor receptor, c-MET, beta-catenin, and p53 expression as prognostic indicators in stage II colon cancer : a tissue microarray study. *Clinical Cancer Research* **10:**3069-3075.

Robanus-Maandag, E. C., Koelink, P. J., Breukel, C., Salvatori, D. C. F., Jagmohan-Changur, S. C., Bosch, C. A. J., Verspaget, H. W. *et al.* (2010). A new conditional Apc-mutant mouse model for colorectal cancer. *Carcinogenesis* **31:**946-952.

Robertson, T. B. (1926). The Analysis of the Growth of the Normal White Mouse into its Constituent Processes. *The Journal of General Physiology* **8:**463-507.

Rodrigo, K. A., Rawal, Y., Renner, R. J., Schwartz, S. J., Tian, Q., Larsen, P. E. and Mallery, S. R. (2006). Suppression of the Tumorigenic Phenotype in Human Oral Squamous Cell Carcinoma Cells by an Ethanol Extract Derived From Freeze-Dried Black Raspberries. *Nutrition and cancer* **54:**58-68.

Roper, J., Tammela, T., Cetinbas, N. M., Akkad, A., Roghanian, A., Rickelt, S., Almeqdadi M., *et al.* (2017). *In vivo* genome editing and organoid transplantation models of colorectal cancer and metastasis. *Nature Biotechnology* doi:10.1038/nbt.3836.

Ropka, M. E., Keim, J. and Philbrick, J. T. (2010). Patient Decisions About Breast Cancer Chemoprevention: A Systematic Review and Meta-Analysis. *Journal of Clinical Oncology* **28:**3090-3095.

Rothenberg, M. E., Nusse, Y., Kalisky, T., Lee, J. J., Dalerba, P., Scheeren, F., Lobo, N. *et al.* (2012). Identification of a cKit+ Colonic Crypt Base Secretory Cell That Supports Lgr5+ Stem Cells in Mice. *Gastroenterology* **142:**1195-1205.e1196.

Rothwell, P. M., Wilson, M., Elwin, C.-E., Norrving, B., Algra, A., Warlow, C. P. and Meade, T.W. (2010). Long-term eff ect of aspirin on colorectal cancer incidence and mortality: 20-year follow-up of five randomised trials. *Lancet* **376**:1741-50.

Sakar, Y., Duca, F. A., Langelier, B., Devime, F., Blottiere, H., Delorme, C., Renault, P. *et al.* (2014). Impact of high-fat feeding on basic helix-loop-helix transcription factors controlling enteroendocrine cell differentiation. *Int J Obes* **38:**1440-1448.

Samelis, G. F., Ekmektzoglou, K. A., Tsiakou, A. and Konstadoulakis, M. (2011). The continuation of bevacizumab following disease progression in patients with metastatic colorectal cancer offers a survival benefit. *Hepatogastroenterology* **58:**1968-1971.

Sánchez-Rivera, F. J. and Jacks, T. (2015). Applications of the CRISPR-Cas9 system in cancer biology. *Nat. Rev. Cancer* **15**:387–395.

Sangiorgi, E. and Capecchi, M. R. (2008). Bmi1 is expressed in vivo in intestinal stem cells. *Nature genetics* **40:**915-920.

Sanjoaquin, M. A., Allen, N., Couto, E., Roddam, A. W. and Key, T. J. (2005). Folate intake and colorectal cancer risk: a meta-analytical approach. *International Journal of Cancer* **113:**825-828.

Sansom, O. J., Reed, K. R., Hayes, A. J., Ireland, H., Brinkmann, H., Newton, I. P., Batlle, E. *et al.* (2004). Loss of Apc in vivo immediately perturbs Wnt signaling, differentiation, and migration. *Genes and Development* **18:**1385-1390.

Sansom, O. J., Meniel, V., Wilkins, J.A., Cole, A. M., Oien, K. A., Marsh, V., Jamieson, T. J., et al. (2006). Loss of Apc allows phenotypic manifestation of the transforming properties of an endogenous K-ras oncogene in vivo. *Proc Natl Acad Sci USA* **103**:14122–14127.

Sasaki, N., Sachs, N., Wiebrands, K., Ellenbroek, S. I. J., Fumagalli, A., Lyubimova, A., Begthel, H. *et al.* (2016). Reg4+ deep crypt secretory cells function as epithelial niche for Lgr5+ stem cells in colon. *Proceedings of the National Academy of Sciences* **113:**E5399-E5407.

Sato, T., Stange, D. E., Ferrante, M., Vries, R. G. J., van Es, J. H., van den Brink, S., van Houdt, W. J. *et al.* (2011a). Long-term Expansion of Epithelial Organoids From Human Colon, Adenoma, Adenocarcinoma, and Barrett's Epithelium. *Gastroenterology* **141:**1762–1772.

Sato, T., van Es, J. H., Snippert, H. J., Stange, D. E., Vries, R. G., van den Born, M., Barker, N. *et al.* (2011b). Paneth cells constitute the niche for Lgr5 stem cells in intestinal crypts. *Nature* **469:**415-418.

Sato, T., Vries, R. G., Snippert, H. J., van de Wetering, M., Barker, N., Stange, D. E., van Es, J. H. *et al.* (2009). Single Lgr5 stem cells build crypt–villus structures *in vitro* without a mesenchymal niche. *Nature* **459:**262-266.

Schepers, A. G., Snippert, H. J., Stange , D. E., van den Born , M., van Es , J. H., van de Wetering , M. and Clevers, H. (2012). Lineage Tracing Reveals $Lgr5^{+}$ Stem Cell Activity in Mouse Intestinal Adenomas. *Science* **337:**730–735.

Schonhoff, S. E., Giel-Moloney, M. and Leiter, A. B. (2004). Minireview: Development and Differentiation of Gut Endocrine Cells. *Endocrinology* **145:**2639-2644.

Schwenk, F., Baron, U. and Rajewsky, K. (1995). A cre-transgenic mouse strain for the ubiquitous deletion of loxP-flanked gene segments including deletion in germ cells. *Nucleic Acids Research* **23:**5080-5081.

Schwitalla, S., Fingerle, Alexander A., Cammareri, P., Nebelsiek, T., Göktuna, Serkan I., Ziegler, Paul K., Canli, O. *et al.* (2013). Intestinal Tumorigenesis Initiated by Dedifferentiation and Acquisition of Stem-Cell-like Properties. *Cell* **152:**25-38.

Scoville, D. H., Sato, T., He, X. C., and Li, L. (2008). Current View: Intestinal Stem Cells and Signaling. *Gastroenterology* **134**:849–864.

Seeram, N. P. (2008). Berry Fruits for Cancer Prevention: Current Status and Future Prospects. *Journal of Agricultural and Food Chemistry* **56:**630-635.

Shay, T., Jojic, V., Zuk, O., Rothamel, K., Puyraimond-Zemmour, D., Feng, T., Wakamatsu, E. *et al.* (2013). Conservation and divergence in the transcriptional programs of the human and mouse immune systems. *Proceedings of the National Academy of Sciences of the United States of America* **110:**2946-2951.

Shen, Z. (2011). Genomic instability and cancer: an introduction. *Journal of Molecular Cell Biology* **3:**1-3.

Shibata, H., Toyama, K., Shioya, H., Ito, M., Hirota, M., Hasegawa, S., Matsumoto, H. *et al.* (1997). Rapid Colorectal Adenoma Formation Initiated by Conditional Targeting of the Apc Gene. *Science* **278:**120.

Shimizu, M., Deguchi, A., Lim, J. T. E., Moriwaki, H., Kopelovich, L. and Weinstein, I. B. (2005). (−)-Epigallocatechin Gallate and Polyphenon E Inhibit Growth and Activation of the Epidermal Growth Factor Receptor and Human Epidermal Growth Factor Receptor-2 Signaling Pathways in Human Colon Cancer Cells. *Clinical Cancer Research* **11:**2735-2746.

Shimizu, M., Shirakami, Y., Sakai, H., Yasuda, Y., Kubota, M., Adachi, S., Tsurumi, H. *et al.* (2010). (−)-Epigallocatechin gallate inhibits growth and activation of the VEGF/VEGFR axis in human colorectal cancer cells. *Chemico-Biological Interactions* **185:**247-252.

Singh-Ranger, G. (2016). The role of aspirin in colorectal cancer chemoprevention. *Critical Reviews in Oncology/Hematology* **104**:87–90.

Shumway, B. S., Kresty, L. A., Larsen, P. E., Zwick, J. C., Lu, B., Fields, H. W., Mumper, R. J. *et al.* (2008). Effects of a Topically Applied Bioadhesive Berry Gel on Loss of Heterozygosity Indices in Premalignant Oral Lesions. *Clinical cancer research : an official journal of the American Association for Cancer Research* **14:**2421-2430.

Singh, S. K., Hawkins, C., Clarke, I. D., Squire, J. A., Bayani, J., Hide, T., Henkelman, R. M. *et al.* (2004). Identification of human brain tumour initiating cells. *Nature* **432:**396-401.

Sinner, D., Kordich, J. J., Spence, J. R., Opoka, R., Rankin, S., Lin, S.-C. J., Jonatan, D. *et al.* (2007). Sox17 and Sox4 Differentially Regulate β-Catenin/T-Cell Factor Activity and Proliferation of Colon Carcinoma Cells. *Molecular and Cellular Biology* **27:**7802-7815.

Siriwoharn, T., Wrolstad, R. E., Finn, C. E. and Pereira, C. B. (2004). Influence of Cultivar, Maturity, and Sampling on Blackberry (Rubus L. Hybrids) Anthocyanins, Polyphenolics, and Antioxidant Properties. *Journal of Agricultural and Food Chemistry* **52:**8021-8030.

Smith, G. H. (2005). Label-retaining epithelial cells in mouse mammary gland divide asymmetrically and retain their template DNA strands. *Development* **132:**681.

Snippert, H. J., van der Flier, L. G., Sato, T., van Es, J. H., van den Born, M., Kroon-Veenboer, C., Barker, N. *et al.* (2010). Intestinal Crypt Homeostasis Results from Neutral Competition between Symmetrically Dividing Lgr5 Stem Cells. *Cell* **143:**134-144.

Soobrattee, M. A., Bahorun, T. and Aruoma, O. I. (2006). Chemopreventive actions of polyphenolic compounds in cancer. *Biofactors* **27:**19-35.

Sporn, M. B. (1976). Approaches to Prevention of Epithelial Cancer during the Preneoplastic Period. *Cancer Research* **36:**2699-2702.

Stevens, R. G., Swede, H., Heinen, C. D., Jablonski, M., Grupka, M., Ross, B., Parente, M. *et al.* (2007). Aberrant crypt foci in patients with a positive family history of sporadic colorectal cancer. *Cancer Letters* **248:**262-268.

Steward, W. P. and Brown, K. (2013). Cancer chemoprevention: a rapidly evolving field. *British Journal of Cancer* **109:**1-7.

Stine, R. R. and Matunis, E. L. (2013). Stem Cell Competition: Finding Balance in the Niche. *Trends in cell biology* **23:**357-364.

Stoian, M., Stoica, V. and Radulian, G. (2016). Stem cells and colorectal carcinogenesis. *Journal of Medicine and Life* **6:**6-11.

Stoner, G. D. (2009). Foodstuffs for Preventing Cancer: The Preclinical and Clinical Development of Berries. *Cancer Prevention Research* **2:**187.

Stoner, G. D., Chen, T., Kresty, L. A., Aziz, R. M., Reinemann, T. and Nines, R. (2006). Protection Against Esophageal Cancer in Rodents With Lyophilized Berries: Potential Mechanisms. *Nutrition and cancer* **54:**33-46.

Stoner, G. D., Sardo, C., Apseloff, G., Mullet, D., Wargo, W., Pound, V., Singh, A. *et al.* (2005). Pharmacokinetics of Anthocyanins and Ellagic Acid in Healthy Volunteers Fed Freeze-Dried Black Raspberries Daily for 7 Days. *The Journal of Clinical Pharmacology* **45:**1153-1164.

Stoner, G. D., Wang, L.-S., Zikri, N., Chen, T., S. Hecht, S., Huang, C., Sardo, C. *et al.* (2007). Cancer Prevention with Freeze-dried Berries and Berry Components. *Seminars in cancer biology* **17:**403-410.

Su, L. K., Kinzler, K. W., Vogelstein, B., Preisinger, A. C., Moser, A. R., Luongo, C., Gould, K. A. *et al.* (1992). Multiple intestinal neoplasia caused by a mutation in the murine homolog of the APC gene. *Science* **256:**668.

Suetsugu, A., Nagaki, M., Aoki, H., Motohashi, T., Kunisada, T. and Moriwaki, H. (2006). Characterization of CD133+ hepatocellular carcinoma cells as cancer stem/progenitor cells. *Biochemical and Biophysical Research Communications* **351:**820-824.

Sun, B., Nishihira, J., Yoshiki, T., Kondo, M., Sato, Y., Sasaki, F. and Todo, S. (2005). Macrophage Migration Inhibitory Factor Promotes Tumor Invasion and Metastasis via the Rho-Dependent Pathway. *Clinical Cancer Research* **11:**1050.

Suzuki, R., Kohno, H., Sugie, S. and Tanaka, T. (2004). Sequential observations on the occurrence of preneoplastic and neoplastic lesions in mouse colon treated with azoxymethane and dextran sodium sulfate. *Cancer Science* **95:**721-727.

Swanson Health Products. (2017). Nutri-Fruit Black Raspberry Powder [Online]. Available at: http://www.swansonvitamins.com/nutri-fruit-freeze-dried-black-raspberry-powder-5-oz-pwdr. [Accessed: 08/02/2017].

Tajima, H., Ohta, T., Kitagawa, H., Okamoto, K., Sakai, S., Kinoshita, J., Makino, I. *et al.* (2012). Neoadjuvant chemotherapy with gemcitabine for pancreatic cancer increases in situ expression of the apoptosis marker M30 and stem cell marker CD44. *Oncology Letters* **3:**1186-1190.

Takeda, N., Jain, R., LeBoeuf, M. R., Wang, Q., Lu, M. M. and Epstein, J. A. (2011). Interconversion Between Intestinal Stem Cell Populations in Distinct Niches. *Science* **334:**1420.

Tan, B. T., Park, C. Y., Ailles, L. E. and Weissm, I. R. (2006). The cancer stem cell hypothesis: a work in progress. *Laboratory Investigation* **86:**1203–1207.

Tetteh, Paul W., Basak, O., Farin, Henner F., Wiebrands, K., Kretzschmar, K., Begthel, H., van den Born, M. *et al.* (2016a). Replacement of Lost Lgr5-Positive Stem Cells through Plasticity of Their Enterocyte-Lineage Daughters. *Cell Stem Cell* **18:**203-213.

Tetteh, P. W., Kretzschmar, K., Begthel, H., van den Born, M., Korving, J., Morsink, F., Farin, H. *et al.* (2016b). Generation of an inducible colon-specific Cre enzyme mouse line for colon cancer research. *Proceedings of the National Academy of Sciences* **113:**11859-11864.

Tian, H., Biehs, B., Warming, S., Leong, K. G., Rangell, L., Klein, O. D. and de Sauvage, F. J. (2011). A reserve stem cell population in small intestine renders Lgr5-positive cells dispensable. *Nature* **478:**255-259.

Tian, Q., Giusti, M. M., Stoner, G. D. and Schwartz, S. J. (2006). Characterization of a new anthocyanin in black raspberries (*Rubus occidentalis*) by liquid chromatography electrospray ionization tandem mass spectrometry. *Food Chemistry* **94:**465-468.

Toden, S., Tran, H.-M., Tovar-Camargo, O. A., Okugawa, Y. and Goel, A. (2016). Epigallocatechin-3-gallate targets cancer stem-like cells and enhances 5-fluorouracil chemosensitivity in colorectal cancer. *Oncotarget* **7:**16158-16171.

Tomasetti, C. and Vogelstein, B. (2015). Variation in cancer risk among tissues can be explained by the number of stem cell divisions. *Science (New York, N.Y.)* **347:**78-81.

Tunster, S. J., McNamara, G. I., Creeth, H. D. J. and John, R. M. (2016). Increased dosage of the imprinted Ascl2 gene restrains two key endocrine lineages of the mouse Placenta. *Developmental Biology* **418:**55-65.

Ulrich, C. M., Bigler, J., and Potter, J. D. (2006). Non-steroidal anti-inflammatory drugs for cancer prevention: promise, perils and pharmacogenetics. *Nat Rev Cancer* **6**:130.

Umar, S. (2010). Intestinal Stem Cells. *Current gastroenterology reports* **12:**340-348.

U.S. Preventive Services Task Force. (2007). Routine Aspirin or Nonsteroidal Anti-inflammatory Drugs for the Primary Prevention of Colorectal Cancer: U.S. Preventive Services Task Force Recommendation Statement. *Ann Intern Med* **146**:361-364.

Valko, M., Leibfritz, D., Moncol, J., Cronin, M. T., Mazur, M. and Telser, J. (2007). Free radicals and antioxidants in normal physiological functions and human disease. *The International Journal of Biochemistry & Cell Biology* **39:**44-84.

van der Flier, L. G., Haegebarth, A., Stange, D. E., van de Wetering, M. and Clevers, H. (2009a). OLFM4 Is a Robust Marker for Stem Cells in Human Intestine and Marks a Subset of Colorectal Cancer Cells. *Gastroenterology* **137:**15-17.

van der Flier, L. G., van Gijn, M. E., Hatzis, P., Kujala, P., Haegebarth, A., Stange, D. E., Begthel, H. *et al.* (2009b). Transcription Factor Achaete Scute-Like 2 Controls Intestinal Stem Cell Fate. *Cell* **136:**903-912.

van Dop, W. A., Heijmans, J., Büller, N. V., Snoek, S. A., Rosekrans, S. L., Wassenberg, E. A., van den Bergh Weerman, M. A. *et al.* (2010). Loss of Indian Hedgehog activates multiple aspects of a wound healing response in the mouse intestine. *Gastroenterology* **139:**1665-1676.

van Es, J. H., de Geest, N., van de Born, M., Clevers, H. and Hassan, B. A. (2010). Intestinal stem cells lacking the Math1 tumour suppressor are refractory to Notch inhibitors. *Nature Communications* **1:**1-5.

van Es, J. H., Sato, T., van de Wetering, M., Lyubimova, A., Yee Nee, A. N., Gregorieff, A., Sasaki, N. *et al.* (2012). Dll1+ secretory progenitor cells revert to stem cells upon crypt damage. *Nat Cell Biol* **14:**1099-1104.

van Es, J. H., van Gijn, M. E., Riccio, O., van den Born, M., Vooijs, M., Begthel, H., Cozijnsen, M. *et al.* (2005). Notch/[gamma]-secretase inhibition turns proliferative cells in intestinal crypts and adenomas into goblet cells. *Nature* **435:**959-963.

van Staveren, W. C. G., Solís, D. Y. W., Hébrant, A., Detours, V., Dumont, J. E. and Maenhaut, C. (2009). Human cancer cell lines: Experimental models for cancer cells in situ? For cancer stem cells? *Biochimica et Biophysica Acta (BBA) - Reviews on Cancer* **1795:**92-103.

VanDussen, K. L., Carulli, A. J., Keeley, T. M., Patel, S. R., Puthoff, B. J., Magness, S. T., Tran, I. T. *et al.* (2012). Notch signaling modulates proliferation and differentiation of intestinal crypt base columnar stem cells. *Development* **139:**488.

VanDussen, K. L., Marinshaw, J. M., Shaikh, N., Miyoshi, H., Moon, C., Tarr, P. I., Ciorba, M. A. *et al.* (2015). Development of an enhanced human gastrointestinal epithelial culture system to facilitate patient-based assays. *Gut* **64:**911-920.

VanDussen, K. L. and Samuelson, L. C. (2010). Mouse Atonal Homolog 1 Directs Intestinal Progenitors to Secretory Cell Rather than Absorptive Cell Fate. *Developmental Biology* **346:**215–223.

Vargo-Gogola, T. and Rosen, J. M. (2007). Modelling breast cancer: one size does not fit all. *Nat Rev Cancer* **7:**659-672.

Velcich, A., Yang, W., Heyer, J., Fragale, A., Nicholas, C., Viani, S., Kucherlapati, R. *et al.* (2002). Colorectal Cancer in Mice Genetically Deficient in the Mucin Muc2. *Science* **295:**1726.

Vermeulen, L., Morrissey, E., van der Heijden, M., Nicholson, A. M., Sottoriva, A., Buczacki, S., Kemp, R. *et al.* (2013). Defining Stem Cell Dynamics in Models of Intestinal Tumor Initiation. *Science* **342:**995.

Vermeulen , L., Todaro , M., de Sousa Mello , F., Sprick , M. R., Kemper , K., Perez Alea , M., Richel , D. J. *et al.* (2008). Single-cell cloning of colon cancer stem cells reveals a multi-lineage differentiation capacity. *Proceedings of the National Academy of Sciences of the United States of America* **105:**13427–13432.

Vidal, S. J., Rodriguez-Bravo, V., Galsky, M., Cordon-Cardo, C. and Domingo-Domenech, J. (2014). Targeting cancer stem cells to suppress acquired chemotherapy resistance. *Oncogene* **33:**4451-4463.

Volk-Draper, L., Hall, K., Griggs, C., Rajput, S., Kohio, P., DeNardo, D. and Ran, S. (2014). Paclitaxel therapy promotes breast cancer metastasis in a TLR4-dependent manner. *Cancer Research* **74:**5421-5434.

Wada, L. and Ou, B. (2002). Antioxidant Activity and Phenolic Content of Oregon Caneberries. *Journal of Agricultural and Food Chemistry* **50:**3495-3500.

Wang, F., Flanagan, J., Su, N., Wang, L.-C., Bui, S., Nielson, A., Wu, X. *et al.* (2012). RNAscope: A Novel in Situ RNA Analysis Platform for Formalin-Fixed, Paraffin-Embedded Tissues. *The Journal of Molecular Diagnostics : JMD* **14:**22-29.

Wang, F., Scoville, D., He, X. C., Mahe, M. M., Box, A., Perry, J. M., Smith, N. R. *et al.* (2013a). Isolation and Characterization of Intestinal Stem Cells Based on Surface Marker Combinations and Colony-Formation Assay. *Gastroenterology* **145:**383-395.e381-321.

Wang, L.-S., Arnold, M., Huang, Y.-W., Sardo, C., Seguin, C., Martin, E., Huang, T. H. M. *et al.* (2011). Modulation of Genetic and Epigenetic Biomarkers of Colorectal Cancer in Humans by Black Raspberries: A Phase I Pilot Study. *Clinical Cancer Research* **17:**598.

Wang, L.-S., Burke, C. A., Hasson, H., Kuo, C.-T., Molmenti, C. L. S., Seguin, C., Liu, P. *et al.* (2014). A Phase Ib Study of the Effects of Black Raspberries on Rectal Polyps in Patients with Familial Adenomatous Polyposis. *Cancer Prevention Research* **7:**666.

Wang, L.-S., Hecht, S. S., Carmella, S. G., Yu, N., Larue, B., Henry, C., McIntyre, C. *et al.* (2009). Anthocyanins in Black Raspberries Prevent Esophageal Tumors in Rats. *Cancer prevention research (Philadelphia, Pa.)* **2:**84-93.

Wang, L.-S., Kuo, C.-T., Cho, S.-J., Seguin, C., Siddiqui, J., Stoner, K., Weng, Y.-I. *et al.* (2013b). Black Raspberry-Derived Anthocyanins Demethylate Tumor Suppressor Genes Through the Inhibition of DNMT1 and DNMT3B in Colon Cancer Cells. *Nutrition and Cancer* **65:**118-125.

Wang, L.-S., Kuo, C.-T., Huang, T. H. M., Yearsley, M., Oshima, K., Stoner, G. D., Yu, J. *et al.* (2013c). Black Raspberries Protectively Regulate Methylation of Wnt Pathway Genes in Precancerous Colon Tissue. *Cancer prevention research (Philadelphia, Pa.)* **6:**1317-1327.

Wang, L.-S., Kuo, C.-T., Stoner, K., Yearsley, M., Oshima, K., Yu, J., Huang, T. H. M. *et al.* (2013d). Dietary black raspberries modulate DNA methylation in dextran sodium sulfate (DSS)-induced ulcerative colitis. *Carcinogenesis* **34:**2842-2850.

Wang, L.-S. and Stoner, G. D. (2008). Anthocyanins and their role in cancer prevention. *Cancer Letters* **269:**281-290.

Wang, S. Y. (2006). Effect of Pre-harvest Conditions on Antioxidant Capacity in Fruits. *Acta Horticulturae* **712:**299-305.

Wang, Z.-J., Ohnaka, K., Morita, M., Toyomura, K., Kono, S., Ueki, T., Tanaka, M. *et al.* (2013e). Dietary polyphenols and colorectal cancer risk: The Fukuoka colorectal cancer study. *World Journal of Gastroenterology* **19:**2683–2690.

Watanabe, K., Ueno, M., Kamiya, D., Nishiyama, A., Matsumura, M., Wataya, T., Takahashi, J. B. *et al.* (2007). A ROCK inhibitor permits survival of dissociated human embryonic stem cells. *Nat Biotech* **25:**681-686.

Webster, M. T., Rozycka, M., Sara, E., Davis, E., Smalley, M., Young, N., Dale, T. C. *et al.* (2000). Sequence variants of the axin gene in breast, colon, and other cancers: an analysis of mutations that interfere with GSK3 binding. *Genes Chromosomes Cancer* **28:**443–453.

Whitehead, R. H., Demmler, K., Rockman, S. P. and Watson, N. K. (1999). Clonogenic Growth of Epithelial Cells From Normal Colonic Mucosa From Both Mice and Humans. *Gastroenterology* **117:**858–865.

Wiedenmann, B., Franke, W. W., Kuhn, C., Moll, R. and Gould, V. E. (1986). Synaptophysin: A marker protein for neuroendocrine cells and neoplasms. *Proceedings of the National Academy of Sciences* **83:**3500-3504.

Willett, W. C., Stampfer, M. J., Colditz, G. A., Rosner, B. A. and Speizer, F. E. (1990). Relation of meat, fat, and fiber intake to the risk of colon cancer in a prospective study among women. *The New England Journal of Medicine* **323:**1664-1672.

Williams, J. M., Duckworth, C. A., Watson, A. J. M., Frey, M. R., Miguel, J. C., Burkitt, M. D., Sutton, R. *et al.* (2013). A mouse model of pathological small intestinal epithelial cell apoptosis and shedding induced by systemic administration of lipopolysaccharide. *Disease Models & Mechanisms* **6:**1388-1399.

Williams, P. L., Warwick, R., Dyson, M. and Bannister, L. H. (1989). Gray's anatomy. 37th ed. Churchill Livingstone.

Wright, N. A. and Alison, M. (1984). The Biology of the Epithelial Cell Populations. Clarendon, Oxford.

Wu, S., Powers, S., Zhu, W. and Hannun, Y. A. (2016). Substantial contribution of extrinsic risk factors to cancer development. *Nature* **529:**43-47.

Wu, X., Gu, L., Prior, R. L. and McKay, S. (2004). Characterization of Anthocyanins and Proanthocyanidins in Some Cultivars of Ribes, Aronia, and Sambucus and Their Antioxidant Capacity. *Journal of Agricultural and Food Chemistry* **52:**7846-7856.

Yamada, Y. and Mori, H. (2007). Multistep carcinogenesis of the colon in ApcMin/+ mouse. *Cancer Science* **98:**6-10.

Yan, K. S., Chia, L. A., Li, X., Ootani, A., Su, J., Lee, J. Y., Su, N. *et al.* (2012). The intestinal stem cell markers Bmi1 and Lgr5 identify two functionally distinct populations. *Proceedings of the National Academy of Sciences of the United States of America* **109:**466-471.

Yan, K.S. and Kuo, C.J. (2015). Ascl2 Reinforces Intestinal Stem Cell Identity. *Cell Stem Cell* **16:**105-106.

Yang, Q., Bermingham, N. A., Finegold, M. J. and Zoghbi, H. Y. (2001). Requirement of Math1 for secretory cell lineage commitment in the mouse intestine. *Science* **294:**2155-2158.

Ying, H.,Kimmelman, A. C.,Lyssiotis, C. A.,Hua, S.,Chu, G. C.,Fletcher-Sananikone, E.,Locasale, J. W. *et al.* (2012).Oncogenic Kras maintains pancreatic tumors through regulation of anabolic glucose metabolism. *Cell* **149**:656-70.

Young, M. A. (2013). The effects of aberrant Wnt signalling on the murine intestinal stem cell compartment. Thesis Ph.D., Cardiff University.

Yu, Y., Kanwar, S. S., Patel, B. B., Nautiyal, J., Sarkar, F. H. and Majumdar, A. P. (2009). Elimination of colon cancer stem-like cells by the combination of curcumin and FOLFOX. *Translat Oncol* **2**.

Zallen, J. A. (2007). Planar polarity and tissue morphogenesis. *Cell* **129:**1051-1063.

Zhang, Z., Knobloch, T. J., Seamon, L. G., Stoner, G. D., Cohn, D. E., Paskett, E. D., Fowler, J. M. *et al.* (2011). A black raspberry extract inhibits proliferation and regulates apoptosis in cervical cancer cells. *Gynecologic oncology* **123:**401-406.

Zhu, L., Gibson, P., Currle, D. S., Tong, Y., Richardson, R. J., Bayazitov, I. T., Poppleton, H. *et al.* (2009). Prominin 1 marks intestinal stem cells that are susceptible to neoplastic transformation. *Nature* **457:**603-607.

Zikri, N. N., Riedl, K. M., Wang, L.-S., Lechner, J. F., Schwartz, S. J. and Stoner, G. D. (2009). Black Raspberry Components Inhibit Proliferation, Induce Apoptosis and Modulate Gene Expression in Rat Esophageal Epithelial Cells. *Nutrition and cancer* **61:**816-826.

8 Supplementary Material

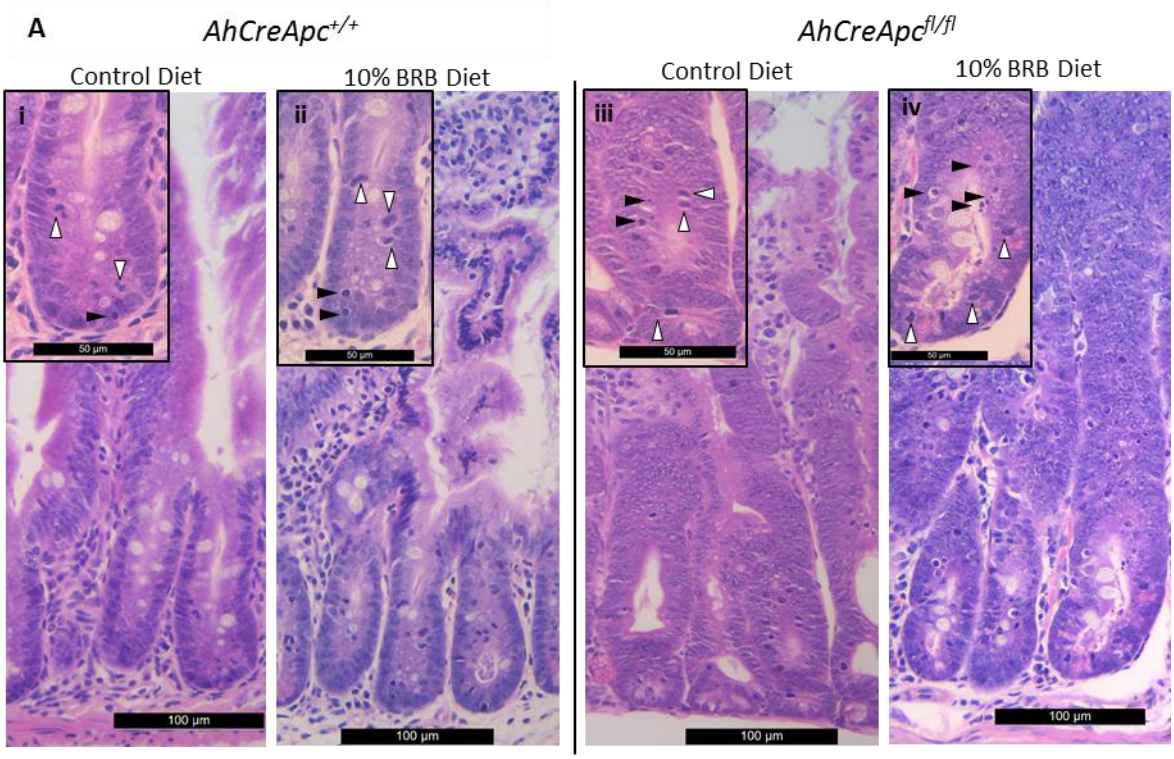

Figure S 8.1 H&E stained intestinal sections showing mitotic and apoptotic bodies in *AhCre Apc*$^{+/+}$ and *Apc*$^{fl/fl}$ mice fed control and 10% BRB diet

(A) Scoring of mitotic figures (white arrows) and apoptotic bodies (black arrows) were analsyed from H&E stained intestinal sections. BRB feeding in wildtype mice had no significant effect on the number of mitoses but significantly increased apoptosis when compared to wildtype control fed mice. (iii) Acute loss of *Apc* resulted in more mitotic bodies per crypt when compared to wildtype control fed mice (i). *Apc*$^{fl/fl}$ mice exposed to BRB diet had more mitotic figures than *Apc*$^{fl/fl}$ mice control fed mice but this was not significant. However, BRB feeding significantly increased apoptosis in *Apc*$^{fl/fl}$ mice. *P value ≤ 0.05, n ≥ 3, one-tailed Mann Whitney U test.

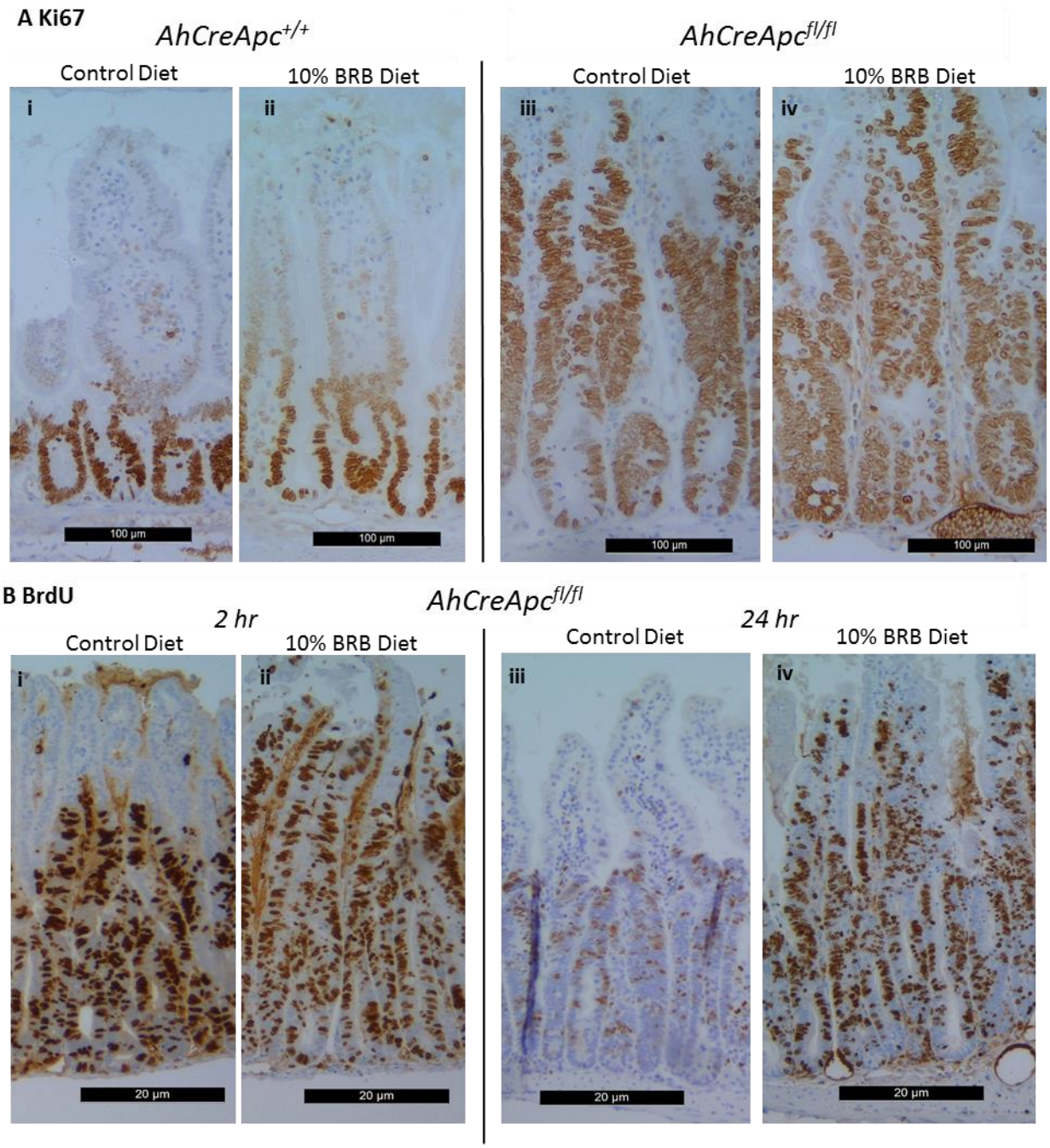

Figure S 8.2 Representative images of Ki67 and BrdU stained intestinal sections of *AhCre Apc*$^{+/+}$ and *Apc*$^{fl/fl}$ mice fed control and 10% BRB diet

(A) Scoring of Ki67 positive cells indicated no alteration in proliferation in wildtype mice in the context of BRB feeding. Loss of *Apc* significantly increased the proliferative compartment as seen with an increased Ki67 positivity in *Apc*$^{fl/fl}$ crypts. Exposure of *Apc*$^{fl/fl}$ mice to BRB diet had no effect on the number of Ki67 positive cells per crypt. (B) BrdU IHC was utilised to score the number of cells in S phase of the cell cycle in *Apc*$^{fl/fl}$ mice at 2 and 24 hrs in the context of BRB exposure. At the 2 hr timepoint, there were more BrdU positive cells (ii) in BRB exposed *Apc*$^{fl/fl}$ intestine compared to control fed *Apc*$^{fl/fl}$ mice (i) however, this was not found to be statistically significant. After 24 hrs, the number of BrdU positive cells in BRB-treated *Apc*$^{fl/fl}$ mice (iv) had almost doubled compared to control fed *Apc*$^{fl/fl}$ mice at 24 hrs (iii). This suggests that BRB diet increased proliferation. *P value ≤ 0.05, n ≥ 3, one-tailed Mann Whitney U test. Scale bars represent 100 µm.

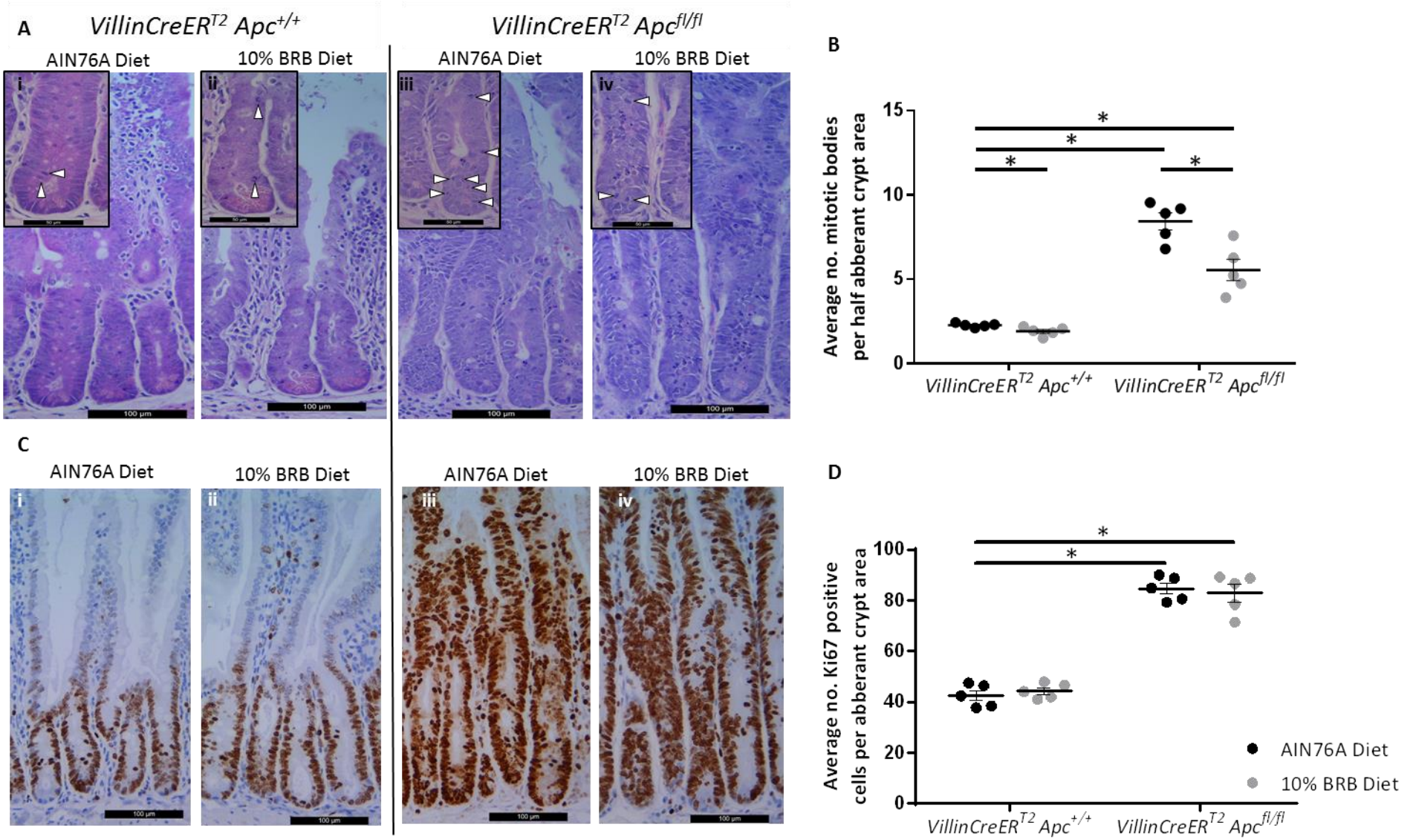

Figure S 8.3 Assessment of proliferation in *VillinCreER^{T2} Apc$^{+/+}$* and *Apc$^{fl/fl}$* mice in the context of 10% BRB diet.

(A) Representative images of mitotic bodies (white arrows) from H&E stained intestinal sections from *VillinCreER^{T2} Apc$^{+/+}$* and *Apc$^{fl/fl}$* exposed to control (AIN76A) and 10% BRB diet. (B) Scoring of mitotic figures from H&E stained sections revealed that BRBs had no effect on mitosis in wildtype mice, but significantly decreased mitosis in *Apc$^{fl/fl}$* mice when compared to control fed *Apc$^{fl/fl}$* mice. Proliferation in these models was also assessed using Ki67 IHC. (C) Representative images of Ki67 staining in control and BRB fed wildtype and *Apc$^{fl/fl}$* mice. (D) Scoring of Ki67 positive cells revealed that 2-week BRB feeding had no effect on the number of Ki67 positive cells per crypt in wildtype or *Apc$^{fl/fl}$* mice when compared to their respective controls. *P value ≤ 0.05, n ≥ 4, two-tailed Mann Whitney U test. Scale bars represent 100 µm, unless otherwise specified.Error bars represent SEM.

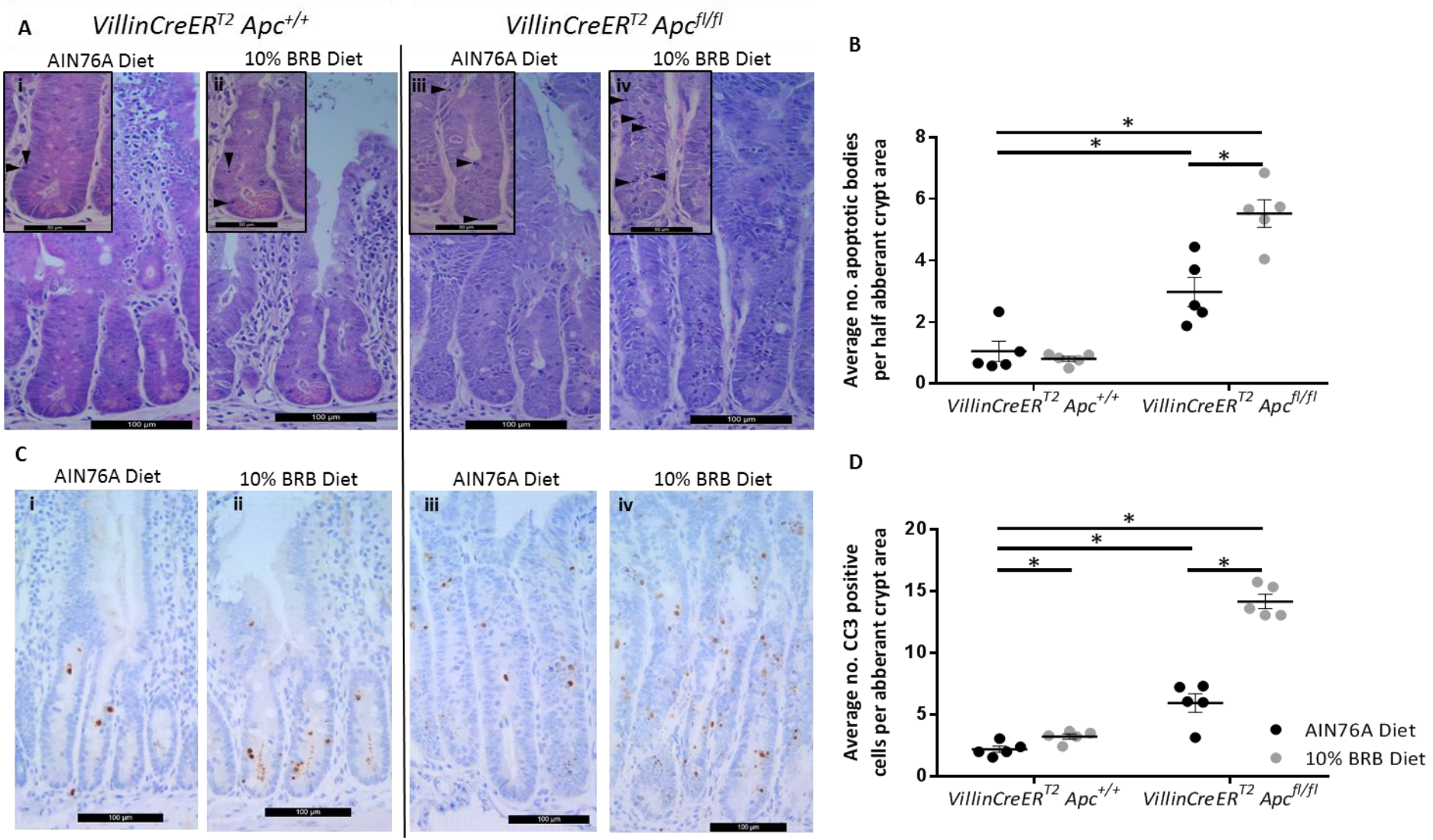

Figure S 8.4 Assessment of cell death in *VillinCreER^{T2} Apc$^{+/+}$* and *Apc$^{fl/fl}$* mice in the context of 10% BRB diet.

(A) Representative images of apoptotic bodies (black arrows) from H&E stained intestinal sections from *VillinCreER^{T2} Apc$^{+/+}$* and *Apc$^{fl/fl}$* exposed to control (AIN76A) and 10% BRB diet. (B) Scoring of apoptotic bodies from H&E stained sections revealed that BRBs had no effect on cell death in wildtype mice, but significantly increased apoptosis in *Apc$^{fl/fl}$* mice when compared to control fed *Apc$^{fl/fl}$* mice. Cell death was also analysed by cleaved caspase 3 (CC3) IHC. (C) Representative images of CC3 staining in control and BRB fed wildtype and *Apc$^{fl/fl}$* mice. (D) Scoring of CC3 positive cells revealed that 2-week feeding on BRBs resulted in a significant increased in cell death in Apc deficient intestine when compared to *Apc$^{fl/fl}$* control fed mice. *P value ≤ 0.05, n ≥ 4, two-tailed Mann Whitney U test. Scale bars represent 100 µm unless otherwise specified.Error bars represent SEM.

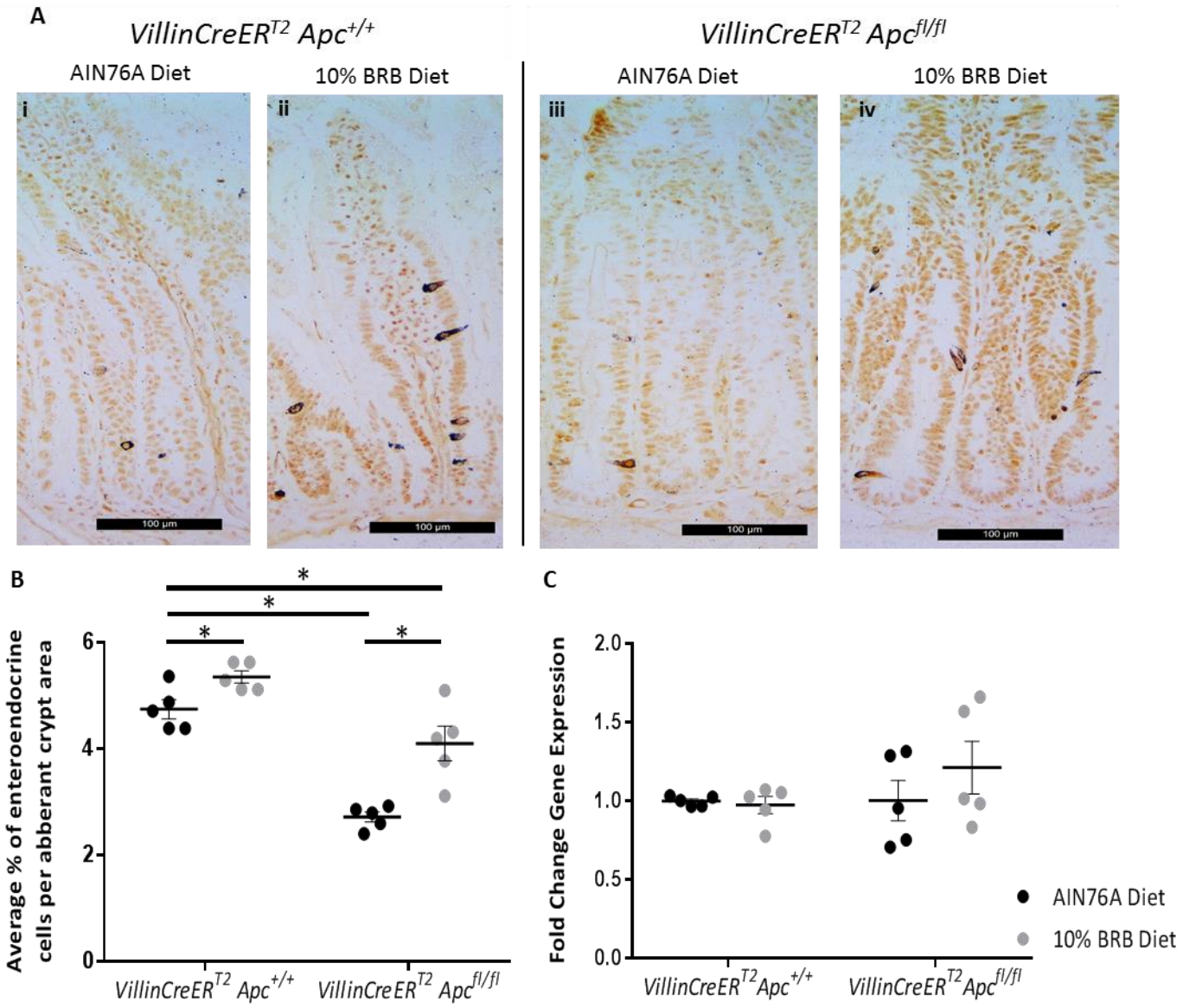

Figure S 8.5 Two-week feeding of 10% BRBs increased enteroendocrine cells in *VillinCreER^{T2} Apc$^{+/+}$* and *Apc$^{fl/fl}$* small intestine

(A) Representative images of grimelius silver stained intestinal tissue sections that highlight enteroendocrine cells marked by black deposits. (B) Scoring of black deposits revealed that BRBs significantly increased the number of enteroendocrine cells in both wildtype and *VillinCreER^{T2} Apc$^{fl/fl}$* small intestine. (C) Gene expression analysis of the enteroendocrine marker *Synaptophysin* was not altered as a result of BRB feeding or *Apc* loss. * P value ≤ 0.05, n ≥ 4, two-tailed Mann Whitney U test. Error bars represent SEM. Scale bars represent 100 µm.

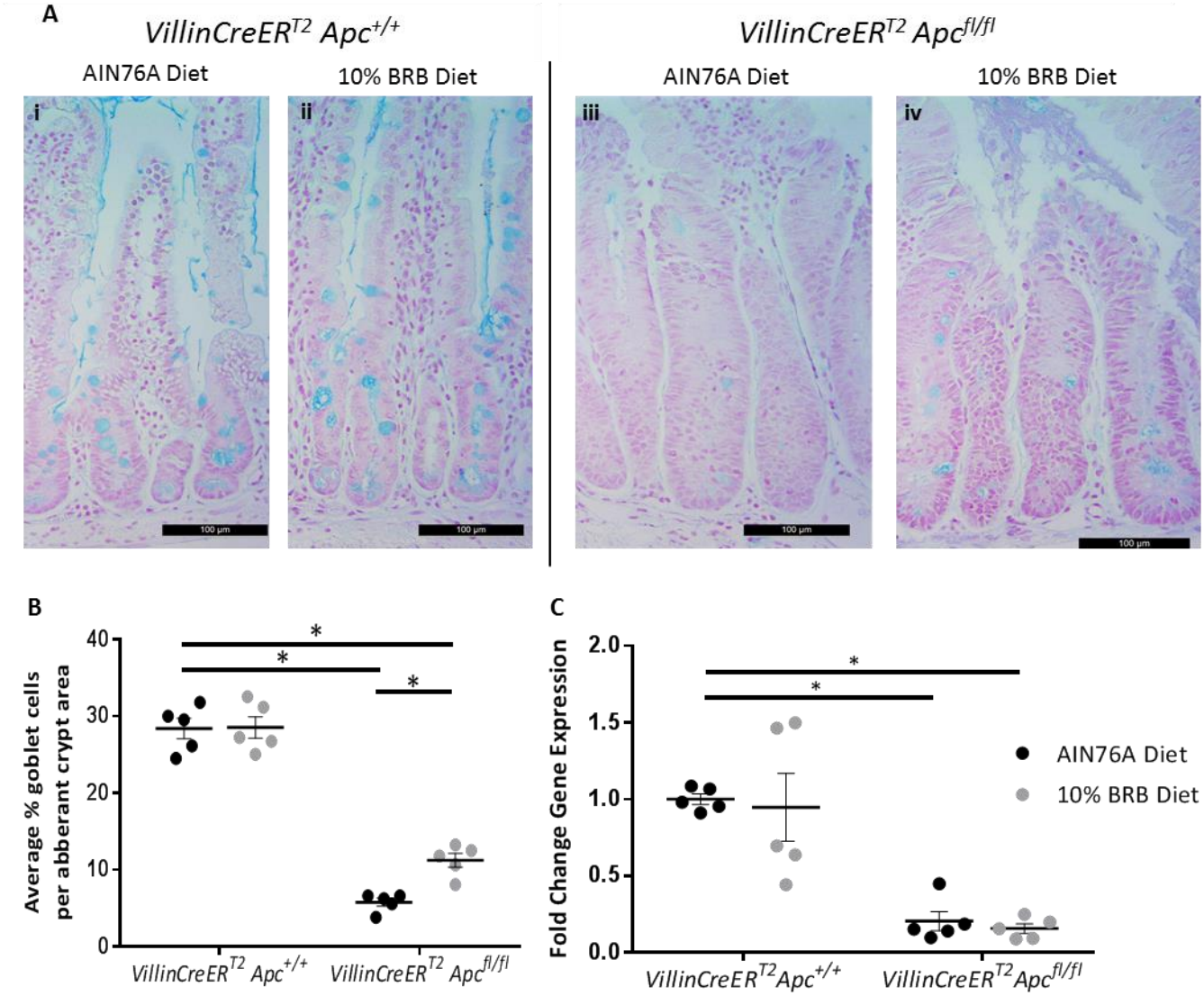

Figure S 8.6 Two-week feeding of 10% BRBs increased the number of goblet cells in *VillinCreER^{T2} Apc$^{fl/fl}$* small intestine

(A) Representative images of alcian blue stained intestinal tissue sections that show goblet cells in blue. (B) BRBs had no effect on the number of goblet cells in wildtype intestine but significantly increased the average percent of goblet cells in the aberrant crypt region following acute loss of *Apc* in the intestine driven by the *VillinCreER^{T2}* transgene. (C) Gene expression analysis of the goblet cell marker *Muc2* was not altered in wildtype or *Apc$^{fl/fl}$* small intestine in the context of BRBs. * P value ≤ 0.05, n ≥ 4, two-tailed Mann Whitney U test. Error bars represent SEM. Scale bars represent 100 µm.

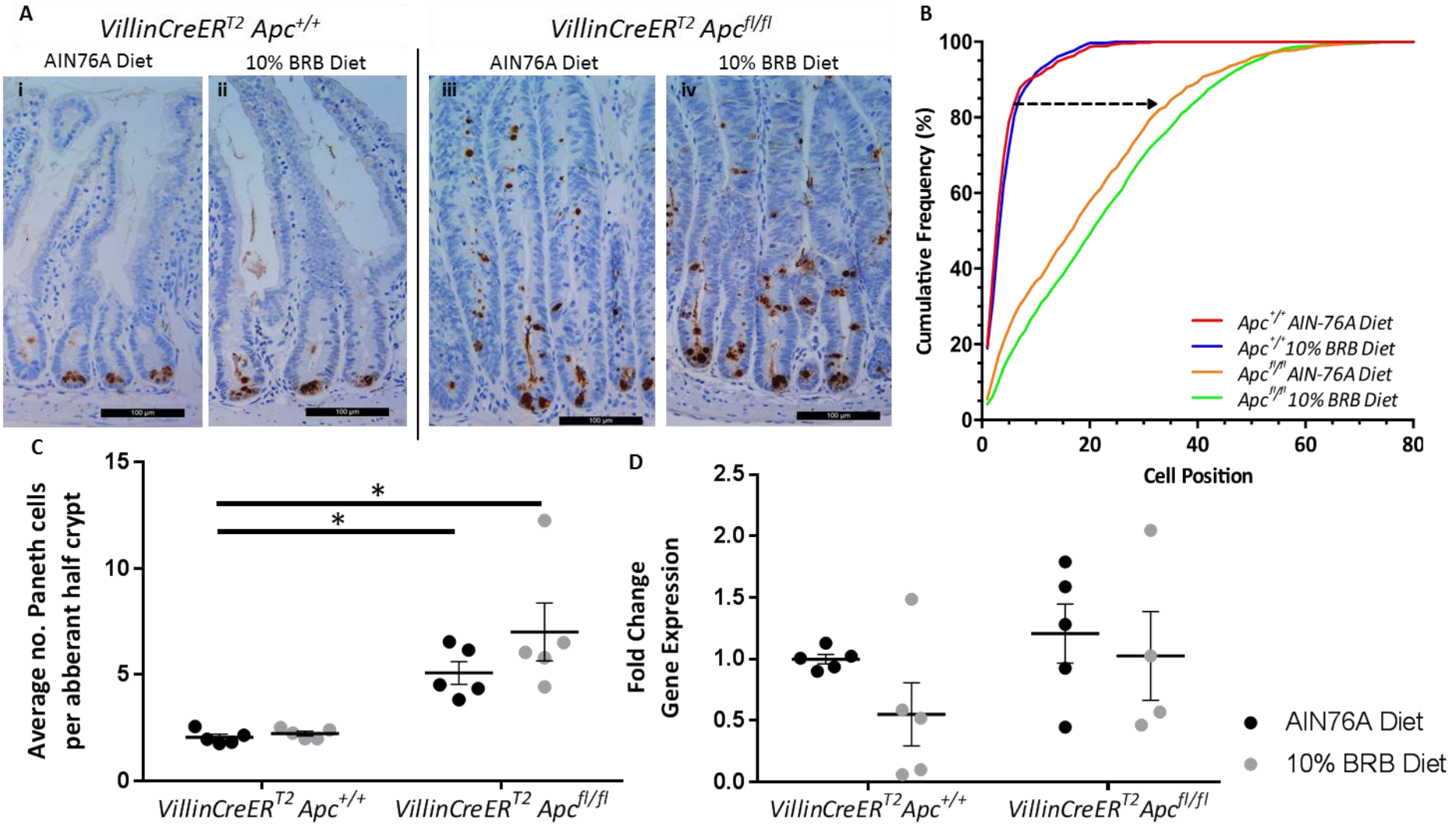

Figure S 8.7 Two-week feeding of 10% BRBs had no effect on Paneth cell differentiation in *VillinCreER^{T2} Apc$^{+/+}$* and *Apc$^{fl/fl}$* mice

(A) Representative images of lysozyme immunohistochemistry that marks Paneth cells with brown staining. (C) Scoring of Paneth cell numbers revealed that BRBs had no effect on the number of these cells in the wildtype crypt and highlighted that the cells were confined to the base of the crypt (B) as normal. Paneth cells are increased in number in *Apc$^{fl/fl}$* crypts and no longer found exclusively at the crypt base (Aiii, B orange line vs red line, C). Feeding of BRBs had no effect on the number or position of Paneth cells in *Apc$^{fl/fl}$* crypts when compared to control fed *Apc$^{fl/fl}$* mice. (D) Gene expression analysis showed that BRB feeding had no effect on the Paneth cell marker *Lysozyme1* in wildtype or *Apc$^{fl/fl}$* intestine. * P value ≤ 0.05, n ≥ 4, two-tailed Mann Whitney U test (C and D) or Kolmogorov-Smirnov test (B). Error bars represent SEM. Scale bars represent 100 µm.

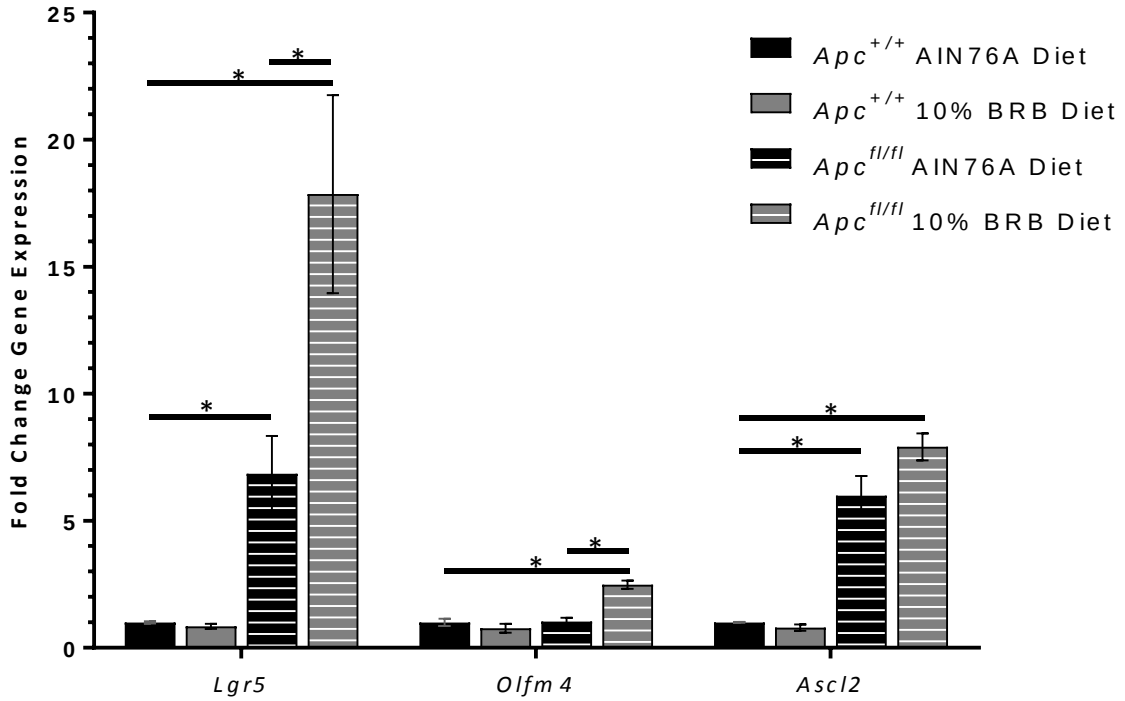

Figure S 8.8 Alterations in ISC marker gene expression in *VillinCreER^{T2} Apc$^{+/+}$* and *Apc$^{fl/fl}$* in the context of 10% BRB diet

qRT-PCR was performed on RNA extracted from epithelial cell extracts from *VillinCreER^{T2} Apc$^{+/+}$* and *Apc$^{fl/fl}$*. BRB feeding had no effect on *Lgr5*, *Olfm4* or *Ascl2* gene expression in wildtype mice. Acute loss of *Apc* resulted in a significant increase in *Lgr5* and *Ascl2* gene expression, however *Olfm4* expression was not altered. Feeding of BRBs in *VillinCreER^{T2} Apc$^{fl/fl}$* mice resulted in a significant up-regulation in *Lgr5* and *Olfm4* gene expression.

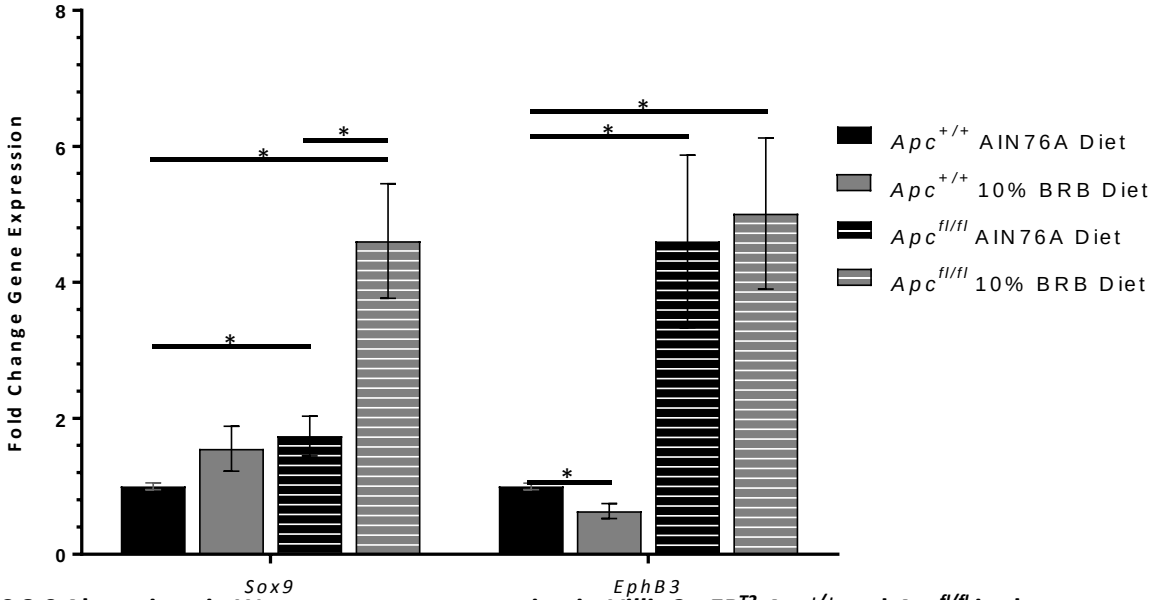

Figure S 8.9 Alterations in Wnt target gene expression in *VillinCreER^{T2} Apc$^{+/+}$* and *Apc$^{fl/fl}$* in the context of 10% BRB diet

qRT-PCR was performed on RNA extracted from epithelial cell extracts from *VillinCreER^{T2} Apc$^{+/+}$* and *Apc$^{fl/fl}$*. BRB feeding had no effect on *Sox9* gene expression in wildtype mice, but significantly down-regulated *EphB3* gene expression. Acute loss of *Apc* resulted in a significant increase in both *Sox9* and *EphB3* gene expressio. Feeding of BRBs in *VillinCreER^{T2} Apc$^{fl/fl}$* mice resulted in a further increase in *Sox9* gene expression however, *EphB3* expression was not altered.